THE IMPORTANCE OF LOW SALINITY HABITAT TO RED DRUM (*SCIAENOPS OCELLATUS*)

A Thesis

by

LOUISA E. TORRANCE

BS, University of Texas at Austin, 2012

Submitted in Partial Fulfillment of the Requirements for the Degree of

MASTER of SCIENCE

in

FISHERIES

Texas A&M University-Corpus Christi
Corpus Christi, Texas

May 2018

May 2018

THE IMPORTANCE OF LOW SALINITY HABITAT TO RED DRUM (*SCIANEOPS OCELLATUS*)

A Thesis

by

LOUISA E. TORRANCE

This thesis meets the standards for scope and quality of
Texas A&M University-Corpus Christi and is hereby approved.

Benjamin Walther, PhD
Chair

J. Derek Hogan, PhD
Committee Member

Robert Vega, PhD
Committee Member

May 2018

ABSTRACT

Red drum (*Sciaenops ocellatus*) is an estuarine-dependent species capable of survival in fresh and low salinity habitats. Standardized sampling by Texas Parks and Wildlife Department (TPWD) for various life stages of red drum occurs in estuaries, but not in tidal creeks and rivers. The goal of this study was to examine the individual variability of red drum low salinity occupancy patterns within the Mission-Aransas and Nueces estuaries using natural chemical tracer approaches.

TPWD personnel obtained age 0-2 red drum using gill nets between November 2016 and June 2017. Stable isotope analysis of muscle tissue (n=201) and otolith microchemistry (n=99) were conducted to obtain migratory and dietary histories of individuals. Ward's Hierarchical clustering analysis of muscle tissue $\delta^{13}C$ and $\delta^{15}N$ values was employed to determine distinct groupings of fish according to isotopic niche occupancy and derived partition coefficients for otolith chemistry (Sr:Ca and Ba:Ca ratios) were derived from the literature to identify movements into low salinity habitats.

Based on analyses of muscle tissue stable isotopes and otolith microchemistry, two groups were found. The first group had an isotopic signature with lower $\delta^{13}C$ and higher $\delta^{15}N$ values compared to the second group. However, spatial analysis indicated that unique stable isotope compositions of bays explained differences between groups, and therefore all sampled red drum were most likely feeding within an estuarine environment. Ba:Ca otolith chemistry threshold values indicated 2-35% of individuals showed low salinity movement during life. Stable isotope signatures were not directly correlated with otolith microchemistry.

The primary pattern of habitat use by red drum appears to be residency within specific bays of the estuary. However, the potential for red drum to move into areas of low salinity could be a useful facultative behavior for populations in a region experiencing inter-annual flood and drought events. Individuals that move into the tributaries of south Texas estuaries may also be important for understanding trophic connectivity between estuarine and freshwater environments should be considered by fisheries managers when prioritizing habitat.

DEDICATION

This work is dedicated to my wonderful family and friends who were constant sources of inspiration and laughter during my time at Texas A&M University-Corpus Christi and to the late Mr. Schwarz, my aquatic science teacher who first introduced me the world of marine ecology. Finally, I am most appreciative of my fiancé, Alan Sosa. Thank you for your unconditional love and support; I'm so happy to be starting this next chapter of life together.

ACKNOWLEDGEMENTS

I would like to thank Dr. Benjamin Walther for his excellence in advising and dedication to my success, Dr. Robert Vega for providing invaluable resources and wisdom, and Dr. J. Derek Hogan for his insight and ecological expertise. I would also like to thank the Fisheries and Mariculture Program for the financial support necessary to complete my stable isotope analysis and Texas Parks and Wildlife Department Coastal Fisheries personnel (Brian Bartram, Justin Dunn, Stephen Hale, Jacob Harris, Moises Hinojosa, Jr., Cindy Kelly, Dr. Christopher Mace, Evan Pettis, Johnny Rios, Jason Slocum, Caleb Taylor, Luis Uballe, Jr., Tom Wagner) for providing me with red drum samples. I am grateful to Dr. Ryan Hladynuik at the University of Texas Marine Science Institute and Dr. Paula Rose at Texas A&M University-Corpus Christi for their exceptional services involving stable isotope analysis, as well as to Dr. Nathaniel Miller at the University of Texas at Austin Jackson School of Geosciences for his skill in otolith microchemistry. Dr. Blair Sterba-Boatwright was indispensable for his statistical expertise, and Dr. John Scarpa and Dr. James Tolan were very helpful in providing advice throughout my project. The Institutional Animal Care and Use Committee Protocol Number for this thesis is AUP#11-15.

TABLE OF CONTENTS

CONTENTS PAGE

ABSTRACT v

DEDICATION vii

ACKNOWLEDGEMENTS viii

TABLE OF CONTENTS ix

LIST OF FIGURES xi

LIST OF TABLES xiii

CHAPTER I: Literature Review of Movement Ecology and Red Drum in Texas 1

CHAPTER II: Determining diet and movement of Red Drum (*Sciaenops ocellatus*) using stable isotope analysis and otolith microchemistry 6

Introduction 6

Stable Isotope Analysis 6

Otolith Microchemistry 9

MATERIALS AND METHODS 14

Study Area 14

Sampling 16

Sample Processing 16

Stable Isotope Analysis 17

Otolith Processing 18

Otolith Aging 19

Determination of Partition Coefficients 20

Otolith Transect Analysis 21

Combined Stable Isotope and Otolith Approach 22

RESULTS 24

Physical Characteristics 24

Stable Isotope Analysis 24

Partition Coefficients 28

DISCUSSION 30

Stable Isotopes 31

Otoliths 34

Implications for Stock Enhancement and Recreational Fishing 36

CONCLUSION 37

REFERENCES 38

LIST OF APPENDICES 73

Appendix 1. Supplemental Isotope Data 73

Appendix 2. Supplemental Otolith Graphs 84

LIST OF FIGURES

FIGURES PAGE

Figure 1. Sampling map of the Nueces and Mission-Aransas Estuaries, Texas, USA.....52

Figure 2. Ward's Hierarchical clustering analysis of all individuals (*n*=201) showing two clusters, designated as Group 1 and Group 2 53

Figure 3. SIBER biplot of $\delta^{13}C$ and $\delta^{15}N$ of all sampled individuals and subsample used for otolith interpretation including convex hull total area and Standard Ellipse Area.....54

Figure 4. Boxplot of $\delta^{13}C$ values from Aransas Bay (AB), Copano Bay (CB), Corpus Christi Bay (CC), Mesquite Bay (MB), Corpus Christi Bay – Mustang Island (MI), and Nueces Bay (NB) .55

Figure 5. Boxplot of $\delta^{15}N$ values from Aransas Bay (AB), Copano Bay (CB), Corpus Christi Bay (CC), Mesquite Bay (MB), Corpus Christi Bay – Mustang Island (MI), and Nueces Bay (NB) .56

Figure 6. Stable isotope signatures ($\delta^{13}C$ and $\delta^{15}N$) of individuals collected at different locations within the Mission-Aransas and Nueces estuaries.....57

Figure 7. Non-parametric Kruskal Wallis post hoc test results of $\delta^{13}C$ values between Mesquite Bay (MB), Nueces Bay (NB), Copano Bay (CB), Corpus Christi Bay – Mustang Island (MI), Aransas Bay (AB), and Corpus Christi Bay (CC) 58

Figure 8. Averaged stable isotope signatures ($\delta^{13}C$ and $\delta^{15}N$) of Group 1 and Group 2 (mixtures), riverine and estuary SPOM, potential prey, and other consumers within the Mission-Aransas estuary 59

Figure 9a. Frequency histogram of individuals grouped by the proportion of their Sr:Ca life history profile that exceeded a threshold for low salinity residence.....60

Figure 9b. Frequency histogram of individuals grouped by the proportion of their Ba:Ca life history profile that exceeded a threshold for low salinity residence.....61

Figure 10a. Average Ba:Ca ratios of 250, 500, and 1000 μm sections of otolith correlated with $\delta^{13}C$ values of individual fish.....62

Figure 10b. Average Sr:Ca ratios for 250, 500, and 1000 μm sections of otolith correlated with $\delta^{13}C$ values for individual fish.....63

LIST OF TABLES

TABLES PAGE

Table 1a. Laser pre-ablation parameters used for sample analysis 64

Table 1b. Laser ablation parameters used for sample analysis 65

Table 2. Age, sample size, and SD of total length (mm) of collected red drum 66

Table 3. Mean and standard deviation of total length (mm) and wet weight (g) of individuals sampled in the Mission-Aransas and Nueces estuaries 67

Table 4. $\delta^{13}C$ and $\delta^{15}N$ means and standard deviation for each group 68

Table 5. Mean and standard deviation of $\delta^{13}C$ and $\delta^{15}N$ of individuals sampled in the Mission-Aransas and Nueces estuaries 69

Table 6. $\delta^{13}C$ and $\delta^{15}N$ values in the Mission-Aransas estuary 70

Table 7. $\delta^{13}C$ and $\delta^{15}N$ values in the Nueces estuary 72

CHAPTER I: Literature Review of Movement Ecology and Red Drum in Texas

Animal movement has been studied by ecologists across a variety of ocean taxa, including the great migrations of marine mammals (Boyd 2004), spawning runs of salmon (Dittman and Quinn 1996), and nesting site preferences of green sea turtles (Robinson et al. 2017). For many species, movement is an essential part of survival as individuals seek shelter, prey, escape from predation, or more favorable environmental conditions (Stewart and Scharf 2008; Dance and Rooker 2016). For others, movement is associated with ontogenetic niche shifts as an individual organism develops from its earliest stage to maturity (Abel 2005; Albuquerque et al. 2012; Werner and Gilliam 1984). The resulting temporal and spatial linkages between ecosystems are important to examine when investigating trophic connections and food web interactions. For example, freshwater communities can depend on the punctuated annual transfer of marine derived nutrients from upstream Pacific salmon migrations (Limburg and Waldman 2009; Naiman et al. 2002). Additionally, hundreds of studies have been conducted along coastlines worldwide in an effort to better understand the life history of fishes that move across salinity gradients (Maggs and Cowley 2016; Le Pape and Cognez 2016; Kynard 1997).

Patterns of fish movement vary greatly among species. Diadromy describes the regular and predictable migration of fish species between marine and freshwater environments (McDowall 1997), although less than 1% of the world's fish are considered diadromous (Limburg and Waldman 2009). Physiological changes in osmoregulation such as altered drinking habits and the transition of gills between absorptive and excretory epithelia allow diadromous species to survive drastic changes in their ionic environment (Gross et al. 1988; Esbaugh and Cutler 2016). Anadromous species such as Chinook salmon (*Oncorhynchus tshawytscha*) grow at sea

before spawning in freshwater rivers. Species dependent on movement across salinity during their life history are considered obligate (Helfman et al. 2009). Catadromous species such as the American eel (*Anguilla rostrata*) spend a majority of their lives in freshwater before returning to their native Sargasso Sea to spawn (Potter et al. 2015). However, not all individuals move into freshwater and may instead reside in coastal bays and estuaries (Lamson et al. 2006). Individuals that are capable of but not restricted to crossing salinity gradients are deemed facultative (McCormick et al. 2013; Kim and Montagna 2012). Euryhaline migration can be driven by increased food availability, latitudinal differences in aquatic productivity, or cues during early life stages, although the timing of these migrations is often variable (Gross et al. 1988; Dunham et al. 2008).

Non-diadromous fish species can also exhibit euryhaline behavior. Varying usage exists to describe marine spawned species that move into estuaries, including "marine stragglers" which may only enter the estuary on occasion, "marine estuarine-opportunists" which use the estuary on a regular basis, and "marine estuarine-dependent species" such as the red drum (*Sciaenops ocellatus*) which complete the juvenile stage of their life cycle in the estuary before moving back into the marine environment (Potter et al. 2015; Sheppard et al. 2012; Nims and Walther 2014; Secor and Kerr 2009).

Additional classification terms have emerged as more is learned about variation between individuals within a population. The term "contingent" was used to describe distinct, possibly non-inherited patterns of behavior by Clark (1968) and was revised by Secor and Piccoli (2007) as "groups of individuals that share similar migration behaviors with some, but not all, members of their population" (Clark 1968; Secor and Piccoli 2007, p. 72). Recently, an investigation of

Southern flounder (*Paralichthys lethostigma*) movement in south Texas found over half of the analyzed individuals never used low salinity habitats, contrary to their accepted life history model (Nims and Walther 2014). This contingent variation could provide increased resiliency during environmental changes, such as the droughts and floods common to the region (Kerr et al. 2010; Secor 1999; Nims and Walther 2014). Similarly, a study of estuarine white perch (*Morone americana*) found the relative abundance of either migratory or resident contingents affected the stability and productivity of the entire population (Kerr et al. 2010).

The red drum is an estuarine-dependent species vital to the economy of Texas with an annual recreational fisheries value of $350 million (Vega et al. 2011). However, in 1975 Texas Parks and Wildlife Department (TPWD) conducted an independent sampling of Texas bays using gill nets and concluded that red drum populations were declining (Matlock 1984). 56 million red drum eggs, fry and fingerlings were released in the same year into Sabine Lake, Galveston Bay, East Matagorda Bay, Matagorda Bay, San Antonio Bay, Aransas Bay, Corpus Christi Bay, and the Upper Laguna Madre with 49,194 tagged to help evaluate stocking success (Matlock 1984). To aid in their recovery the 1981 Texas Legislature passed House Bill 1000 (known as the Redfish Bill) declaring red drum as a game fish and prohibited their sale (Bengston et al. 2003). Since then, stock enhancement programs have continued to supplement wild red drum and Texas bay populations have recovered to near record numbers (Vega et al. 2011).

Ecologically, red drum contribute greatly to the structure of prey assemblages in coastal estuaries (Scharf and Schlicht 2000). Adult red drum are found throughout the Gulf of Mexico, typically in salinities between 20 and 40 (Neill 1990). Their greatest concentrations are found along the coasts of Louisiana and Texas (Pattillo et al. 1997; Reagan 1985). Spawning occurs during the late summer and fall when adults move towards the mouths of bays and inlets from

offshore (Comyns et al. 1991; Wilson and Nieland 1994). Their eggs and pre-settlement larvae are carried into the estuaries via tidal currents, where they settle and remain until about age 3-5 (Holt et al. 1983). It has been hypothesized that spawning females demonstrate philopatry and return to or remain near natal estuaries in addition to exhibiting limited coastwise movement while in the Gulf of Mexico (Gold et al. 1999). Tagging studies in the Mission-Aransas Estuary in Texas found that red drum maintained high residency to particular regions within bays with a preference for boundaries of differing habitat types, such as salt marsh edges (Moulton et al. 2017; Stunz et al. 2002).

During estuarine residence, juvenile red drum feed primarily on crustaceans and fishes, with relative proportions of prey items varying by season. Red drum are the dominant predator of blue crab (*Callinectes sapidus*) in Louisiana (Scharf and Schlicht 2000; Guillory and Elliot 2001), although polychaetes, amphipods, stomatopods, echinoids, algae, and detritus have also been identified in gut content analyses (Overstreet and Heard 1978). A number of red drum prey items themselves move between low salinity habitats and the estuary, including brown shrimp (*Penaeus aztecus*) and blue crab which red drum may follow into tidal creeks and river mouths (Riera et al. 2000; Bourgeois et al. 2014). Several studies have investigated the rapid transcriptional responses in red drum that result in their short and long-term tolerance of freshwater, including down-regulation of ion excretion pathways (Crocker et al. 1981; Watson et al. 2014). An experiment measuring blood osmolality shifts of juveniles observed a 98% survival rate after abrupt movement from seawater to freshwater (Crocker et al. 1983). Juveniles in the wild show wide ranges of habitat use across salinity and have been sampled in river channels along the western and eastern coasts of Florida and in shallow creeks and river channels of South Carolina

(Bacheler et al. 2008; Adams and Tremain 2000; Stevens et al. 2013; Wenner 1992). These individuals may select oligohaline habitat to access prey, avoid predators, or as a response to decreased winter temperatures (Peters and McMichael 1987). Thus, red drum have the physiological capacity to live as partial or full-time residents in freshwater.

However, red drum use of low salinity (≤5) habitats in south Texas remains unclear. A primary objective of this study was to establish if red drum in the Mission-Aransas and Nueces estuary move into low salinity habitats and if so, what percentage and how frequently. A more thorough understanding of the habitats fish use is important for fisheries managers, especially when defining Essential Fish Habitat (EFH). The intent of this provision is to describe and identify "those waters and substrate necessary to fish for spawning, breeding, feeding and/or growth to maturity" and consider habitat and the role that it plays during different stages of development of a species (MSFCMA 2007, p. 6). All estuaries in the Gulf of Mexico are designated as red drum EFH, while freshwater habitats are not currently included.

CHAPTER II: Determining diet and movement of Red Drum (*Sciaenops ocellatus*) using stable isotope analysis and otolith microchemistry

Introduction

Studies to address animal movement can be conducted directly using underwater visual observations (Mumby et al. 2004; Ambrose and Swarbrick 1989) and satellite tagging (Tupper 2007), or indirectly using biochemical markers such as otoliths (Walther and Limburg 2012; Rooker et al. 2010; Campana et al. 2000), and tissue stable isotopes (Rubenstein and Hobson 2004; MacKenzie et al. 2011). Direct methods can be cost prohibitive or difficult to achieve in certain environments, leaving indirect methods as an ideal alternative.

Stable Isotope Analysis

As an organism feeds in a new food web, the existing isotopic signature of their tissues is both diluted by and replaced with newly synthesized material created with the new signature (Buccheister and Latour 2010), and the isotope ratios of $\delta^{13}C$ and $\delta^{15}N$ can be used to examine movement of an organism between distinct food webs with isotopically unique baseline signatures (Herzka 2005). When an organism migrates to a habitat with a different food web (e.g. marine to low salinity), the new isotopic composition of prey items becomes incorporated into its tissues over time, leaving an isotopic signature that is offset from the diet isotope value in a process called fractionation (Herzka 2005), particularly when moving between freshwater and estuaries or offshore regions (Fry 2002; Michener and Kaufman 2007; Fry 1983; Fry 1999). An important assumption when analyzing food webs is that the fractionation between diet and organism is ~3.4‰ for nitrogen and a conservative 0-1‰ for carbon (Buccheister and Latour 2010;

Post 2002; Peterson and Fry 1987). Because tissues are time integrated and do not immediately reflect the stable isotopes of a dietary change, a turnover rate, or time required for equilibrium with the new diet, must be known in order to interpret food web dynamics (Vander Zanden et al. 2015). Turnover rates for specific tissues and species are often established in laboratory studies (Buchheister and Latour 2010; Gorokhova and Hansson 1999; Herzka and Holt 2000; Mohan et al. 2016). Factors affecting turnover rate include growth rate, metabolism, age, and tissue type (Perga and Gerdeaux 2005; Hesslein et al. 1993; Herzka and Holt 2000). Red drum experience rapid growth during the first year of life which results in turnover rates more greatly influenced by the dilution of existing tissue isotopes with the isotopic signatures of new dietary items than by tissue replacement through metabolic turnover (Herzka et al. 2002; Hesslein et al. 1993; Trueman et al. 2005). Time or growth-based models can be used to estimate the relative contribution of either growth or metabolism (Buccheister and Latour 2010). However, turnover rates and metabolic variations between individuals as a whole and within tissues must be accounted for during analysis (Bowes and Thorpe 2015; Vander Zanden and Rasmussen 2001). Muscle tissue is often selected to obtain diet isotopic ratios because of the longer time scale of diet accumulated over several weeks rather than short term feeding behavior (Trueman et al. 2005; Maruyama et al. 2017; Suzuki et al. 2005; Mohan et al. 2016).

A sufficient difference in stable isotope ratios between food webs the organism is feeding in must be discernible in order to interpret the isotopic compositions of tissues within the context of migration (Herzka and Holt 2000). Established maps of distinct stable isotope signatures, or "isoscapes" are often an important reference when designing a diet study using stable isotopes

(West et al. 2009; Graham et al. 2010; Hobson et al. 2010). For instance, the isoscapes constructed within of the Gulf of Mexico by Radabaugh et al. (2013) have been useful for many subsequent studies ranging from sea turtle locations to the validation of fish eye lenses as trackers of fish movement (Wallace et al. 2014; Vander Zanden et al. 2016). The $\delta^{13}C$ values of dissolved organic carbon in seawater are a result of marine dissolved bicarbonate and slow exchange with carbon dioxide in the atmosphere. $\delta^{13}C$ values in rivers are related to geologic weathering of limestone and soils, and exchange with atmospheric and soil carbon dioxide (Mook and DeVries 2000; Peterson and Fry 1987). This results in a contrast of stable isotope signatures that are found between fresh and marine water. Generally, $\delta^{13}C$ values increase with salinity (Fry 2002; Qian et al. 1966). $\delta^{15}N$ values can increase or decrease across salinity gradients depending on factors such as anthropogenic inputs of nitrogen (i.e. wastewater discharge or artificial fertilizer) or varied flow conditions that cause particulate organic nitrogen $\delta^{15}N$ values to either reflect human pollution more closely resemble the landscape of the watershed (Mooney and McClelland 2012; Fry 2002). These differences in baseline sources of carbon and nitrogen are ultimately incorporated by phytoplankton and consumers (Michener and Kaufman 2007). Studies conducted from the Aransas River mouth to the Gulf of Mexico and from the Guadalupe River to the Aransas Pass ship channel confirmed an increase in $\delta^{13}C$ values and found a decrease in $\delta^{15}N$ values with salinity within the Mission-Aransas estuary (Lebreton et al. 2016; Bishop et al. 2017). As organisms move across salinities and begin feeding, as when brown shrimp move from Corpus Christi Bay into areas of freshwater inundation in the Rincon Bayou, $\delta^{13}C$ values representative of a diet primarily composed of oceanic plankton ($\delta^{13}C$ = -21.7 to -20.7‰) will shift to a food web based on terrestrial derived organic matter, as indicated by more negative $\delta^{13}C$ values ($\delta^{13}C$ = -24.0 to -21.0‰; Riera et al. 2000). In freshwater systems influenced by C_3 plants such

as trees, shrubs, and temperate grasses, $\delta^{13}C$ values average -26.5‰, while estuarine seagrasses can exhibit $\delta^{13}C$ values that average -10.0‰ (Tykot 2004; Fry 2006) Because tissues isotope signatures reflect diet, insight regarding individual movement can be gained as dietary shifts in novel regimes occur due to gradients across and between estuaries with distinct salinities and anthropogenic inputs.

Otolith Microchemistry

Otoliths are calcium carbonate accretionary structures found in the inner ear system of all bony fishes and are contained within the otic chamber in a fluid called endolymph and assist the fish with hearing and balance (Secor 1999; Payan et al. 2004). The otolith grows continuously and accretes increments with alternating opacities on a daily and annual basis (Pannella 1971; Campana and Neilson 1985). These increments can be counted and measured to identify age and growth rates, and their chemical composition can be assayed to identify spawning stocks or populations, or to reconstruct migratory histories (Campana and Jones 1992; Campana et al. 2000). Otolith chemistry has major advantages over alternative methodologies such as mark-recapture studies, including cost effectiveness, avoidance of tag loss, and ability to capture the entire life history of an individual.

The concentrations of certain elements in otoliths are proportional to ambient water concentrations, making the otolith a valuable tool for understanding movement across natural chemical gradients among habitats (Wheeler 2016; Campana 1992). An essential assumption that must be met for otolith-based chemical reconstructions is that the assayed element does not undergo

significant physiological regulation that decouples the otolith composition from the ambient environment (Campana et al. 2000; Kalish 1991). The pathway of elements from the environment into the otolith includes multiple biological barriers. First, elements enter the fish across branchial or intestinal membranes and are transported via blood plasma to the inner ear where they cross another membrane into the endolymph and are finally crystallized directly into the calcium carbonate or adhered to the protein lattice of the aragonite otolith layers (Campana 1999; Bath et al. 2000). Highly physiologically regulated elements that are subject to significant discrimination or elevated uptake along points in this pathway do not allow environmental reconstructions because the otolith composition is decoupled from ambient water compositions (Campana et al. 2000; Sturrock et al. 2014). Useful trace elements in otoliths that primarily reflect water chemistry include strontium, barium, and manganese (Mohan et al. 2012; Secor and Rooker 2000; Walther and Thorrold 2006). In order to estimate the relative discrimination of a given element between water and otoliths, researchers commonly calculate a partition coefficient, which is the ratio of the elemental concentration in the otolith to the ambient concentration in the water (Bath et al. 2000; DiMaria et al. 2010). This partition coefficient allows estimations of expected otolith elemental ratios to be made for fish inhabiting certain habitats with unique water chemical compositions if the water elemental ratios are known.

There are environmental parameters such as salinity that correlate predictably with water chemistry and subsequently otolith chemistry. For instance, barium (Ba) concentrations in marine environments are generally low (10.0-30.0 μg/kg), while freshwater concentrations can be enriched in dissolved Ba due to river flow and resulting weathering of continental rocks (Bernat

et al. 1972; Shaw et al. 1998). This results in Ba:Ca ratios that typically decrease as salinity increases, a pattern observed in the Nueces River in particular (Shaw et al. 1998, Nims and Walther 2014). Reduction of erosional and weathering processes by human activities such as construction can reduce the amount of dissolved Ba downstream and affect Ba:Ca levels between rivers within the same watershed and is important to consider when interpreting otoliths (Characklis and Wisener 1997). The Ba:Ca ratio along the salinity gradient from the Nueces River into Corpus Christi Bay revealed a non-linear curve and a rapid change in magnitude in salinities between 0-15, a pattern common among estuaries globally (Nims and Walther 2014; Coffey et al. 1997). Therefore, Ba:Ca in otoliths is an effective recorder of salinity histories, particularly for species that migrate across the full salinity gradient into oligohaline waters.

Strontium can also reflect transitions across salinity regimes (Walther and Nims 2015). Sr:Ca variability in fish otoliths has been used to interpret movement since Sr:Ca is positively correlated with salinity but requires careful consideration due to potential issues regarding the influence of temperature and physiology on the uptake of Sr and subsequent Sr:Ca values reflected in the otolith (Kraus and Secor 2004; Zimmerman 2005; Secor and Rooker 2000). Strontium is supplied to the marine environment through mantle at mid-ocean ridges and by rivers via continental weathering (Godderis and Veizer 2000; Palmer and Edmond 1992). When ratioed to calcium, strontium has a relatively constant concentration (8.5 – 9.0 mmol/mol) in the marine environment (de Villiers 1999) while the end-members of most freshwater coastal tributaries end-members fall below this value (Brown and Severin 2009; Kraus and Secor 2004). The major tributaries of the Mission-Aransas and Nueces estuaries are consistent with freshwater trends for Sr:Ca, although Sr:Ca values are between 4.5 to 6.0 mmol/mol and therefore substantially above

the global freshwater median of 2.39 mmol/mol (Walther and Nims 2015; Brown and Severin 2009; Palmer and Edmond 1992). These high freshwater Sr:Ca values can be attributed to the weathering of Cretaceous limestone common to central Texas, which has high strontium concentrations (Walther and Nims 2015). Consequently, the magnitude of difference between freshwater and marine end-members in South Texas estuaries is narrower than areas with alternative geology, and Ba:Ca is likely a more sensitive indicator of movement into oligohaline habitats for Texas species.

Salinity has been described as a primary hydrobiological parameter and the ecology of Texas estuaries is profoundly influenced by changes in salinity due to freshwater inflow (Copeland 1966; Dunton et al. 2001; Pollack et al. 2011; Chen 2010). The expansion and contraction of salinity gradients changes with season, floods, droughts, and tides, with periods of high inflow contributing nutrients and sediments that are especially important for maintaining high productivity and nursery environments (Polis et al. 1997; Russell et al. 2006). South Texas experiences annual variability in precipitation (Mooney and McClelland 2012; Orlando et al. 1993), and major precipitation events can trigger significant decreases in tidal creek salinities, as seen in the Nueces marsh in 1992 (Dunton et al. 2001) as well as in bays, as seen in Copano Bay after a major storm event in 2007 (Mooney and McClelland 2012). Conversely, saltwater intrusions from Nueces Bay into the Nueces River during high tides or increased evaporation and periods of low freshwater inflow can increase salinity and cause hypersaline conditions (Ockerman 2001). After construction of dams, the reduction in freshwater flow resulted the Nueces Marsh becoming a reverse estuary, which was only negated after precipitation events (Palmer et al. 2002). Groundwater can also impact the physical characteristics of an estuary. In a study of Oso

Bay, significant differences in $\delta^{13}C$ values between 2012 and 2013 were attributed to a change in water sources and submarine groundwater discharge and coastal groundwater discharge during the 2013 drought (Bighash and Murgulet 2015). These scenarios must be considered when interpreting stable isotopes and otolith microchemistry.

This study is an attempt to combine life history transects of otolith chemistry (Sr:Ca and Ba:Ca) with muscle tissue stable isotope analysis ($\delta^{13}C$ and $\delta^{15}N$) in order to examine the habitat use of red drum in south Texas estuaries. This integrated approach provides insight into the duration and frequency of movement as well as feeding of red drum across salinity gradients. The overall objectives of this project are to investigate the life history and habitat use of red drum, a recreationally and ecologically important species in the Gulf of Mexico, by quantifying the number of fish within our geographic study sample that migrate into low salinity habitats (≤5) and how frequently this migration occurs over their life using otolith chemistry. Additionally, we seek to determine if red drum are engaging in low salinity food webs using stable isotope analysis of muscle tissue. Both findings can augment the understanding of energy flow within an estuary and using geochemical tools to describe the ecological interactions and movements of this species and can have important implications for Essential Fish Habitat designation and management.

MATERIALS AND METHODS

Study Area

The coastal estuaries of Texas are defined by the input of terrestrial freshwater into the Gulf of Mexico and include sub-systems such as shallow bays (Chandler et al. 1981). Estuaries in the south receive less freshwater input than the north and are generally more saline (Montagna et al. 2011). However, precipitation, inflow, and salinity can vary on an annual basis due to El Nino Southern Oscillation (Tolan 2007; Bonner and Duke 2015; Montagna and Kalke 1995). Texas bays receive episodic pulses of freshwater and terrestrial nutrients during storm events which can dramatically reduce average salinity for extended periods (Mooney and McClelland 2012; Ward 1997). Conversely, droughts which contribute to high evaporation and low inflow can cause periods of hypersalinity (>35; Evans 2012). With consideration for the effects of increased salinity on dissolved elemental constituents, a study from Galveston Bay, the Mission-Aransas estuary, and the Laguna Madre found that Ba:Ca could still be used as a suitable proxy (Mohan and Walther 2015).

The Nueces estuary spans over 432 km^2 and includes the primary Corpus Christi Bay and secondary Nueces Bay. Nueces Bay is located in the northwestern edge of Corpus Christi Bay and receives an average of 780,000 m^3/yr of freshwater from the Nueces River and the Rincon Delta (Eldridge et al. 2005; Longley 1994). Additional freshwater inflow is provided by Oso Creek which receives water from the Nueces-Rio Grande Coastal Basin (Chandler et al. 1981). Corpus Christi Bay has an average depth between 3.0-4.0 m and exchanges water with Nueces Bay, Redfish Bay to the northeast, Oso Bay to the southwest, and the Gulf of Mexico through the

Aransas east-west shipping channel (Simms et al. 2008; Islam et al. 2014). The average salinity in Nueces Bay is between 21.4 to 25.0, while the average salinity in Corpus Christi Bay is between 26.5 to 31.4 (Longley 1994; Kim and Montagna 2012). *Halodule wrightii* and *Thalassia testidinum* are the dominant species of seagrass and increase in cover with distance from freshwater inflow (Pulich et al. 1998).

The Mission-Aransas Estuary includes Aransas Bay and Copano Bay, with San Jose Island between the bays and the Gulf of Mexico (Bonner and Duke 2015). Copano Bay is a secondary bay located in the northwest edge of Aransas Bay and receives a mean daily inflow of 28.0 m^3/s from the Mission and Aransas Rivers, supplied by the San Antonio-Nueces Coastal Basin (Froeschke et al. 2013; Chandler et al. 1981), both of which supply the estuary with the highest quantity of freshwater (Lebreton et al. 2016). The Aransas River is affected by anthropogenic inputs of inorganic nutrients and nitrogen (resulting in high $\delta^{15}N$) as contributed by Beeville (Mooney and McClelland 2012). Additional freshwater inflow is provided by Copano, Cavasso, and Salt Creeks. Aransas Bay has an average depth of 2.6 m and exchanges water with Copano Bay, St. Charles and Mesquite Bays to the northeast, Redfish Bay to the southwest, and the Gulf of Mexico through the Aransas shipping channel and Cedar Bayou (Chen 2010). The average salinity in Copano Bay is 10.9, and in Aransas Bay is 16.4 (Longley 1994). A substantial exchange of water between Aransas Bay and the Gulf of Mexico occurs from wind driven tides (Ward and Armstrong 1997). The benthic habitat consists of seagrass beds of *H. wrightii* oyster reefs of *Crassostrea virginica*, salt marsh of *Spartina alterniflora*, and sandy bottom mixed with clay and silt (Froeschke et al. 2013). Phytoplankton composition in Aransas Bay and Copano Bay remained uniform in a study by Holland et al. (1975) who found primarily diatoms

(*Coscinodiscus* sp. and *Rhizosolenia alata*), dinoflagellates, and green algae (Freese 1952; Holland et al. 1975). With the exception of the copepod *Acartia tonsa*, zooplankton varied by bay based on species composition and abundance and by season (Matthews et al. 1974).

Sampling

TPWD utilizes gill nets for fisheries-independent monitoring of finfish communities using a random sampling protocol. Juvenile and sub-adult red drum were collected during November 2016 and from April to June of 2017 using standardized sampling gill nets (182.9 m long, 1.2 m deep, separated into 45.7 m sections of 7.6-,10.2-,12.7- and 15.2-cm monofilament meshes) in the Nueces and Mission-Aransas Estuaries (Figure 1; Osburn 1987). Gill nets were set one hour before sunset and collected the following day at sunrise. Spatial and temporal data (sample location and time, depth, turbidity, dissolved oxygen, water temperature, salinity, weather conditions, species caught, and number of species caught) were recorded upon collection. Red drum were placed on ice and transported to lab. Samples were either immediately processed or frozen for later processing at -20 ºC.

Sample Processing

Frozen fish were thawed, rinsed, and stored on ice during processing. Total length, standard length, and wet weight data was recorded. Gut contents were weighed and stored in 190 proof ethanol for identification.

Stable Isotope Analysis

A left epaxial muscle sample was removed using a scalpel and frozen at -20 ºC until further processing. Samples were dried at 60 ºC in a drying oven for 48-72 hours, ground to a fine powder using a mortar and pestle and stored in plastic vials. Approximately 1.0 mg of dried ground muscle was rolled into tin capsules at the University of Texas Marine Science Institute Core Isotope Facility in Port Aransas, Texas. Samples were analyzed using a Carlo Erba NC2500 elemental analyzer connected to a Thermo Fisher Scientific Delta V Plus isotope-ratio-mass-spectrometer. The isotope results are presented using the conventional δ-notation:

$$\delta^{13}C\ (or\ \delta^{15}N) = \left[\frac{R_{sample}}{R_{standard}} - 1\right]\ (in\ ‰)$$

where R_{sample} and $R_{standard}$ = $^{13}C/^{12}C$ (or $^{15}N/^{14}N$) of the unknown sample and the certified reference material, respectively. All δ-values are reported relative to VPDB for carbon and AIR for nitrogen, unless otherwise stated (Coplen 1996). A two-point calibration of $\delta^{13}C$ to VPDB and to $\delta^{15}N$ to AIR was achieved using certified reference materials USGS-40 and USGS-41a.

For USGS-40, the standard deviation (SD) for $\delta^{13}C$ was 0.06‰ (n = 22) and for $\delta^{15}N$ 0.07‰ (n = 22), both within 1 SD of the known value ($\delta^{13}C$ = -26.39‰ and $\delta^{15}N$ = -4.52‰). For USGS-41a, the SD for $\delta^{13}C$ was 0.07‰ (n = 22) and for $\delta^{15}N$ 0.07‰ (n = 22), both within 1 SD of the known value ($\delta^{13}C$ = 36.55‰ and $\delta^{15}N$ = 47.55‰).

A replicate sample was included at least once every 20th sample to assess precision. The mean standard deviation of 19 replicates was 0.14‰ for $\delta^{13}C$ and 0.03‰ for $\delta^{15}N$ values. An internal laboratory Peach Leaf standard was used to evaluate the accuracy and precision of the carbon (-26.2 ± 0.1‰ (SD, n = 12)) and nitrogen (1.53 ± 0.1‰ (SD, n = 5)) isotope results.

An estimate of the rate of change in isotopic composition of red drum muscle tissue after a dietary shift was made using isotope turnover and discrimination factors for the Atlantic croaker (*Micropogonias undulatus*), a species also in the family Sciaenidae, found in a controlled diet switch experiment (Mohan et al. 2016).

Otolith Processing

Sagittal otoliths were extracted, rinsed in deionized water to remove excess tissue, and stored in plastic vials to dry. A left or right sagittal otolith was randomly selected and embedded in EpoxiCure Epoxy Resin mixed with EpoxiCure Epoxy Hardener spiked with indium in an 8:2 ratio. Embedded otoliths were allowed to dry for at least 24 hours, and then cut along their transverse plane using a Buehler Isomet Low Speed Saw into 1 mm sections. Sectioned otoliths were mounted onto petrographic slides using CrystalBond 509 and polished using 30-micron aluminum oxide lapping film followed by 3-micron aluminum oxide lapping film until the surface was uniformly smooth and the core was in view. Polished otolith sections were removed from the petrographic slide and remounted onto a new slide (12 otoliths per slide) for chemical analysis.

Otoliths were analyzed for elemental concentrations of ^{43}Ca, ^{24}Mg, ^{25}Mg, ^{55}Mn, ^{88}Sr, ^{115}In, and ^{138}Ba at the Jackson School for Geosciences at the University of Texas Austin using an

Agilent 7500ce quadrupole ICP-MS coupled to a 193-nm New Wave UP-193FX laser system. Otolith section slides were loaded into the laser and prepped for ablation using imaging software to designate analysis tracks and adjust focus. Transects began at the otolith core and followed a path towards the edge along the longer axis. Analysis tracks were pre-ablated at 80% power and 10Hz using a 75 μm spot at 50 μm/s to reduce surface contamination (Table 1a). Otolith sections were then ablated from core to edge of the otolith at 80% power and 10Hz using a 35 μm spot at 15 μm/s for all runs (Table 1b). Blocks of 8-10 otoliths were bracketed by certified standards (NIST 612 glass for instrument drift and analytical precision and MACS-3 calcium carbonate to convert raw intensity counts to concentrations). Estimates of analytical precisions, accuracies and limits of detection were calculated from repeated measurements (n = 39) of the NIST 612 standard interspersed across the three days of analysis, after correction against MACS-3. For ^{88}Sr, the average limit of detection (LOD) was 9.2 ppb, recovery was 100.5% and residual standard deviation (RSD) was 3.6%. For ^{138}Ba, LOD was 9.4 ppb, recovery was 104.4% and RSD was 11.3%. Beginning and ending positions for analysis were determined using elemental intensity counts of ^{43}Ca and ^{115}In. After, elemental intensity counts of ^{137}Ba and ^{43}Ca were averaged and smoothed using a 7-point running mean, converted from parts per million to moles to Ba:Ca and Sr:Ca molar ratios (using the sagittal otolith reference material FEBS-1 certified quantity value of 38.3 wt% assumed for calcium). These molar ratios were then graphed against distance along the otolith from core to edge.

Otolith Aging

Otoliths were photographed and aged using the procedure described in Campana (1992) using a Zeiss Discovery V8 Stereo microscope and ZEN 2.3 (Blue Edition) software. Opaque

bands were counted as yearly increments (Wenner 1992). If no opaque bands were present, the individual was determined to be <1 year of age.

Determination of Partition Coefficients

Partition coefficients were calculated and used to determine threshold elemental ratios in otoliths corresponding to movements into low salinity (salinities < 5) environments. This allowed for interpretation of potential low salinity habitat use based on otolith chemistry life history transects.

The partition coefficient (*D*) was calculated using the following equation:

$$D_{[element]} = \frac{element{:}\,Ca_{otolith}}{element{:}\,Ca_{water}}$$

where $[element{:}Ca]_{otolith}$ was calculated using average Sr:Ca and Ba:Ca values for one-year-old red drum reared in control conditions at the University of Texas Marine Science Institute with fully marine water sourced from the ship channel at Port Aransas, Texas (average otolith Sr:Ca = 3.27 and Ba:Ca = 6.99; Woodcock and Walther 2014; Woodcock et al. 2013).

The $[element{:}Ca]_{water}$ parameter was calculated using the following regional equations relating salinity to elemental ratios derived from extensive field sampling of water compositions across the coast of Texas by Mohan and Walther (2015):

$$Sr{:}\,Ca\ mmol/mol\ =\ 0.033x\ +\ 6.99$$

$$Ba{:}\,Ca\ \mu mol/mol\ =\ -3.21x\ +\ 175$$

where x is the salinity of water. A salinity of 35 was used to represent seawater for this purpose.

Once the partition coefficients were calculated using values for local marine waters and experimentally reared fish, they were used to estimate expected otolith chemistry values for fish inhabiting low salinity habitats. Water values for Sr:Ca and Ba:Ca in local streams and rivers were measured by Walther and Nims (2015) and used here for this purpose. The mean elemental ratios for freshwater sources feeding into the Nueces and Mission-Aransas estuaries were calculated for Sr:Ca and Ba:Ca values by averaging across water samples (salinities < 5) taken from the Guadalupe, San Antonio, Mission, Aransas, and Nueces Rivers and Oso Creek. In addition, given that water chemistry was variable among rivers, alternative otolith chemistry thresholds were calculated using either low (minus one standard deviation of average river water elemental ratios) and high (plus one standard deviation) thresholds water chemistry values. These three threshold values were used to account for chemical variability among streams and thus determine how sensitive determinations of movement into low salinity habitats were to the specific choice of a given threshold.

Otolith Transect Analysis

Otolith run data were separated into Excel files for each individual. Run data included time, ^{43}Ca (CPS), ^{24}Mg (ppm), ^{25}Mg (ppm), ^{55}Mn (ppm), ^{88}Sr (ppm), ^{115}In (CPS), and ^{138}Ba (ppm). The starting and ending position for each transect was located and graphs were truncated

using ^{43}Ca, and ^{115}In intensities. This was possible because Ca intensities were high when the laser spot completely ablated otolith material and Ca intensities dropped and In intensities rose when the laser spot moved off the otolith and began ablating the surrounding spiked epoxy. Using the truncated transects, a 7-point running mean was calculated for ^{88}Sr and ^{138}Ba to remove high frequency variation that reflected instrumental noise. Using the smoothed values, ^{88}Sr in parts per million units were converted to moles, ratioed to Ca, and converted to mmol/mol assuming a constant Ca concentration in the otolith of 38.3% by weight. ^{138}Ba in parts per million units were converted to moles, ratioed to Ca, and converted to μmol/mol. Sr:Ca and Ba:Ca ratios were graphed against distance to qualitatively observe patterns. The Excel function "IF" was then used with low, mean, and high threshold values for Sr and Ba to designate a "Pass/Fail" assignment for each value of Sr:Ca and Ba:Ca within individual transects. A "Pass" assignment for a data point was indicative of low salinity movement while a "Fail" assignment represented estuarine or marine use. Percent "Pass" for each threshold and ratio was calculated and graphed as a histogram.

Combined Stable Isotope and Otolith Approach

To determine if a relationship between muscle tissue δ^{13}C and otolith Sr:Ca and Ba:Ca values existed, Sr:Ca and Ba:Ca ratios were averaged for the exterior 250, 500, and 1000 μm sections of each individual otolith representing the most recently accreted material prior to capture. These three distances were chosen given the potential for variability in otolith accretion rates and therefore uncertainty about how much material in the otolith represented comparable periods of time required for equilibration of muscle tissue isotopes as determined by Mohan et al. (2016). However, each distance could constitute varying amounts of time integration depending

on growth rates. Growth rates for red drum are affected by both age and temperature, so care must be taken during interpretation to account for increased growth rates of younger individuals and during warmer months (Porch et al. 2002). Linear regressions were calculated comparing mean elemental values of Sr:Ca and Ba:Ca to $\delta^{13}C$ values for individual fish, with separate regressions calculated for each of the three exterior distance intervals.

RESULTS

Physical Characteristics

A total of 201 wild individuals were collected from bays within the Mission-Aransas (n = 113) and Nueces (n = 88) estuaries and analyzed for stable isotope analysis. Of these, a representative sub-set of 99 fish were analyzed for otolith chemistry composition. The majority of individuals aged and used for laser ablation analyses were age-1 fish and the remainder were either age-0 or age-2 (Table 2). Fish collected from the Mission-Aransas estuary ranged in total length from 335.0 to 719.0 mm with a mean of 423.5 ± 68.3 mm. Wet weight ranged from 375.0 to 3875.0 g with a mean of 823.0 ± 468.9 g. Fish collected from the Nueces estuary ranged in total length from 303.0 to 628.0 mm with a mean of 421.1 ± 77.3 mm. Wet weight ranged from 271.0 to 2580.0 g with a mean of 831.5 ± 487.6 g (Table 3). Water temperature and salinity at time of collection ranged from 21.8 to 29.2 °C and 7.7 to 31.7. Fish sampled in this study were <3 years of age with the earliest capture date of November 2016 and the most recent capture date of June 2017. Using USGS Surface Water Annual Statistics, 2013 and 2014 showed discharges lower than 2015, followed by an increase in 2015, followed by a decrease in 2016 and 2017 (https://txpub.usgs.gov/txwaterdashboard/index.html). A pulse in freshwater flow could temporarily mask the chemical signature of the estuary with a more riverine signature and is important to note while interpreting otoliths.

Stable Isotope Analysis

Isotope ratios were checked against biometric and chemical metrics to ensure that ontogeny or tissue composition alone were not the primary drivers of variability in isotope signatures.

Linear regressions were calculated comparing $\delta^{13}C$ and $\delta^{15}N$ values with C:N ratios (indicative of lipid content which could bias isotope signatures) and total length and wet weight (as a proxy for size and age). No significant relationship was found between $\delta^{13}C$ and $\delta^{15}N$ values and C:N ratios ($p = 0.485$ and $p = 0.141$), therefore no lipid correction was necessary (Vander Zanden and Rasmussen 2001; DeNiro and Epstein 1977; Post et al. 2007). There were significant relationships between $\delta^{13}C$ values and total length ($p = <0.001$) and wet weight ($p = <0.001$), however both variables show low adjusted R-squared (AR^2) values which each explain less than 12% of the $\delta^{13}C$ value ($AR^2 = 0.11$ for length and $AR^2 = 0.12$ for mass). There were also significant relationships between $\delta^{15}N$ values and total length ($p = 0.002$) and wet weight ($p = 0.006$), however the low AR^2 values each explain less than 8% of the $\delta^{15}N$ value ($AR^2 = 0.04$ for length and $AR^2 = 0.03$ for mass). Given that length and mass explained only a minor amount of variance in isotope values, size corrections were not applied to isotope values used for subsequent analyses. While there was a statistically significant difference in $\delta^{13}C$ values between age 0 and age 1 individuals ($p = 0.027$), no significant differences were found between age 0 and age 2 individuals. In addition, age explained less than 5% of the relationship between $\delta^{13}C$ values and age 0 and age 1. No significant relationships were found between $\delta^{15}N$ values and fish of any age, further contributing to the conclusion that ontogeny was not a significant driver of observed isotope variability.

The Ward technique of hierarchical clustering analysis was used to group individuals that exhibit maximally similar values to determine innate differences in $\delta^{13}C$ and $\delta^{15}N$ isotope signatures among individuals (Ward 1963). The $\delta^{13}C$ and $\delta^{15}N$ values of all samples were ordinated and organized by similarity. Two distinct groups were identified (Group 1, $n = 130$ and Group 2,

n = 71; Figure 2). Group 1 had a mean $\delta^{13}C$ value of -17.65 ± 0.89 and a mean $\delta^{15}N$ value of 14.25 ± 1.39 while Group 2 had a mean $\delta^{13}C$ of -14.19 ± 0.68 and a mean $\delta^{15}N$ of 12.01 ± 0.89 (Table 4). Both groups were significantly different in $\delta^{13}C$ and $\delta^{15}N$ values (p = < 0.001). The isotope values for the sub-set of individuals selected from each group for otolith chemistry analyses were compared to the values for the original groups to ensure subsamples were representative of each group. No significant differences in mean isotope values were found between subsamples and their respective original group values (Figure 3).

Collection sites were grouped by bay of sampling (Aransas Bay, Copano Bay, Corpus Christi Bay, Mustang Island – Corpus Christi Bay, Mesquite Bay, and Nueces Bay). Corpus Christi Bay was further subdivided to distinguish samples taken along the bay side of Mustang Island (Table 5; Figure 4, 5, 6). Non-parametric Kruskal Wallis post hoc tests were selected due to residual heteroscedasticity. $\delta^{13}C$ values in Mesquite and Nueces Bays were significantly different from Aransas and Corpus Christi Bays, while Copano Bay overlapped with bays from both groups (Figure 7).

Assignments for $\delta^{13}C$ and $\delta^{15}N$ values of baselines and prey items across low salinity and estuarine habitats were compiled from the literature for isotopic composition data in the Nueces and Mission-Aransas estuaries (Table 6). $\delta^{13}C$ values for suspended particulate organic matter (SPOM) for this system was taken over ten months (November 2010 to August 2011) and ranged from -35.5 to -20.8‰. The average Aransas and Mission Rivers $\delta^{13}C$ values were less ^{13}C-enriched than the average $\delta^{13}C$ values of estuarine sampling stations across salinities of 5-20, 21-30, and 30+ (Lebreton et al. 2016). $\delta^{13}C$ riverine particular organic matter (POM) from the

Nueces River ranged from -28.8 to -26.3‰ (Riera et al. 2000). In the Mission-Aransas estuary, the average $\delta^{13}C$ values of *Halodule* and *Spartina* were higher than their respective epiphytes. Amphipods and isopods resembled the isotopic signatures of the marsh plant epiphytes while the plicate horn shell more closely resembled the marsh plants themselves. Crab, shrimp, and fish including sheepshead, Gulf killifish, Atlantic croaker, mullet, chain pipefish, pinfish, inland silversides, Atlantic needlefish, and naked goby had average $\delta^{13}C$ values closer to the values found in estuarine SPOM (Rezek 2017). In the Nueces estuary, Salicornia species in the Rincon Bayou mouth ranged from -27.8 to -26.3‰ and zooplankton ranged from -26.3 to -25.6‰. As expected, brown shrimp sampled in the Rincon Bayou mouth were more ^{13}C-enriched than those in the Nueces River (Riera et al. 2000).

Values of $\delta^{15}N$ for SPOM for this system ranged from 3.6 to 17.5‰. Average Aransas and Mission Rivers $\delta^{15}N$ values had greater variability than the average $\delta^{13}C$ values. Riverine POM in the Nueces River ranged from 8.8 to 10.8 (Riera et al. 2000). Estuarine sampling stations across salinities of 5-20, 21-30, and 30+ (Lebreton et al. 2016) showed decreasing averages with increasing salinity. The average $\delta^{15}N$ values of *Halodule* and *Spartina* were higher than their respective epiphytes. Amphipods, isopods, and the plicate horn shell had similar values. Crab, shrimp, and fish including sheepshead, Gulf killifish, Atlantic croaker, mullet, chain pipefish, pinfish, inland silversides, Atlantic needlefish, and naked goby showed $\delta^{15}N$ differences larger than 3.4‰, which could be representative of increasing trophic level feeding (Rezek 2017; DeNiro and Epstein 1981; Post 2002).

A muscle tissue turnover rate was estimated at $t_{95\%}$ = 129 ± 47 days for $\delta^{13}C$ and $t_{95\%}$ = 115 ± 12 days for $\delta^{15}N$ using an experimental study of Atlantic croaker (Mohan et al. 2016), but it is important to consider variability around this time scale. For example, wild Southern flounder required an average of 213.4 days to reach 95% turnover (Buchhestier and Latour 2010).

Partition Coefficients

Using values from Walther and Nims (2015), the average salinities of river water samples to our study system used to calculate partition coefficients were 1.38 ± 1.15. River samples with salinities above 5 were not included since the non-linear relationship of barium to calcium to salinity has the largest increase at low salinities. The calculated partition coefficients for D_{Sr} and D_{Ba} were 0.40 and 0.11, respectively. Low and high thresholds were estimated using plus or minus one standard deviation of the average elemental ratios across river water samples. Estimated Sr:Ca and Ba:Ca thresholds in otolith life history profiles were Sr:Ca = 2.1 mmol/mol, Ba:Ca= 39.9 µmol/mol (low threshold), Sr:Ca = 2.0 mmol/mol, Ba:Ca = 65.5 µmol/mol (mean threshold), and Sr:Ca = 2.4 mmol/mol, Ba:Ca = 106.2 µmol/mol (high threshold; Walther and Nims 2015).

First, the number of individuals which showed low salinity movement were counted using each threshold. Using the low, mean, and high Sr:Ca thresholds, 99%-100% of sampled individuals exhibited low salinity occupancy at some point in their individual transects (n = 98, 99, and 99, respectively). Comparatively, 35% of sampled individuals exhibited low salinity occupancy at some point in their transects using the low Ba:Ca threshold (n = 35), which decreased to 2% of individuals when using mean or high Ba:Ca thresholds (n= 2 and 2, respectively). The

narrow degree of difference between low salinity and marine values of Sr in south Texas systems may account for the disparity in estimates. The percent of each transect that crossed the low, mean, and high salinity thresholds for each individual was calculated using the "IF" function in Excel and graphed. Low Sr:Ca had a range of 0 to 89% and a mean of 19%, mean Sr:Ca had a range of 28 to 100% and a mean of 63%, and high Sr:Ca had a range of 59 to 100% and a mean of 89%. Low Ba:Ca had a range of 0 to 37% and a mean of 2%, mean Ba:Ca had a range of 0 to 3% and a mean of .0004%, and high Ba:Ca had a range of 0 to 0.01% and a mean of .0002% (Figure 9a and 9b).

The average elemental ratios across the exterior 250, 500, and 1000 μm sections of otolith transects were correlated with $\delta^{13}C$ values for individual fish to determine if elemental and isotope ratios were significantly correlated, as would be expected if isotope values depended on recently inhabited salinity regimes. Ba:Ca ratios were not statistically significant for any distance. Although Sr:Ca was significant at both 500 μm ($p = 0.019$) and 1000 μm ($p = 0.001$), the AR^2 was only 5% and 9%. These results indicated that differences in isotope values among and within groups were not primarily driven by variable salinity experiences in the few months prior to capture.

DISCUSSION

This project was an attempt to detect movement of red drum from the estuary into low salinity habitats by using otolith chemistry and stable isotope analysis of muscle tissue. Stable isotope analysis indicated that there are distinct groups among the red drum sample as seen by significant differences in $\delta^{13}C$ and $\delta^{15}N$ means for clusters defined by Ward's Hierarchical clustering analysis. In addition, otolith microchemistry revealed individually variable instances of residence in low salinity habitat based on Ba:Ca thresholds applied to life history graphs. However, most otolith chemistry thresholds used indicated that low salinity residence was not common.

Stable isotope composition was significantly different between the two groups present in this system. The first group was characterized by lower $\delta^{13}C$ values and higher $\delta^{15}N$ than the second group. Based on $\delta^{13}C$ and $\delta^{15}N$ trends with salinity in this region, it was initially hypothesized that the first group represented individuals feeding in or on prey items from low salinity habitats and the second group represented estuarine feeders (Bishop et al. 2017). However, once groups were spatially analyzed, differences in stable isotope signatures are more likely explained by individual residency within local bays with unique stable isotope baselines.

Evidence of individuals with otolith chemistry life history transects indicating low salinity movement was found using both Ba:Ca and Sr:Ca thresholds. Although Sr:Ca ratios indicated almost 100% of individuals experienced low salinity, this tracer is less trustworthy for assigning salinity histories for fish moving into Texas rivers given the high Sr content in freshwaters in the

region. Thus, the results based on Ba:Ca ratios are likely a more robust estimation of true movement histories. In addition, the lack of correlations between tissue isotopes and otolith exterior elemental ratios further indicated that major movements across salinity gradients were infrequent and not responsible for differences in isotope niche occupancy. Together, this work supports the conclusion that post settlement red drum have high rates of fidelity to individual bays and only rarely make excursions into low salinity habitats.

Stable Isotopes

Because of the random sampling protocol for gill net setting employed by Texas Parks and Wildlife, red drum samples represented multiple major and minor bays throughout the Mission-Aransas and Nueces estuaries. Numerous tagging studies have confirmed that red drum in Texas estuaries show evidence of strong site fidelity (Osburn et al. 1982; Simmons and Breuer 1962; Moulton et al. 2017). Additionally, schools of juvenile red drum tend to swim together and revisit specific sites over the course of several months, increasing the likelihood of similar isotopic signatures between individuals captured in the same bay area (Osburn et al. 1982). Because red drum juveniles tend to stay in or revisit similar locations together for several weeks, the physical and chemical characteristics of each sampling location is likely the primary cause for isotopic differences between individuals (Osburn et al. 1982).

Geographically, all Texas estuaries share commonalities such as barrier islands that run parallel to the shorelines and lagoons that are cut by river valleys that produce estuarine systems (Montagna and Kalke 1995). However, salinity regimes differ between and within estuaries due to north to south decreases in average annual precipitation, relative amount of freshwater inflow

to bay size, and proximity to river inflows (Montagna and Kalke 1995). Known relationships between $\delta^{13}C$ and $\delta^{15}N$ and salinity in this region can be used to help with stable isotope interpretation. The first group (Group 1) identified by Ward's Hierarchical clustering analysis was primarily composed of individuals from Mesquite Bay (97.4%) and Nueces Bay (97.4%). The second group (Group 2) was primarily composed of individuals from Corpus Christi Bay – Mustang Island (100%), Aransas Bay (97.3%), Corpus Christi Bay (95.2%), and Copano Bay (53.6%). Thus, capture location was strongly predictive of observed differences in muscle stable isotope values. This result suggested that fish had been resident in their capture locations for long enough to equilibrate with their local food webs, which varied with distance from freshwater inputs.

The capture locations differed geographically and whether bays were primary or secondary, and thus had differing degrees of influence of freshwater inputs from creeks and rivers. Mesquite Bay exchanges water with San Antonio Bay (within the Guadalupe estuary) which receives higher annual freshwater inflows than the Mission-Aransas estuary (Texas Department of Water Resources 1982), perhaps accounting for the lower mean $\delta^{13}C$ values found in individuals sampled in that location. Additionally, Mesquite Bay is lower in overall seagrass cover (583 acres), a ^{13}C enriched food web base ($\delta^{13}C$ = -10.0 to 12.0‰), than bays such as Aransas Bay (3,277 acres) and may reflect organic matter derived from phytoplankton ($\delta^{13}C$ = -19.0 to 21.0‰; Handley et al. 2007; Rooker et al. 2010). Nueces Bay is a secondary bay within the Nueces estuary, and unsurprisingly, individuals had lower $\delta^{13}C$ values indicative of a terrestrial carbon source supplied by the Nueces River. Corpus Christi and Aransas Bay varied little in $\delta^{13}C$, although $\delta^{15}N$ was slightly higher in Aransas Bay. High $\delta^{15}N$ values from anthropogenic contributions

(wastewater inputs, agricultural runoff) are seen in the Aransas River during periods of low flow but do not show a significant effect on particulate organic nitrogen (PON) in Copano Bay (Mooney and McClelland 2012). Therefore, differences may be attributed to the trophic influence of prey items. Finally, the variability in $\delta^{13}C$ (-21.3 to -13.3‰) within Copano Bay could be attributed to sampling that occurred in two locations, once at the mouth of the Aransas River and once at the mouth of Copano Creek. Individuals feeding in a food web sourced from SPOM supplied by the Aransas River ($\delta^{13}C$ = -30.8 ± 3.2‰) would likely show lower $\delta^{13}C$ values than individuals feeding near the mouth of Copano Creek, which is supported by sampling location data (Lebreton et al. 2016).

Next, a $\delta^{13}C$ and $\delta^{15}N$ biplot was graphed using values of SPOM, primary producers, and consumers within the estuaries to compare with Group 1 and Group 2 means (Figure 8; Lebreton et al. 2016; Rezek 2017). Because mean $\delta^{13}C$ values more closely matched SPOM $\delta^{13}C$ values for Aransas Bay (range: -23.5 to -20.8‰, mean of -22.3‰ ± 0.8) than for the Mission and Aransas Rivers (range: -35.5 to -27.7‰, mean: -30.7‰ ± 2.9), both red drum groups more likely had estuarine diets contributing to their stable isotope signatures (Lebreton et al. 2016). Additionally, a fractionation of ~1‰ in $\delta^{13}C$ and 3.4‰ in $\delta^{15}N$ from the isotopic signatures of potential prey items (i.e. amphipods, crabs, and shrimp) and mean $\delta^{15}N$ values ($\delta^{15}N$ = 14.3‰ ± 1.4 and 12.0‰ ± .8) consistent with other estuarine consumer isotope compositions such as the naked goby and Atlantic croaker was seen for both groups (Rezek 2017). However, the generalized diet of red drum can result in signatures that are challenging to directly assign to particular prey items (Scharf and Schlicht 2000). For instance, prey can migrate between the estuarine and low salinity and therefore imprint a riverine signature into the tissues of consumers, it is possible that

individuals in Group 1 reflect a ~1‰ offset in the $\delta^{13}C$ values associated with brown shrimp that had inhabited or were inhabiting the Nueces River (Riera et al. 2000).

Otoliths

The present study examined the full life history of Sr:Ca and Ba:Ca ratios in otoliths to predict the relative frequency of low salinity movement an individual experienced. For each elemental ratio, the mean threshold value was interpreted in conjunction with low and high thresholds to account for the variability of low salinity end-member signatures in this region. The low, mean, and high Sr:Ca thresholds predicted low salinity movement by nearly all individuals while the low, mean, and high Ba:Ca thresholds predicted far fewer individuals moving into low salinity at some point during their lives. In terms of frequency, the mean Sr:Ca threshold indicated that individuals spent between 28% to 100% of their life history profiles in low salinity. Conversely, the mean Ba:Ca threshold indicated that individuals spent 0% to 1% of their life history profiles in low salinity. However, using the low Ba:Ca threshold, individual use of low salinity increased to 37%. While both Sr:Ca and Ba:Ca suggest movement into low salinity, the proportion of the study sample varies greatly depending on which ratio is used. In these south Texas systems, Sr:Ca values can approach the marine value due to watersheds that drain over bedrock containing marine derived carbonates that are high in Sr. The resulting difference between end-members is 3.54 to 4.04 mmol/mol, and makes it a less reliable proxy for salinity than Ba:Ca.

It is possible that estimates of low salinity movement in this study fall short of actual movement events. Brief (<24 hours) movements may not be recorded in the otolith due to limitations in LA-ICPMS methodology to obtain enough newly synthesized material to analyze chemically novel environments. However, results seen from these wild captured individuals do illustrate predominant trends in salinity shifts over their entire life history. Also, the relative amounts of trace elements within the tidal creeks and rivers in our study system cause substantial variability around our average threshold estimate and should be taken into consideration when interpreting thresholds. Low Ba:Ca thresholds may better represent systems with lower dissolved Ba concentrations, such as Oso Creek. Using this tributary alone, the Ba:Ca partition coefficient decreases to over half of the average of all six rivers and creeks. Conversely, using the tributary with the highest Ba:Ca ratio results in a Ba:Ca partition coefficient of almost twice the average of all tributaries.

The lack of significance and/or low AR^2 values between average Ba:Ca and Sr:Ca ratios for each of the exterior 250, 500, and 1000 µm sections and $\delta^{13}C$ values indicates that the stable isotope diet groups are unlikely related to low salinity movements (Figure 10a and 10b). Red drum do not appear to use low salinity with as high frequency as compared with other species in the estuary such as southern flounder, but still show differences in overall life history profiles indicative that at least some individuals visit tidal creeks and rivers at some point during their lives (Nims and Walther 2014).

Implications for Stock Enhancement and Recreational Fishing

Delineating EFH became a federally mandated provision for fisheries management councils after the 1996 Sustainable Fisheries Act recognized that one of the greatest threats to sustainable fisheries was the continued loss of aquatic habitats. Because of limited resources for designating Essential Fish Habitat, approaches for determining the most valuable habitats have been explored (Beck et al. 2001). In a study of best management practices, it was recommended that habitat used by larval and juvenile stages should be given conservation priority (Levin and Stunz 2005). This life history period coincides with their time in the estuary. Nutrient subsidies and freshwater inflow clearly provide habitat to red drum inhabiting secondary bays, and if a small proportion of red drum are using rivers and tidal creeks as habitat or feeding groups, it then becomes important to consider those areas when prioritizing habitat for management. Even if red drum are simply transients within those regions, there is still ecological justification to consider the complete habitat use of this species throughout its life history.

CONCLUSION

The present study suggests that differences in $\delta^{13}C$ and $\delta^{15}N$ values of red drum muscle tissue that exist in the Mission-Aransas and Nueces estuaries are driven by individual residency within bays with unique isotopic compositions. Secondary bays that receive more freshwater inflow from tributaries exhibit food webs with lower $\delta^{13}C$ values than primary bays and Mesquite Bay exchanges water with the Guadalupe estuary that receives higher precipitation and freshwater inflow from Guadalupe and San Antonio Rivers. Both situations are most likely explained by salinity. Differences in $\delta^{15}N$ values may be best explained by a combination of salinity and androgenic inputs. Although red drum have the physiological capacity for movement into low salinity habitats, it does not appear that individuals are entering or feeding in those habitats often, as seen by a majority of Ba:Ca values representative of estuarine salinities in otoliths and $\delta^{13}C$ and $\delta^{15}N$ values that more closely resemble estuarine prey items.

Still, groups of red drum with similar stable isotope signatures were caught near the mouths of tributaries in secondary bays and could feed on prey items that use low salinity. Also, knowledge that at least a small proportion of individuals show low salinity movement could be helpful for understanding red drum behavior during periods of drought. Therefore, it is still important to consider the flow of nutrients and energy and physical boundaries between freshwater and the estuaries in red drum management.

REFERENCES

Able, K. W. 2005. A re-examination of fish estuarine dependence: evidence for connectivity between estuarine and ocean habitats. Estuarine, Coastal and Shelf Science, 64(1), 5-17.

Adams, D. H., & Tremain, D. M. 2000. Association of large juvenile red drum, *Sciaenops ocellatus,* with an estuarine creek on the Atlantic coast of Florida. Environmental Biology of Fishes, 58(2), 183-194.

Albuquerque, C. Q., Miekeley, N., Muelbert, J. H., Walther, B. D., & Jaureguizar, A. J. 2012. Estuarine dependency in a marine fish evaluated with otolith chemistry. Marine Biology, 159(10), 2229-2239.

Ambrose, R.F. & Swarbrick, S.L. 1989. Comparison of fish assemblages on artificial and natural reefs off the coast of southern California. Bulletin of Marine Science, 44(2), 718-733.

Bacheler, N. M., Paramore, L. M., Buckel, J. A., & Scharf, F. S. 2008. Recruitment of juvenile red drum in North Carolina: spatiotemporal patterns of year-class strength and validation of a seine survey. North American Journal of Fisheries Management, 28(4), 1086-1098.

Bath, G. E., Thorrold, S. R., Jones, C. M., Campana, S. E., McLaren, J. W., & Lam, J. W. 2000. Strontium and barium uptake in aragonitic otoliths of marine fish. Geochimica et Cosmochimica Acta, 64(10), 1705-1714.

Beck, M. W., Heck Jr, K. L., Able, K. W., Childers, D. L., Eggleston, D. B., Gillanders, B. M., & Orth, R. J. 2001. The identification, conservation, and management of estuarine and marine nurseries for fish and invertebrates: a better understanding of the habitats that serve as nurseries for marine species and the factors that create site-specific variability in nursery quality will improve conservation and management of these areas. Bioscience, 51(8), 633-641.

Bengston, S., Blankinship, R., & Bonds, C. 2003. Texas Parks and Wildlife Department History 1963-2003. Retrieved from Texas Parks and Wildlife website: http://tpwd.texas.gov/about/history. Accessed January 20, 2018.

Bernat, M., Church, T., & Allegre, C. J. 1972. Barium and strontium concentrations in Pacific and Mediterranean Sea water profiles by direct isotope dilution mass spectrometry. Earth and Planetary Science Letters, 16(1), 75-80.

Bighash, P., & Murgulet, D. 2015. Application of factor analysis and electrical resistivity to understand groundwater contributions to coastal embayments in semi-arid and hypersaline coastal settings. Science of The Total Environment, 532, 688-701.

Bishop, K. A., McClelland, J. W., & Dunton, K. H. 2017. Freshwater contributions and nitrogen sources in a south Texas estuarine ecosystem: a time-integrated perspective from stable isotopic ratios in the eastern oyster (*Crassostrea virginica*). Estuaries and Coasts, 40(5), 1314-1324.

Bonner, T., & Duke, J. 2015. Guadalupe, San Antonio, Mission, and Aransas Rivers and Mission, Copano, Aransas, and San Antonio Bays Basin. Retrieved from: https://www.tceq.texas.gov/permitting/water_rights/wr.../guadalupe-sanantonio-bbsc. Accessed January 20, 2018.

Bourgeois M., Marx J., & Semon K. 2014. Louisiana Blue Crab Fishery Management Plan. Retrieved from: http://www.wlf.louisiana.gov/fishing/fishery-management-plans-marine. Accessed January 20, 2018.

Bowes, R. E., & Thorp, J. H. 2015. Consequences of employing amino acid vs. bulk-tissue, stable isotope analysis: a laboratory trophic position experiment. Ecosphere, 6(1), 1-12.

Boyd, I.L. 2004. Migration of Marine Mammals. *In:* Biological Resources and Migration. Springer, Berlin, Heidelberg, pp. 203-210.

Brown, R. J., & Severin, K. P. 2009. Otolith chemistry analyses indicate that water Sr:Ca is the primary factor influencing otolith Sr:Ca for freshwater and diadromous fish but not for marine fish. Canadian Journal of Fisheries and Aquatic Sciences, 66(10), 1790-1808.

Buchheister, A., & Latour, R. J. 2010. Turnover and fractionation of carbon and nitrogen stable isotopes in tissues of a migratory coastal predator, summer flounder (*Paralichthys dentatus*). Canadian Journal of Fisheries and Aquatic Sciences, 67(3), 445-461.

Campana, S. E. 1992. Measurement and interpretation of the microstructure of fish otoliths. Canadian Special Publication of Fisheries and Aquatic Sciences, 117, 59-71.

Campana, S. E. 1999. Chemistry and composition of fish otoliths: pathways, mechanisms and applications. Marine Ecology Progress Series, 263-297.

Campana, S. E., & Jones, C. M. 1992. Analysis of otolith microstructure data. Otolith microstructure examination and analysis. Canadian Special Publication of Fisheries and Aquatic Sciences, 117, 73-100.

Campana, S. E., & Neilson, J. D. 1985. Microstructure of fish otoliths. Canadian Journal of Fisheries and Aquatic Sciences, 42(5), 1014-1032.

Campana, S.E., Chouinard, G.A., Hanson, J.M., Frechet, A., & Brattey, J. 2000. Otolith elemental fingerprints as biological tracers of fish stocks. Fisheries Research, 46(1), 343-357.

Chandler, C., Knox, J., & Byrd, L. 1981. Nueces and Mission-Aransas estuaries; a study of influence of freshwater inflows. Limited Publication, 108. Texas Department of Water Resources, Austin, Texas, 362 pp.

Characklis, G., and M. Wiesner. 1997. Particles, metals, and water quality in runoff from large urban watershed. Journal of Environmental Engineering, 123, 753–759.

Chen, G.F. 2010. Freshwater Inflow Recommendations for the Mission-Aransas Estuarine System. Texas Parks and Wildlife Department, Austin, TX. 120 pp.

Clark, J. 1968. Seasonal movements of striped bass contingents of Long Island Sound and the New York Bight. Transactions of the American Fisheries Society, 97(4), 320-343.

Coffey, M., Dehairs, F., Collette, O., Luther, G., Church, T., & Jickells, T. 1997. The behaviour of dissolved barium in estuaries. Estuarine, Coastal and Shelf Science, 45(1), 113-121.

Comyns, B.H., Lyczkowski-Shultz, J., Nieland, D.L., Wilson, C.A. 1991. Reproduction of red drum, *Sciaenops ocellatus*, in the northcentral Gulf of Mexico: seasonality and spawner biomass. NOAA Technical Report NMFS, 95, 17–26.

Copeland, B. J. 1966. Effects of decreased river flow on estuarine ecology. Journal (Water Pollution Control Federation), 38(11), 1831-1839.

Coplen, T. B. 1996. New guidelines for reporting stable hydrogen, carbon, and oxygen isotope-ratio data. Geochimica et Cosmochimica Acta, 60, 3359.

Crocker, P. A., Arnold, C. R., DeBoer, J. A., & Holt, G. J. 1983. Blood osmolality shift in juvenile red drum, *Sciaenops ocellatus* L. exposed to fresh water. Journal of Fish Biology, 23(3), 315-319.

Crocker, P. A., Arnold, C. R., Holt, J. D., & DeBoer, J. A. 1981. Preliminary evaluation of survival and growth of juvenile red drum (*Sciaenops ocellata*) in fresh and salt water. Journal of the World Aquaculture Society, 12(1), 122-134.

Dance, M. A., & Rooker, J. R. 2016. Stage-specific variability in habitat associations of juvenile red drum across a latitudinal gradient. Marine Ecology Progress Series, 557, 221-235.

DiMaria, R. A., Miller, J. A., & Hurst, T. P. 2010. Temperature and growth effects on otolith elemental chemistry of larval Pacific cod, *Gadus macrocephalus*. Environmental Biology of Fishes, 89(3-4), 453-462.

de Villiers, S. 1999. Seawater strontium and Sr/Ca variability in the Atlantic and Pacific oceans. Earth and Planetary Science Letters, 171, 623–634.

DeNiro, M. J., & Epstein, S. 1977. Mechanism of carbon isotope fractionation associated with lipid synthesis. Science, 197(4300), 261-263.

DeNiro, M. J., & Epstein, S. 1981. Influence of diet on the distribution of nitrogen isotopes in animals. Geochimica et Cosmochimica Acta, 45(3), 341-351.

Dittman, A. & Quinn, T. 1996. Homing in Pacific Salmon: mechanisms and ecological basis. Journal of Experimental Biology, 199(1), 83-91.

Dunham, J., Baxter, C., Fausch, K., Fredenberg, W., Kitano, S., Koizumi, I., & Stanford, J. 2008. Evolution, ecology, and conservation of Dolly Varden, white spotted char, and bull trout. Fisheries, 33(11), 537-550.

Dunton, K. H., Hardegree, B., & Whitledge, T. E. 2001. Response of estuarine marsh vegetation to interannual variations in precipitation. Estuaries and Coasts, 24(6), 851-861.

Eldridge, P. M., Cifuentes, L. A., & Kaldy, J. E. 2005. Development of a stable-isotope constraint system for estuarine food-web models. Marine Ecology Progress Series, 303, 73-90.

Esbaugh, A. J., & Cutler, B. 2016. Intestinal Na^+, K^+, $2Cl^-$ cotransporter 2 plays a crucial role in hyperosmotic transitions of a euryhaline teleost. Physiological Reports, 4(22), e13028.

Evans, A., Madden, K., & Morehead, S.P. 2012. The Ecology and Sociology of the Mission-Aransas Estuary: An Estuarine and Watershed Profile. University of Texas Marine Science Institute, Port Aransas, Texas, 183 pp.

Freese, L.R. 1952. Marine diatoms of the Rockport, Texas, Bay area. Texas Journal of Science, 4, 331-386.

Froeschke, B. F., Stunz, G. W., Robillard, M. M. R., Williams, J., & Froeschke, J. T. 2013. A modeling and field approach to identify essential fish habitat for juvenile Bay Whiff (*Citharichthys spilopterus*) and Southern Flounder (*Paralichthys lethostigma*) within the Aransas Bay complex, TX. Estuaries and Coasts, 36(5), 881-892.

Fry, B. 1983. Fish and shrimp migrations in the northern Gulf of Mexico analyzed using stable C, N, and S isotope ratios. Fishery Bulletin, 81, 789- 801.

Fry, B. 1999. Using stable isotopes to monitor watershed influences on aquatic trophodynamics. Canadian Journal of Fisheries and Aquatic Sciences, 56(11), 2167-2171.

Fry, B. 2002. Conservative mixing of stable isotopes across estuarine salinity gradients: a conceptual framework for monitoring watershed influences on downstream fisheries production. Estuaries, 25(2), 264-271.

Fry, B. 2006. Stable Isotope Ecology. Springer-Verlag New York.

Godderis, Y., & Veizer, J. 2000. Tectonic control of chemical and isotopic composition of ancient oceans; the impact of continental growth. American Journal of Science, 300(5), 434-461.

Gold, J. R., Richardson, L. R., & Turner, T. F. 1999. Temporal stability and spatial divergence of mitochondrial DNA haplotype frequencies in red drum (*Sciaenops ocellatus)* from coastal regions of the western Atlantic Ocean and Gulf of Mexico. Marine Biology, 133(4), 593-602.

Gorokhova, E., & Hansson, S. 1999. An experimental study on variations in stable carbon and nitrogen isotope fractionation during growth of *Mysis mixta* and *Neomysis integer*. Canadian Journal of Fisheries and Aquatic Sciences, 56(11), 2203-2210.

Graham, B. S., Koch, P. L., Newsome, S. D., McMahon, K. W., & Aurioles, D. 2010. Using isoscapes to trace the movements and foraging behavior of top predators in oceanic ecosystems. Isoscapes, 299-318.

Gross, M. R., Coleman, R. M., & McDowall, R. M. 1988. Aquatic productivity and the evolution of diadromous fish migration. Science, 239(4845), 1291-1293.

Guillory, V. & Elliot, M. (2001). A review of blue crab predators. Proceedings of the Blue Crab Mortality Symposium, 90, 69-83.

Handley, L., Altsman, D., DeMay, R. 2007. Seagrass Status and Trends in the Northern Gulf of Mexico: 1940–2002. US Geological Survey Scientific Investigations Report 2006-5287 and US Environmental Protection Agency 855-R-04-003, 267 pp.

Helfman, G., Collette, B. B., Facey, D. E., & Bowen, B. W. 2009. The diversity of fishes: biology, evolution, and ecology. Blackwell Science, Oxford.

Herzka, S. Z. 2005. Assessing connectivity of estuarine fishes based on stable isotope ratio analysis. Estuarine, Coastal and Shelf Science, 64(1), 58-69.

Herzka, S. Z., & Holt, G. J. 2000. Changes in isotopic composition of red drum (*Sciaenops ocellatus)* larvae in response to dietary shifts: potential applications to settlement studies. Canadian Journal of Fisheries and Aquatic Sciences, 57(1), 137-147.

Herzka, S. Z., Holt, S. A., & Holt, G. J. 2002. Characterization of settlement patterns of red drum *Sciaenops ocellatus* larvae to estuarine nursery habitat: a stable isotope approach. Marine Ecology Progress Series, 226, 143-156.

Hesslein, R. H., Hallard, K. A., & Ramlal, P. 1993. Replacement of sulfur, carbon, and nitrogen in tissue of growing broad whitefish (*Coregonus nasus*) in response to a change in diet traced by $\delta^{34}S$, $\delta^{13}C$, and $\delta^{15}N$. Canadian Journal of Fisheries and Aquatic Sciences, 50(10), 2071-2076.

Hobson, K. A., Barnett-Johnson, R., & Cerling, T. 2010. Using isoscapes to track animal migration. Isoscapes, 273-298.

Holland, J. S., Maciolek, N., Kalke, R., Mullins, L., & Oppenheimer, C.H. 1975. A Benthos and Plankton Study of the Corpus Christi, Copano, and Aransas Bay Systems. III, Report on Data Collected During the Period July, 1974-May, 1975 and Summary of the Three-year Project: Final report. University of Texas Marine Science Institute, Port Aransas, Texas, 174 pp.

Holt, S. A., Kitting, C. L., & Arnold, C. R. 1983. Distribution of young red drums among different sea-grass meadows. Transactions of the American Fisheries Society, 112(2B), 267-271.

Islam, M. S., Bonner, J. S., Edge, B. L., & Page, C. A. 2014. Hydrodynamic characterization of Corpus Christi Bay through modeling and observation. Environmental Monitoring and Assessment, 186(11), 7863-7876.

Kalish, J. M. 1991. Determinants of otolith chemistry: seasonal variation in the composition of blood plasma, endolymph and otoliths of bearded rock cod *Pseudophycis barbatus*. Marine Ecology Progress Series, 137-159.

Kerr, L. A., Cadrin, S. X., & Secor, D. H. 2010. The role of spatial dynamics in the stability, resilience, and productivity of an estuarine fish population. Ecological Applications, 20(2), 497-507.

Kim, H. C., & Montagna, P. A. 2012. Effects of climate-driven freshwater inflow variability on macrobenthic secondary production in Texas lagoonal estuaries: a modeling study. Ecological Modelling, 235, 67-80.

Kraus, R. T., & Secor, D. H. 2004. Incorporation of strontium into otoliths of an estuarine fish. Journal of Experimental Marine Biology and Ecology, 302(1), 85-106.

Kynard, B. 1997. Life history, latitudinal patterns, and status of the shortnose sturgeon, *Acipenser brevirostrum*. Environmental Biology of Fishes, 48(1-4), 319-334.

Lamson, H. M., Shiao, J. C., Iizuka, Y., Tzeng, W. N., & Cairns, D. K. 2006. Movement patterns of American eels (*Anguilla rostrata*) between salt-and freshwater in a coastal watershed, based on otolith microchemistry. Marine Biology, 149(6), 1567-1576.

Lebreton, B., Pollack, J. B., Blomberg, B., Palmer, T. A., Adams, L., Guillou, G., & Montagna, P. A. 2016. Origin, composition and quality of suspended particulate organic matter in relation to freshwater inflow in a South Texas estuary. Estuarine, Coastal and Shelf Science, 170, 70-82.

Le Pape, O., & Cognez, N. 2016. The range of juvenile movements of estuarine and coastal nursery dependent flatfishes: estimation from a meta-analytical approach. Journal of Sea Research, 107, 43-55.

Levin, P. S., & Stunz, G. W. 2005. Habitat triage for exploited fishes: Can we identify essential "Essential Fish Habitat?". Estuarine, Coastal and Shelf Science, 64(1), 70-78.

Limburg, K.E., & Waldman, J.R. 2009. Dramatic declines in North Atlantic diadromous fishes. BioScience, 59(11), 955-965.

Longley, W.L. 1994. Freshwater Inflows to Texas Bays and Estuaries: Ecological Relationships and Methods for Determination of Needs. Texas Water Development Board, Austin, Texas, 386 pp.

MacKenzie, K.M., Palmer, M.R., Moore, A., Ibbotson, A.T., Beaumont, W.R., Poulter, D.J., & Trueman, C.N. 2011. Locations of marine animals revealed by carbon isotopes. Scientific Reports, 1, 21.

Maggs, J.Q., & Cowley, P.D. 2016. Nine decades of fish movement research in southern Africa: A synthesis of research and findings from 1928 to 2014. Reviews in Fish Biology and Fisheries, 26(3), 287-302.

Magnuson-Stevens Fishery Conservation and Management Act as Amended Through January 12, 2007. 16 U.S.C. § 1802-1891. 2007.

Maruyama, A., Tanahashi, E., Hirayama, T., & Yonekura, R. 2017. A comparison of changes in stable isotope ratios in the epidermal mucus and muscle tissue of slow-growing adult catfish. Ecology of Freshwater Fish, 26(4), 636-642.

Matlock, G. 1984. A Summary of 7 Years of Stocking Texas Bays with Red Drum. Management Data Series, 60, 14 pp.

Matthews, G.A., Marcin, C.A., and Clements, G.L. (1974). A Plankton and Benthos Survey of the San Antonio Bay System: March 1972-July 1974. Texas Parks and Wildlife Department, Austin, Texas, 76 pp.

McCormick, S. D., Farrell, A. P., & Brauner, C. J. 2013. Fish Physiology: Euryhaline Fishes, Volume 32. Academic Press.

McDowall, R. M. 1997. The evolution of diadromy in fishes (revisited) and its place in phylogenetic analysis. Reviews in Fish Biology and Fisheries, 7(4), 443-462.

Michener, R. H., & Kaufman, L. 2007. Stable isotope ratios as tracers in marine food webs: an update. Stable isotopes in ecology and environmental science, 2, 238-282.

Mohan, J. A., & Walther, B. D. 2015. Spatiotemporal variation of trace elements and stable isotopes in subtropical estuaries: II. Regional, local, and seasonal salinity-element relationships. Estuaries and Coasts, 38(3), 769-781.

Mohan, J. A., Rulifson, R. A., Corbett, D. R., & Halden, N. M. 2012. Validation of oligohaline elemental otolith signatures of striped bass by use of in situ caging experiments and water chemistry. Marine and Coastal Fisheries, 4(1), 57-70.

Mohan, J. A., Smith, S. D., Connelly, T. L., Attwood, E. T., McClelland, J. W., Herzka, S. Z., & Walther, B. D. 2016. Tissue-specific isotope turnover and discrimination factors are affected by diet quality and lipid content in an omnivorous consumer. Journal of Experimental Marine Biology and Ecology, 479, 35-45.

Montagna, P. A., & Kalke, R. D. 1995. Ecology of infaunal mollusca in South Texas estuaries. American Malacological Bulletin, 11, 163-175.

Montagna, P., Ward, G., & Vaughan, B. 2011. The importance of freshwater inflows to Texas estuaries. Water policy in Texas: responding to the rise of scarcity. The RFF Press, Washington, DC, 107-127.

Mook, W. G., & De Vries, J. J. 2000. Volume I, Introduction: theory methods review. Environmental Isotopes in the Hydrological Cycle—Principles and Applications, International Hydrological Programme (IHP-V), Technical Documents in Hydrology (IAEA/UNESCO) No, 39, 75-76.

Mooney, R. F., & McClelland, J. W. 2012. Watershed Export Events and Ecosystem Responses in the Mission–Aransas National Estuarine Research Reserve, South Texas. Estuaries and Coasts, 35(6), 1468-1485.

Moulton, D. L., Dance, M. A., Williams, J. A., Sluis, M. Z., Stunz, G. W., & Rooker, J. R. 2017. Habitat Partitioning and Seasonal Movement of Red Drum and Spotted Seatrout. Estuaries and Coasts, 40(3), 905-916.

Mumby, P.J., Edwards, A.J., Arias-Gonzalez, J.E., Lendeman, K.C., Blackwell, P.G., Gall, A., Gorczynska, M.I., Harborne, A.R., Pescod, C.L., Renken, H., Wabnitz, C.C.C. and Llewellyn, G. 2004. Mangroves enhance the biomass of coral reef fish communities in the Caribbean. Nature, 427(6974), 533-536.

Naiman, R. J., Bilby, R. E., Schindler, D. E., & Helfield, J. M. 2002. Pacific salmon, nutrients, and the dynamics of freshwater and riparian ecosystems. Ecosystems, 5(4), 399-417.

Neill, W.H. 1990. Environmental requirements of red drum. Red drum aquaculture. Publ. 90 603, Texas A&M University Sea Grant, Galveston, 105-108.

Nims, M. K., & Walther, B. D. 2014. Contingents of southern flounder from subtropical estuaries revealed by otolith chemistry. Transactions of the American Fisheries Society, 143(3), 721-731.

Ockerman, D. J. 2001. Water Budget for the Nueces Estuary, Texas, May-October 1998 (No. 081-01). US Geological Survey.

Orlando Jr., S.P., L.P. Rozas, G.H. Ward, & C.J. Klein. 1993. Characteristics of Gulf of Mexico estuaries. Silver Spring: National Oceanic and Atmospheric Administration, Office of Ocean Resources Conservation and Assessment.

Osburn, H.R. 1987. Comparison of Offshore and Onshore Gill Net Catches in Corpus Christi Bay. Texas Parks and Wildlife Department, Coastal Fisheries Branch.

Osburn, H.R., Matlock, G.C., & Green, A.W. 1982. Red drum (*Sciaenops ocellatus*) movement in Texas bays. Contributions in Marine Science 25, 85–97.

Overstreet, R. M., & Heard, R. W. 1978. Food of the red drum, *Sciaenops ocellata*, from Mississippi Sound. Gulf and Caribbean Research, 6(2), 131-135.

Palmer, M. R., & Edmond, J. M. 1992. Controls over the strontium isotope composition of river water. Geochimica et Cosmochimica Acta, 56(5), 2099-2111.

Palmer, T. A., Montagna, P. A., & Kalke, R. D. 2002. Downstream effects of restored freshwater inflow to Rincon Bayou, Nueces Delta, Texas, USA. Estuaries, 25(6), 1448-1456.

Pannella, G. 1971. Fish otoliths: daily growth layers and periodical patterns. Science, 173 (4002), 1124-1127.

Pattillo, M. E., Czapla, T. E., Nelson, D. M., & Monaco, M. E. 1997. Distribution and abundance of fishes and invertebrates in Gulf of Mexico estuaries, Volume II: Species life history summaries. ELMR Rep. No. 11. NOAA/NOS Strategic Environmental Assessments Division, Silver Springs, MD, 377 pp.

Payan, P., De Pontual, H., Bœuf, G., & Mayer-Gostan, N. 2004. Endolymph chemistry and otolith growth in fish. Comptes Rendus Palevol, 3(6-7), 535-547.

Perga, M. E., & Gerdeaux, D. 2005. 'Are fish what they eat' all year round? Oecologia, 144(4), 598-606.

Peters, K. M., & McMichael, R. H. 1987. Early life history of the red drum, *Sciaenops ocellatus* (Pisces: Sciaenidae), in Tampa Bay, Florida. Estuaries and Coasts, 10(2), 92-107.

Peterson, B. J., & Fry, B. 1987. Stable isotopes in ecosystem studies. Annual Review of Ecology and Systematics, 18(1), 293-320.

Polis, G. A., Anderson, W. B., & Holt, R. D. 1997. Toward an integration of landscape and food web ecology: the dynamics of spatially subsidized food webs. Annual Review of Ecology and Systematics, 28(1), 289-316.

Pollack, J. B., Kim, H. C., Morgan, E. K., & Montagna, P. A. 2011. Role of flood disturbance in natural oyster (*Crassostrea virginica*) population maintenance in an estuary in South Texas, USA. Estuaries and Coasts, 34(1), 187-197.

Porch, C., Wilson, C., and Nieland, D. 2002. A new growth model for red drum (*Sciaenops ocellatus*) that accommodates seasonal and ontogenic changes in growth rates. Fishery Bulletin, 100(1), 149-152.

Post, D. M. 2002. Using stable isotopes to estimate trophic position: models, methods, and assumptions. Ecology, 83(3), 703-718.

Post, D. M., Layman, C. A., Arrington, D. A., Takimoto, G., Quattrochi, J., & Montana, C. G. 2007. Getting to the fat of the matter: models, methods and assumptions for dealing with lipids in stable isotope analyses. Oecologia, 152(1), 179-189.

Potter, I. C., Tweedley, J. R., Elliott, M., & Whitfield, A. K. 2015. The ways in which fish use estuaries: a refinement and expansion of the guild approach. Fish and Fisheries, 16(2), 230-239.

Pulich, W., Dunton, K.H., Roberts, L.R., Calnan, T., Lester, J., & McKinney, L.D. 1998. Seagrass conservation plan for Texas. Texas Parks and Wildlife Department. Austin, Texas. 79 pp.

Qian, Y., Kennicutt II, M. C., Svalberg, J., Macko, S. A., Bidigare, R. R., & Walker, J. 1996. Suspended particulate organic matter (SPOM) in Gulf of Mexico estuaries: compound-specific isotope analysis and plant pigment compositions. Organic Geochemistry, 24(8-9), 875-888.

Radabaugh, K.R., Hollander, D. J., & Peebles, E.B. 2013. Seasonal δ13C and δ15N isoscapes of fish populations along a continental shelf trophic gradient. Continental Shelf Research, 68, 112-122.

Reagan, R. E. 1985. Species Profiles. Life Histories and Environmental Requirements of Coastal Fishes and Invertebrates (Gulf of Mexico): red drum. Biol Rep 82(11.36) TR EL-82-4. US Fish and Wildlife Service, Washington, DC.

Rezek, R. J., Lebreton, B., Roark, E. B., Palmer, T. A., & Pollack, J. B. 2017. How does a restored oyster reef develop? An assessment based on stable isotopes and community metrics. Marine Biology, 164(3), 54.

Riera, P., Montagna, P. A., Kalke, R. D., & Richard, P. 2000. Utilization of estuarine organic matter during growth and migration by juvenile brown shrimp *Penaeus aztecus* in a South Texas estuary. Marine Ecology Progress Series, 205-216.

Robinson, D. P., Jabado, R. W., Rohner, C. A., Pierce, S. J., Hyland, K. P., & Baverstock, W. R. 2017. Satellite tagging of rehabilitated green sea turtles *Chelonia mydas* from the United Arab Emirates, including the longest tracked journey for the species. PloS one, 12(9), e0184286.

Rooker, J. R., Stunz, G. W., Holt, S. A., & Minello, T. J. 2010. Population connectivity of red drum in the northern Gulf of Mexico. Marine Ecology Progress Series, 407, 187-196.

Rubenstein, D. R., & Hobson, K. A. 2004. From birds to butterflies: animal movement patterns and stable isotopes. Trends in Ecology & Evolution, 19(5), 256-263.

Russell, M. J., Montagna, P. A., & Kalke, R. D. 2006. The effect of freshwater inflow on net ecosystem metabolism in Lavaca Bay, Texas. Estuarine, Coastal and Shelf Science, 68(1-2), 231-244.

Scharf, F. S., & Schlicht, K. K. 2000. Feeding habits of red drum (*Sciaenops ocellatus*) in Galveston Bay, Texas: Seasonal diet variation and predator-prey size relationships. Estuaries, 23(1), 128-139.

Secor, D. H. 1999. Specifying divergent migrations in the concept of stock: the contingent hypothesis. Fisheries Research, 43(1-3), 13-34.

Secor, D. H., & Kerr, L. A. 2009. Lexicon of life cycle diversity in diadromous and other fishes. American Fisheries Society Symposium, 69, 537-556.

Secor, D. H., & Piccoli, P. M. 2007. Oceanic migration rates of upper Chesapeake Bay striped bass (*Morone saxatilis*), determined by otolith microchemical analysis. Fishery Bulletin, 105(1), 62-73.

Secor, D. H., & Rooker, J. R. 2000. Is otolith strontium a useful scalar of life cycles in estuarine fishes?. Fisheries Research, 46(1-3), 359-371.

Shaw, T. J., Moore, W. S., Kloepfer, J., & Sochaski, M. A. 1998. The flux of barium to the coastal waters of the southeastern USA: the importance of submarine groundwater discharge. Geochimica et Cosmochimica Acta, 62(18), 3047-3054.

Sheppard, J. N., Whitfield, A. K., Cowley, P. D., & Hill, J. M. 2012. Effects of altered estuarine submerged macrophyte bed cover on the omnivorous Cape stumpnose *Rhabdosargus holubi*. Journal of Fish Biology, 80(3), 705-712.

Simmons, E.G., and Breuer, J.P. 1962. A study of redfish, *Sciaenops ocellata* Linn., and the black drum, *Pogonias cromis,* Linn. Publications of the Institute of Marine Science, 8, 184-211.

Simms, A. R., Anderson, J. B., Rodriguez, A. B., & Taviani, M. 2008. Mechanisms controlling environmental change within an estuary: Corpus Christi Bay, Texas, USA. Evidence for Rapid Change in Estuarine Environments: Geologic Society of America, Special Paper, 443, 121-146.

Stevens, P. W., Greenwood, M. F., & Blewett, D. A. 2013. Fish assemblages in the oligohaline stretch of a southwest Florida river during periods of extreme freshwater inflow variation. Transactions of the American Fisheries Society, 142(6), 1644-1658.

Stewart, C. B., & Scharf, F. S. 2008. Estuarine Recruitment, Growth, and First-Year Survival of Juvenile Red Drum in North Carolina. Transactions of the American Fisheries Society, 137(4), 1089-1103.

Stunz, G. W., Minello, T. J., & Levin, P. S. 2002. Growth of newly settled red drum *Sciaenops ocellatus* in different estuarine habitat types. Marine Ecology Progress Series, 238, 227-236.

Sturrock, A. M., Trueman, C. N., Milton, J. A., Waring, C. P., Cooper, M. J., & Hunter, E. 2014. Physiological influences can outweigh environmental signals in otolith microchemistry research. Marine Ecology Progress Series, 500, 245-264.

Suzuki, K. W., Kasai, A., Nakayama, K., & Tanaka, M. 2005. Differential isotopic enrichment and half-life among tissues in Japanese temperate bass (*Lateolabrax japonicus*) juveniles: implications for analyzing migration. Canadian Journal of Fisheries and Aquatic Sciences, 62(3), 671-678.

Texas Department of Water Resources. 1982. The influence of freshwater inflows upon the major bays and estuaries of the Texas gulf coast: executive summary. 2nd ed. Report LP-115. Texas Department of Water Resources, Austin, Texas, 1 v.

Tolan, J. M. 2007. El Niño-Southern Oscillation impacts translated to the watershed scale: estuarine salinity patterns along the Texas Gulf coast, 1982 to 2004. Estuarine, Coastal and Shelf Science, 72(1-2), 247-260.

Trueman, C. N., McGill, R. A., & Guyard, P. H. 2005. The effect of growth rate on tissue-diet isotopic spacing in rapidly growing animals. An experimental study with Atlantic salmon (*Salmo salar*). Rapid Communications in Mass Spectrometry, 19(22), 3239-3247.

Tupper, M. 2007. Identification of nursery habitats for commercially valuable humphead wrasse *Cheilinus undulatus* and large groupers (Pisces: Serranidae) in Palau. Marine Ecology Progress Series, 332, 189-199.

Tykot, R. H. 2004. Stable isotopes and diet: you are what you eat. Proceedings-International School of Physics Enrico Fermi, 154, 433-444.

Vander Zanden, H. B., Bolten, A. B., Tucker, A. D., Hart, K. M., Lamont, M. M., Fujisaki, I., & Pajuelo, M. 2016. Biomarkers reveal sea turtles remained in oiled areas following the Deepwater Horizon oil spill. Ecological Applications, 26(7), 2145-2155.

Vander Zanden, M. J., Clayton, M. K., Moody, E. K., Solomon, C. T., & Weidel, B. C. 2015. Stable isotope turnover and half-life in animal tissues: a literature synthesis. PLoS One, 10(1), e0116182.

Vander Zanden, M.J., & Rasmussen, J. B. 2001. Variation in $\delta^{15}N$ and $\delta^{13}C$ trophic fractionation: implications for aquatic food web studies. Limnology and Oceanography, 46(8), 2061-2066.

Vega, R. R., Neill, W. H., Gold, J. R., & Ray, M. S. 2011. Enhancement of Texas Sciaenids (red drum and spotted seatrout). NOAA Technical Memorandum NMFS-F/SPO-113, 85-92.

Wallace, A. A., Hollander, D. J., & Peebles, E. B. 2014. Stable isotopes in fish eye lenses as potential recorders of trophic and geographic history. PloS one, 9(10), e108935.

Walther, B. D., & Limburg, K. E. 2012. The use of otolith chemistry to characterize diadromous migrations. Journal of Fish Biology, 81(2), 796-825.

Walther, B. D., & Nims, M. K. 2015. Spatiotemporal variation of trace elements and stable isotopes in subtropical estuaries: I. Freshwater endmembers and mixing curves. Estuaries and Coasts, 38(3), 754-768.

Walther, B. D., & Thorrold, S. R. 2006. Water, not food, contributes the majority of strontium and barium deposited in the otoliths of a marine fish. Marine Ecology Progress Series, 311, 125-130.

Ward, G. H. 1997. Processes and trends of circulation within the Corpus Christi Bay national estuary program study area. Corpus Christi Bay National Estuary Program, Corpus Christi, Texas, CCBNEP-21, 287.

Ward, G.H. and Armstrong, N.E. 1997. Current Status and Historical Trends of Ambient Water, Sediment, Fish, and Shellfish Tissue Quality in the Corpus Christi Bay National Estuary Program Study Area. Publication CCBNEP-13. Texas Natural Resource Conservation Commission, Austin, Texas, 807 pp.

Ward, J. 1963. Hierarchical grouping to optimize an objective function. Journal of American Statistics Association, 58, 236-244.

Watson, C. J., Nordi, W. M., & Esbaugh, A. J. 2014. Osmoregulation and branchial plasticity after acute freshwater transfer in red drum, *Sciaenops ocellatus*. Comparative Biochemistry and Physiology Part A: Molecular & Integrative Physiology, 178, 82-89.

Wenner, C. 1992. Red drum: natural history and fishing techniques in South Carolina. South Carolina Department of Natural Resources. Technical Report 17, Charleston.

Werner, E. E., & Gilliam, J. F. 1984. The ontogenetic niche and species interactions in size-structured populations. Annual Review of Ecology and Systematics, 15(1), 393-425.

West, J. B., Bowen, G. J., Dawson, T. E., & Tu, K. P. 2009. Isoscapes: understanding movement, pattern, and process on Earth through isotope mapping. Springer Science & Business Media.

Wheeler, S. G., Russell, A. D., Fehrenbacher, J. S., & Morgan, S. G. 2016. Evaluating chemical signatures in a coastal upwelling region to reconstruct water mass associations of settlement-stage rockfishes. Marine Ecology Progress Series, 550, 191-206.

Wilson, C. A., & Nieland, D. L. 1994. Reproductive biology of red drum, *Sciaenops ocellatus*, from the neritic waters of the northern Gulf of Mexico. Fishery Bulletin, 92(4), 841-850.

Woodcock, S. H., Grieshaber, C. A., & Walther, B. D. 2013. Dietary transfer of enriched stable isotopes to mark otoliths, fin rays, and scales. Canadian Journal of Fisheries and Aquatic Sciences, 70(1), 1-4.

Woodcock, S. H., & Walther, B. D. 2014. Trace elements and stable isotopes in Atlantic tarpon scales reveal movements across estuarine gradients. Fisheries Research, 153, 9-17.

Zimmerman, C. E. 2005. Relationship of otolith strontium-to-calcium ratios and salinity: experimental validation for juvenile salmonids. Canadian Journal of Fisheries and Aquatic Sciences, 62(1), 88-97.

LIST OF FIGURES

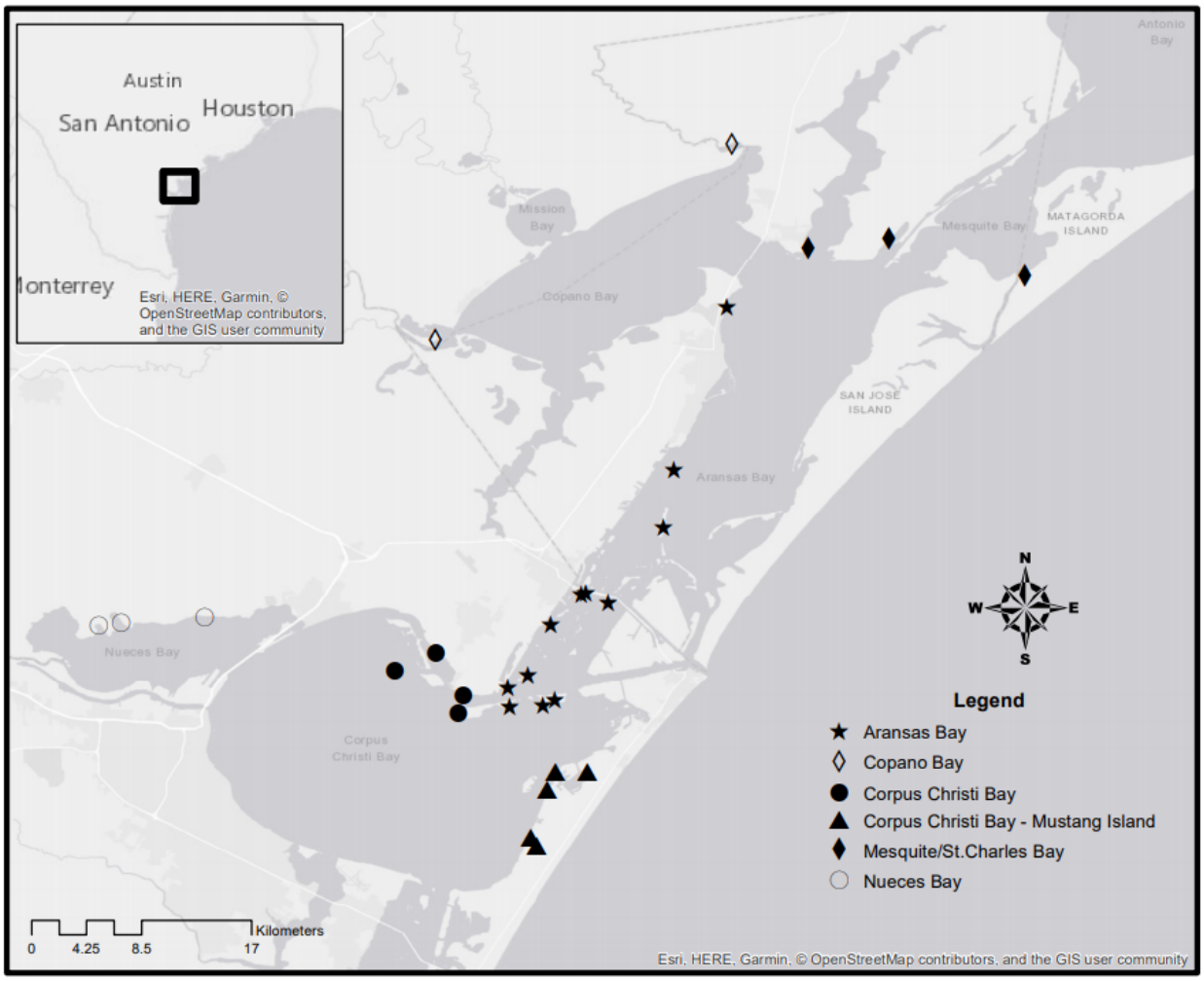

Figure 1. Sampling map of the Nueces and Mission-Aransas Estuaries, Texas, USA.

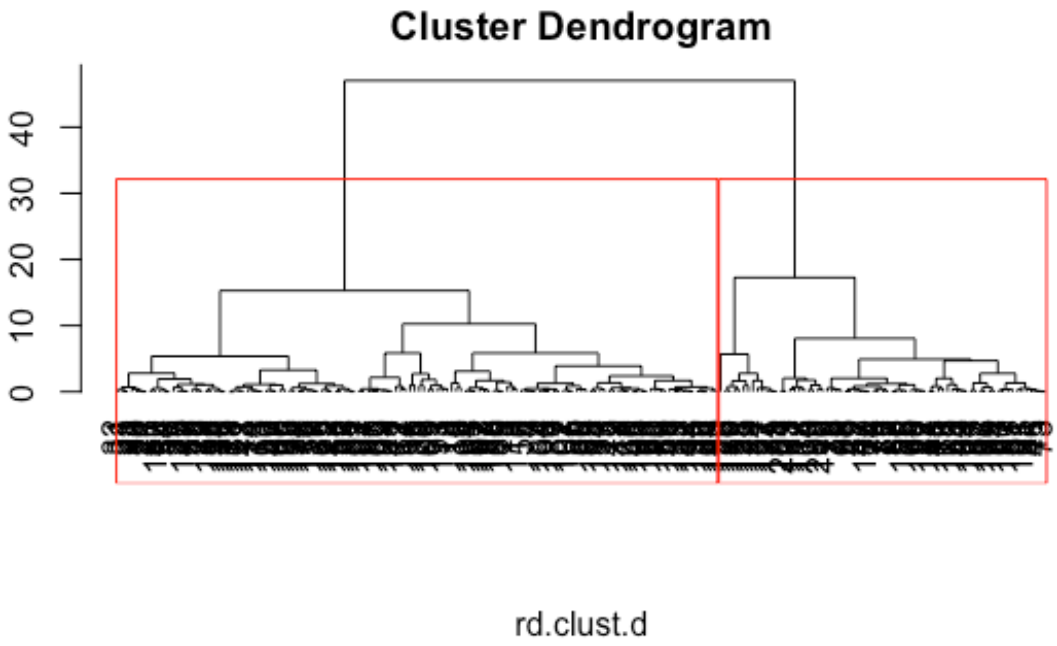

Figure 2. Ward's Hierarchical clustering analysis of all individuals (*n*=201) showing two clusters, designated as Group 1 and Group 2.

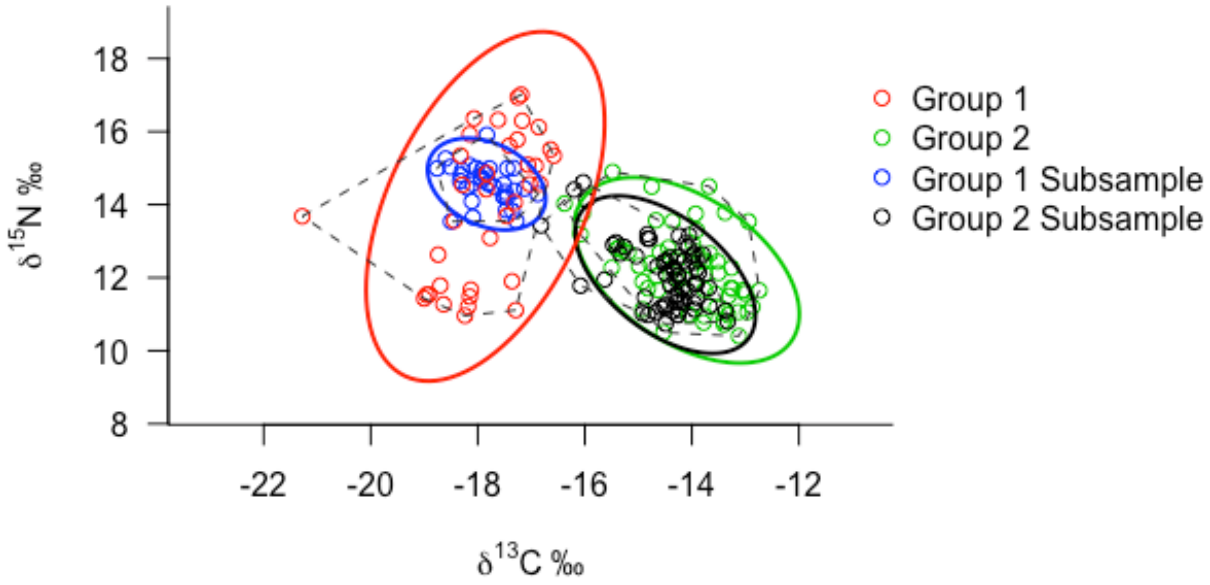

Figure 3. SIBER biplot of $\delta^{13}C$ and $\delta^{15}N$ of all sampled individuals and subsample used for otolith interpretation including convex hull total area and Standard Ellipse Area.

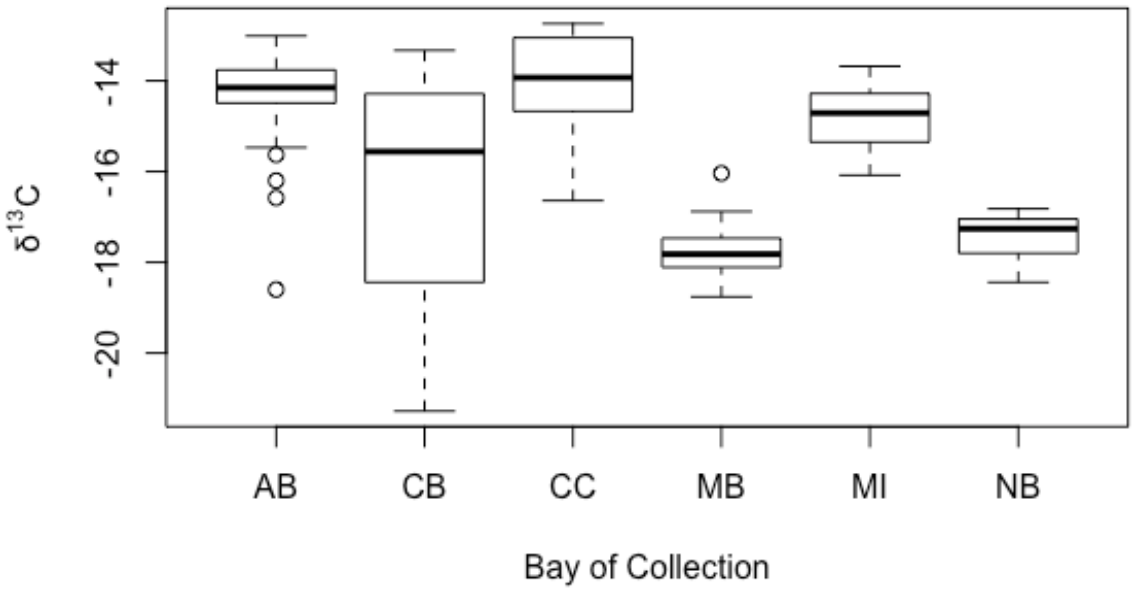

Figure 4. Boxplot of $\delta^{13}C$ values from Aransas Bay (AB), Copano Bay (CB), Corpus Christi Bay (CC), Mesquite Bay (MB), Corpus Christi Bay – Mustang Island (MI), and Nueces Bay (NB).

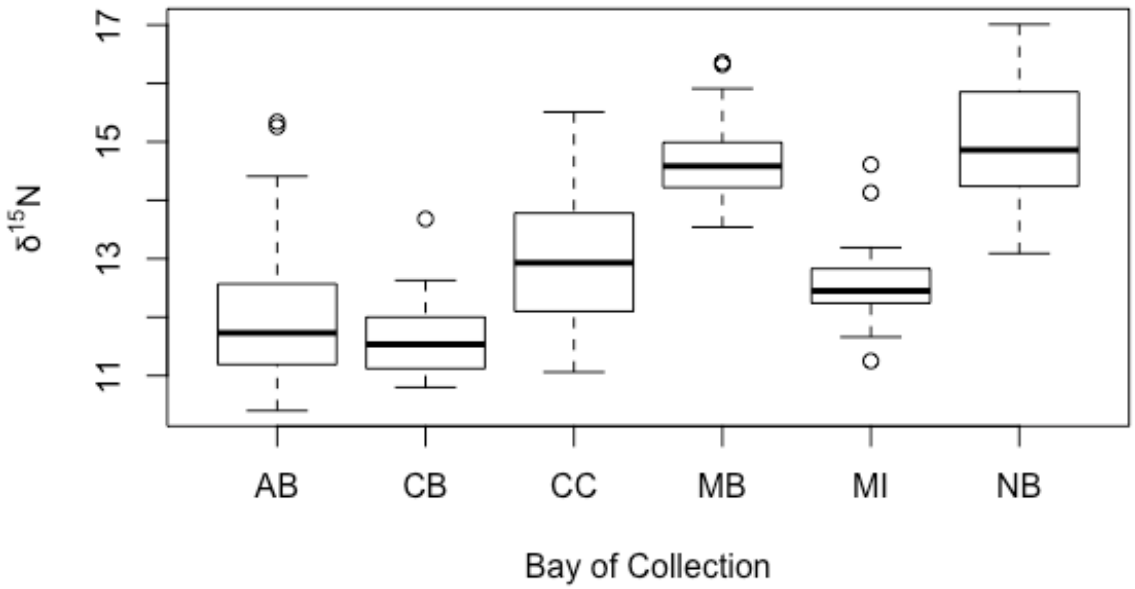

Figure 5. Boxplot of $\delta^{15}N$ values from Aransas Bay (AB), Copano Bay (CB), Corpus Christi Bay (CC), Mesquite Bay (MB), Corpus Christi Bay – Mustang Island (MI), and Nueces Bay (NB).

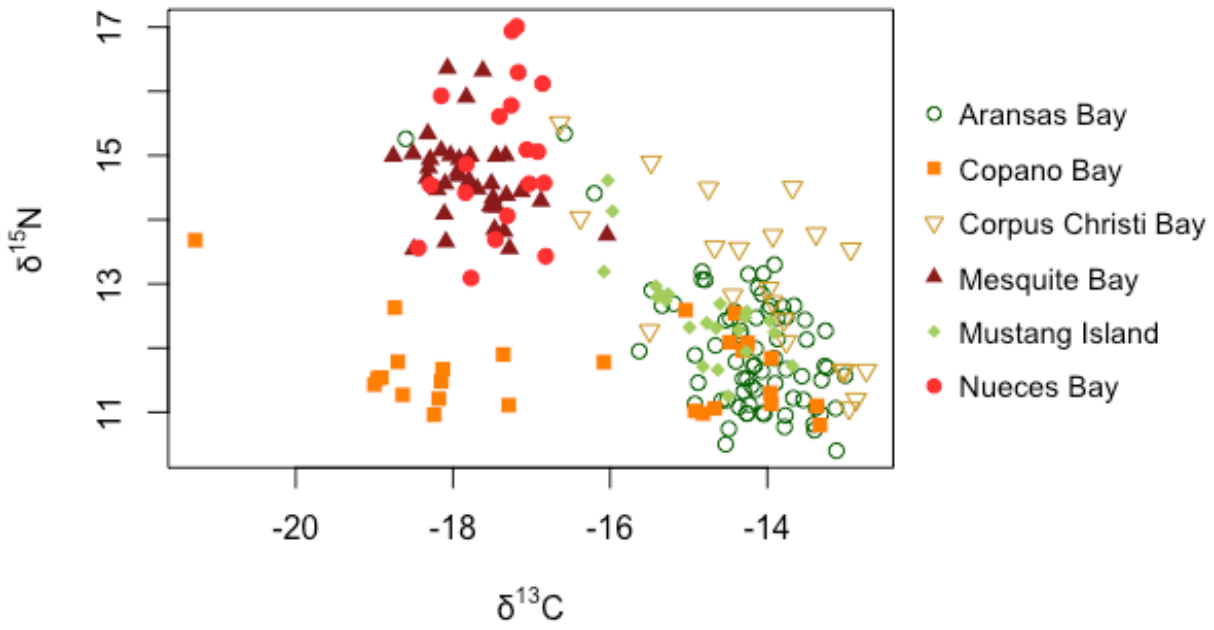

Figure 6. Stable isotope signatures ($\delta^{13}C$ and $\delta^{15}N$) of individuals collected at different locations within the Mission-Aransas and Nueces estuaries.

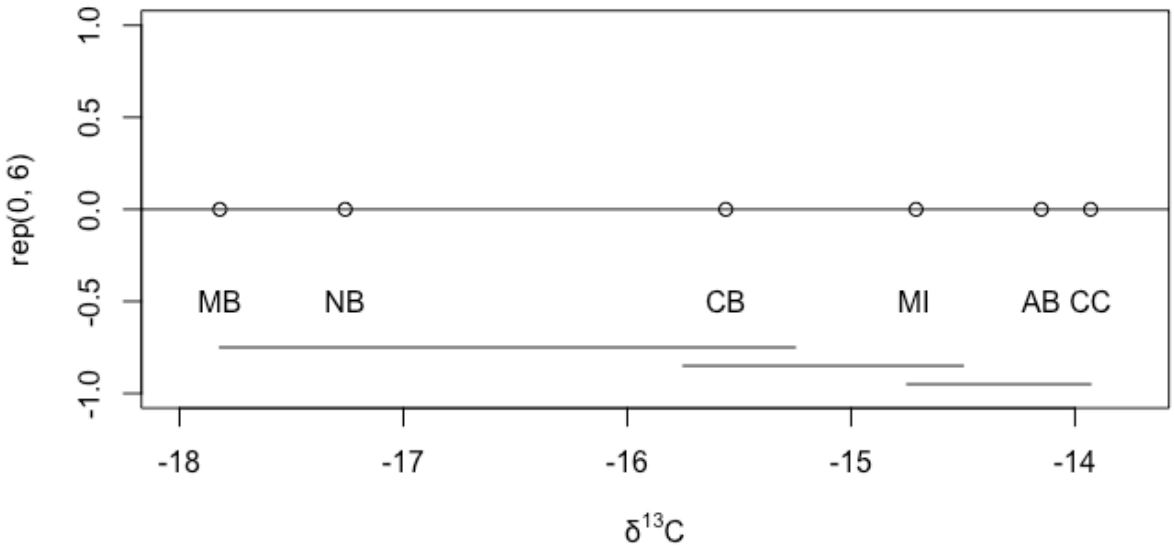

Figure 7. Non-parametric Kruskal Wallis post hoc test results of $\delta^{13}C$ values between Mesquite Bay (MB), Nueces Bay (NB), Copano Bay (CB), Corpus Christi Bay – Mustang Island (MI), Aransas Bay (AB), and Corpus Christi Bay (CC).

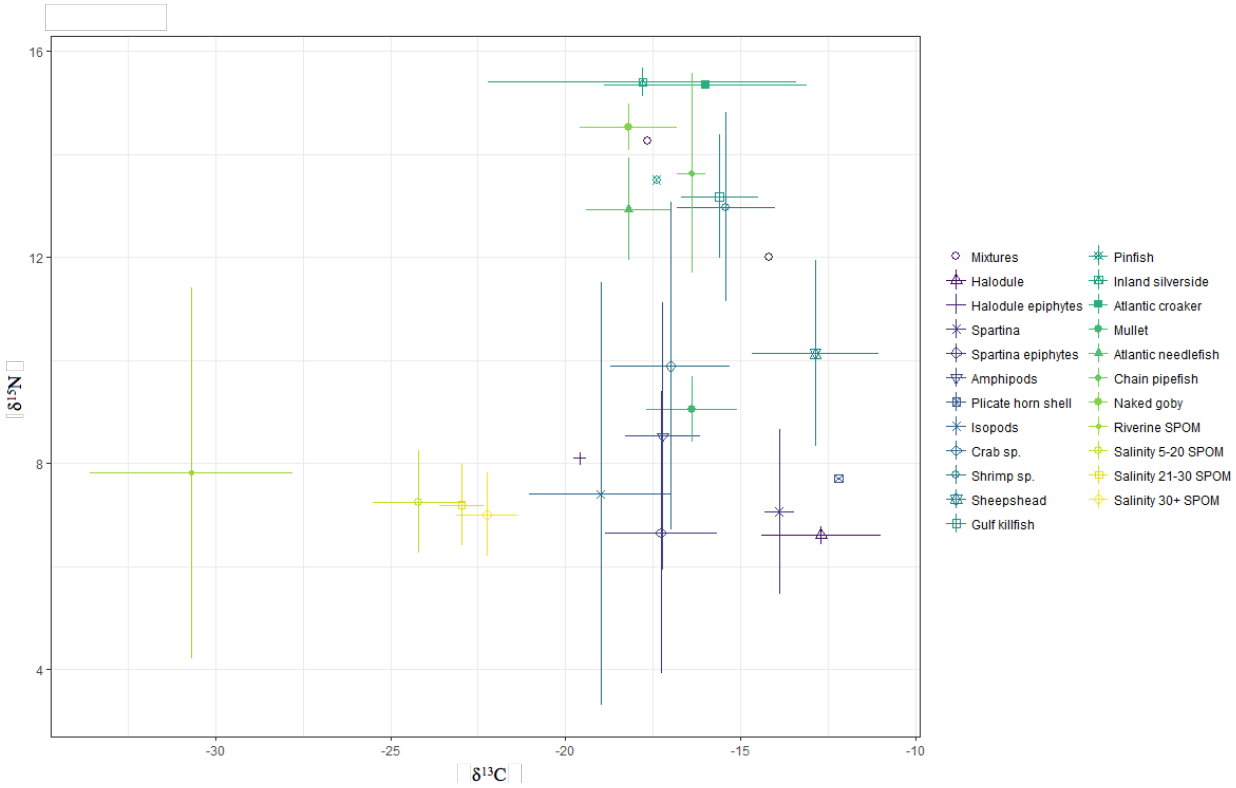

Figure 8. Averaged stable isotope signatures ($\delta^{13}C$ and $\delta^{15}N$) of Group 1 and Group 2 (mixtures), riverine and estuary SPOM, potential prey, and other consumers within the Mission-Aransas estuary.

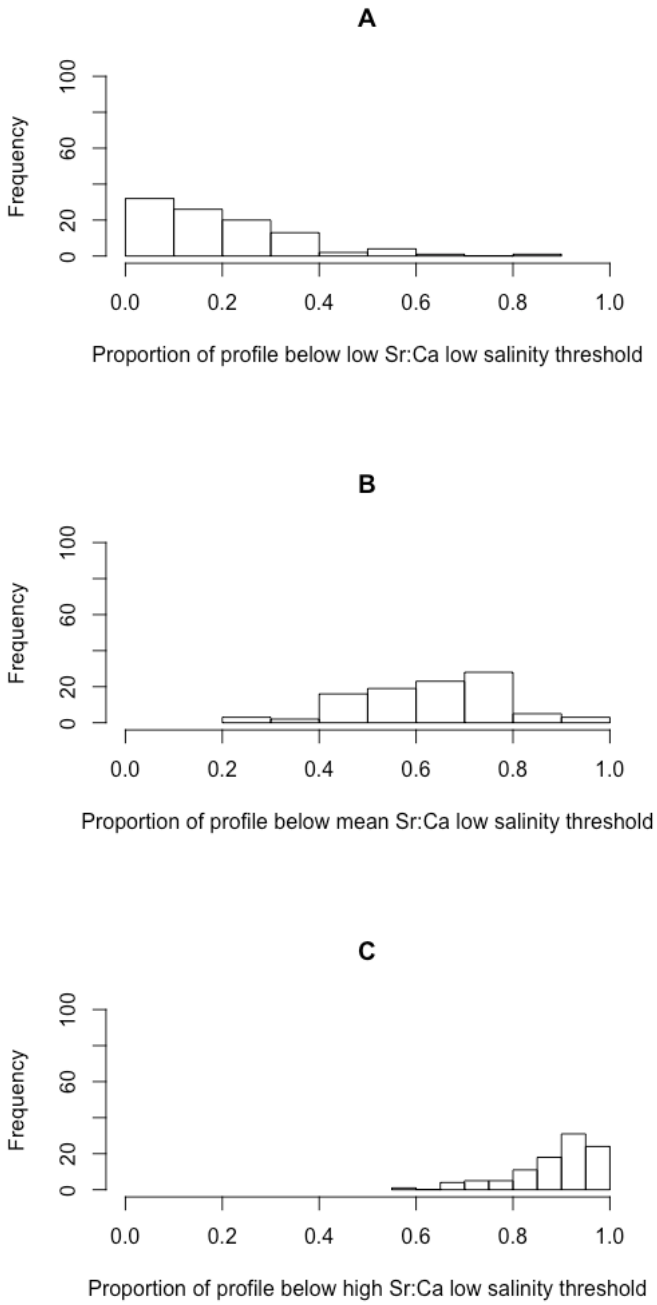

Figure 9a. Frequency histogram of individuals grouped by the proportion of their Sr:Ca life history profile that exceeded a threshold for low salinity residence. (**A**) Frequencies of low salinity proportions calculated for all individuals using the high Sr:Ca low salinity threshold. (**B**) Frequencies of low salinity proportions calculated for all individuals using the mean Sr:Ca low salinity threshold. (**C**) Frequencies of low salinity proportions calculated for all individuals using the low Sr:Ca low salinity threshold.

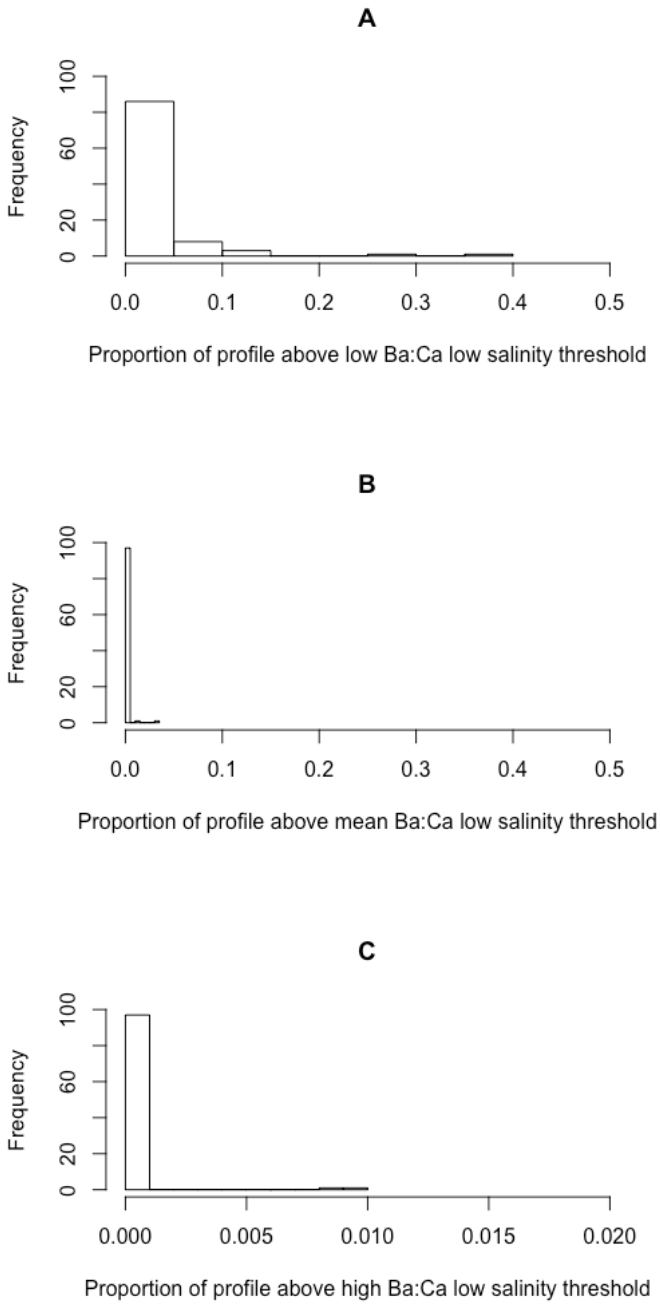

Figure 9b. Frequency histogram of individuals grouped by the proportion of their Ba:Ca life history profile that exceeded a threshold for low salinity residence. (**A**) Frequencies of low salinity proportions calculated for all individuals using the low Ba:Ca low salinity threshold. (**B**) Frequencies of low salinity proportions calculated for all individuals using the mean Ba:Ca low salinity threshold. (**C**) Frequencies of low salinity proportions calculated for all individuals using the high Ba:Ca low salinity threshold.

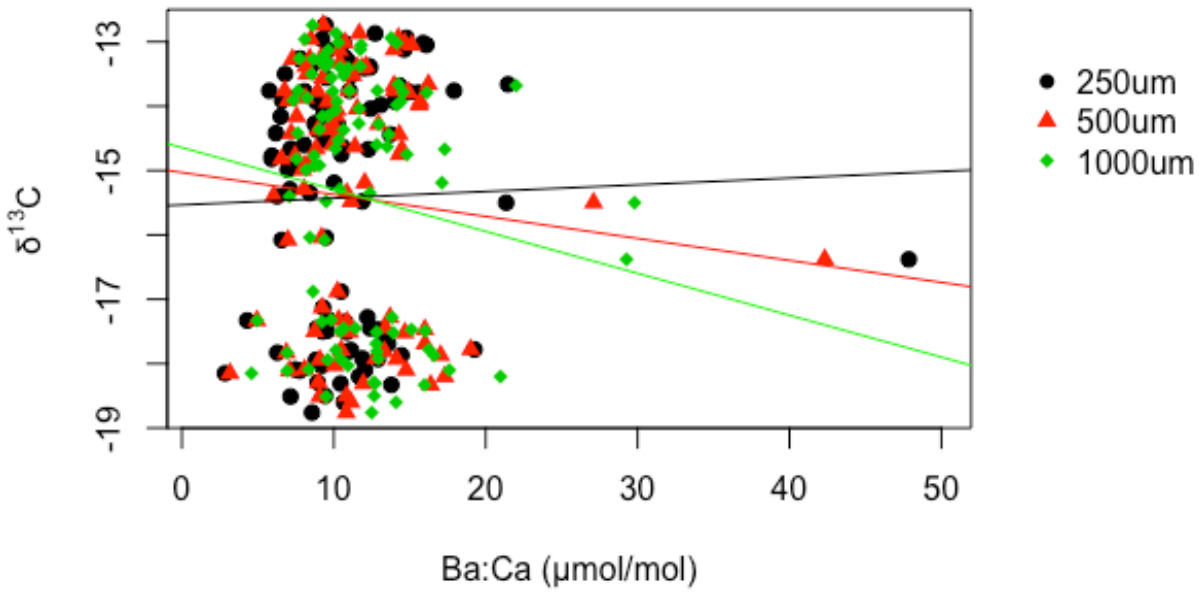

Figure 10a. Average Ba:Ca ratios of 250, 500, and 1000 µm sections of otolith correlated with $\delta^{13}C$ values of individual fish.

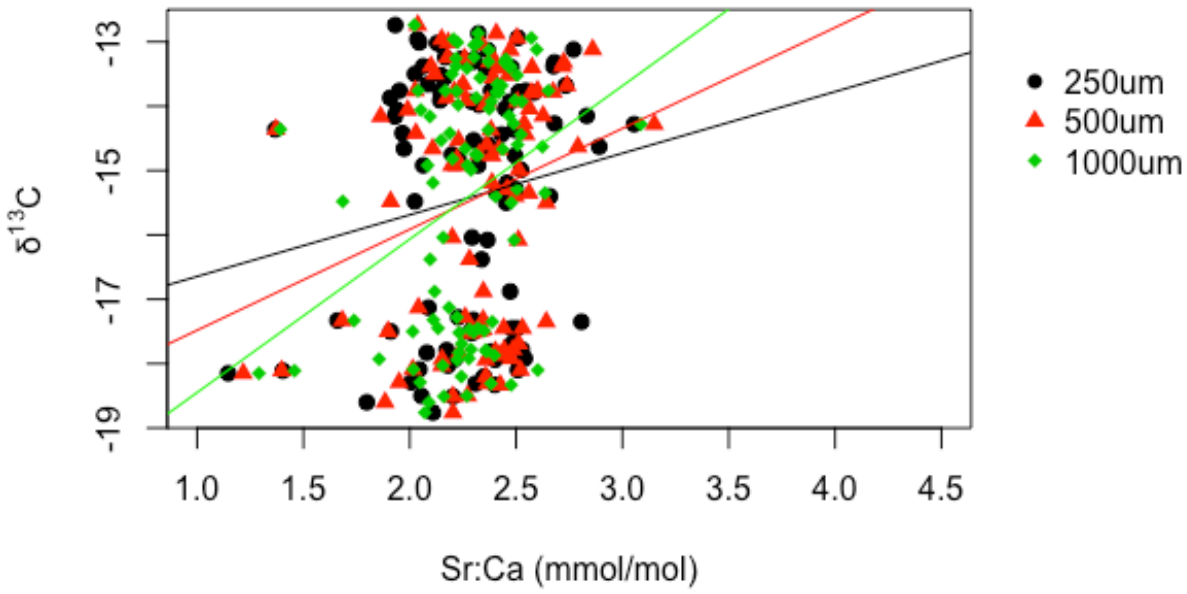

Figure 10b. Average Sr:Ca ratios for 250, 500, and 1000 µm sections of otolith correlated with $\delta^{13}C$ values for individual fish.

LIST OF TABLES

Table 1a. Laser pre-ablation parameters used for sample analysis.

LA-ICPMS Pre-Ablation Parameters	
Laser energy output	80%
Repetition rate	10 Hz
Spot size	75 μm
Laser speed	15 μm/s
He flow	800 mL/min
Ar flow	N/A

Table 1b. Laser ablation parameters used for sample analysis.

LA-ICPMS Ablation Parameters	
Laser energy output	80%
Repetition rate	10 Hz
Spot size	35 μm
Laser speed	15 μm/s
He flow	850 mL/min
Ar flow	700 mL/min

Table 2. Age, sample size, and SD of total length (mm) of collected red drum.

Age	*n*	TL (SD)
0	13	343.2 (42.8)
1	76	403.9 (57.1)
2	10	538.1 (47.1)

Table 3. Mean and standard deviation of total length (mm) and wet weight (g) of individuals sampled in the Mission-Aransas and Nueces estuaries.

Estuary	Collection Site	*n*	Mean (Standard Deviation) TL (mm)	WW (g)
Mission-Aransas	Aransas Bay	73	455.4 (76.3)	1023.4 (547.3)
Mission-Aransas	Copano Bay	28	423.5 (57.8)	801.1 (331.0)
Mission-Aransas	Mesquite Bay	28	389.1 (45.4)	632.9 (252.5)
Nueces	Corpus Christi Bay	21	399.4 (101.1)	789.4 (692.8)
Nueces	Corpus Christi Bay – Mustang Island	22	378.2 (45.3)	577.0 (263.0)
Nueces	Nueces Bay	19	434.4 (59.6)	848.4 (337.2)

Table 4. $\delta^{13}C$ and $\delta^{15}N$ means and standard deviation for each group.

	Group 1 *n*=79	Group 2 *n*=122	T-test
$\delta^{13}C$	-17.65 (0.89)	-14.19 (0.68)	p = < 0.001
$\delta^{15}N$	14.25 (1.39)	12.01 (0.82)	p = < .0001

Table 5. Mean and standard deviation of $\delta^{13}C$ and $\delta^{15}N$ of individuals sampled in the Mission-Aransas and Nueces estuaries.

Estuary	Collection Site	*n*	Mean (Standard Deviation) $\delta^{13}C$	$\delta^{15}N$
Mission-Aransas	Aransas Bay	73	-14.23 (.85)	12.00 (0.98)
Mission-Aransas	Copano Bay	28	-16.34 (2.28)	11.66 (0.65)
Mission-Aransas	Mesquite Bay	28	-17.78 (0.51)	14.64 (0.65)
Nueces	Corpus Christi Bay	21	-14.11 (1.13)	13.05 (1.26)
Nueces	Corpus Christi Bay – Mustang Island	22	-14.84 (0.69)	12.55 (0.76)
Nueces	Nueces Bay	19	-17.42 (0.50)	14.98 (1.16)

Table 6. $\delta^{13}C$ and $\delta^{15}N$ values in the Mission-Aransas estuary. Source: Lebreton et al. 2016; Rezek et al. 2017.

	$\delta^{13}C$	$\delta^{15}N$	Source
SPOM (Mission and Aransas Rivers)	-30.7‰ (2.9)	7.8‰ (3.6)	Lebreton et al. 2016
SPOM (5-20 salinity)	-24.2‰ (1.3)	7.3‰ (1.0)	Rezek et al. 2017
SPOM (21-30 salinity)	-22.9‰ (0.6)	7.2‰ (0.8)	Rezek et al. 2017
SPOM (30+ salinity)	-22.2‰ (0.9)	7.0‰ (0.8)	Rezek et al. 2017
Halodule wrightii	-12.7‰ (1.7)	6.6‰ (0.2)	Rezek et al. 2017
Spartina alterniflora	-13.9‰ (0.4)	7.1‰ (1.6)	Rezek et al. 2017
Halodule epiphyte	-19.6‰	8.1‰	Rezek et al. 2017
Spartina epiphytic algae	-17.3‰ (1.6)	6.7‰ (2.7)	Rezek et al. 2017
Amphipods	-17.3‰ (1.1)	8.5‰ (2.6)	Rezek et al. 2017
Isopods	-19.0‰ (1.0)	7.4‰ (4.0)	Rezek et al. 2017
Cerithideopsis pliculosa	-12.2‰	7.7‰	Rezek et al. 2017
Callinectes sapidus	-17.0‰ (1.7)	9.9‰ (3.2)	Rezek et al. 2017
Shrimp sp.	-15.4‰ (1.4)	13.0‰ (1.8)	Rezek et al. 2017
Cyprinodon variegatus	-12.9‰ (1.8)	10.1‰ (1.8)	Rezek et al. 2017
Fundulus grandis	-15.6‰ (1.1)	13.2‰ (1.2)	Rezek et al. 2017

Table 6. Continued.

	$\delta^{13}C$	$\delta^{15}N$	Source
Micropogonias undulatus	-16.0‰ (2.9)	15.4‰ (0.1)	Rezek et al. 2017
Mugil sp.	-16.4‰ (1.3)	9.1‰ (0.6)	Rezek et al. 2017
Syngnathus louisianae	-16.4‰ (0.4)	13.6‰ (1.9)	Rezek et al. 2017
Lagodon rhomboides	-17.4‰	13.5‰	Rezek et al. 2017
Menidia beryllina	-17.8‰ (4.4)	15.4‰ (0.3)	Rezek et al. 2017
Strongylura marina	-18.2‰ (1.2)	12.9‰ (1.0)	Rezek et al. 2017
Gobiosoma bosc	-18.2‰ (1.4)	14.5‰ (0.5)	Rezek et al. 2017

Table 7. $\delta^{13}C$ and $\delta^{15}N$ values in the Nueces estuary. Source: Riera et al. 2000.

	$\delta^{13}C$	$\delta^{15}N$	Source
POM (Nueces River)	-28.8 to -26.3‰	8.8 to 10.8‰	Riera et al. 2000
Salicornia sp. (fresh leaves)	-27.8 to -26.3‰	-	Riera et al. 2000
Zooplankton	-26.3 to -25.6‰	11.7‰	Riera et al. 2000
Penaeus aztecus (Rincon Bayou)	-20.6 to -14.8‰	4.5 to 13.1‰	Riera et al. 2000
Penaeus aztecus (Nueces River)	-25.2 to 20.4‰	6.6 to 13.9‰	Riera et al. 2000

LIST OF APPENDICES

Appendix 1: Supplemental Isotope Data.

Table A. Sample metadata. Identification number, capture location (CC=Corpus Christi, AB=Aransas Bay, MI= Corpus Christi – Mustang Island, MB = Mesquite Bay, CB = Copano Bay, and NB = Nueces Bay), capture date, total length, $\delta^{13}C$, and $\delta^{15}N$ for all wild fish captured in this study.

Fish ID	Location Captured	Date Captured	TL (mm)	$\delta^{13}C$	$\delta^{15}N$
RD001	CC	11/09/16	303	-16.38	14.03
RD002	CC	11/09/16	327	-13.76	12.10
RD003	CC	11/09/16	610	-14.36	13.55
RD004	AB	11/08/16	510	-13.76	12.48
RD005	AB	11/08/16	407	-13.52	12.44
RD006	AB	11/08/16	491	-13.66	12.66
RD007	CC	11/08/16	323	-13.79	12.44
RD008	CC	11/08/16	421	-13.93	13.75
RD009	CC	11/08/16	322	-13.93	12.72
RD010	CC	11/08/16	345	-13.98	12.93
RD011	CC	11/08/16	328	-15.48	14.90
RD012	CC	11/09/16	345	-15.50	12.27
RD013	CC	11/09/16	325	-14.44	12.82
RD014	CC	11/09/16	320	-13.38	13.78
RD015	CC	11/09/16	311	-12.94	13.54
RD016	CC	11/09/16	341	-14.75	14.49

Table A. Continued.

Fish ID	Location Captured	Date Captured	TL (mm)	$\delta^{13}C$	$\delta^{15}N$
RD017	CC	11/09/16	309	-14.67	13.57
RD018	CC	11/09/16	473	-13.68	14.50
RD019	CC	11/15/16	491	-12.87	11.20
RD020	CC	11/15/16	497	-13.02	11.65
RD021	CC	11/15/16	471	-13.05	11.65
RD022	CC	11/15/16	500	-12.96	11.06
RD023	CC	11/15/16	628	-12.74	11.65
RD024	AB	11/15/16	433	-14.04	10.97
RD025	AB	11/15/16	365	-13.41	10.81
RD026	AB	11/15/16	355	-13.78	10.77
RD027	AB	11/15/16	465	-13.13	11.06
RD028	AB	11/15/16	445	-13.32	10.98
RD029	AB	11/15/16	471	-13.54	11.19
RD030	AB	11/15/16	460	-13.56	11.56
RD031	AB	11/15/16	479	-13.24	11.69
RD032	AB	11/15/16	509	-13.31	11.50
RD033	AB	11/15/16	591	-13.27	11.72
RD034	AB	11/15/16	560	-13.38	11.07
RD035	AB	11/15/16	518	-13.01	11.57
RD036	AB	11/15/18	464	-13.12	10.40

Table A. Continued.

Fish ID	Location Captured	Date Captured	TL (mm)	$\delta^{13}C$	$\delta^{15}N$
RD037	AB	04/24/17	450	-13.40	10.72
RD038	AB	05/08/17	399	-18.60	15.26
RD039	MI	05/08/17	370	-14.37	12.28
RD040	MI	05/08/17	354	-14.63	11.66
RD041	MI	05/08/17	386	-14.27	11.94
RD042	MI	05/08/17	416	-14.60	12.69
RD043	MI	05/11/17	561	-14.28	12.48
RD044	MB	05/11/17	345	-17.35	13.82
RD045	MB	05/11/17	383	-17.52	14.22
RD046	MB	05/11/17	430	-17.45	14.20
RD047	MB	05/11/17	379	-17.87	14.86
RD048	MB	05/11/17	335	-18.09	13.66
RD049	MB	05/11/17	353	-17.78	14.99
RD050	MB	05/11/17	381	-17.69	14.48
RD051	MB	05/11/17	369	-17.32	14.38
RD052	MB	11/15/16	386	-17.92	14.94
RD053	AB	11/15/16	374	-14.53	10.50
RD054	AB	11/15/16	370	-14.06	10.99
RD055	AB	05/16/17	440	-14.16	11.73
RD056	AB	05/16/17	504	-13.87	12.47

Table A. Continued.

Fish ID	Location Captured	Date Captured	TL (mm)	$\delta^{13}C$	$\delta^{15}N$
RD057	AB	05/16/17	536	-13.91	13.30
RD058	AB	05/16/17	456	-14.15	11.99
RD059	AB	05/16/17	529	-13.26	12.27
RD060	AB	05/16/17	398	-14.42	12.57
RD061	AB	05/16/17	395	-14.92	11.89
RD062	AB	05/16/17	385	-15.19	12.69
RD063	AB	05/16/17	380	-14.92	11.13
RD064	AB	05/16/17	438	-14.66	12.04
RD065	AB	05/16/17	397	-13.76	11.67
RD066	AB	05/16/17	445	-13.50	12.13
RD067	AB	05/11/17	337	-13.77	10.95
RD068	MB	05/11/17	370	-17.94	14.75
RD069	MB	05/11/17	383	-18.10	14.56
RD070	MB	05/11/17	405	-18.11	14.09
RD071	MB	05/11/17	358	-17.28	13.55
RD072	MB	05/11/17	367	-18.76	14.99
RD073	MB	05/11/17	355	-17.50	14.20
RD074	MB	05/11/17	371	-18.31	14.81
RD075	MB	05/11/17	373	-18.33	14.65
RD076	MB	05/11/17	391	-18.29	14.94

Table A. Continued.

Fish ID	Location Captured	Date Captured	TL (mm)	$\delta^{13}C$	$\delta^{15}N$
RD077	MB	05/11/17	396	-17.79	14.60
RD078	MB	05/11/17	395	-18.15	15.08
RD079	MB	05/11/17	363	-18.51	15.03
RD080	MB	05/11/17	370	-16.88	14.29
RD081	MB	05/11/17	385	-17.49	14.34
RD082	MB	05/11/17	384	-18.50	13.54
RD083	MB	05/09/17	358	-18.03	15.00
RD084	MI	05/09/17	370	-14.99	12.32
RD085	MI	05/09/17	354	-14.77	12.39
RD086	MI	05/11/17	339	-14.82	11.71
RD087	MB	05/11/17	360	-17.45	14.99
RD088	MB	05/11/17	385	-17.81	14.57
RD089	MB	05/11/17	348	-17.47	13.85
RD090	MB	05/11/17	410	-18.20	14.47
RD091	MB	05/11/17	341	-17.51	14.56
RD092	MB	05/11/17	517	-17.33	15.00
RD093	MB	05/11/17	529	-16.04	13.76
RD094	MB	05/11/17	530	-17.13	14.44
RD095	MB	05/11/17	405	-17.83	15.91
RD096	MB	05/09/17	405	-17.93	14.68

Table A. Continued.

Fish ID	Location Captured	Date Captured	TL (mm)	$\delta^{13}C$	$\delta^{15}N$
RD097	MI	05/09/17	401	-15.35	12.83
RD098	MI	05/09/17	375	-16.08	13.19
RD099	MI	05/09/17	358	-15.29	12.74
RD100	MI	11/09/16	366	-15.40	12.79
RD101	MI	5/9/17	361	-15.26	12.84
RD102	MI	5/9/17	364	-15.42	12.97
RD103	AB	5/24/17	410	-15.34	12.66
RD104	AB	5/24/17	391	-16.58	15.34
RD105	AB	5/24/17	526	-14.47	12.46
RD106	AB	5/24/17	380	-16.20	14.41
RD107	MI	5/9/17	360	-13.91	12.24
RD108	MI	5/9/17	352	-14.65	12.31
RD109	MI	5/9/17	386	-16.03	14.61
RD110	MI	5/9/17	356	-13.97	12.42
RD111	MI	5/9/17	381	-14.26	12.57
RD112	MI	5/9/17	344	-13.68	11.72
RD113	MI	5/9/17	406	-15.97	14.13
RD114	MI	5/9/17	361	-14.50	11.25
RD115	CC	5/23/17	398	-16.64	15.51
RD116	MB	5/17/17	383	-18.32	15.34

Table A. Continued.

Fish ID	Location Captured	Date Captured	TL (mm)	$\delta^{13}C$	$\delta^{15}N$
RD117	MB	5/17/17	395	-17.62	16.32
RD118	MB	5/17/17	394	-18.07	16.36
RD119	AB	6/7/17	719	-14.14	12.47
RD120	CB	6/8/17	358	-21.28	13.68
RD121	NB	6/6/17	385	-16.82	13.43
RD122	NB	6/6/17	429	-18.29	14.54
RD123	CB	5/23/17	428	-18.15	11.48
RD124	CB	5/23/17	395	-18.91	11.54
RD125	CB	5/23/17	403	-18.96	11.53
RD126	CB	5/23/17	407	-18.13	11.67
RD127	CB	5/23/17	427	-19.00	11.43
RD128	CB	5/23/17	366	-17.29	11.11
RD129	CB	5/23/17	368	-18.74	12.63
RD130	CB	5/23/17	370	-18.24	10.96
RD131	CB	5/23/17	380	-18.70	11.79
RD132	CB	5/23/17	415	-18.18	11.21
RD133	CB	5/23/17	379	-17.36	11.90
RD134	CB	5/23/17	399	-18.64	11.27
RD135	CB	6/7/17	424	-13.96	11.30
RD136	CB	6/7/17	371	-14.92	11.02

Table A. Continued.

Fish ID	Location Captured	Date Captured	TL (mm)	$\delta^{13}C$	$\delta^{15}N$
RD137	CB	6/7/17	423	-15.04	12.59
RD138	CB	6/7/17	510	-13.37	11.10
RD139	CB	6/7/17	515	-14.31	11.96
RD140	CB	6/7/17	452	-13.95	11.13
RD141	CB	6/7/17	367	-16.08	11.78
RD142	CB	6/7/17	530	-14.25	12.08
RD143	CB	6/7/17	532	-13.95	11.84
RD144	CB	6/7/17	484	-14.26	12.04
RD145	CB	6/7/17	518	-14.48	12.09
RD146	CB	6/7/17	500	-14.41	12.54
RD147	CB	6/7/17	393	-14.82	10.98
RD148	CB	6/7/17	378	-14.67	11.06
RD149	CB	6/7/17	365	-13.33	10.80
RD150	AB	6/7/17	397	-14.88	11.46
RD151	AB	6/7/17	475	-14.18	11.72
RD152	AB	6/7/17	455	-14.07	11.64
RD153	AB	6/7/17	453	-13.91	11.84
RD154	AB	6/7/17	496	-14.26	11.52
RD155	AB	6/7/17	558	-13.90	11.45
RD156	AB	6/7/17	514	-14.20	11.41

Table A. Continued.

Fish ID	Location Captured	Date Captured	TL (mm)	$\delta^{13}C$	$\delta^{15}N$
RD157	AB	6/7/17	467	-13.87	12.14
RD158	AB	6/7/17	477	-13.67	11.22
RD159	AB	6/7/17	478	-14.40	11.79
RD160	AB	6/7/17	413	-14.49	10.74
RD161	AB	6/7/17	356	-14.36	11.08
RD162	AB	6/7/17	348	-15.63	11.95
RD163	NB	6/7/17	485	-18.15	15.93
RD164	NB	6/7/17	540	-17.41	15.61
RD165	NB	6/7/17	529	-17.31	14.06
RD166	NB	6/7/17	430	-17.06	15.09
RD167	NB	6/7/17	386	-17.03	14.56
RD168	NB	6/7/17	411	-17.77	13.09
RD169	NB	6/7/17	434	-17.46	13.69
RD170	NB	6/7/17	369	-17.26	15.78
RD171	AB	6/7/17	519	-14.23	11.12
RD172	AB	6/7/17	514	-14.31	11.52
RD173	AB	6/7/17	500	-14.51	11.19
RD174	AB	6/7/17	489	-14.58	11.18
RD175	AB	6/7/17	512	-14.26	10.98
RD176	AB	6/7/17	462	-14.30	11.32

Table A. Continued.

Fish ID	Location Captured	Date Captured	TL (mm)	$\delta^{13}C$	$\delta^{15}N$
RD177	AB	6/7/17	512	-14.15	11.35
RD178	AB	6/7/17	512	-14.26	10.98
RD179	NB	6/7/17	546	-16.92	15.06
RD180	NB	6/7/17	520	-17.83	14.86
RD181	NB	6/7/17	432	-18.44	13.56
RD182	NB	6/7/17	416	-17.84	14.42
RD183	NB	6/7/17	365	-16.84	14.57
RD184	AB	5/15/17	470	-13.99	12.59
RD185	AB	5/15/17	345	-14.83	13.19
RD186	AB	5/15/17	325	-14.34	12.27
RD187	AB	5/15/17	340	-13.80	12.64
RD188	AB	5/15/17	321	-14.79	13.06
RD189	AB	5/15/17	383	-14.83	13.07
RD190	AB	5/15/17	375	-14.53	12.43
RD191	AB	5/15/17	493	-14.34	12.20
RD192	AB	5/15/17	334	-15.47	12.90
RD193	AB	5/15/17	561	-14.24	13.15
RD194	AB	5/15/17	518	-14.12	12.94
RD195	AB	5/15/17	562	-14.07	12.84
RD196	AB	5/15/17	573	-13.96	12.65

Table A. Continued.

Fish ID	Location Captured	Date Captured	TL (mm)	$\delta^{13}C$	$\delta^{15}N$
RD197	AB	5/15/17	556	-14.05	13.16
RD198	NB	6/6/17	397	-17.25	16.94
RD199	NB	6/6/17	381	-16.86	16.12
RD200	NB	6/6/17	401	-17.17	16.30
RD201	NB	6/6/17	397	-17.19	17.01

Appendix 2: Supplemental Otolith Graphs.

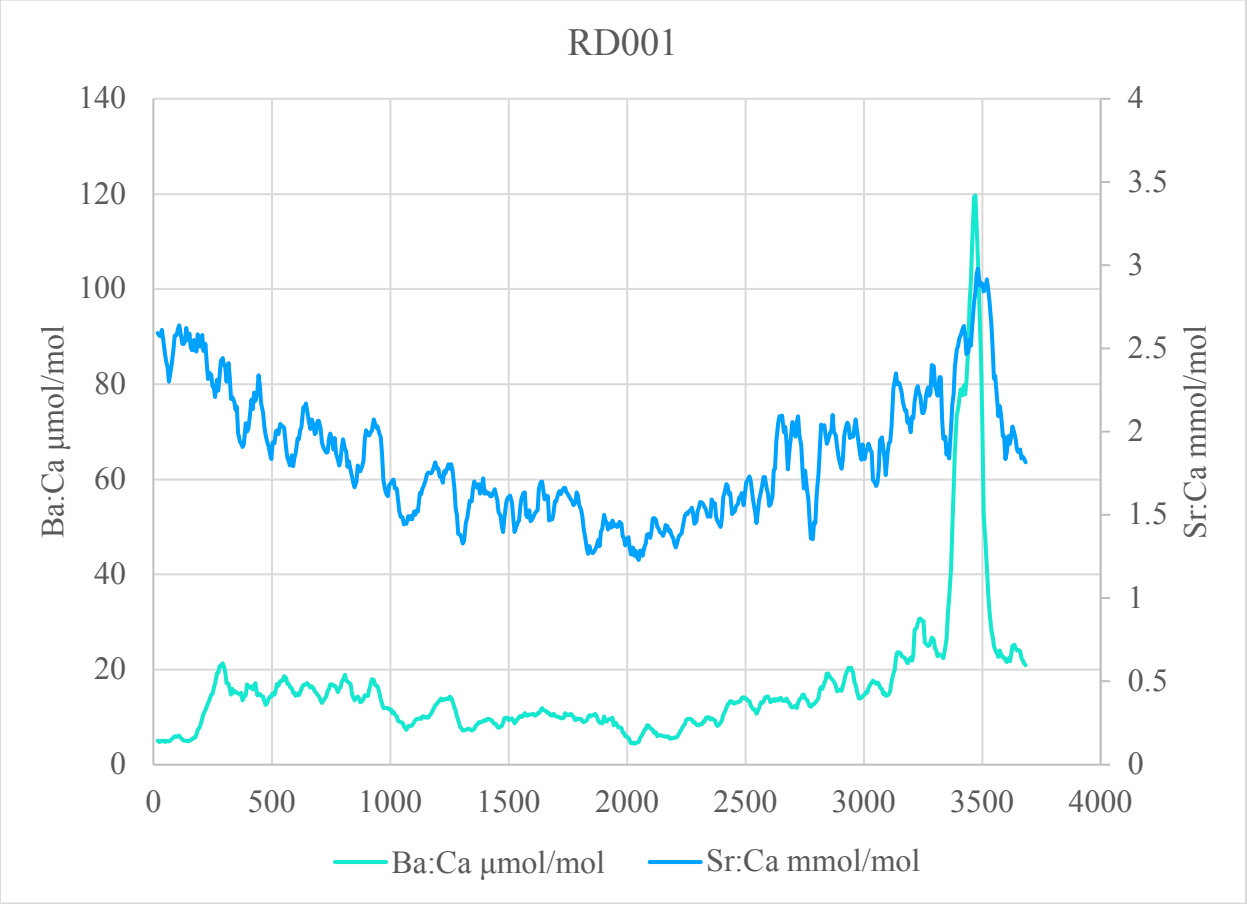

Figure A.1. The Ba:Ca and Sr:Ca life history profile of individual RD001.

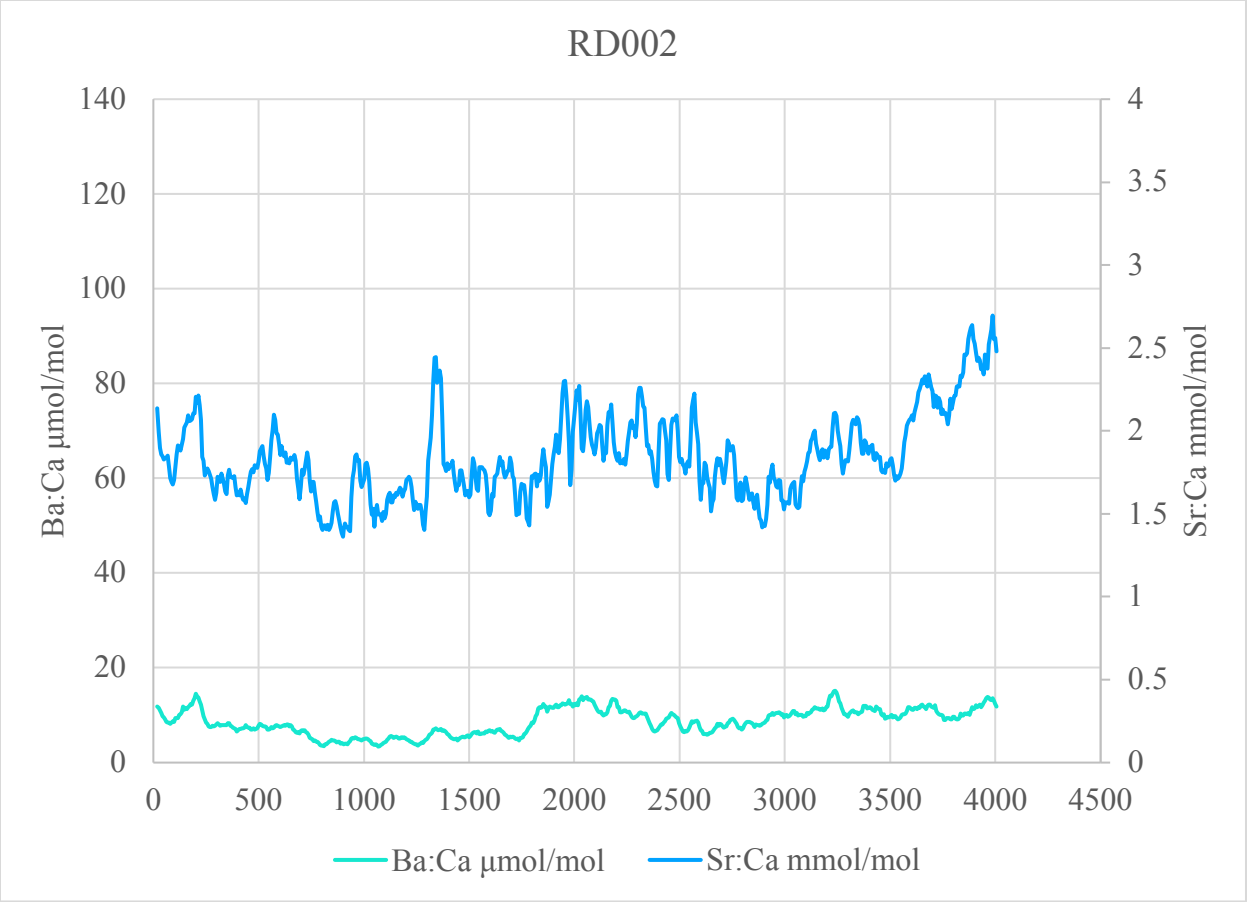

Figure A.2. The Ba:Ca and Sr:Ca life history profile of individual RD002.

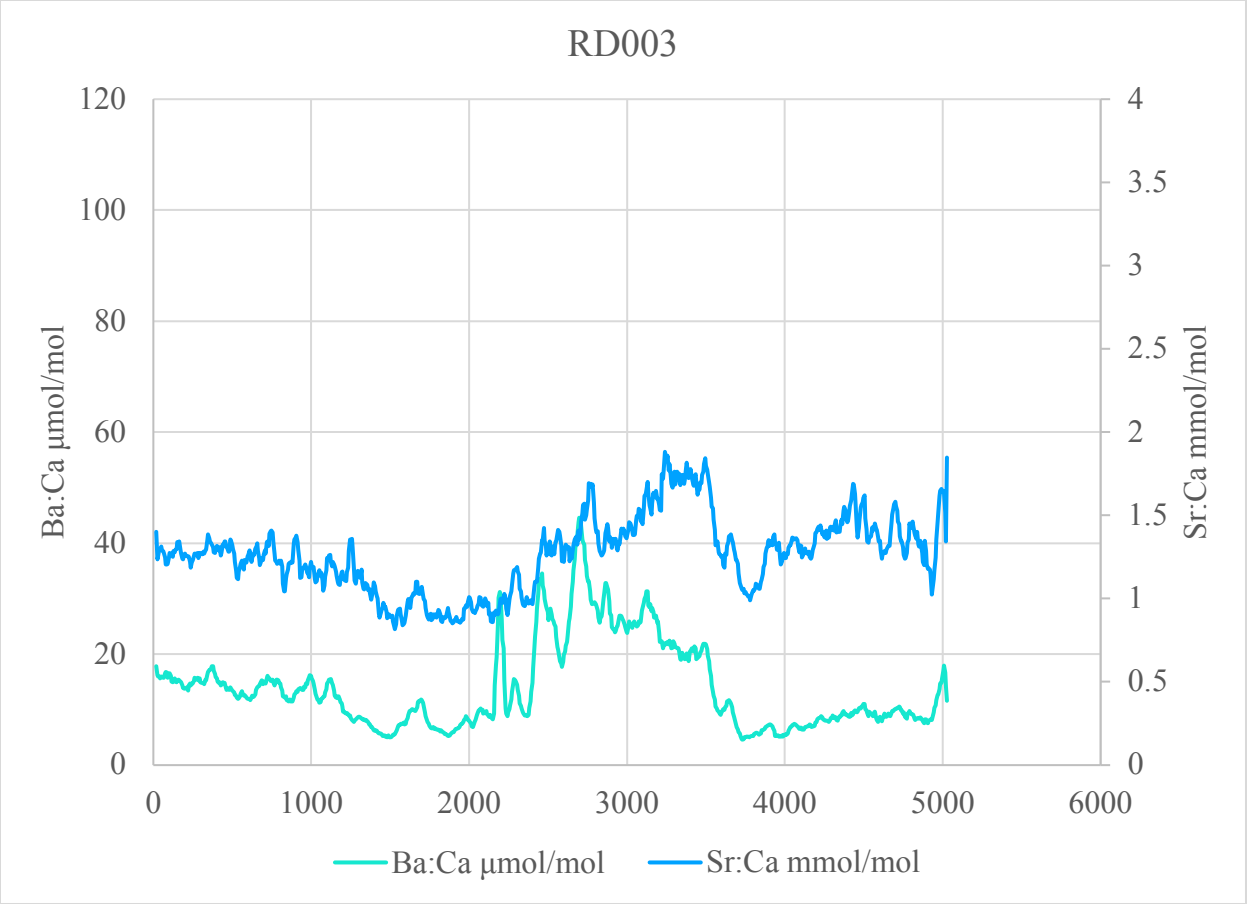

Figure A.3. The Ba:Ca and Sr:Ca life history profile of individual RD003.

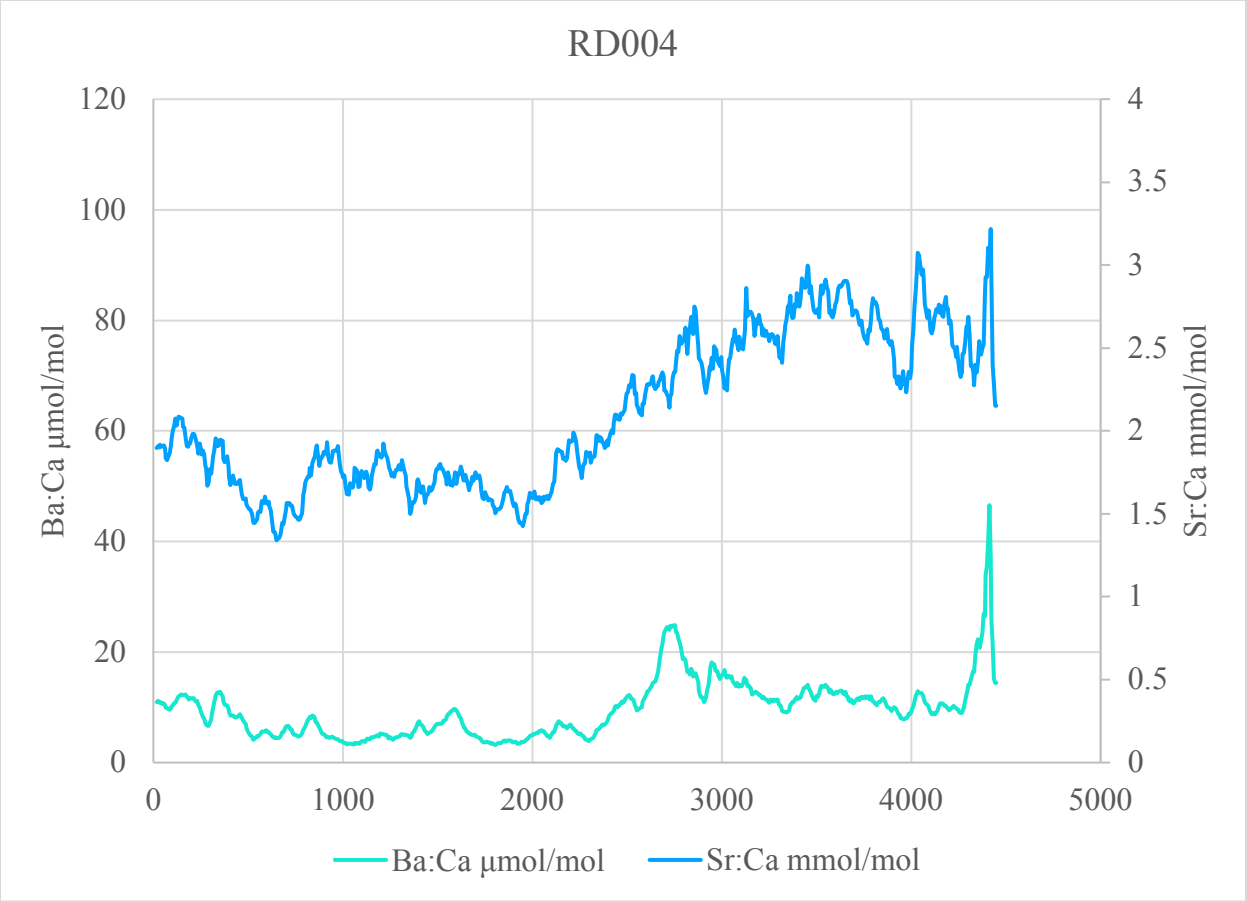

Figure A.4. The Ba:Ca and Sr:Ca life history profile of individual RD004.

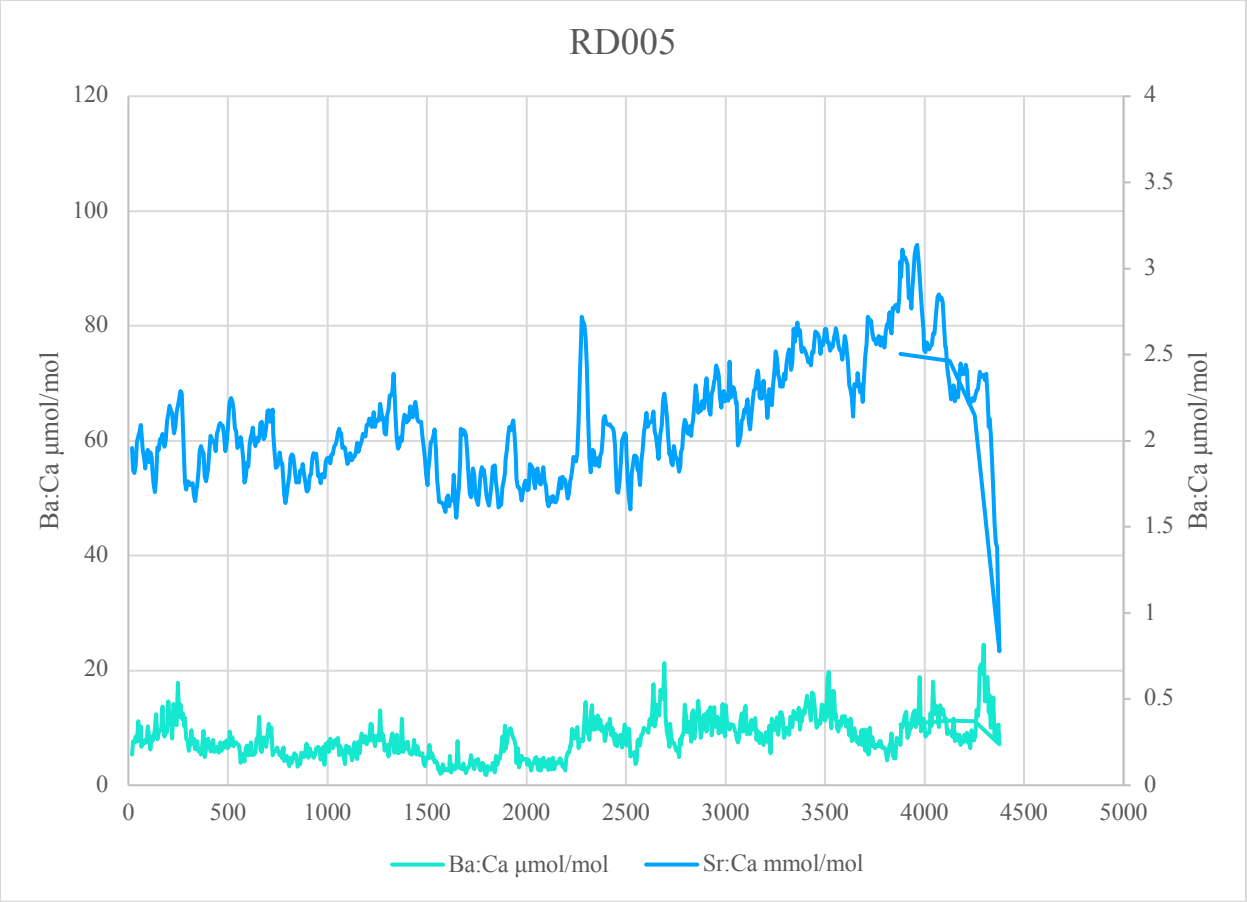

Figure A.5. The Ba:Ca and Sr:Ca life history profile of individual RD005.

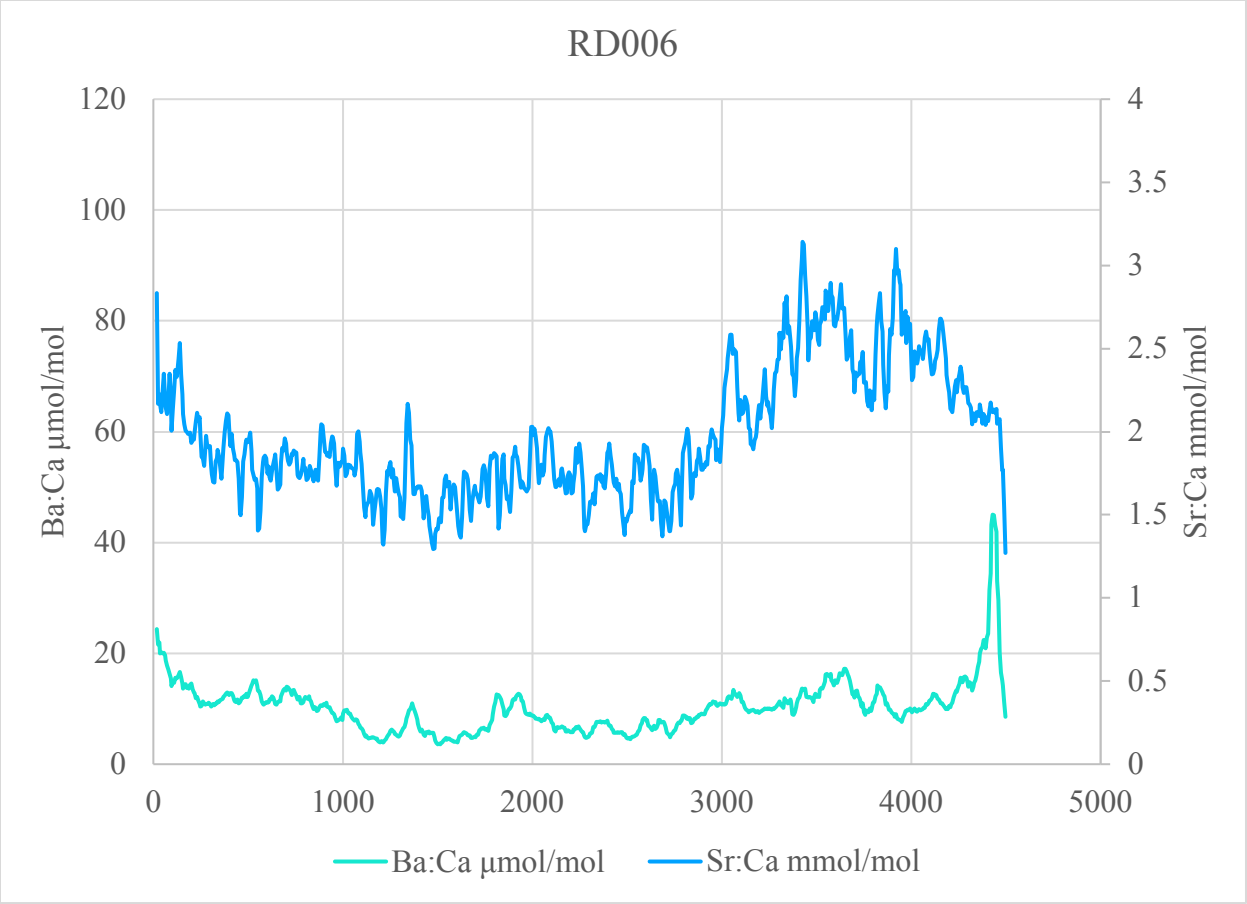

Figure A.6. The Ba:Ca and Sr:Ca life history profile of individual RD006.

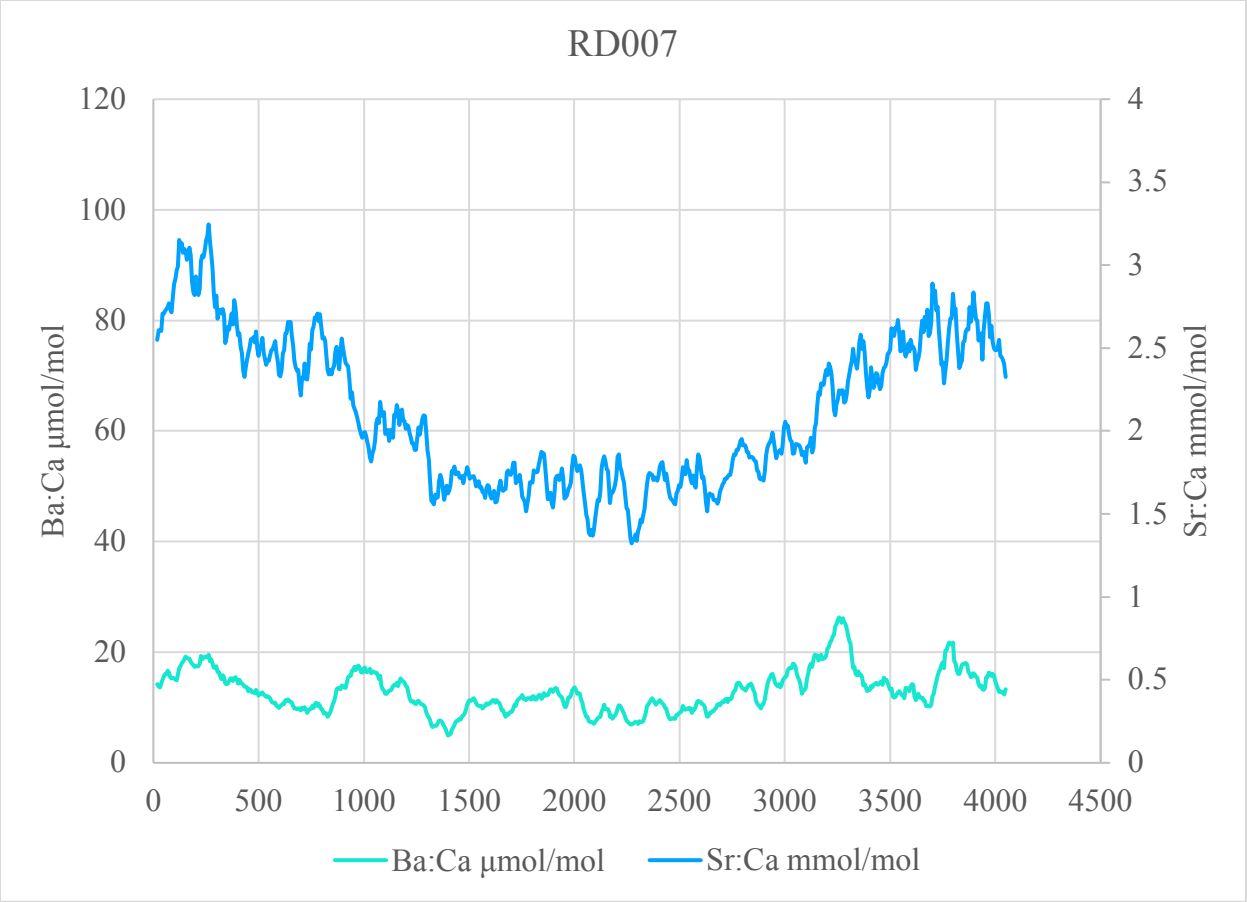

Figure A.7. The Ba:Ca and Sr:Ca life history profile of individual RD007.

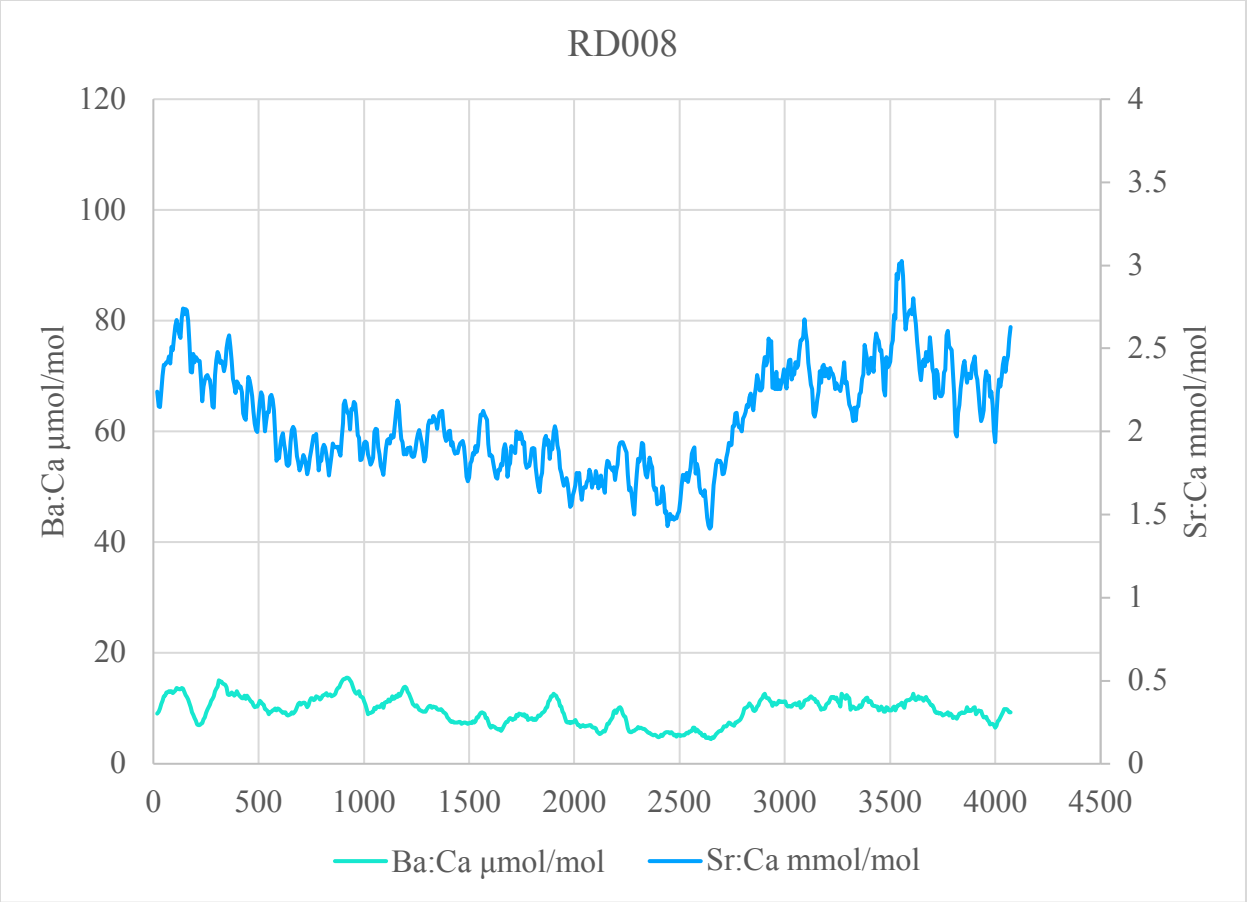

Figure A.8. The Ba:Ca and Sr:Ca life history profile of individual RD008.

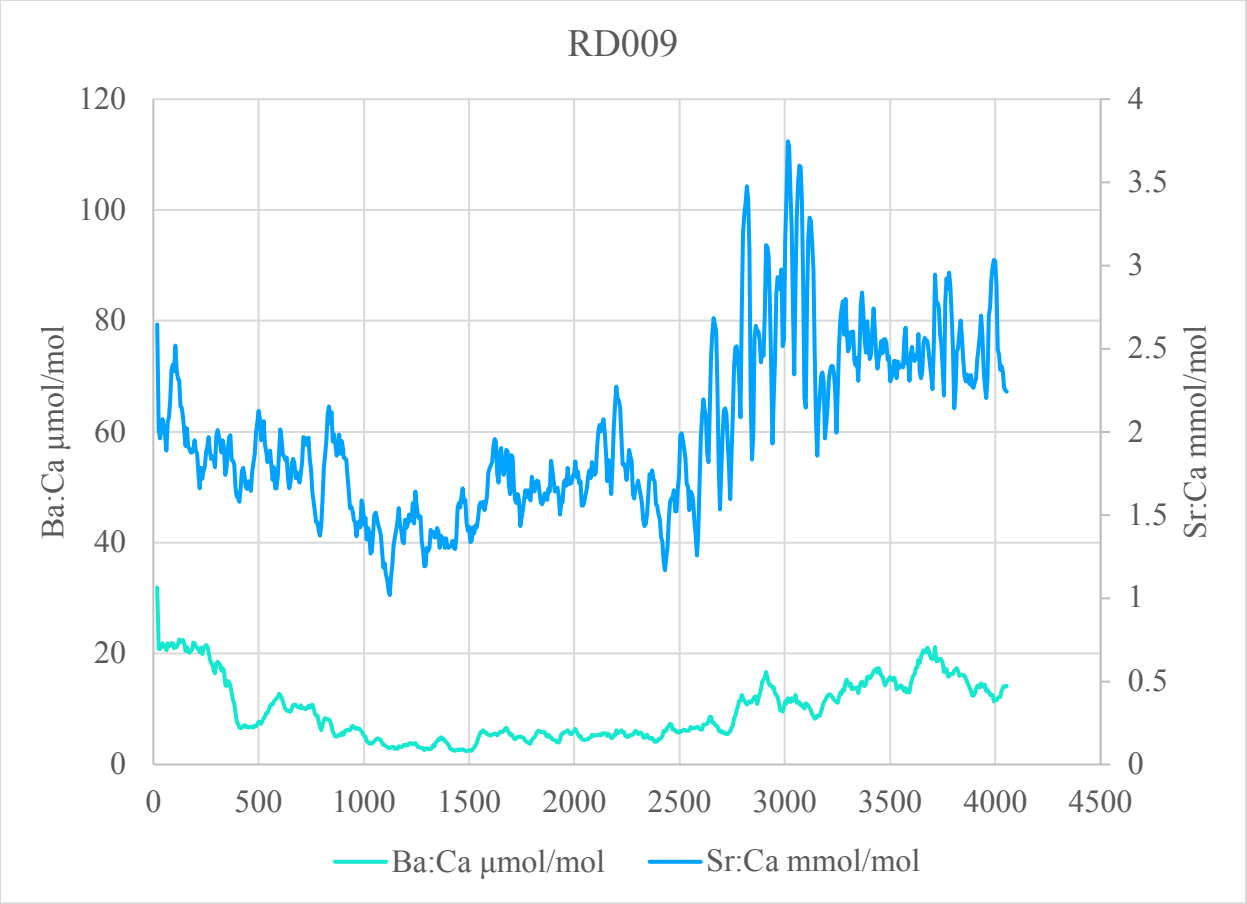

Figure A.9. The Ba:Ca and Sr:Ca life history profile of individual RD009.

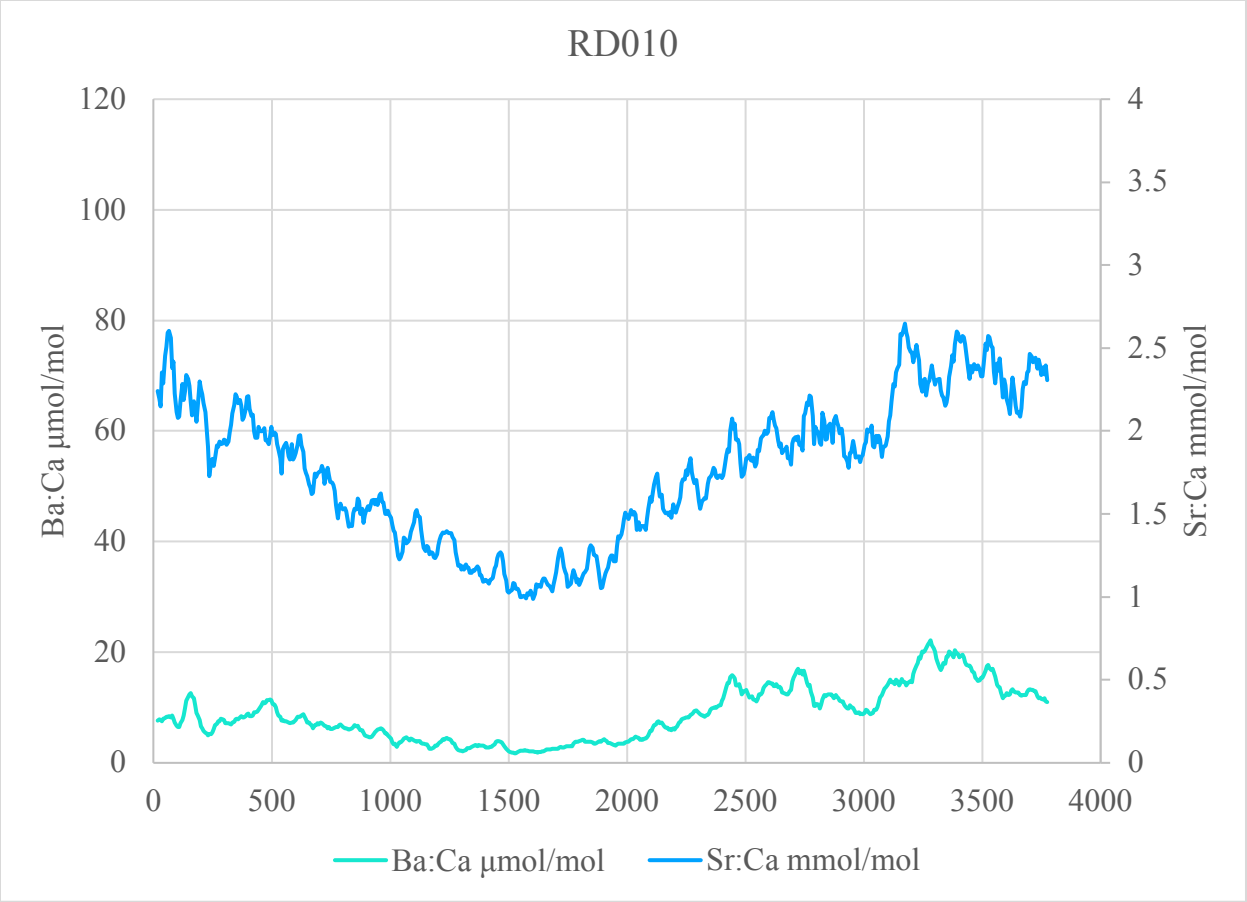

Figure A.10. The Ba:Ca and Sr:Ca life history profile of individual RD010.

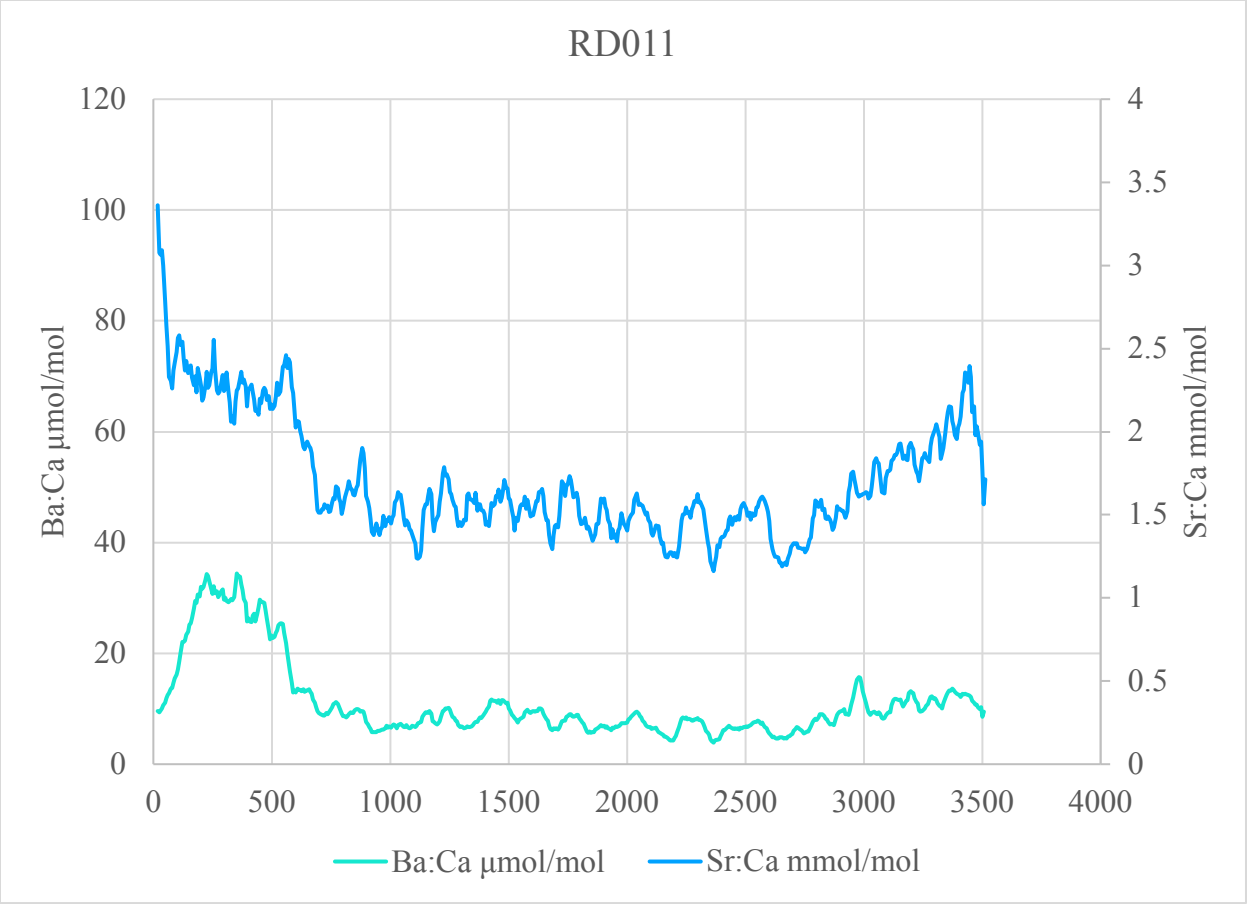

Figure A.11. The Ba:Ca and Sr:Ca life history profile of individual RD011.

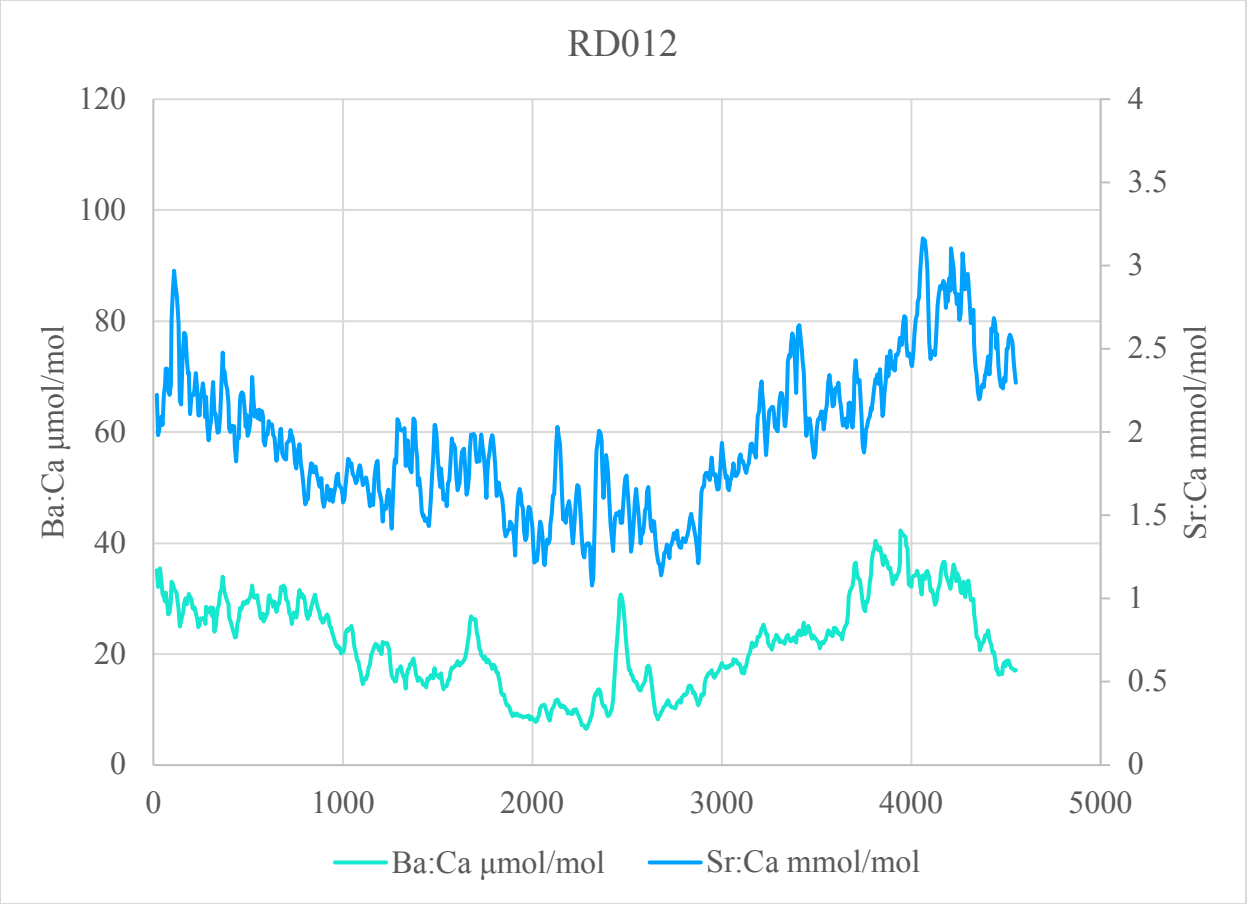

Figure A.12. The Ba:Ca and Sr:Ca life history profile of individual RD012.

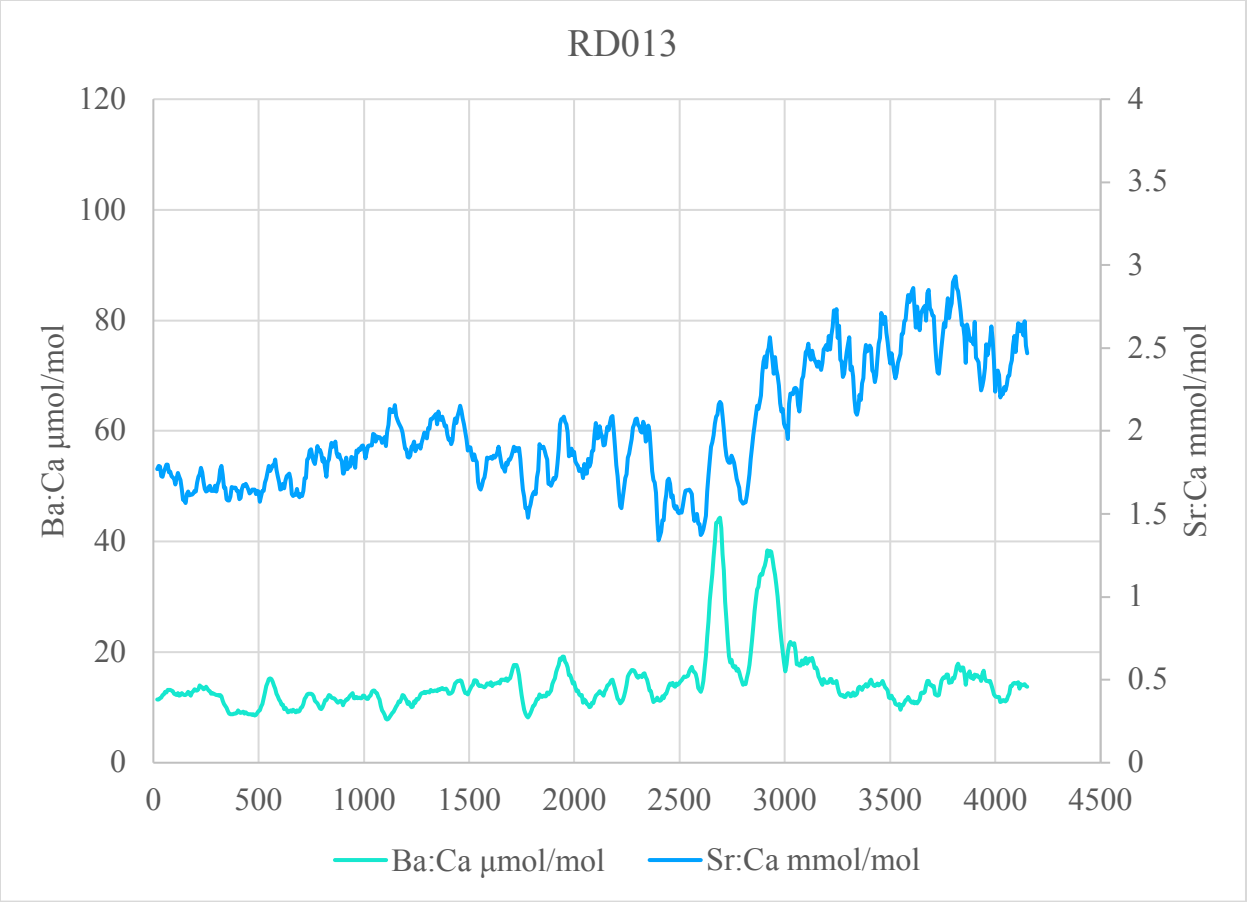

Figure A.13. The Ba:Ca and Sr:Ca life history profile of individual RD013.

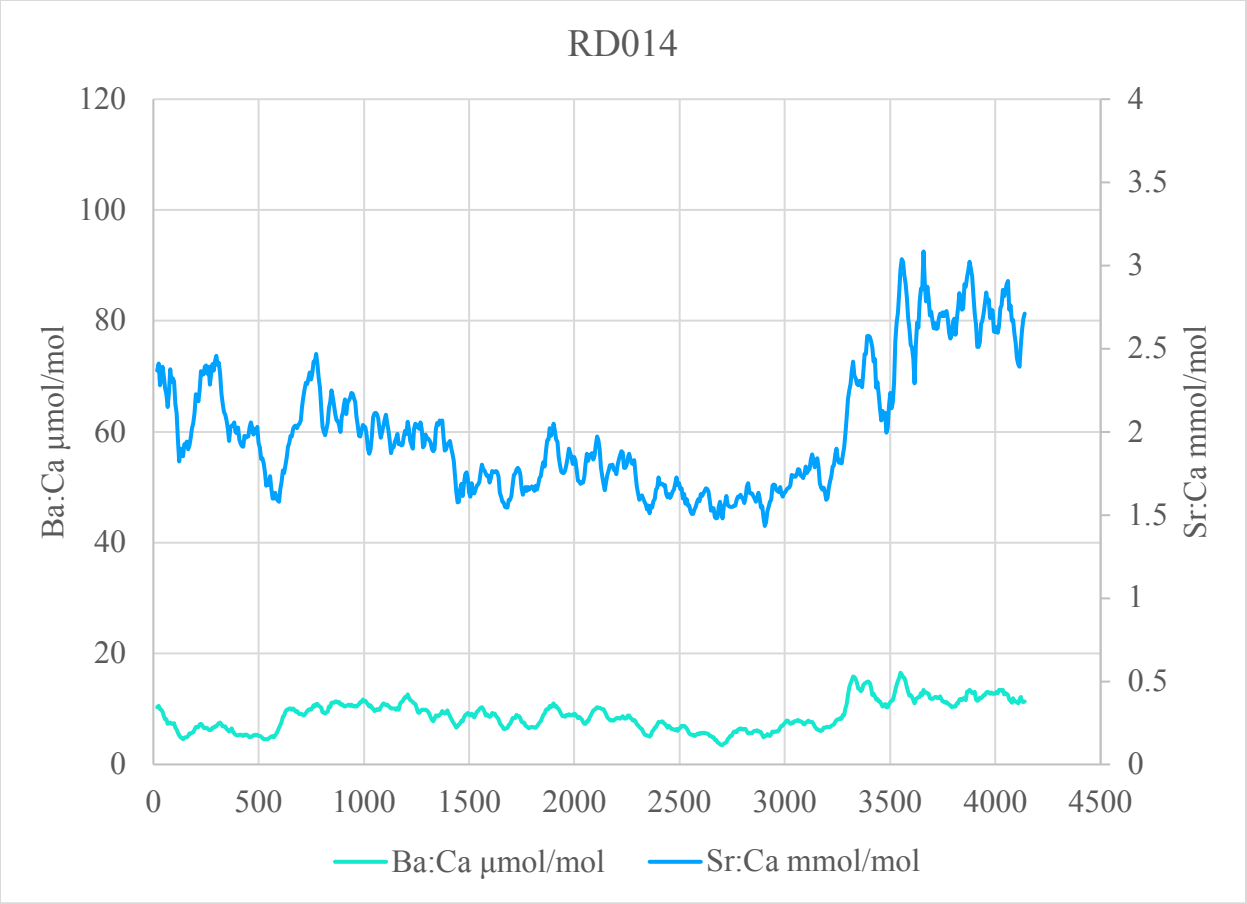

Figure A.14. The Ba:Ca and Sr:Ca life history profile of individual RD014.

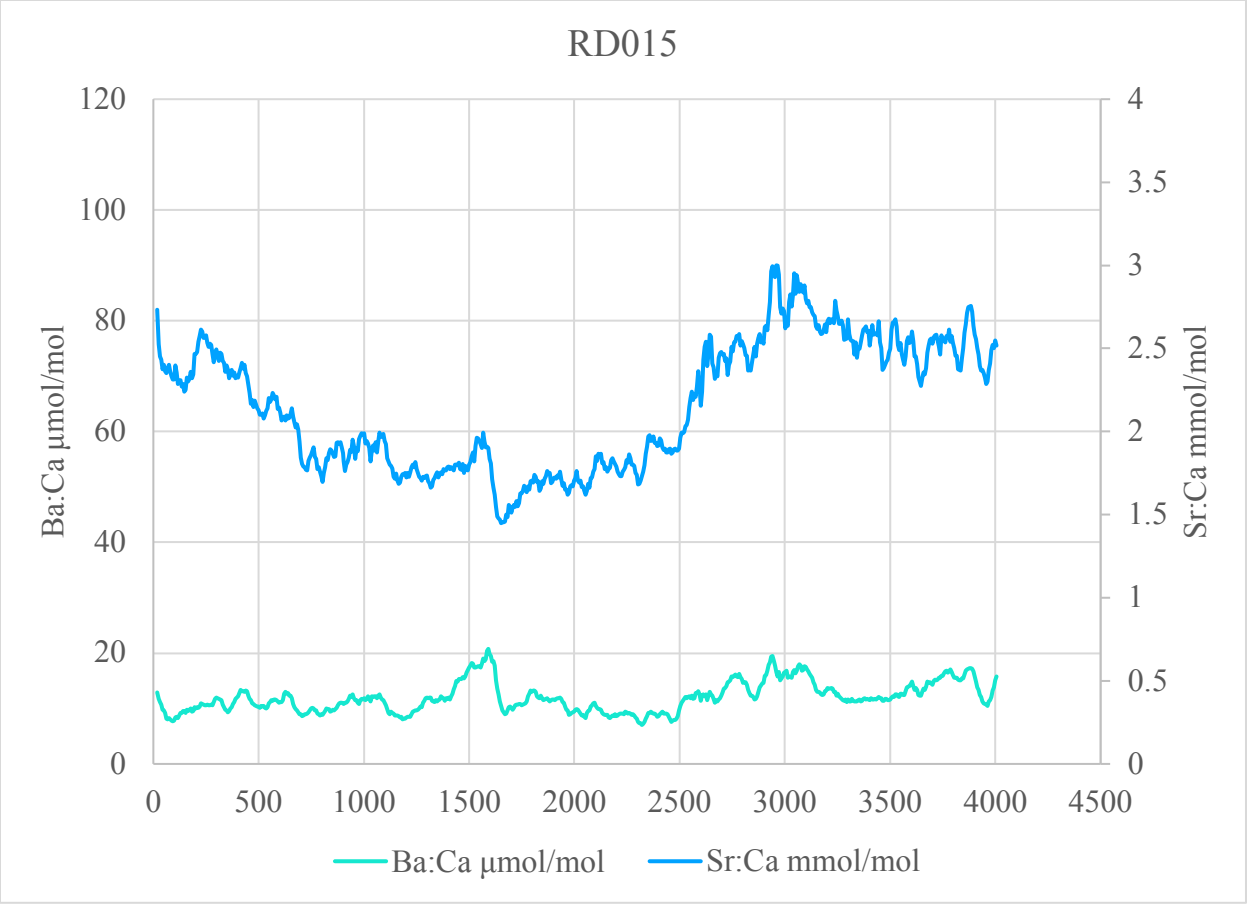

Figure A.15. The Ba:Ca and Sr:Ca life history profile of individual RD015.

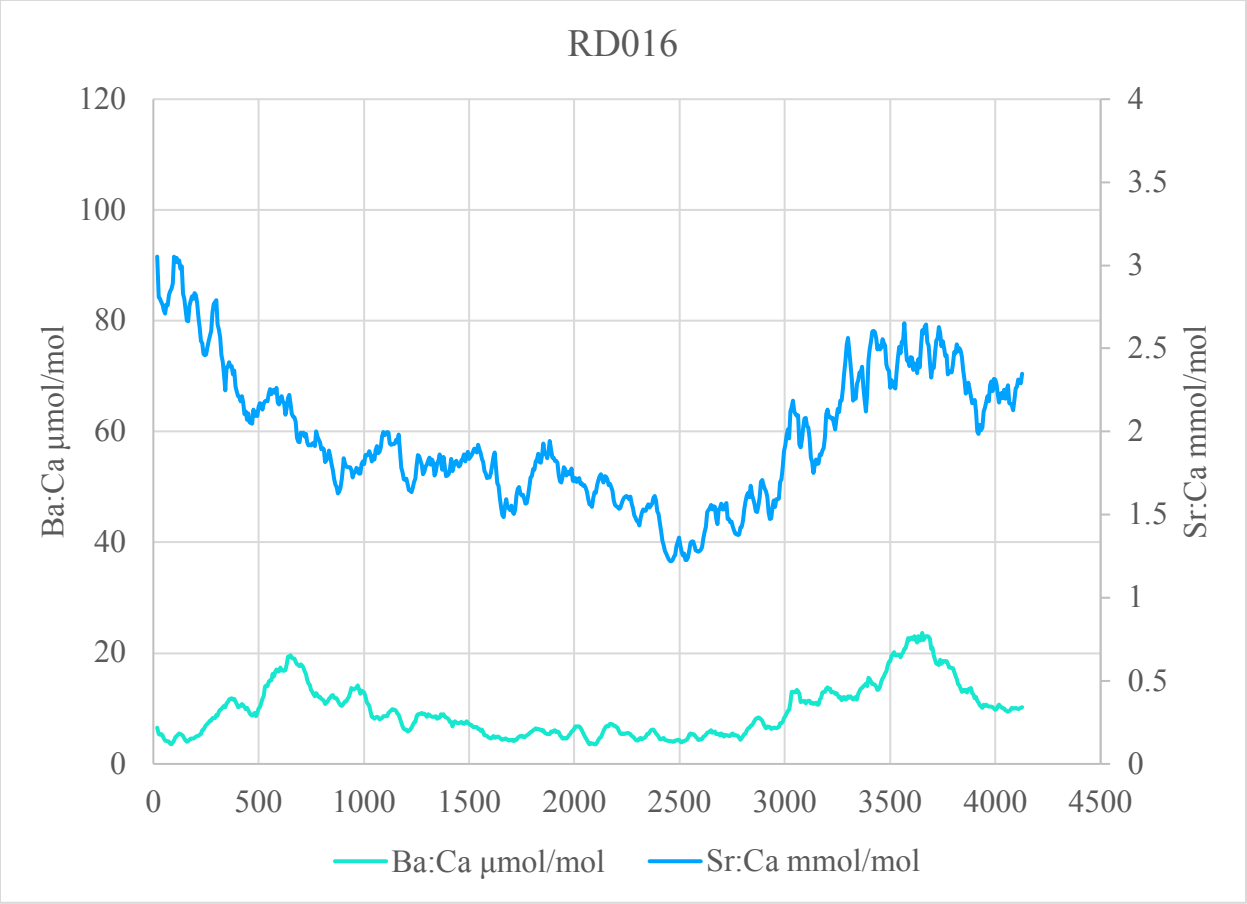

Figure A.16. The Ba:Ca and Sr:Ca life history profile of individual RD016.

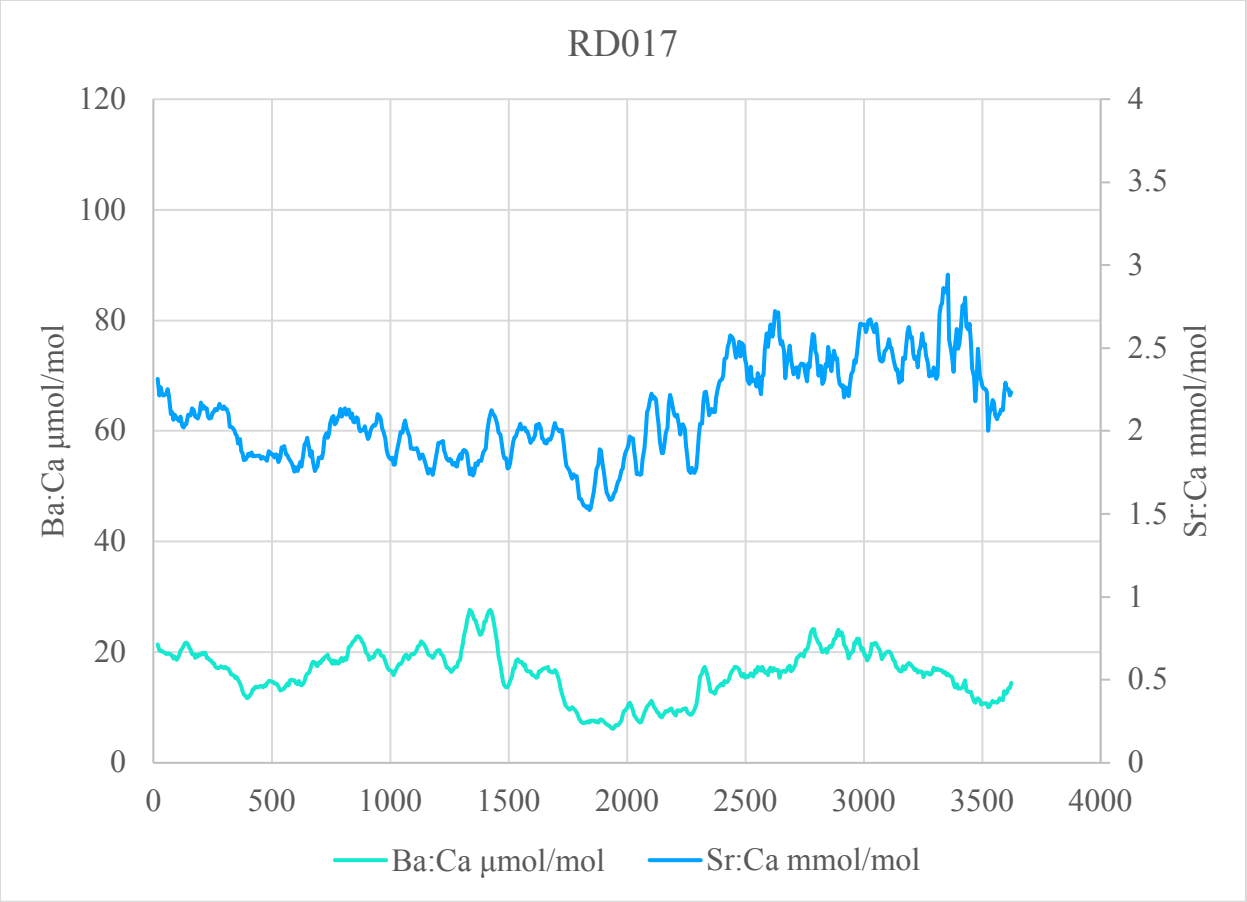

Figure A.17. The Ba:Ca and Sr:Ca life history profile of individual RD017.

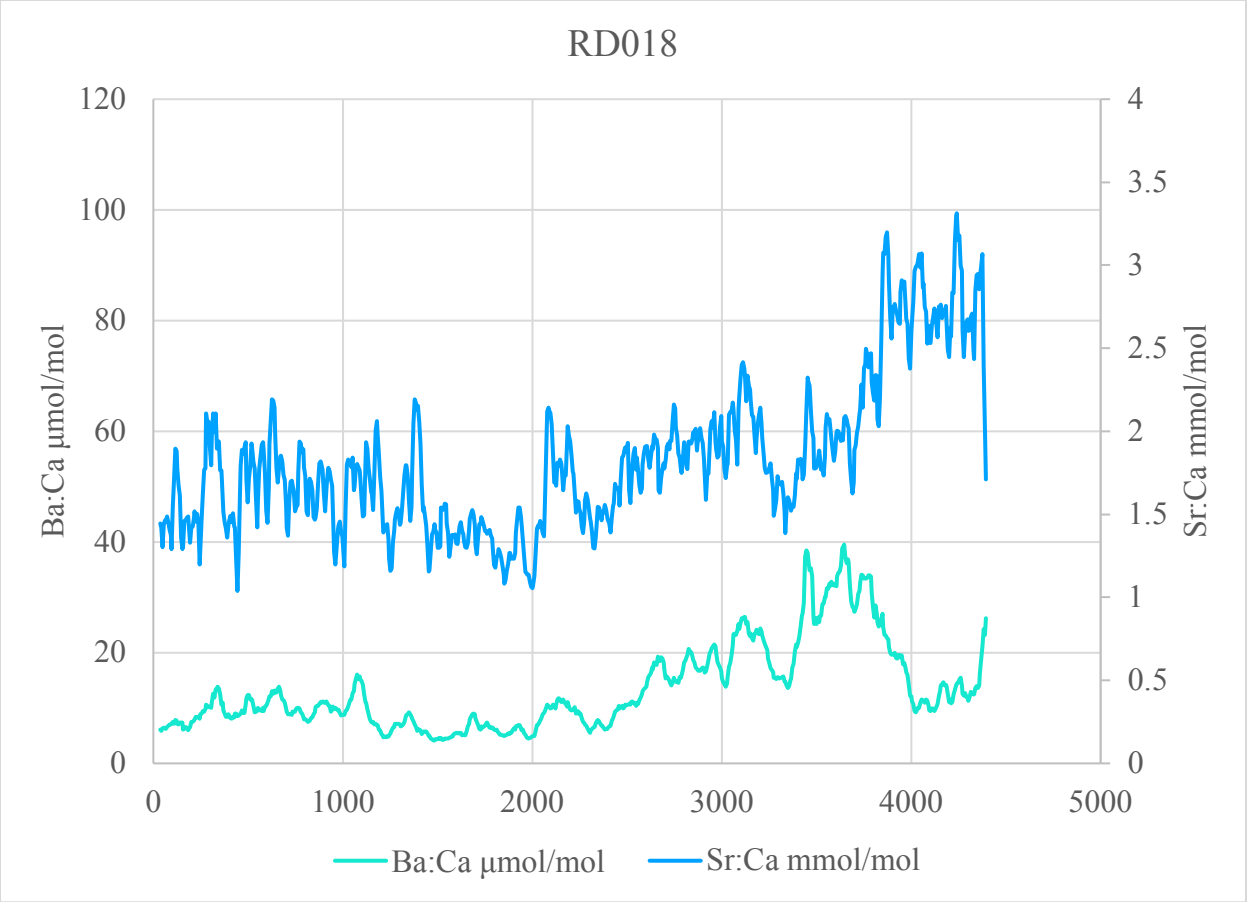

Figure A.18. The Ba:Ca and Sr:Ca life history profile of individual RD018.

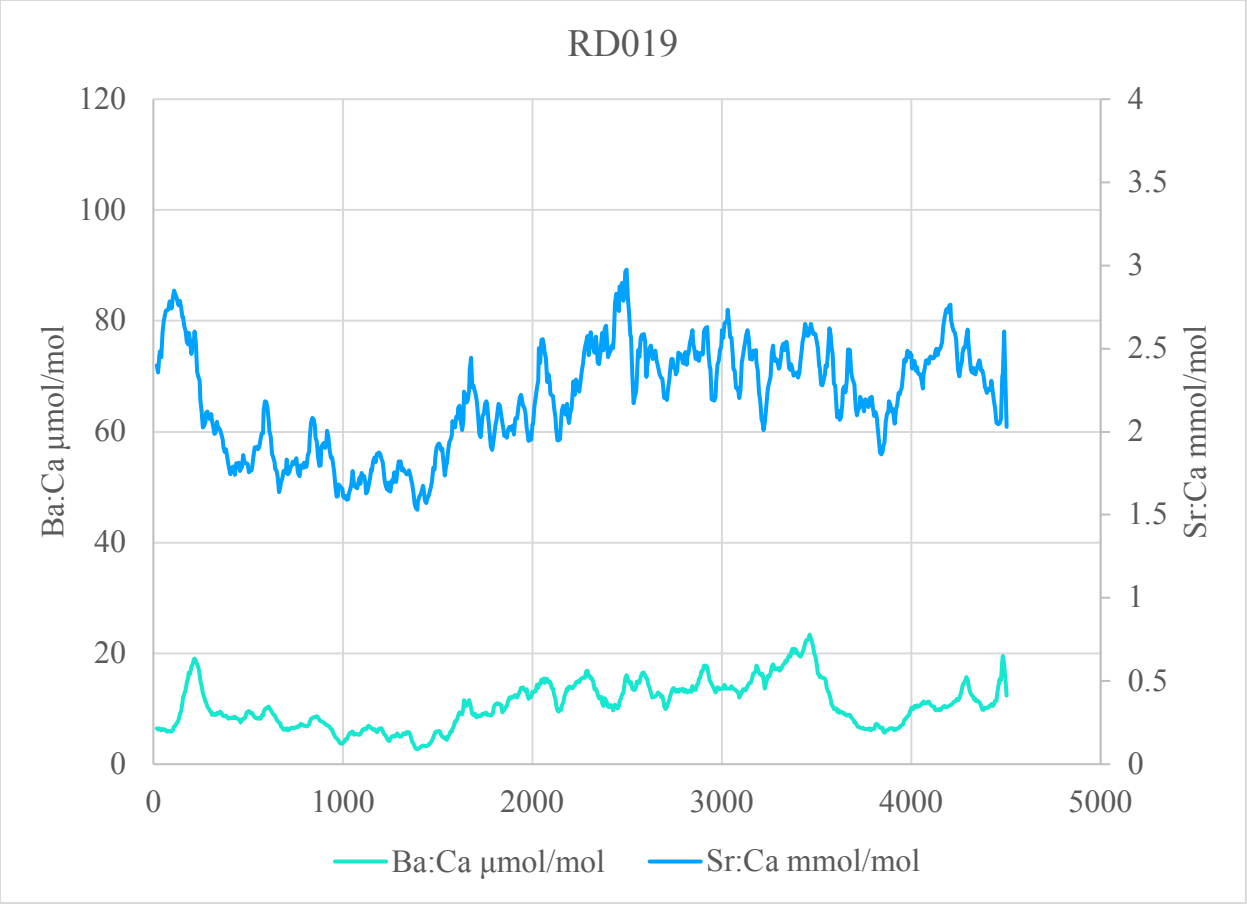

Figure A.19. The Ba:Ca and Sr:Ca life history profile of individual RD019.

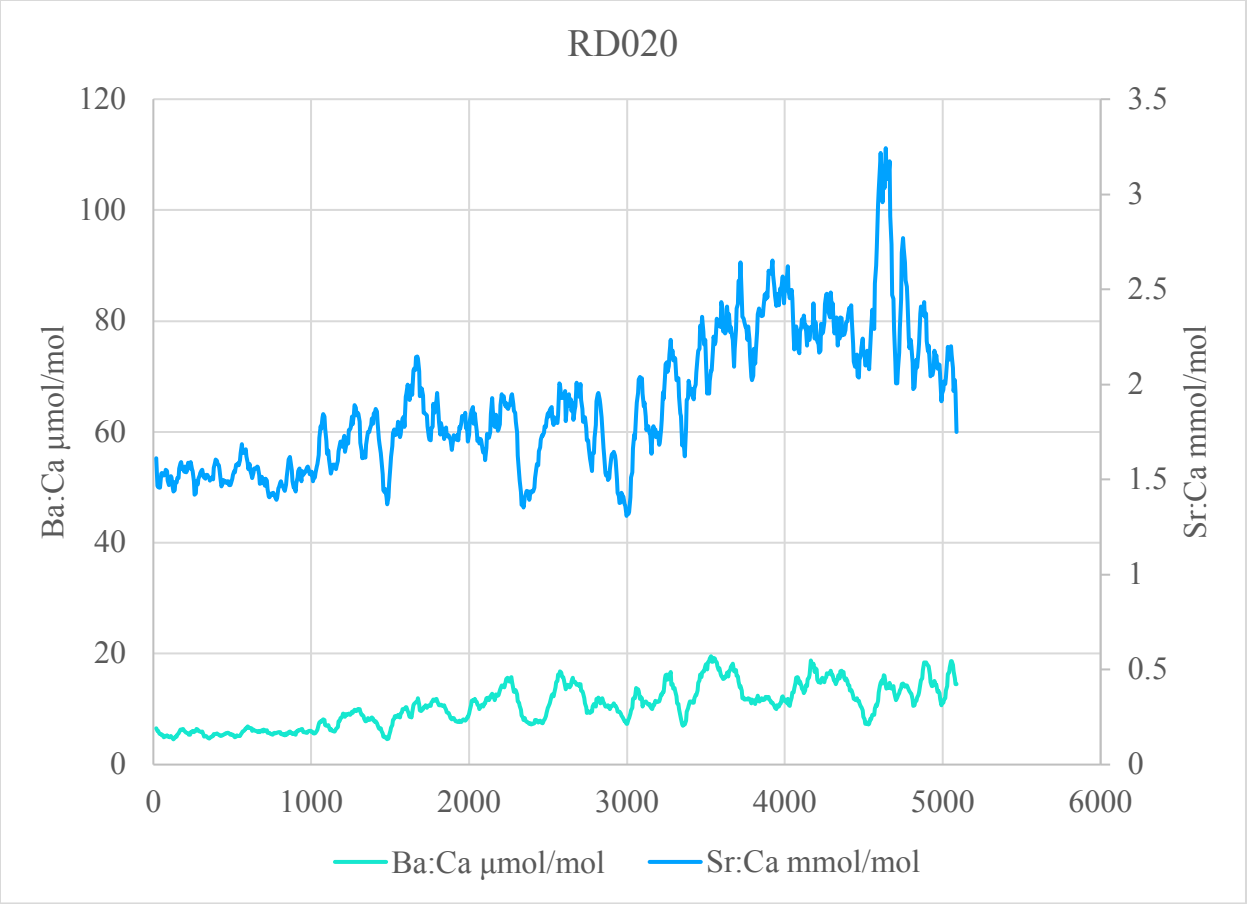

Figure A.20. The Ba:Ca and Sr:Ca life history profile of individual RD020.

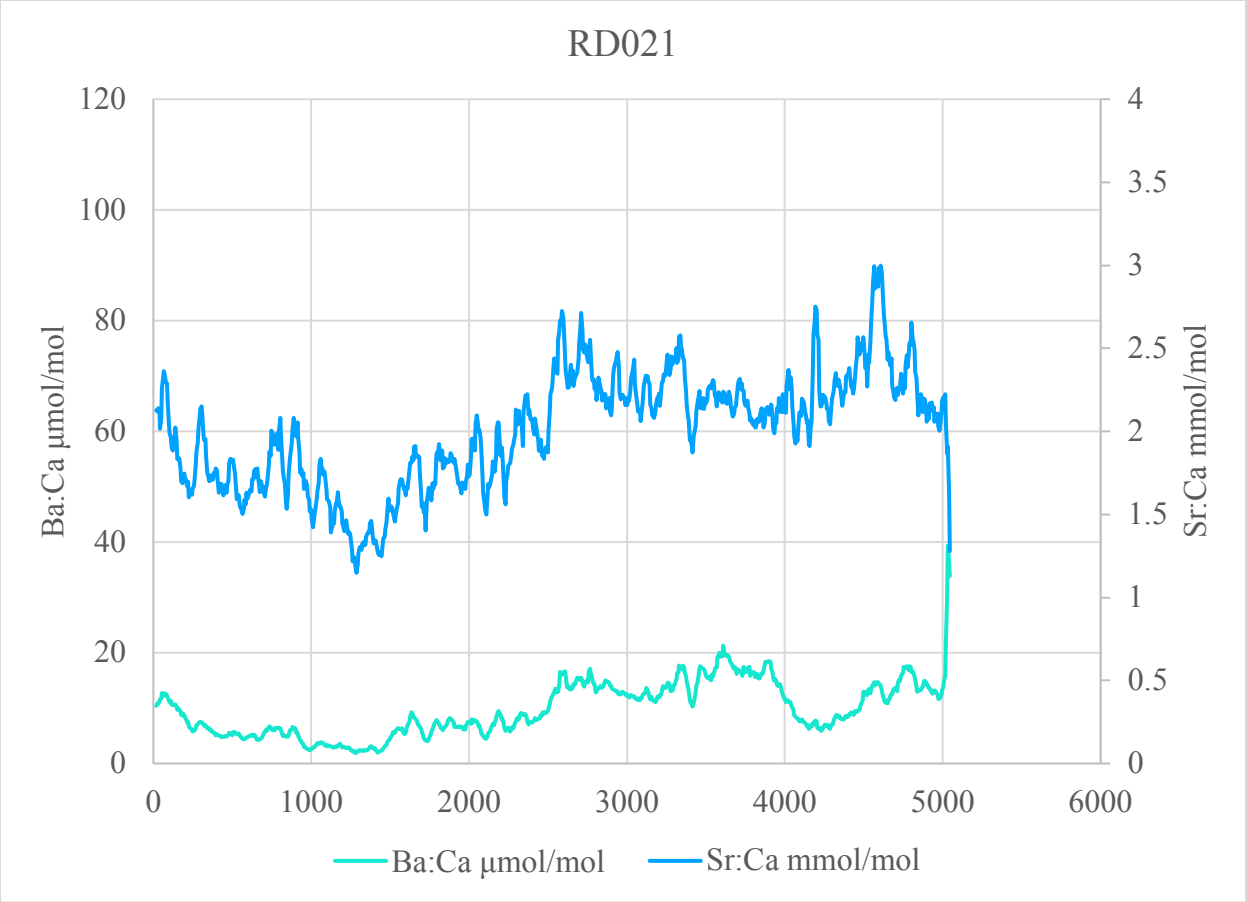

Figure A.21. The Ba:Ca and Sr:Ca life history profile of individual RD021.

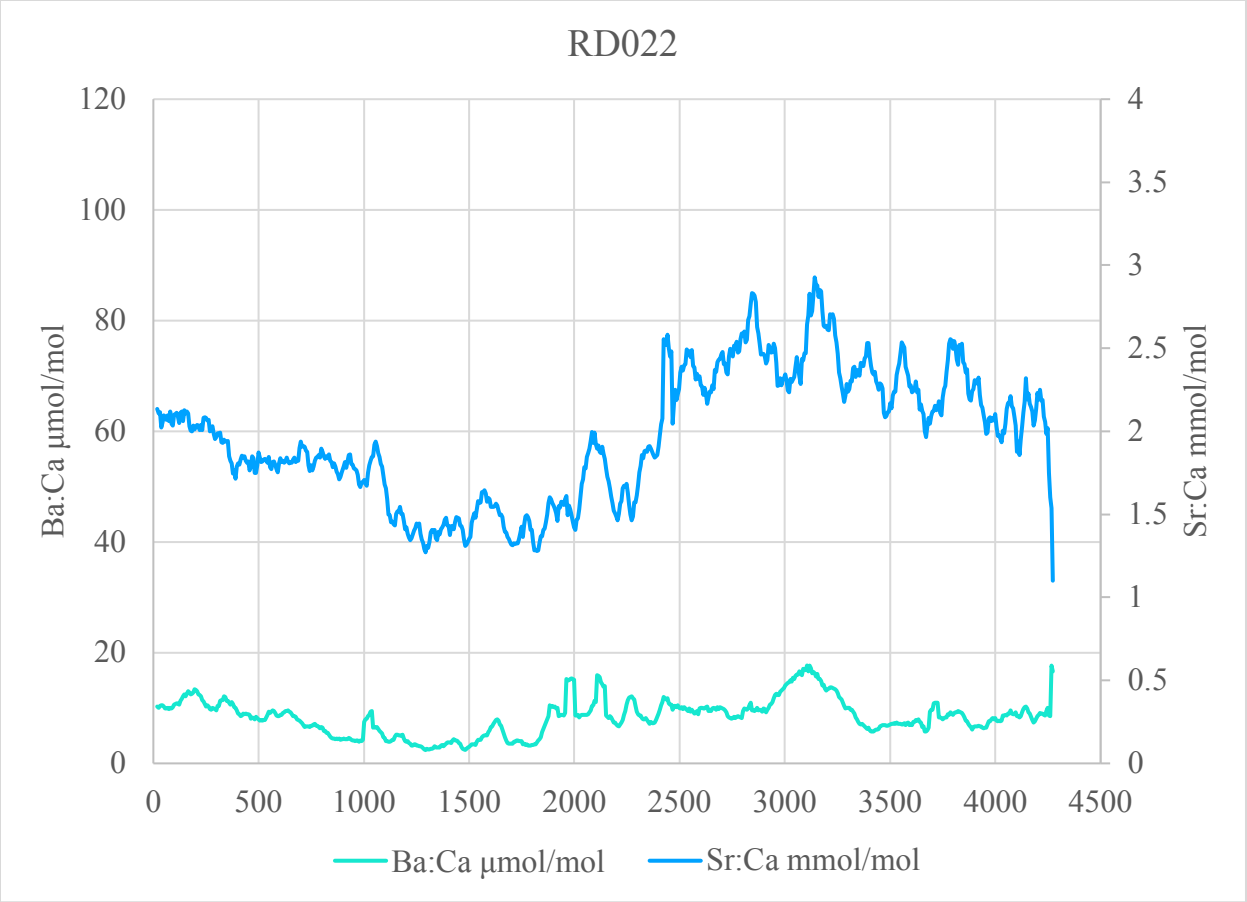

Figure A.22. The Ba:Ca and Sr:Ca life history profile of individual RD022.

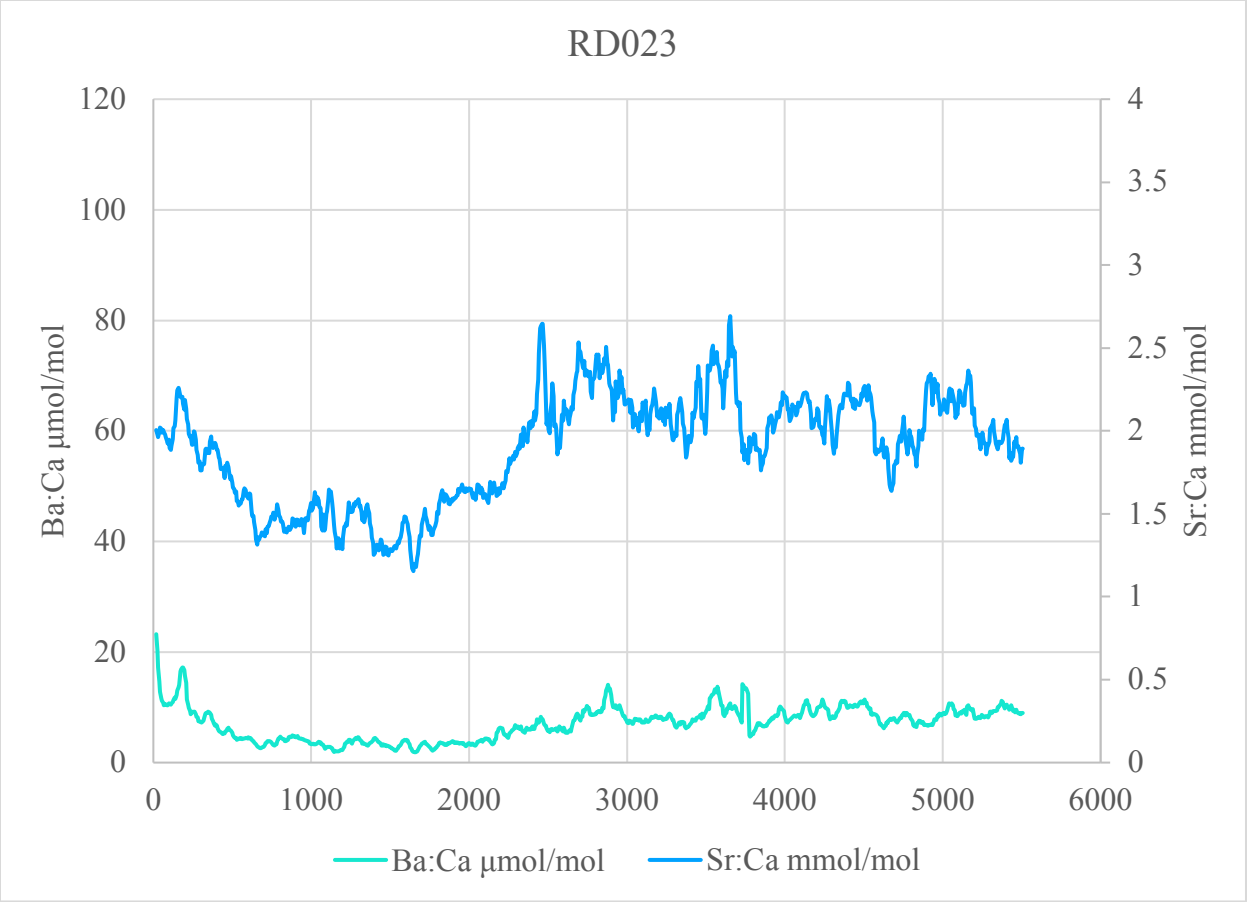

Figure A.23. The Ba:Ca and Sr:Ca life history profile of individual RD023.

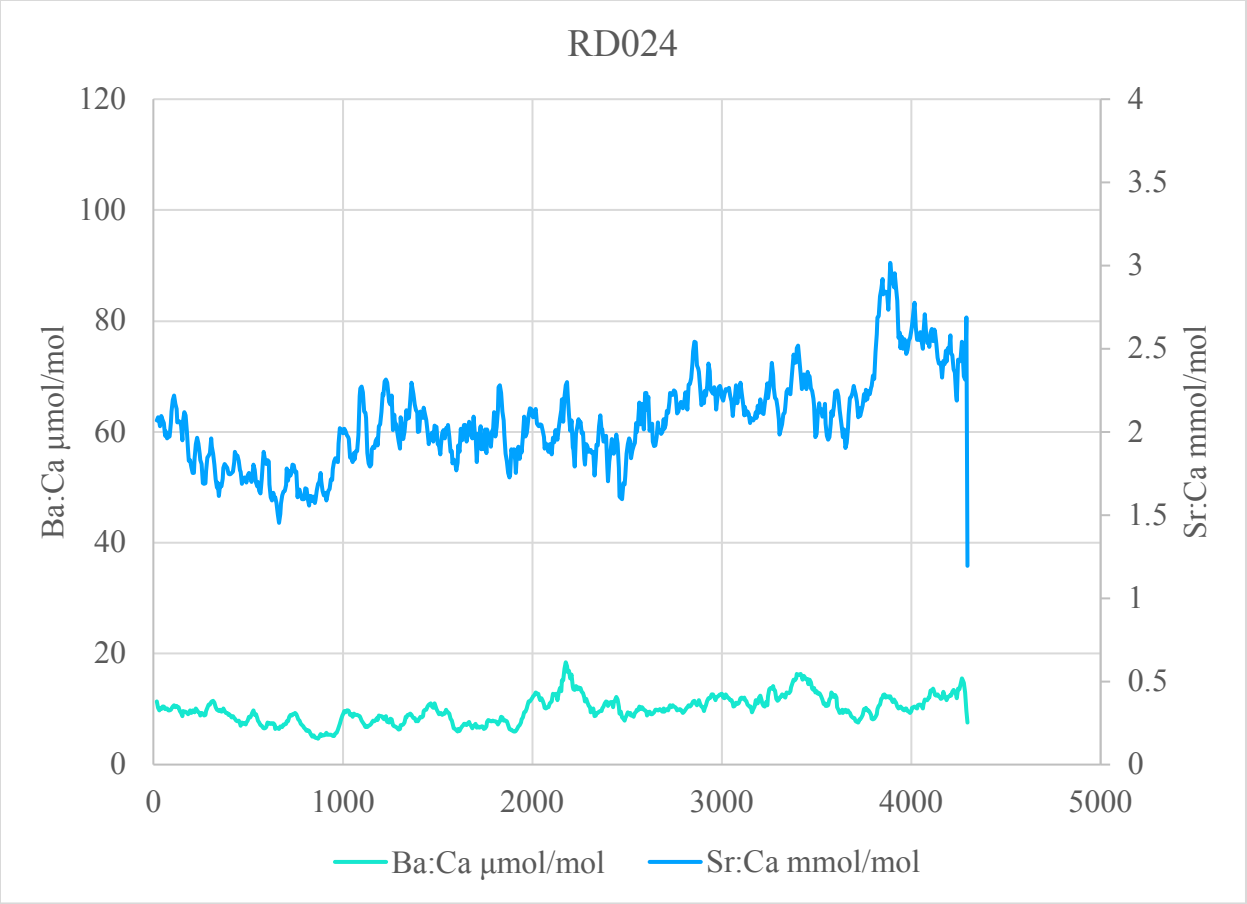

Figure A.24. The Ba:Ca and Sr:Ca life history profile of individual RD024.

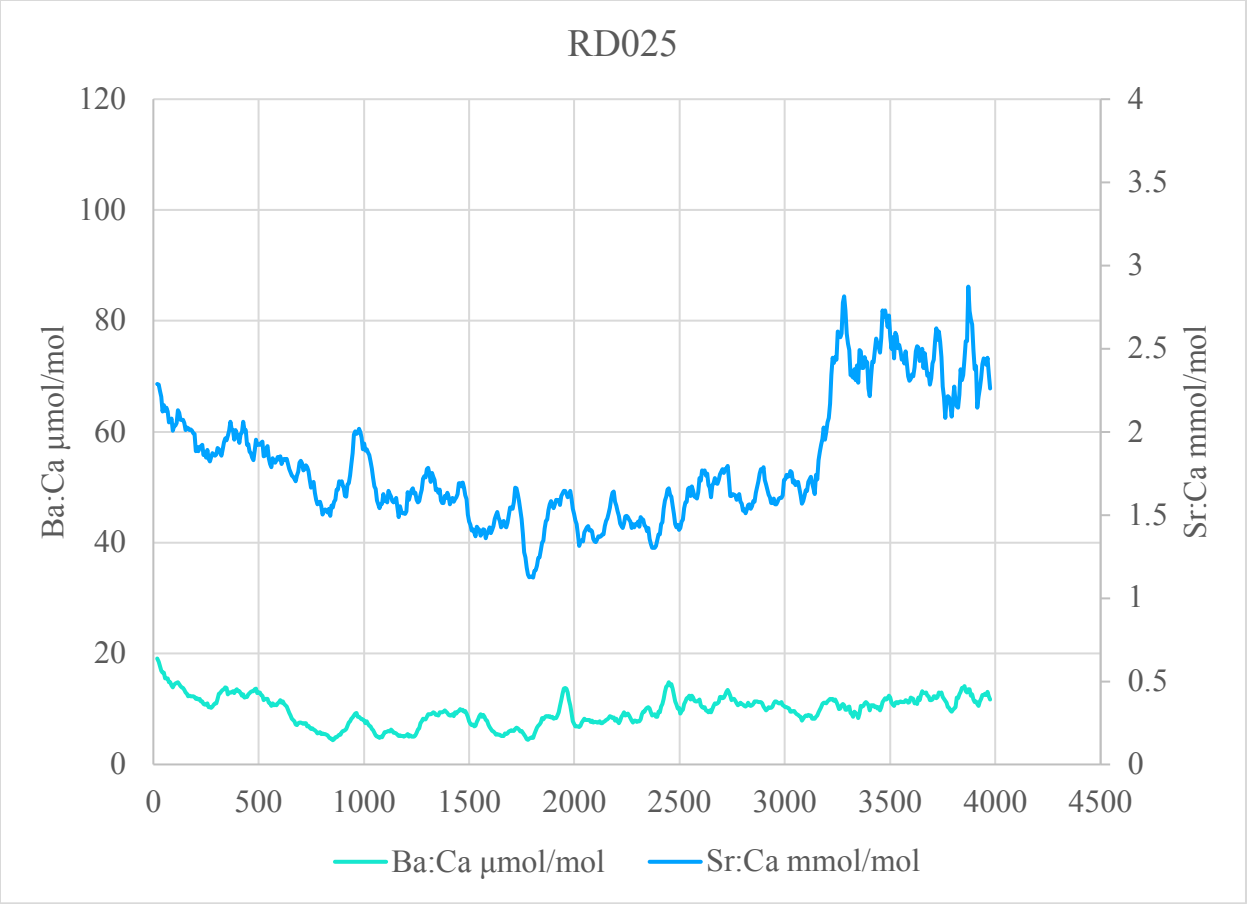

Figure A.25. The Ba:Ca and Sr:Ca life history profile of individual RD025.

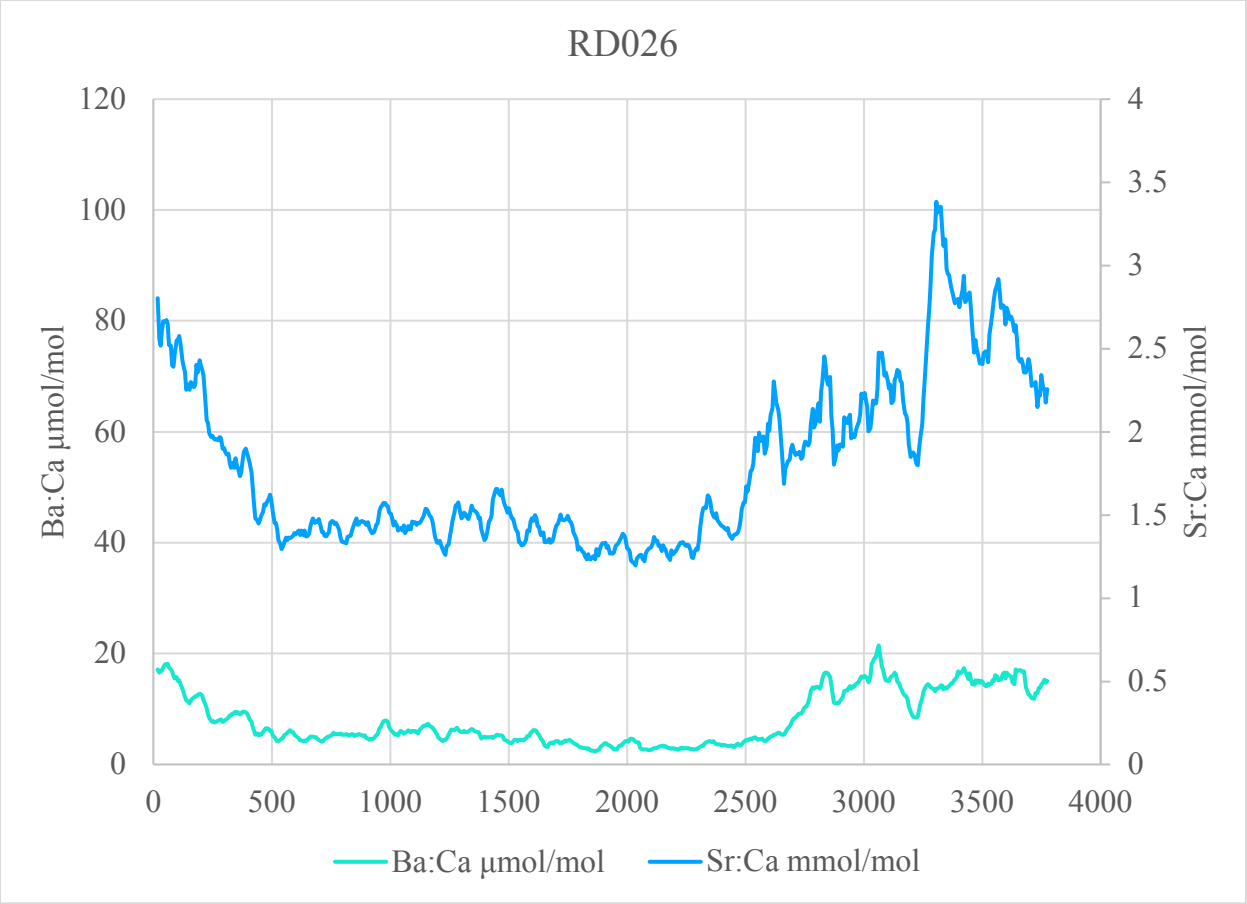

Figure A.26. The Ba:Ca and Sr:Ca life history profile of individual RD026.

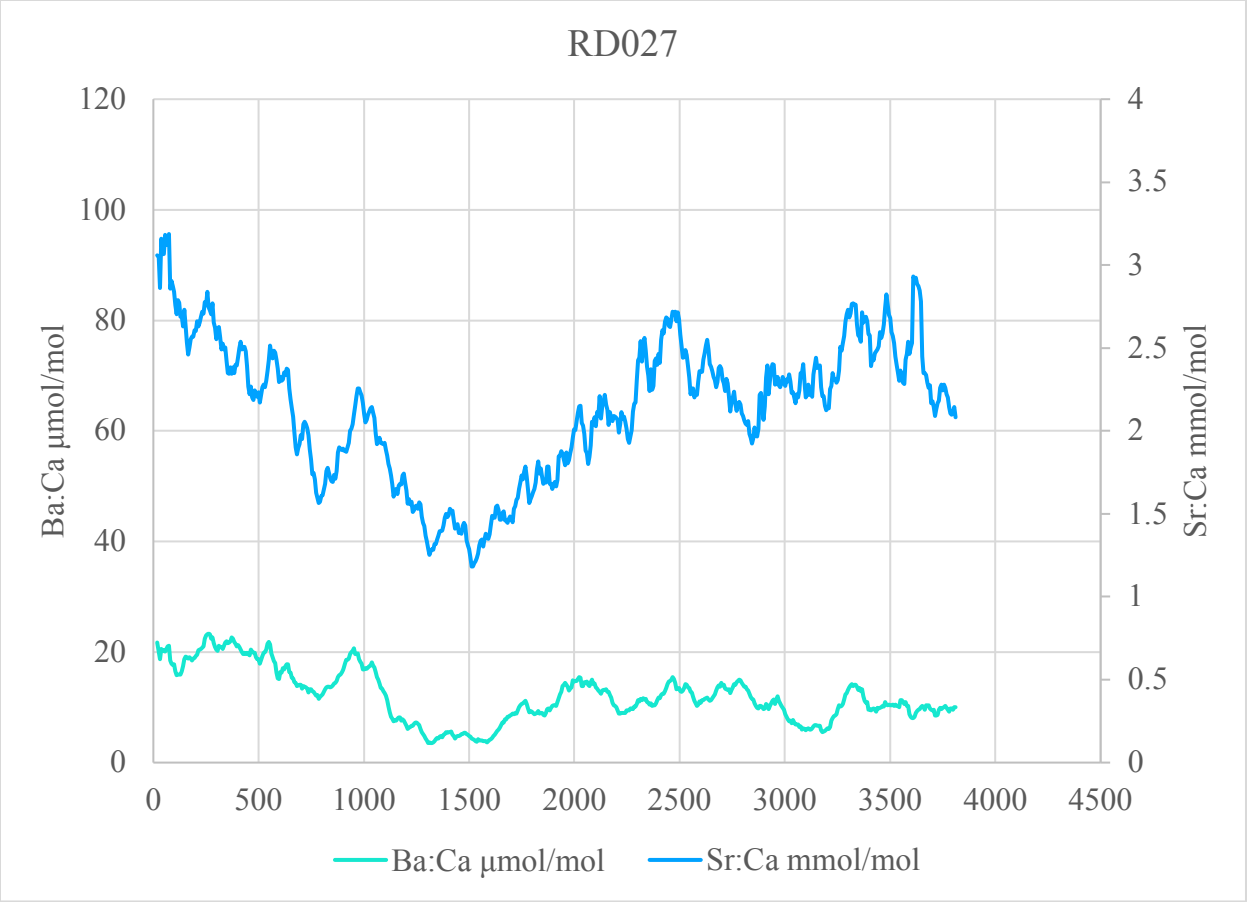

Figure A.27. The Ba:Ca and Sr:Ca life history profile of individual RD027.

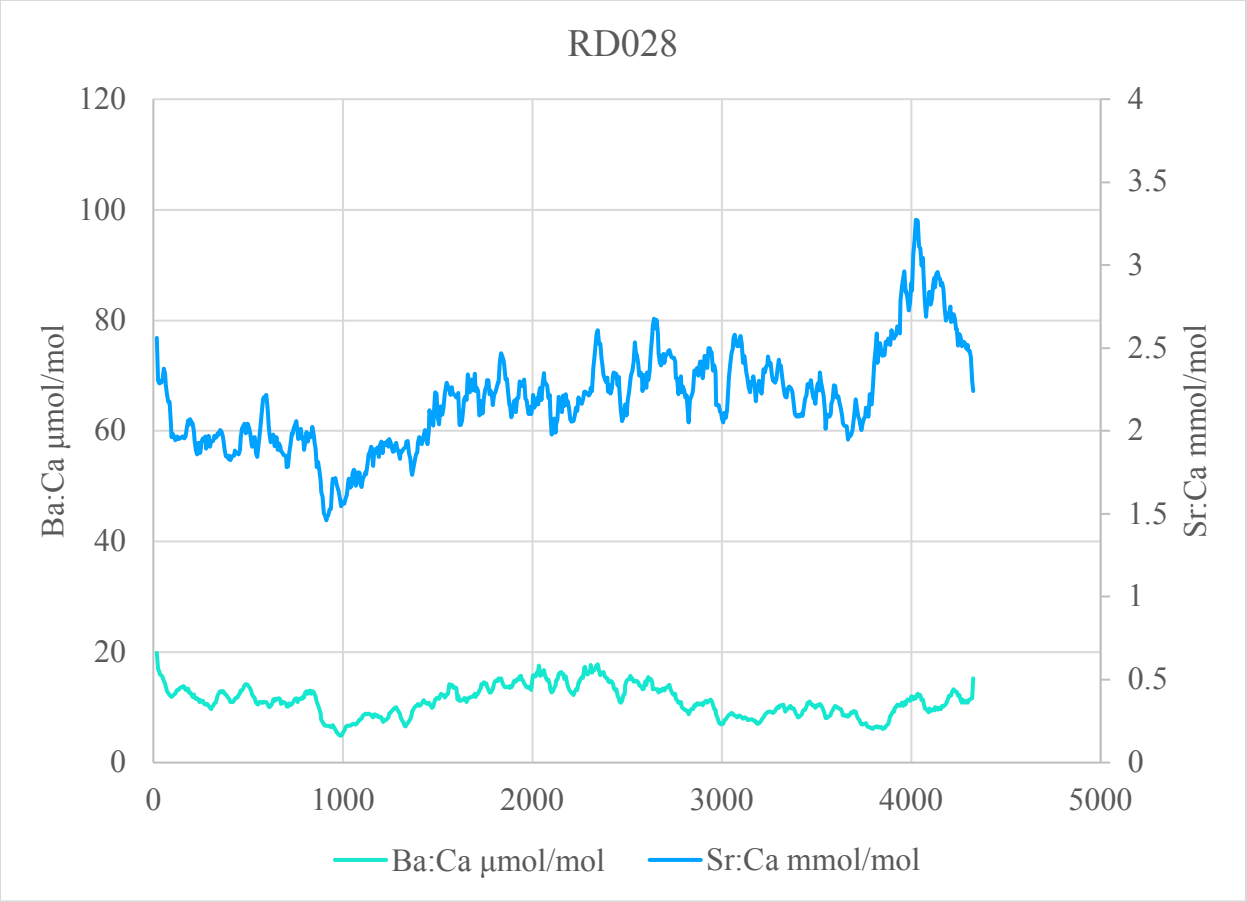

Figure A.28. The Ba:Ca and Sr:Ca life history profile of individual RD028.

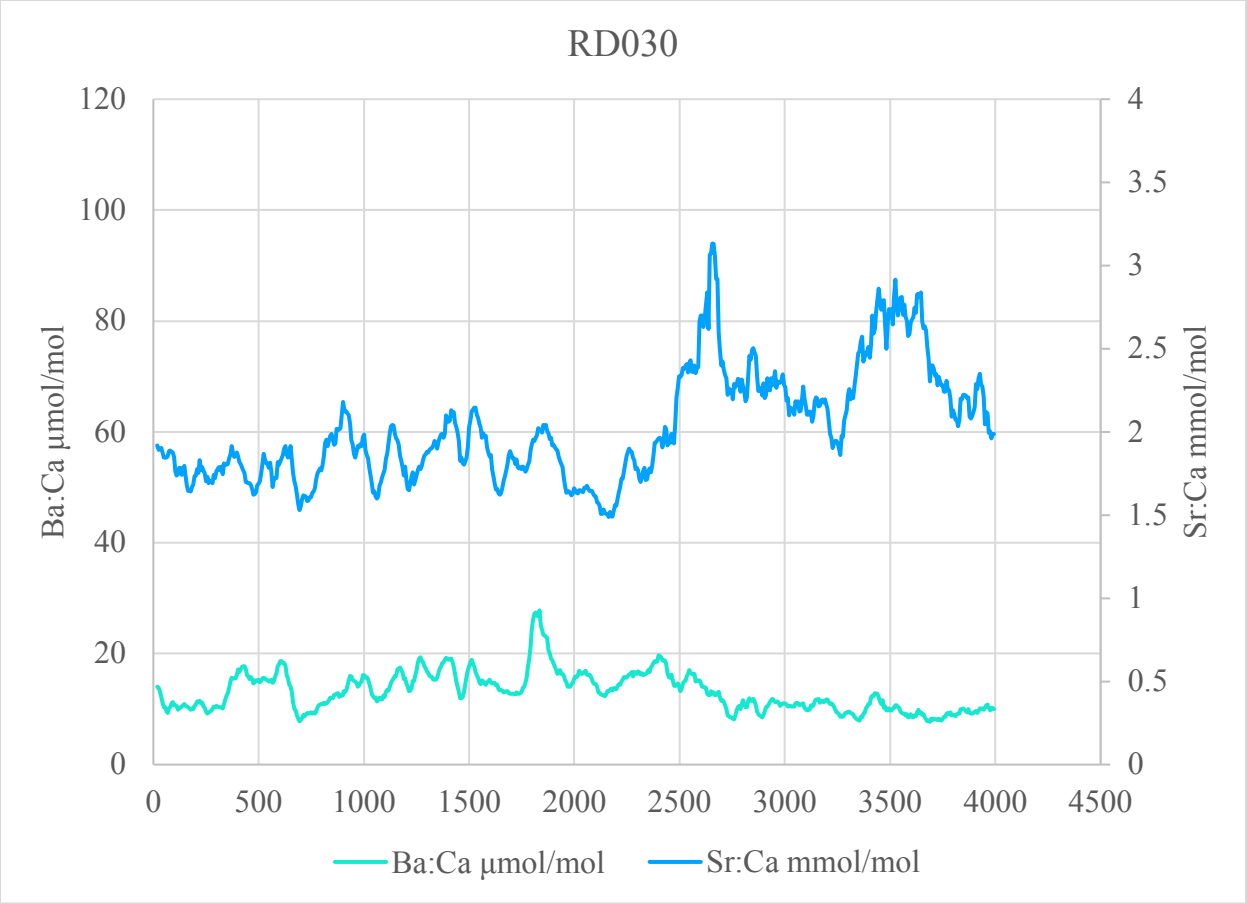

Figure A.30. The Ba:Ca and Sr:Ca life history profile of individual RD030.

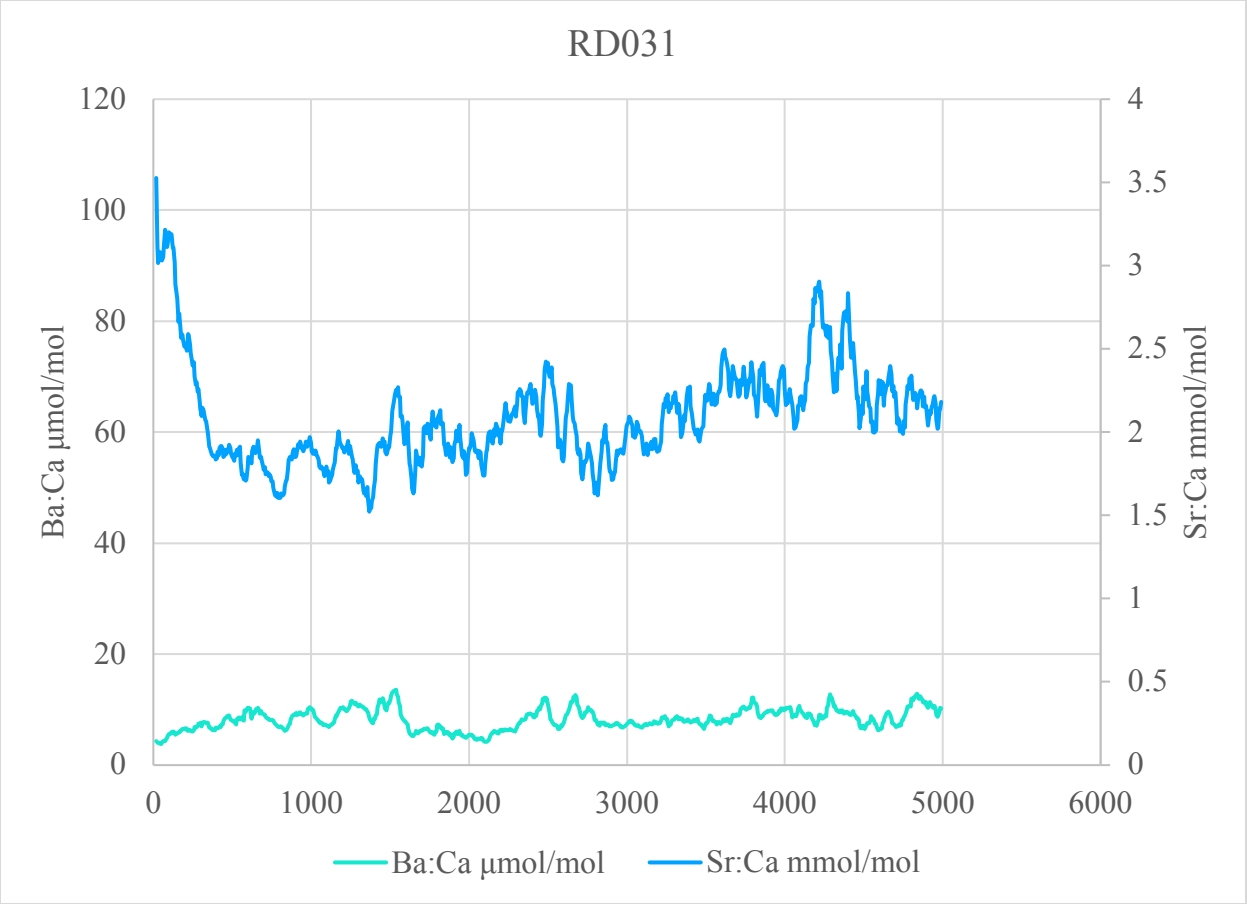

Figure A.31. The Ba:Ca and Sr:Ca life history profile of individual RD031.

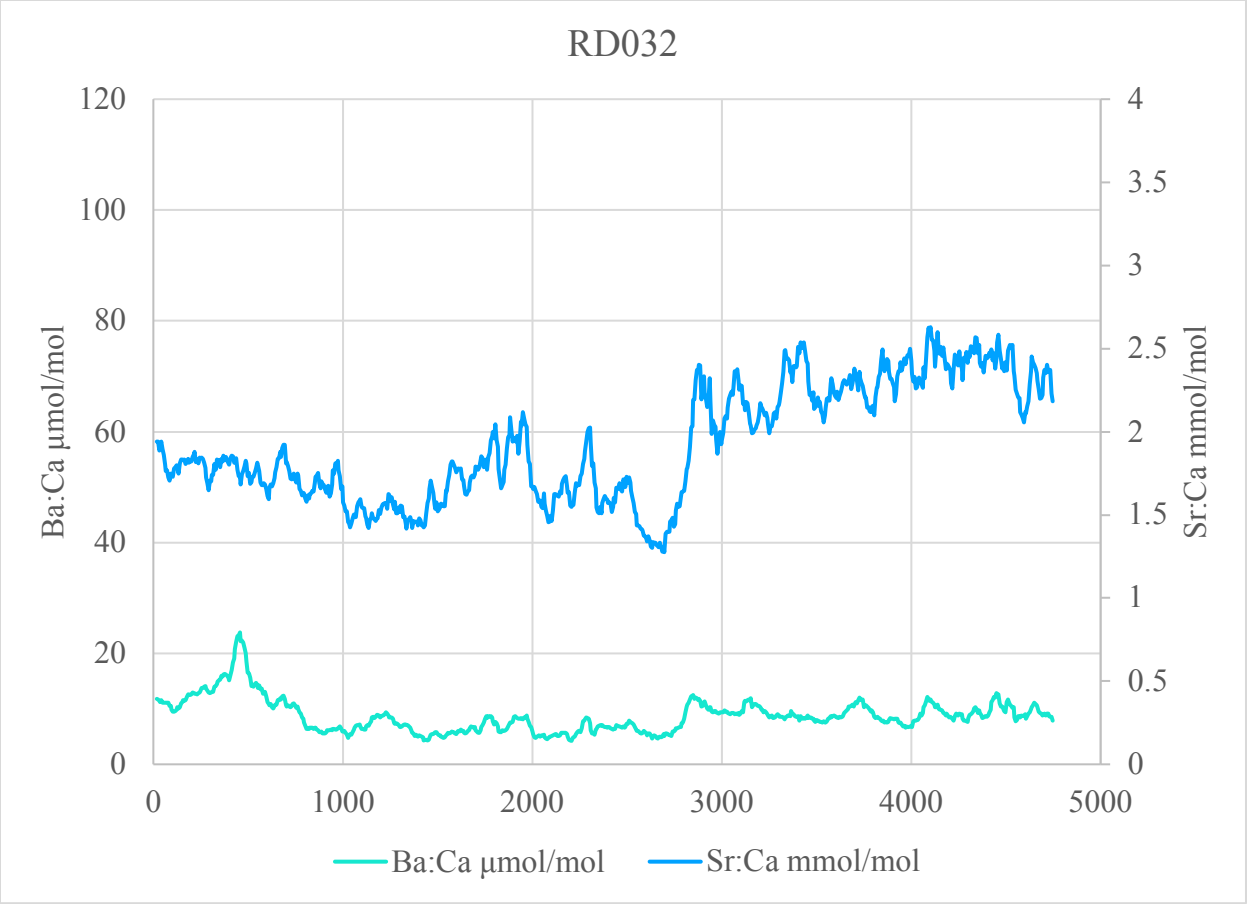

Figure A.32. The Ba:Ca and Sr:Ca life history profile of individual RD032.

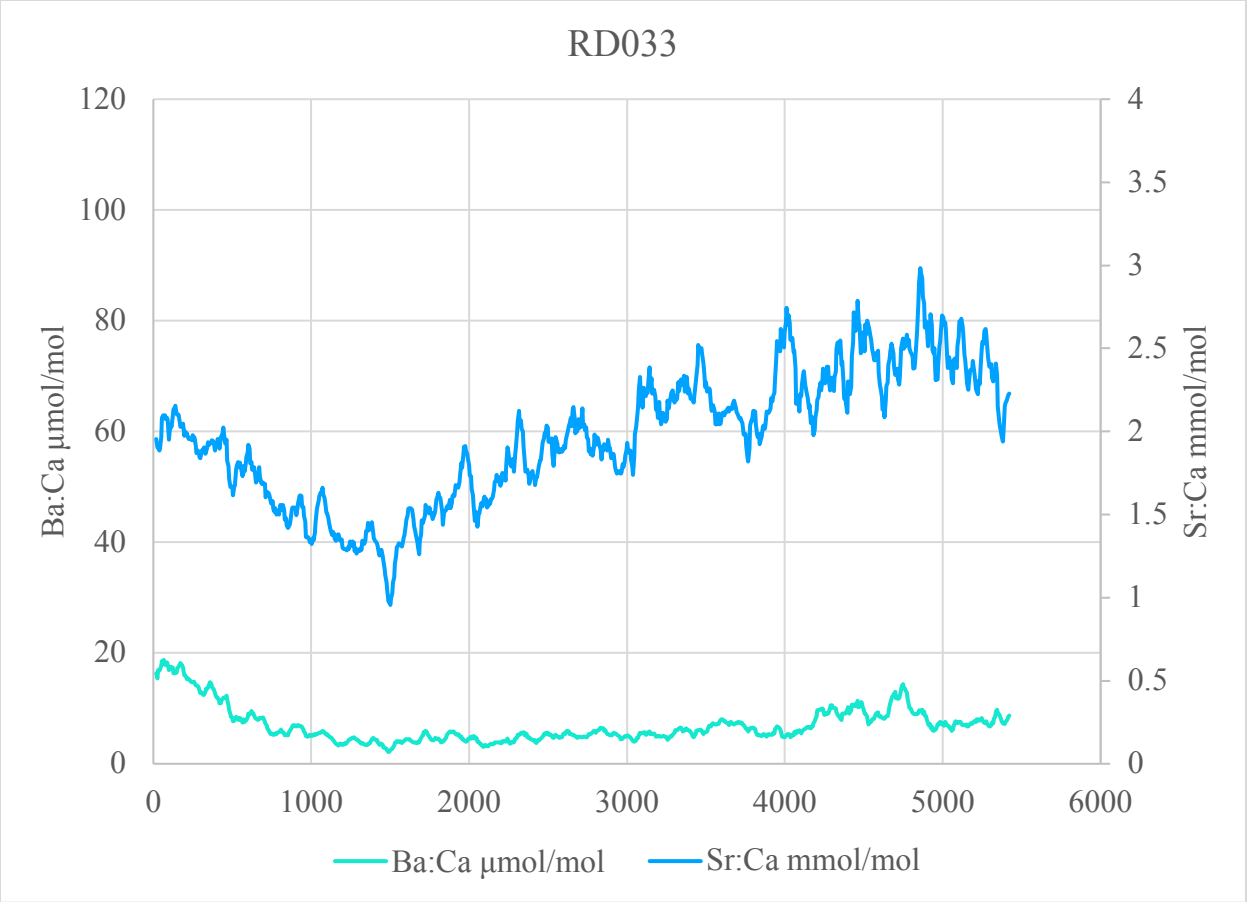

Figure A.33. The Ba:Ca and Sr:Ca life history profile of individual RD033.

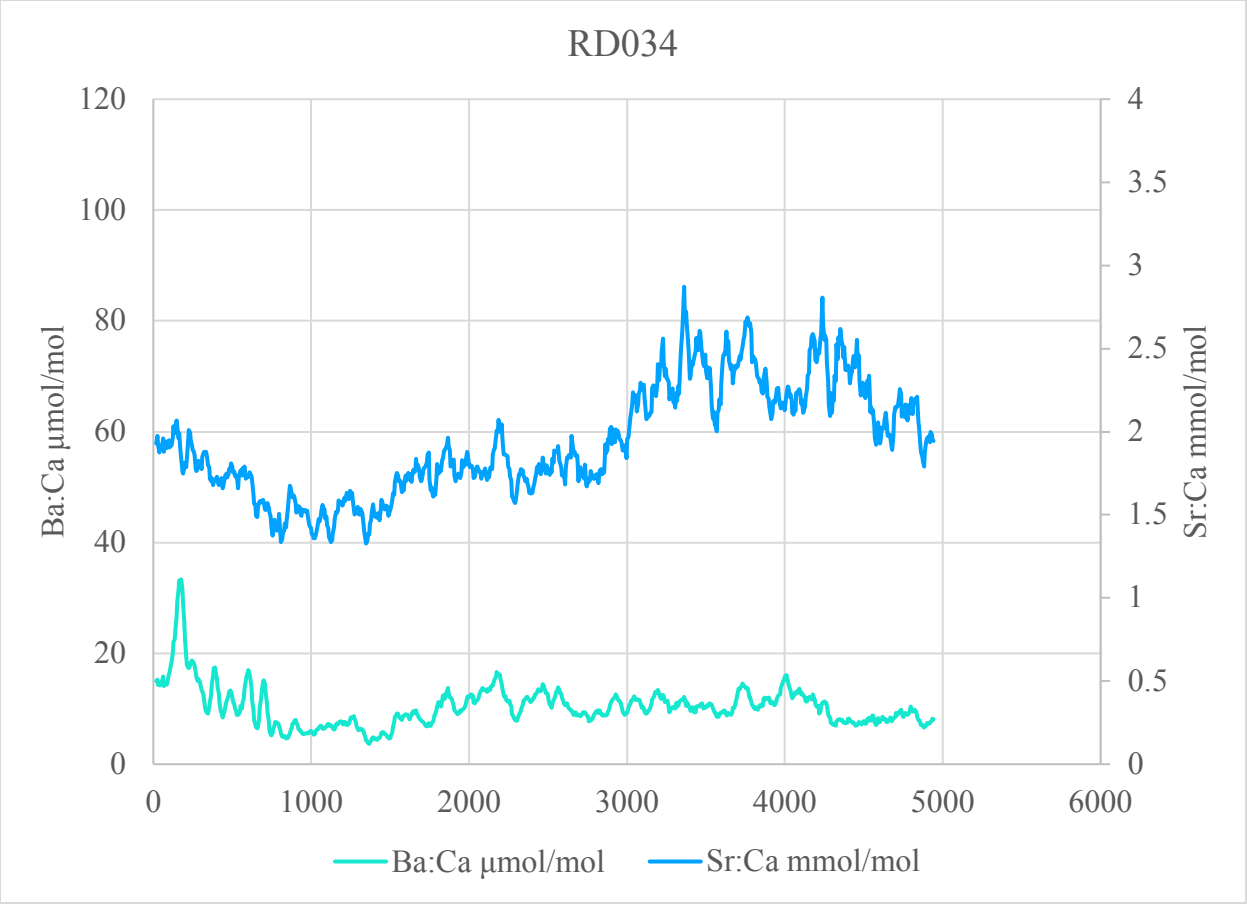

Figure A.34. The Ba:Ca and Sr:Ca life history profile of individual RD034.

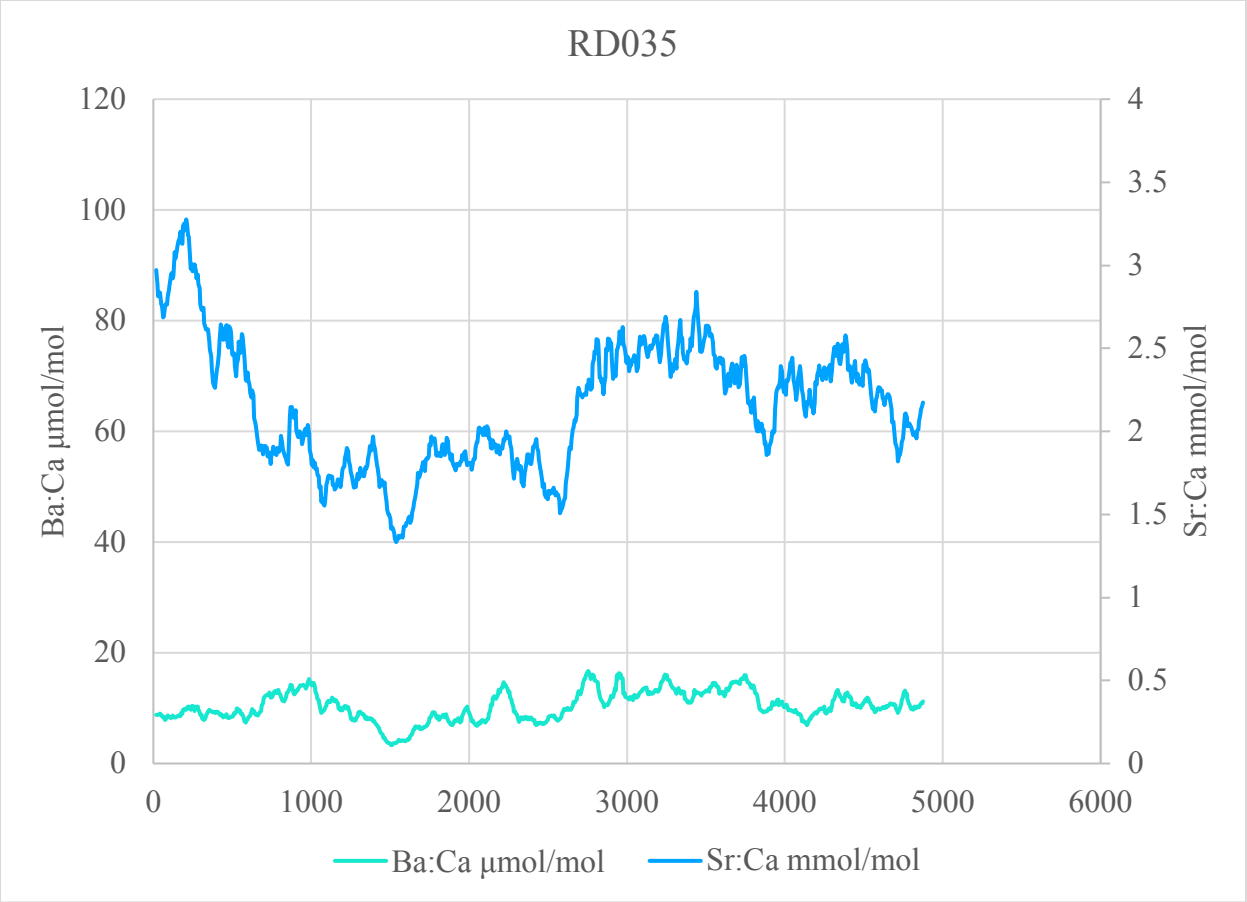

Figure A.35. The Ba:Ca and Sr:Ca life history profile of individual RD035.

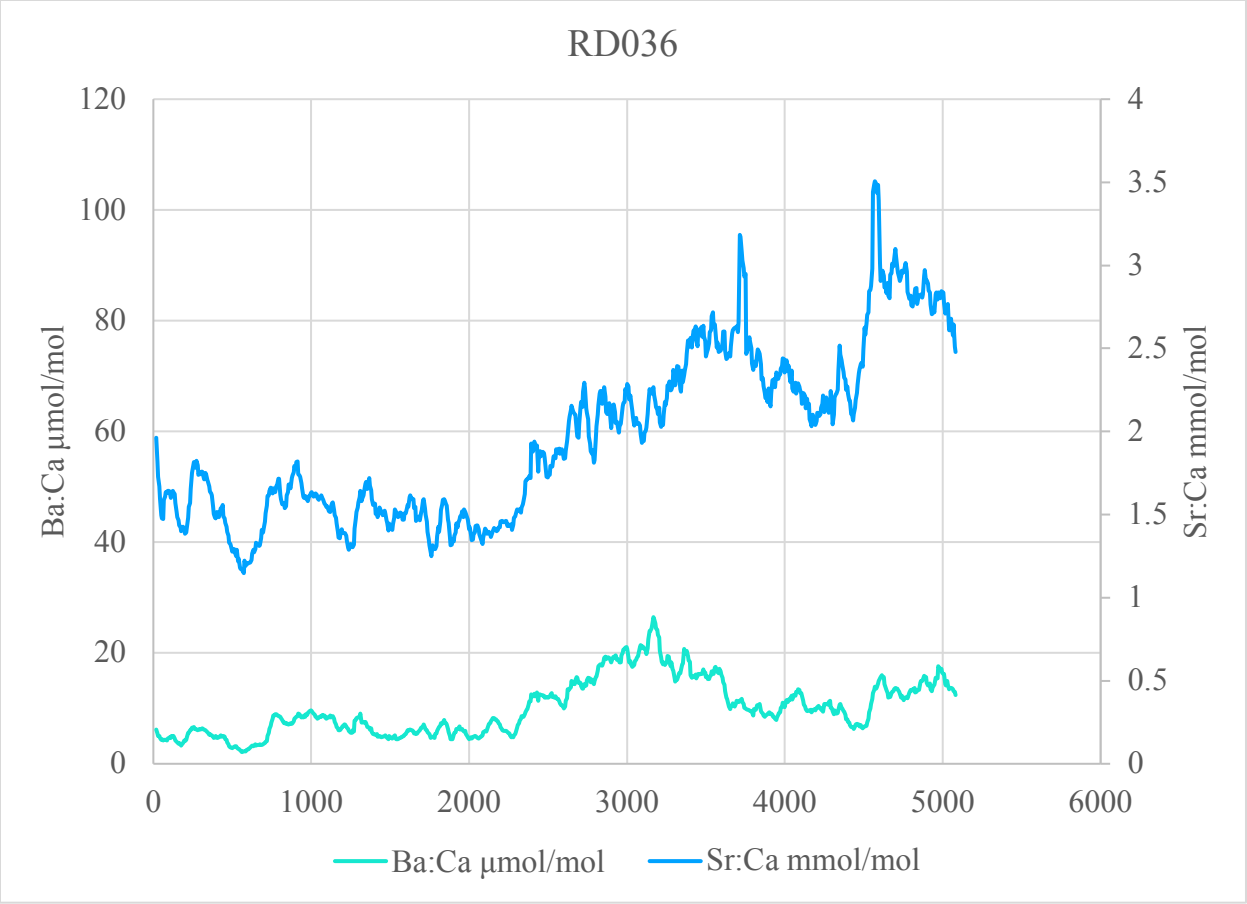

Figure A.36. The Ba:Ca and Sr:Ca life history profile of individual RD036.

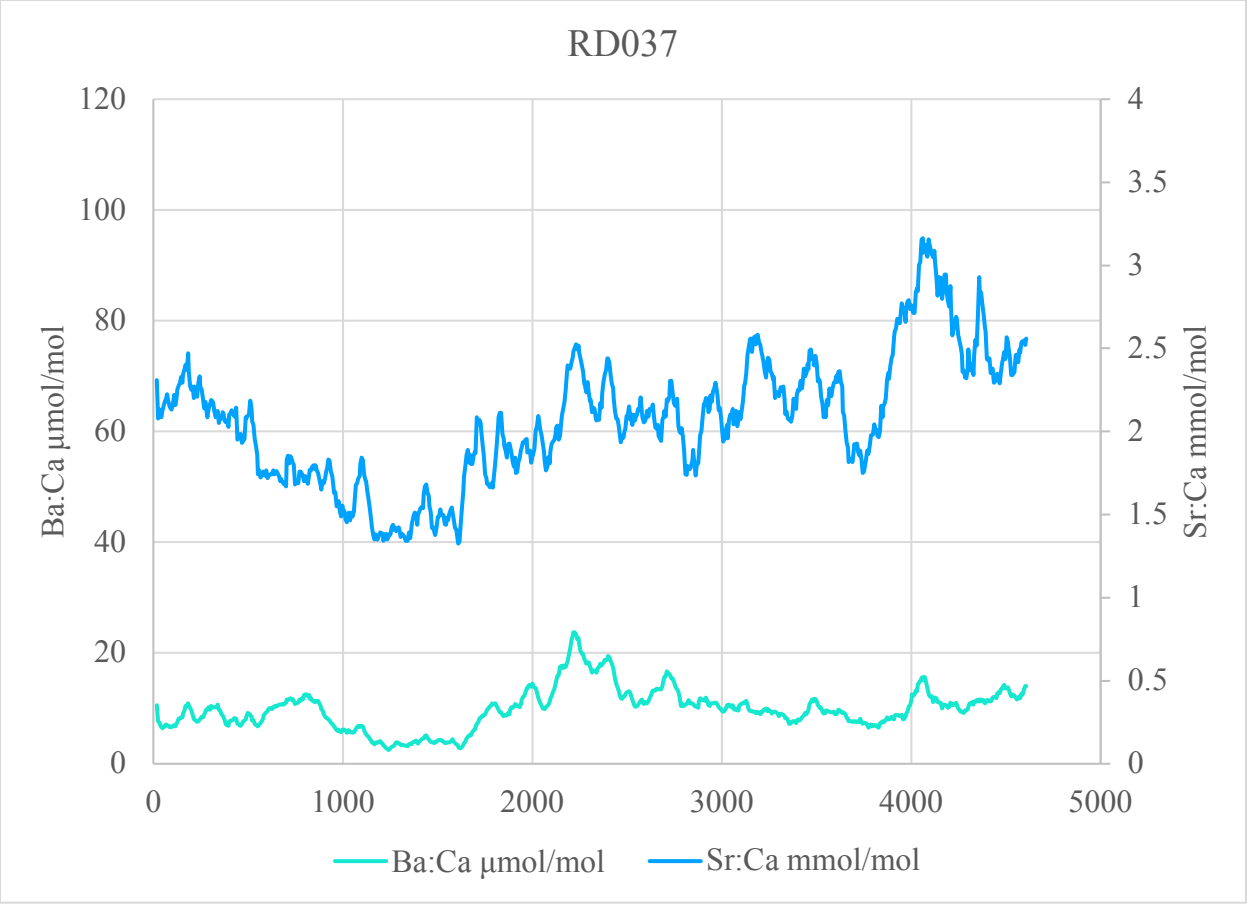

Figure A.37. The Ba:Ca and Sr:Ca life history profile of individual RD037.

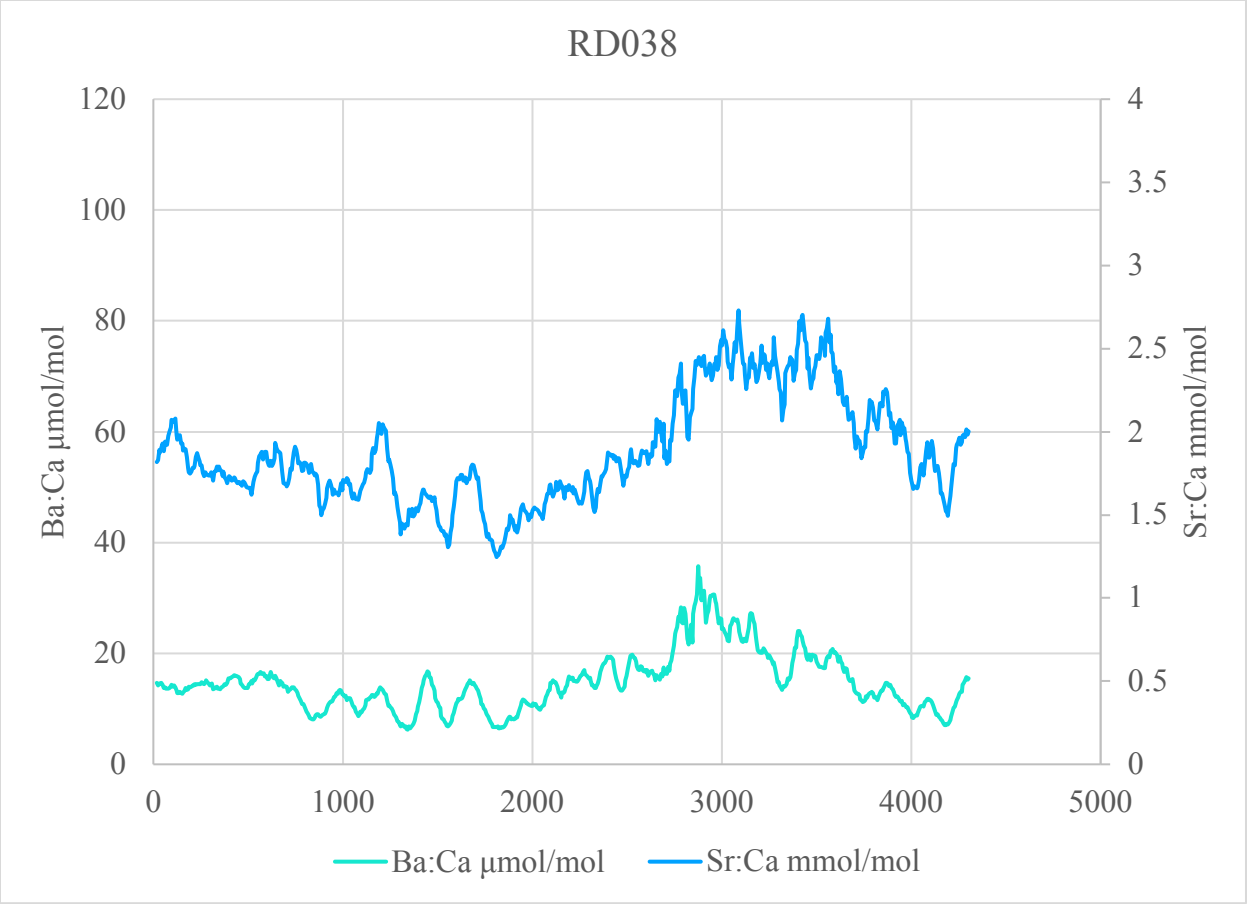

Figure A.38. The Ba:Ca and Sr:Ca life history profile of individual RD038.

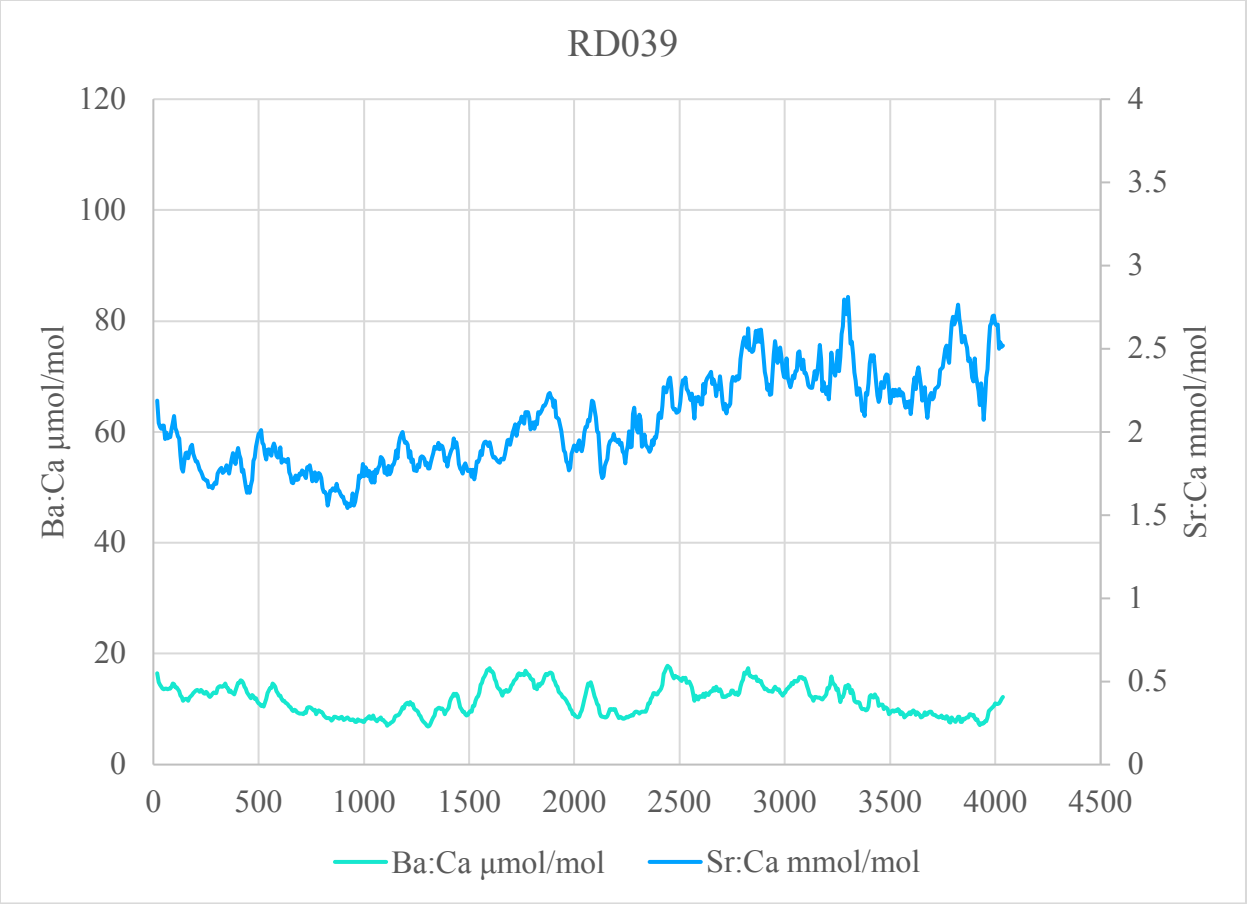

Figure A.39. The Ba:Ca and Sr:Ca life history profile of individual RD039.

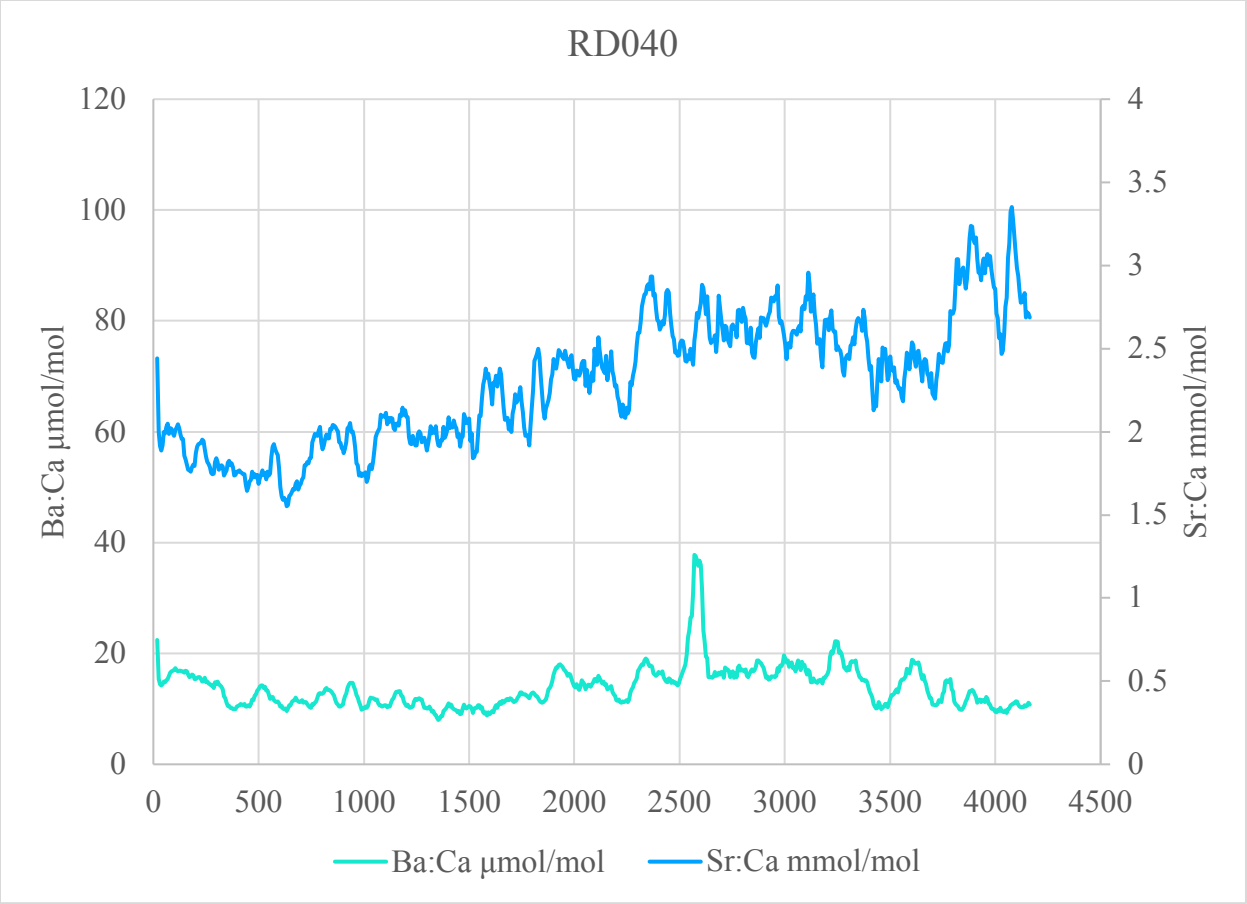

Figure A.40. The Ba:Ca and Sr:Ca life history profile of individual RD040.

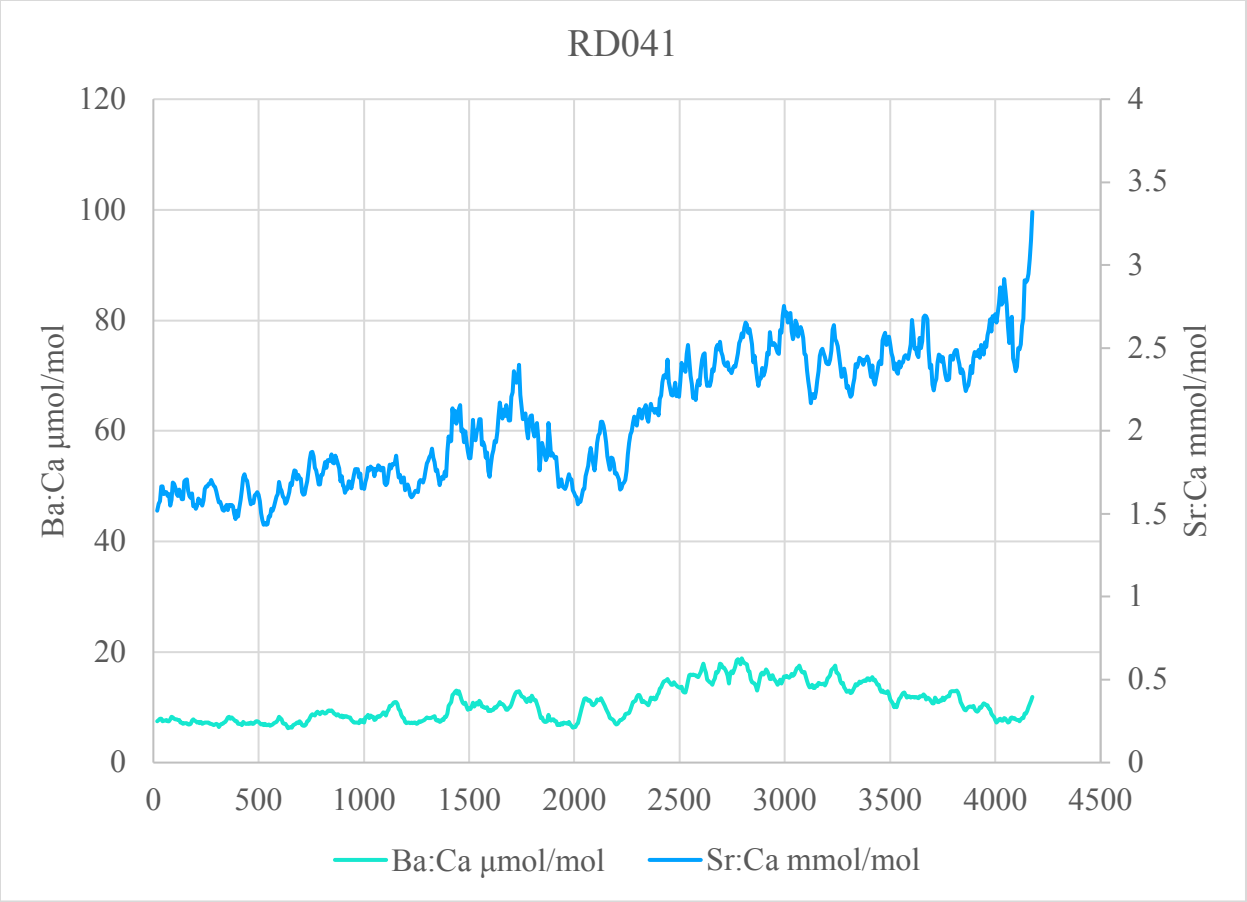

Figure A.41. The Ba:Ca and Sr:Ca life history profile of individual RD041.

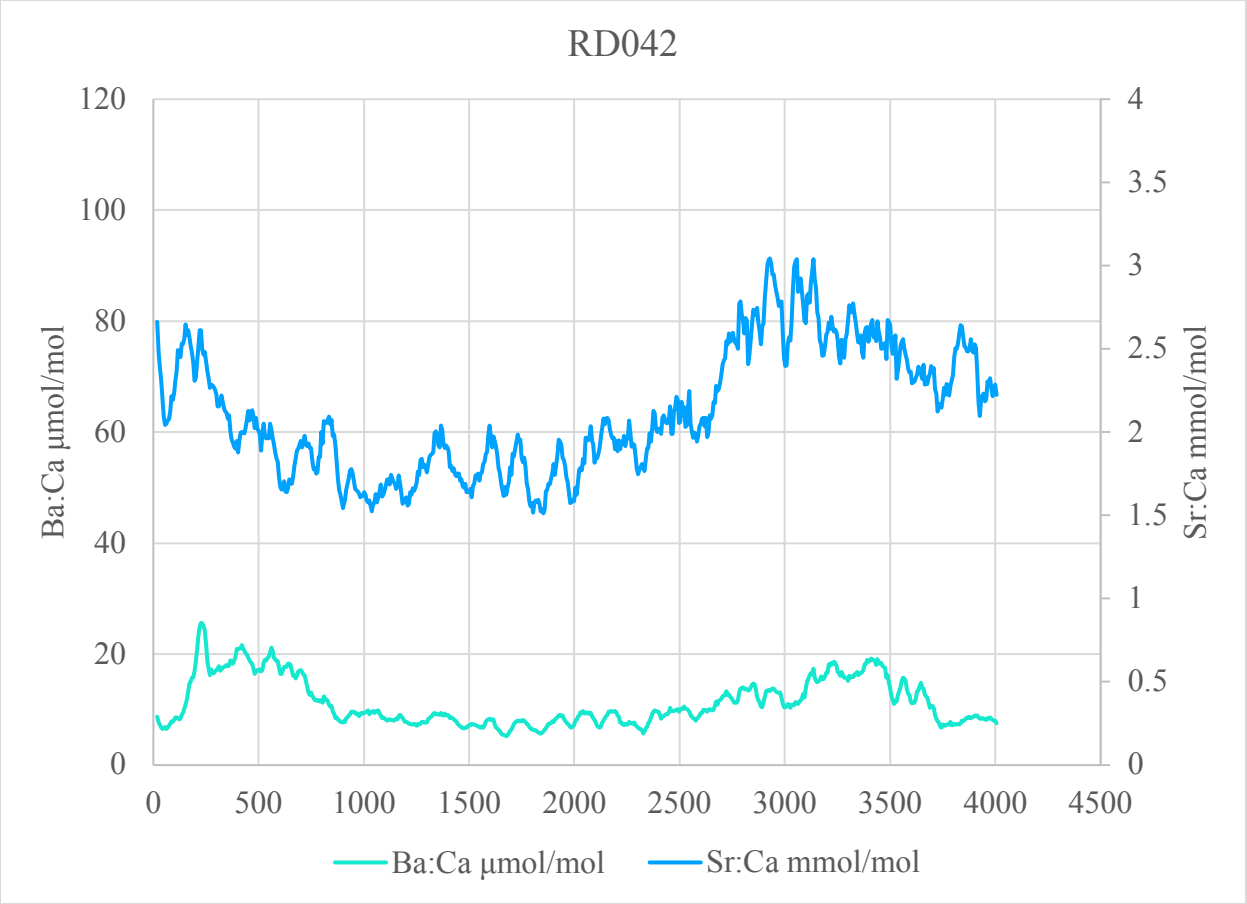

Figure A.42. The Ba:Ca and Sr:Ca life history profile of individual RD042.

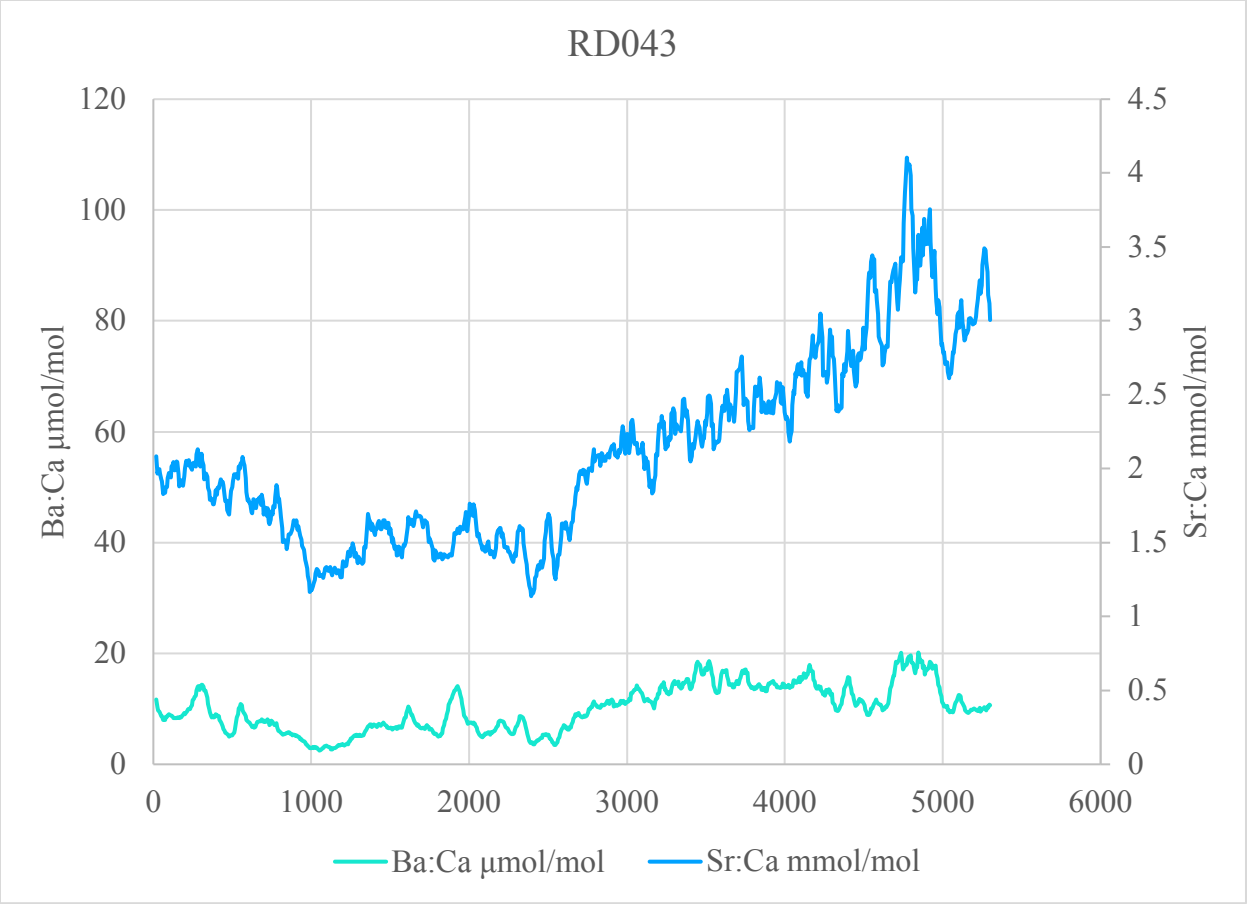

Figure A.43. The Ba:Ca and Sr:Ca life history profile of individual RD043.

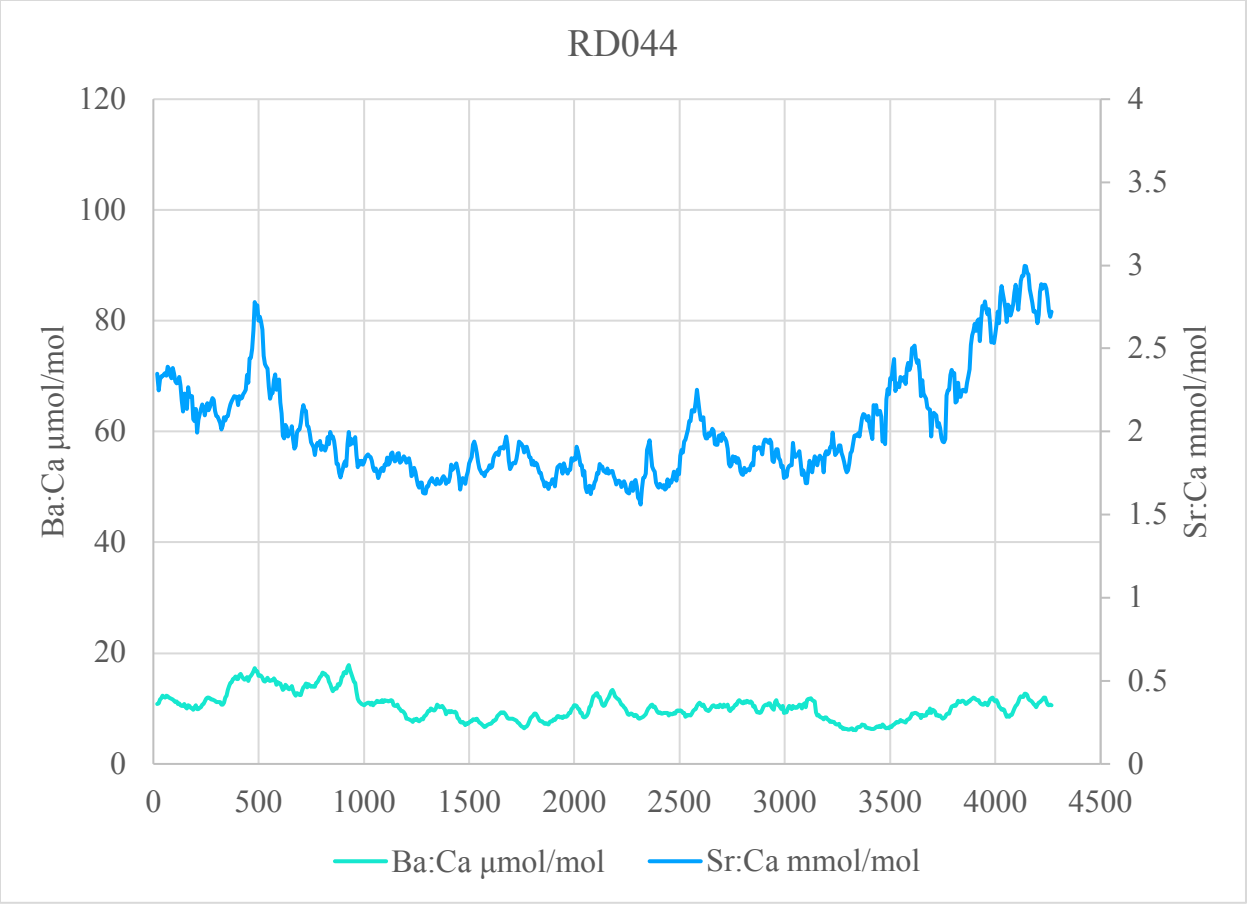

Figure A.44. The Ba:Ca and Sr:Ca life history profile of individual RD044.

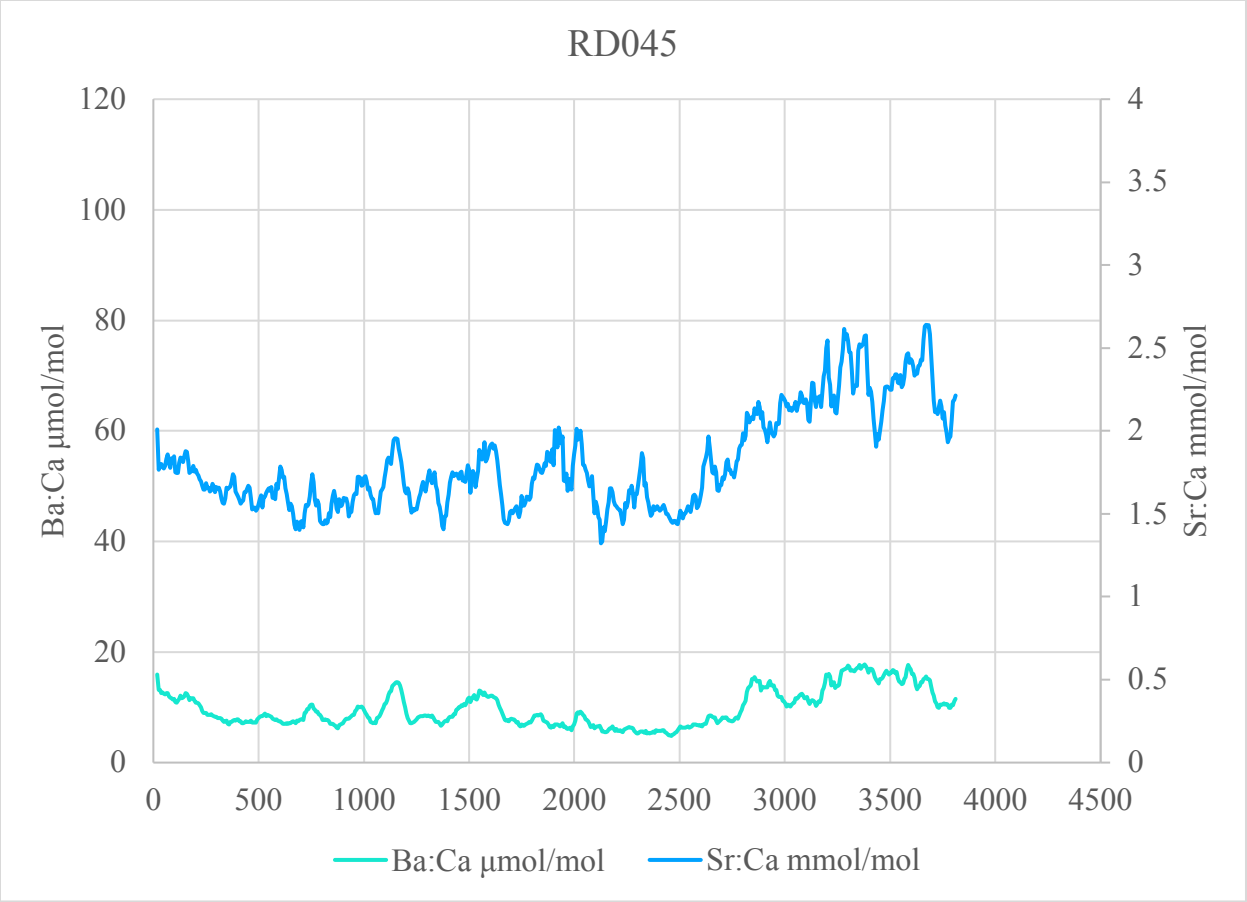

Figure A.45. The Ba:Ca and Sr:Ca life history profile of individual RD045.

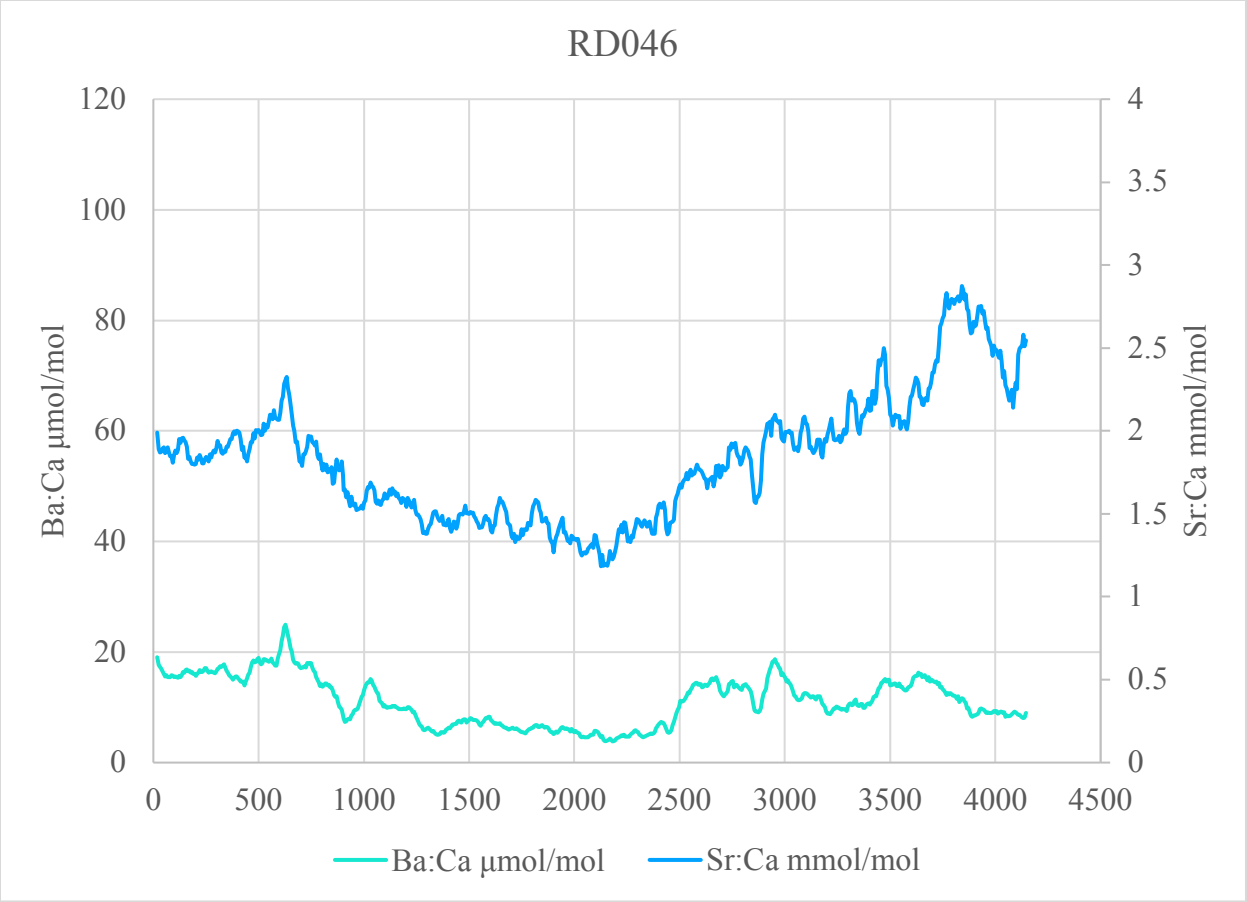

Figure A.46. The Ba:Ca and Sr:Ca life history profile of individual RD046.

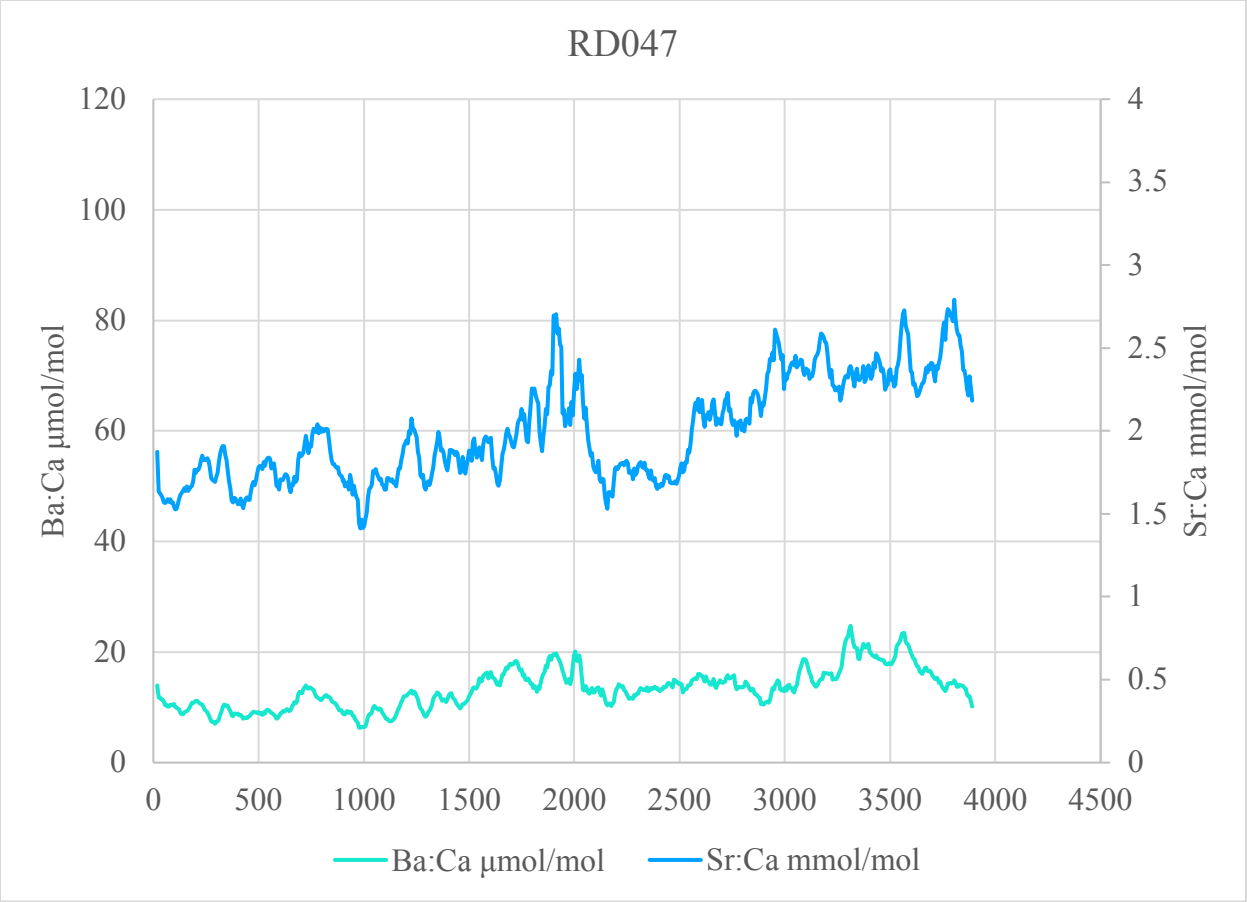

Figure A.47. The Ba:Ca and Sr:Ca life history profile of individual RD047.

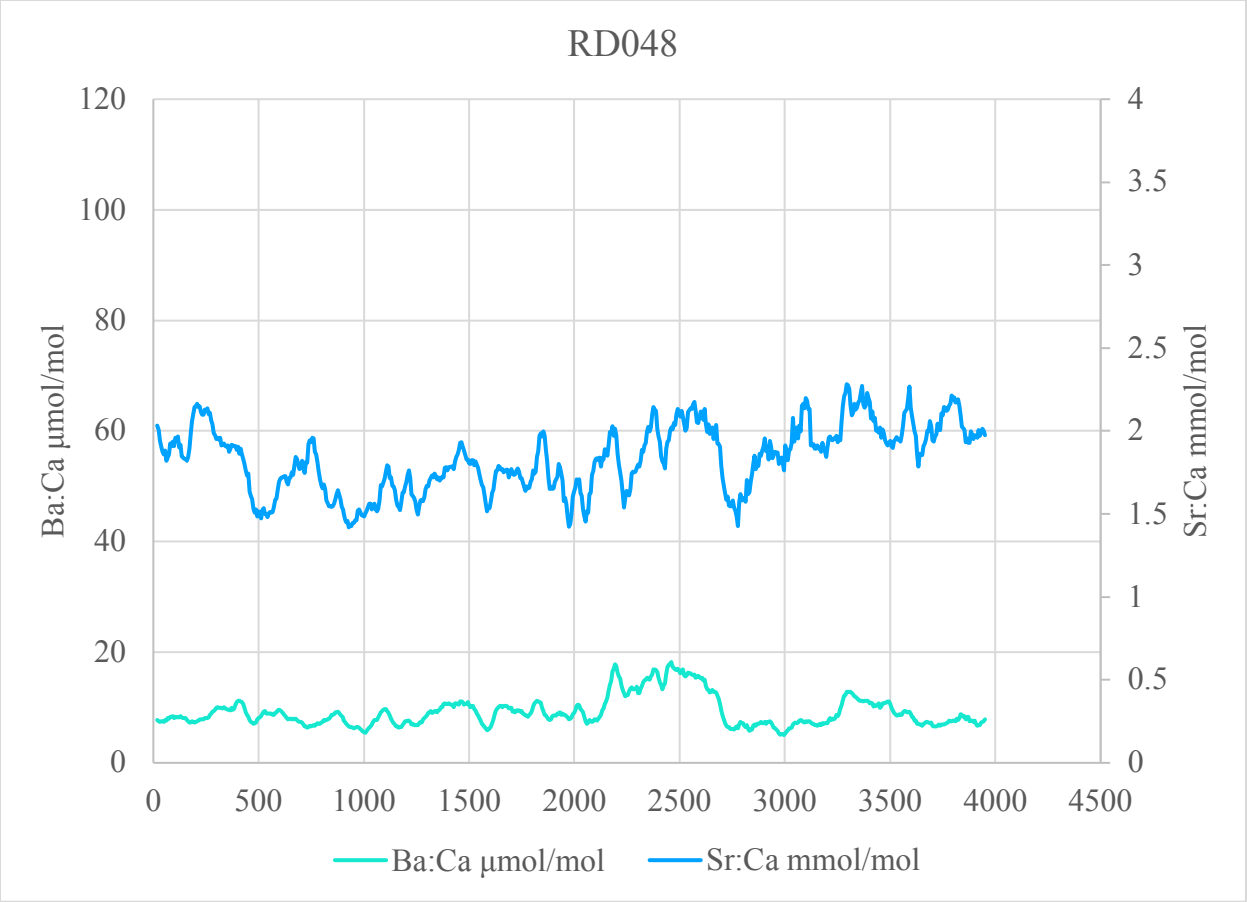

Figure A.48. The Ba:Ca and Sr:Ca life history profile of individual RD048.

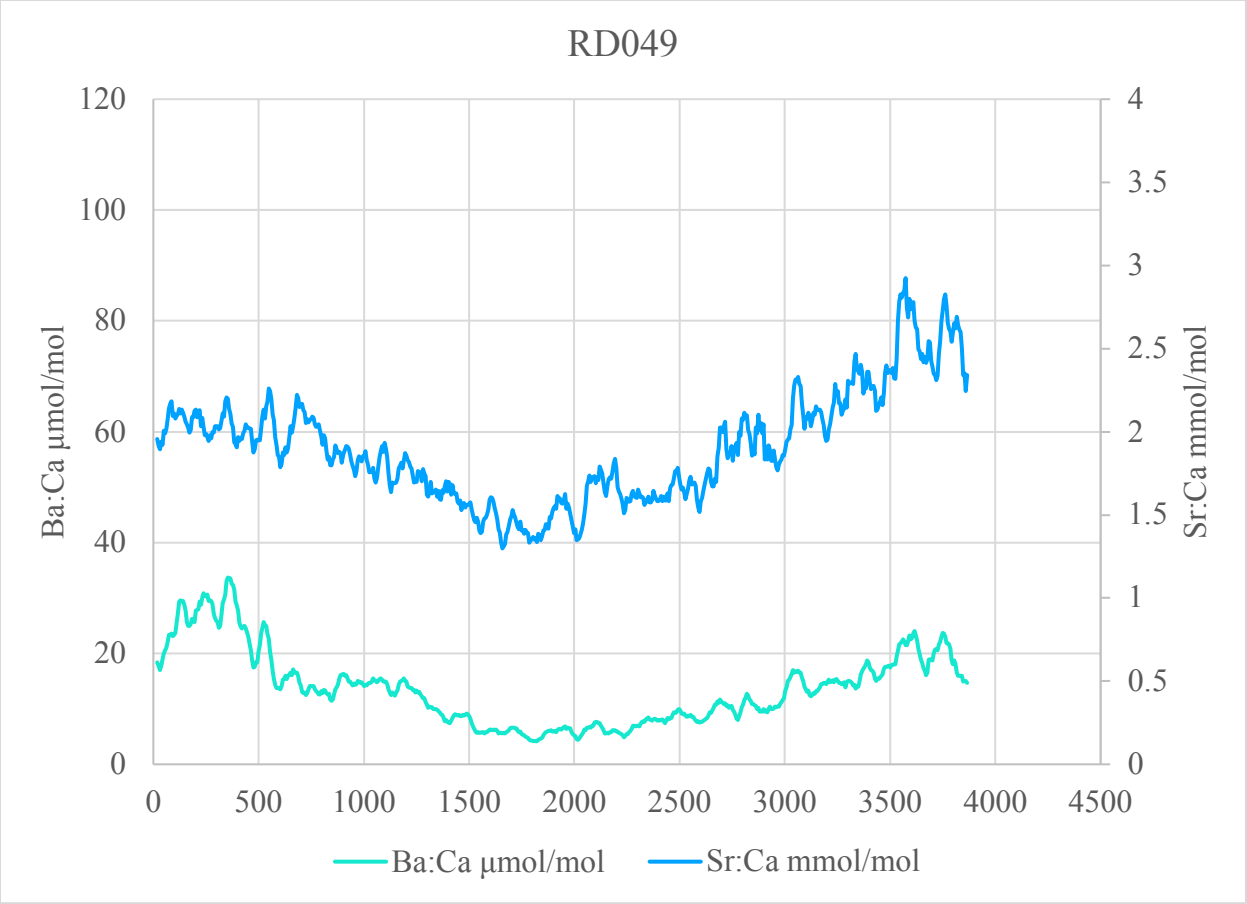

Figure A.49. The Ba:Ca and Sr:Ca life history profile of individual RD049.

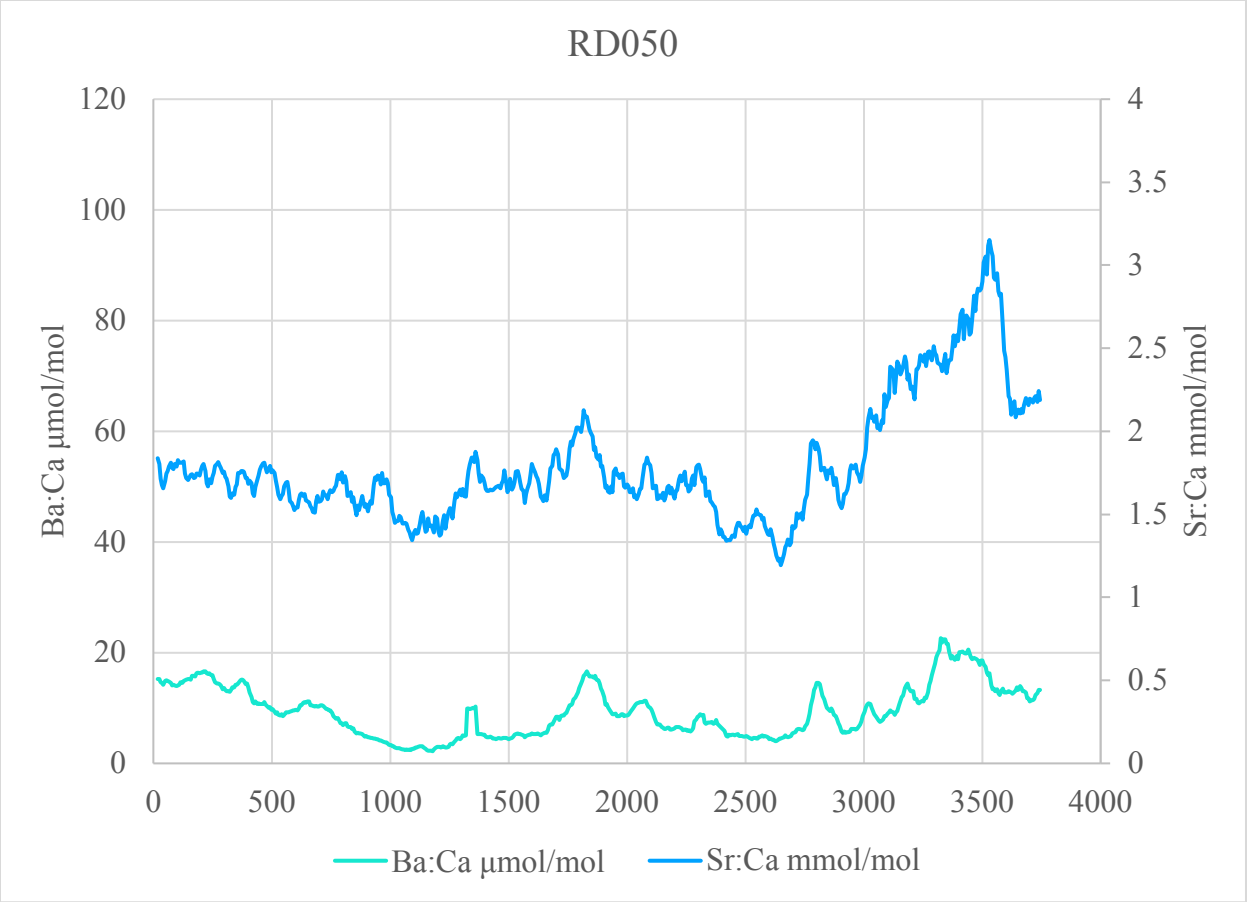

Figure A.50. The Ba:Ca and Sr:Ca life history profile of individual RD050.

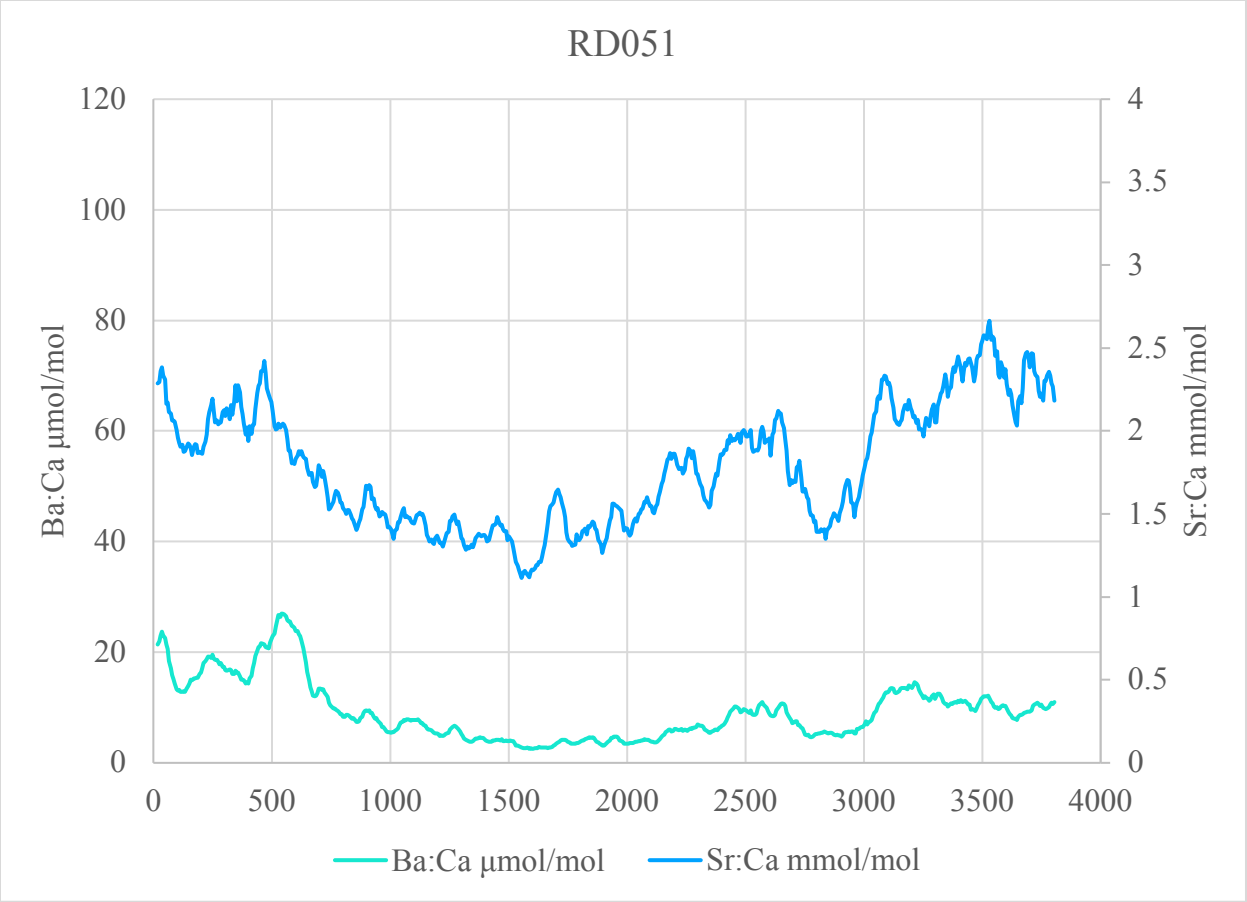

Figure A.51. The Ba:Ca and Sr:Ca life history profile of individual RD051.

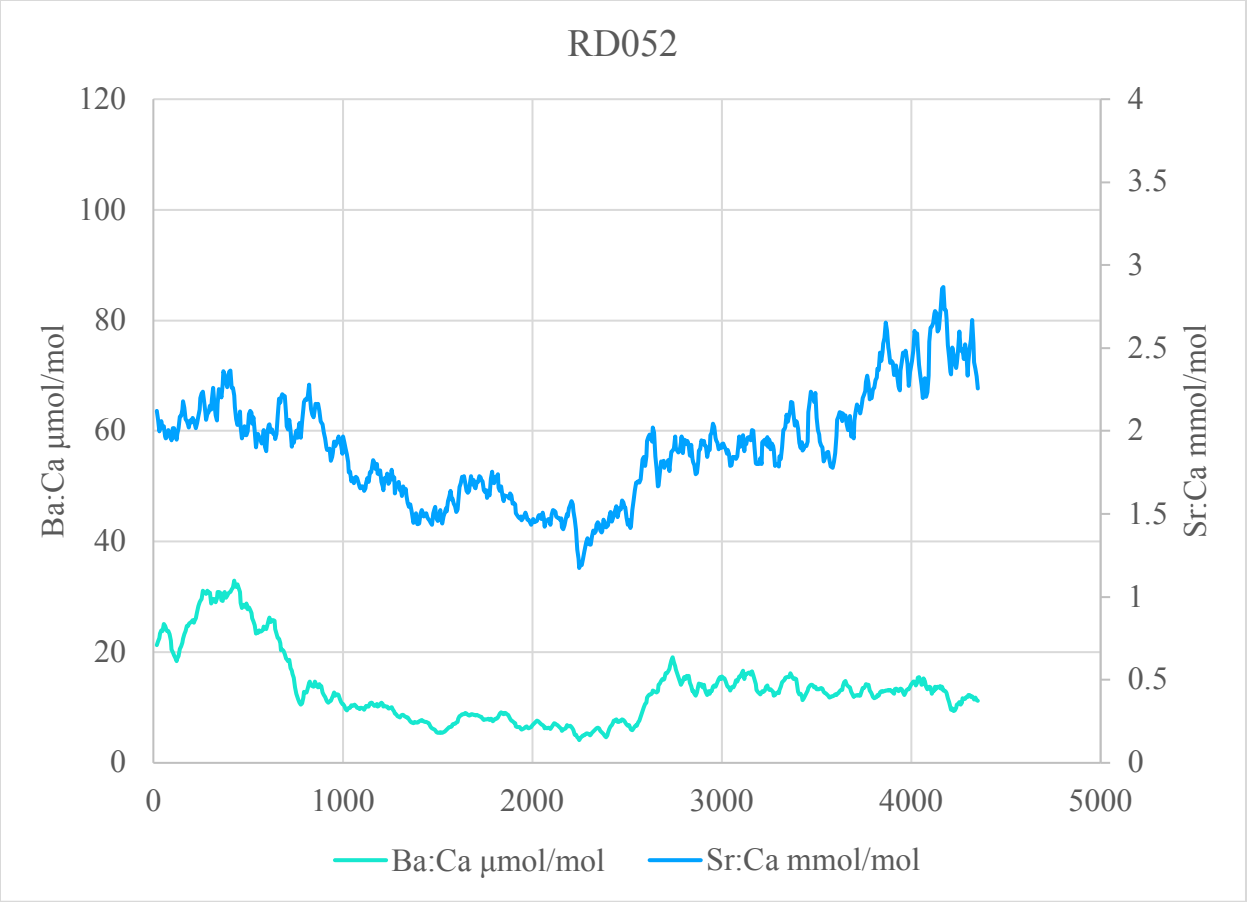

Figure A.52. The Ba:Ca and Sr:Ca life history profile of individual RD052.

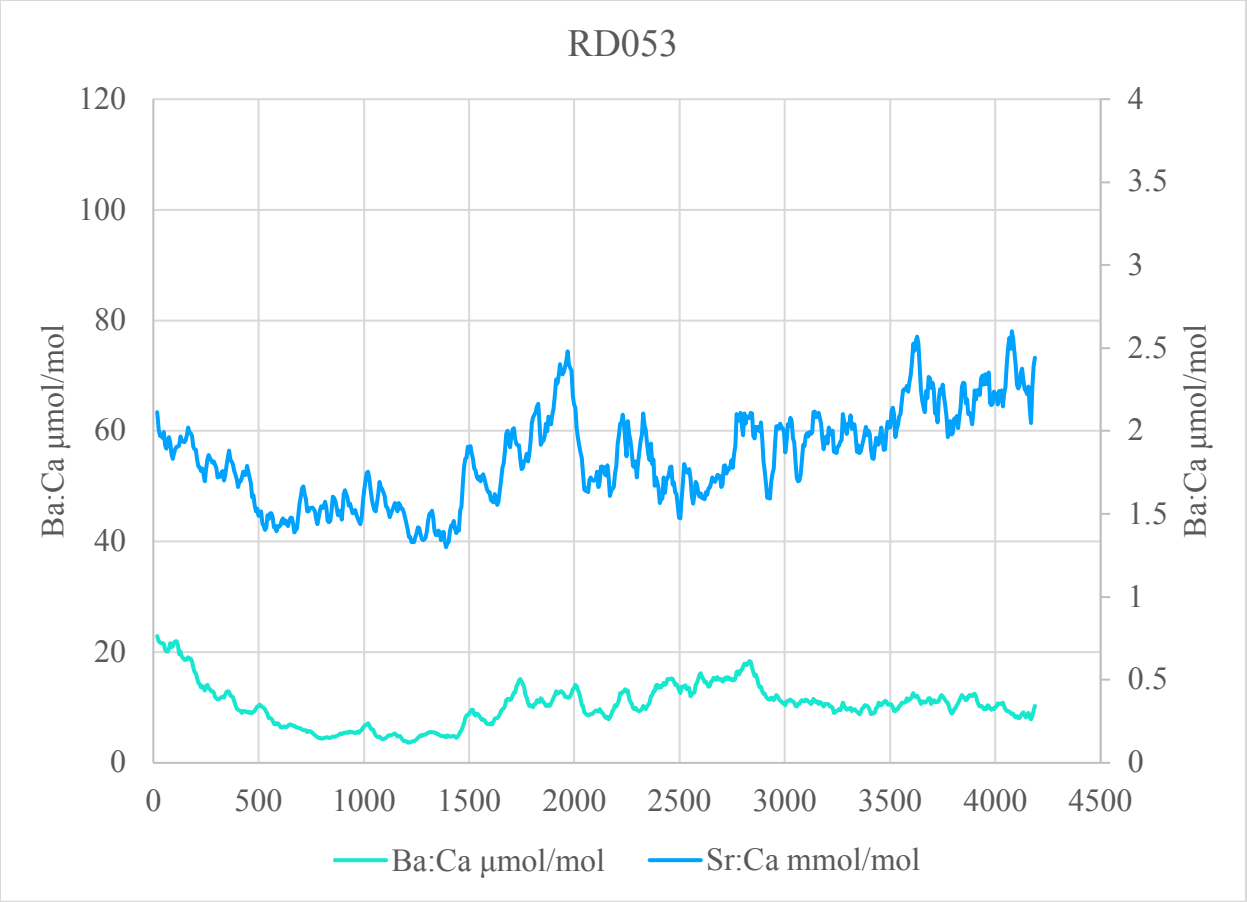

Figure A.53. The Ba:Ca and Sr:Ca life history profile of individual RD053.

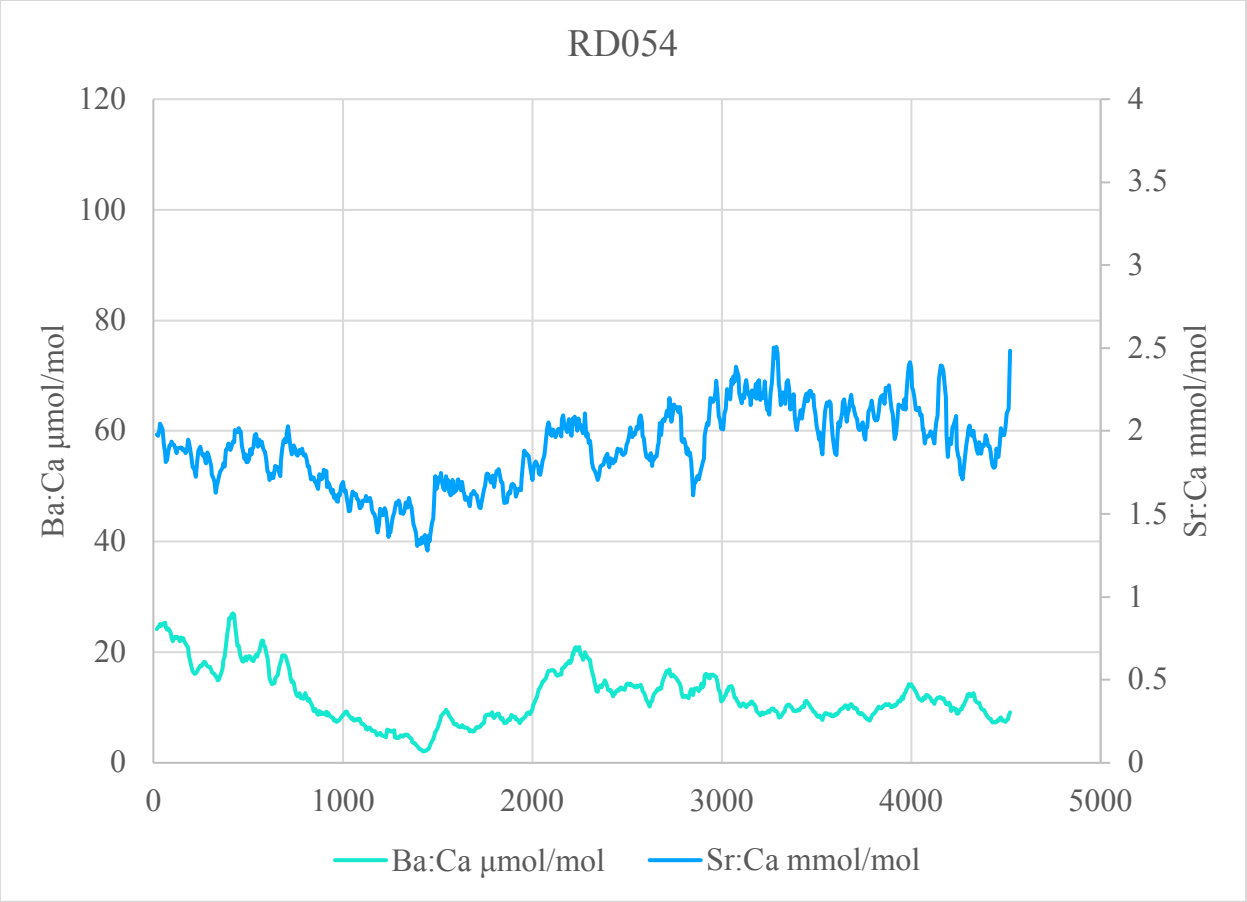

Figure A.54. The Ba:Ca and Sr:Ca life history profile of individual RD054.

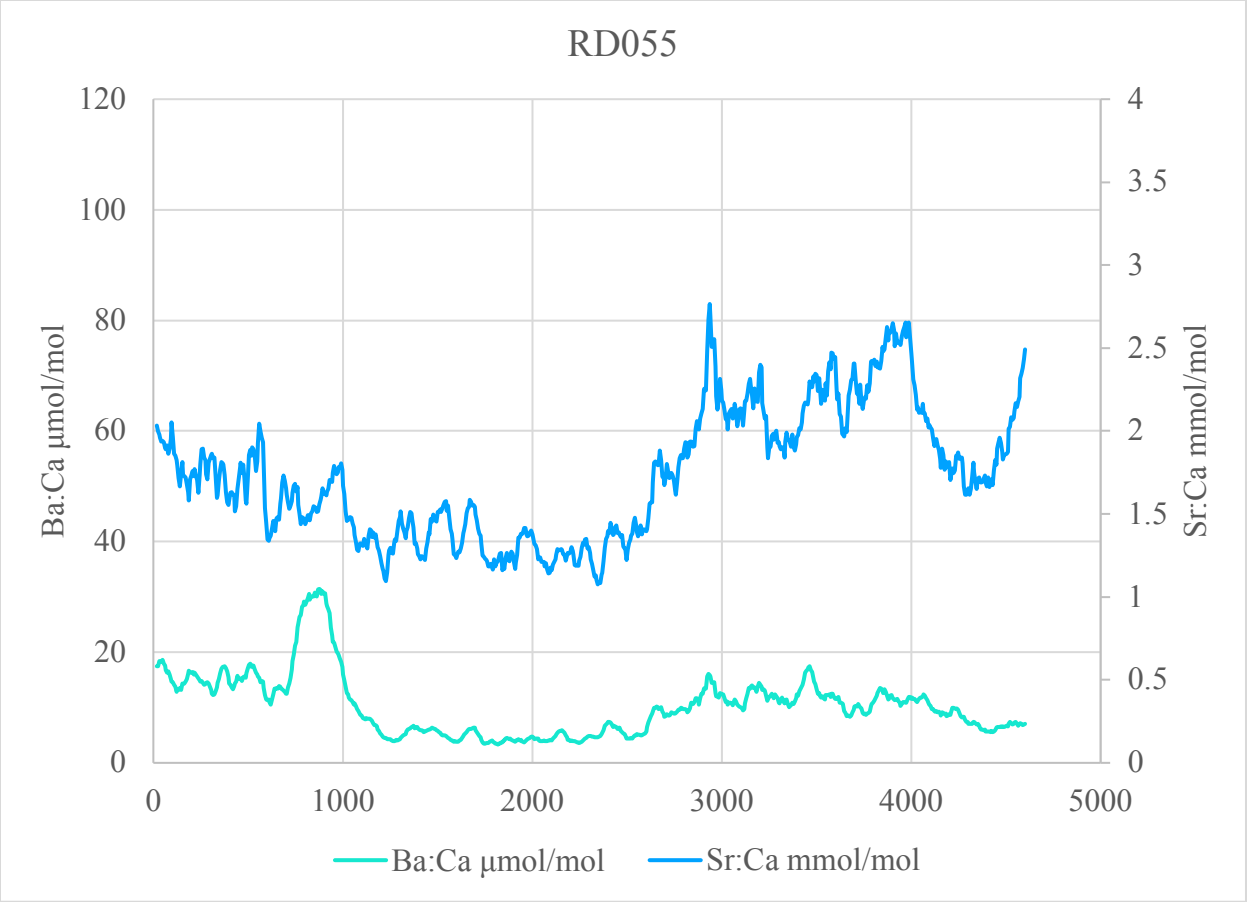

Figure A.55. The Ba:Ca and Sr:Ca life history profile of individual RD055.

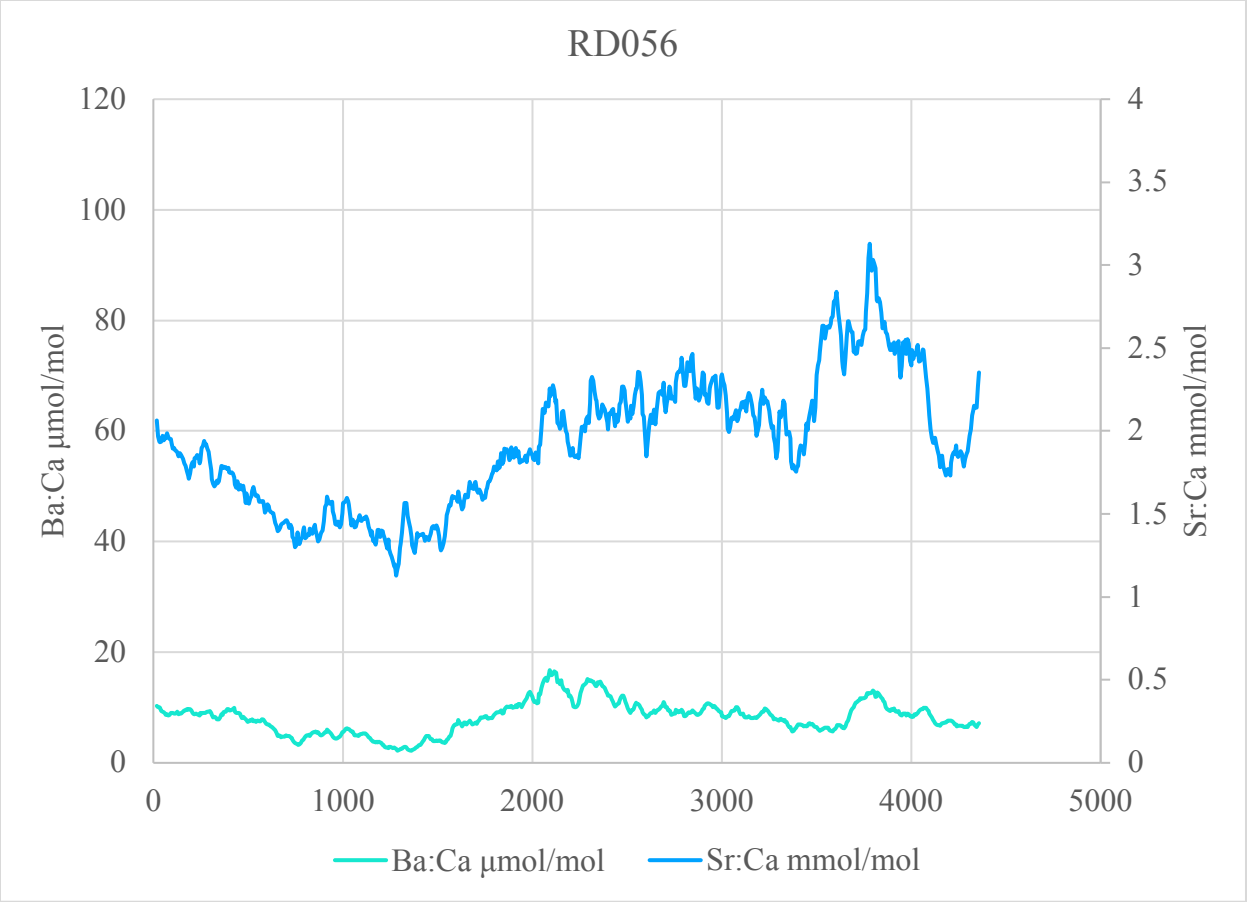

Figure A.56. The Ba:Ca and Sr:Ca life history profile of individual RD056.

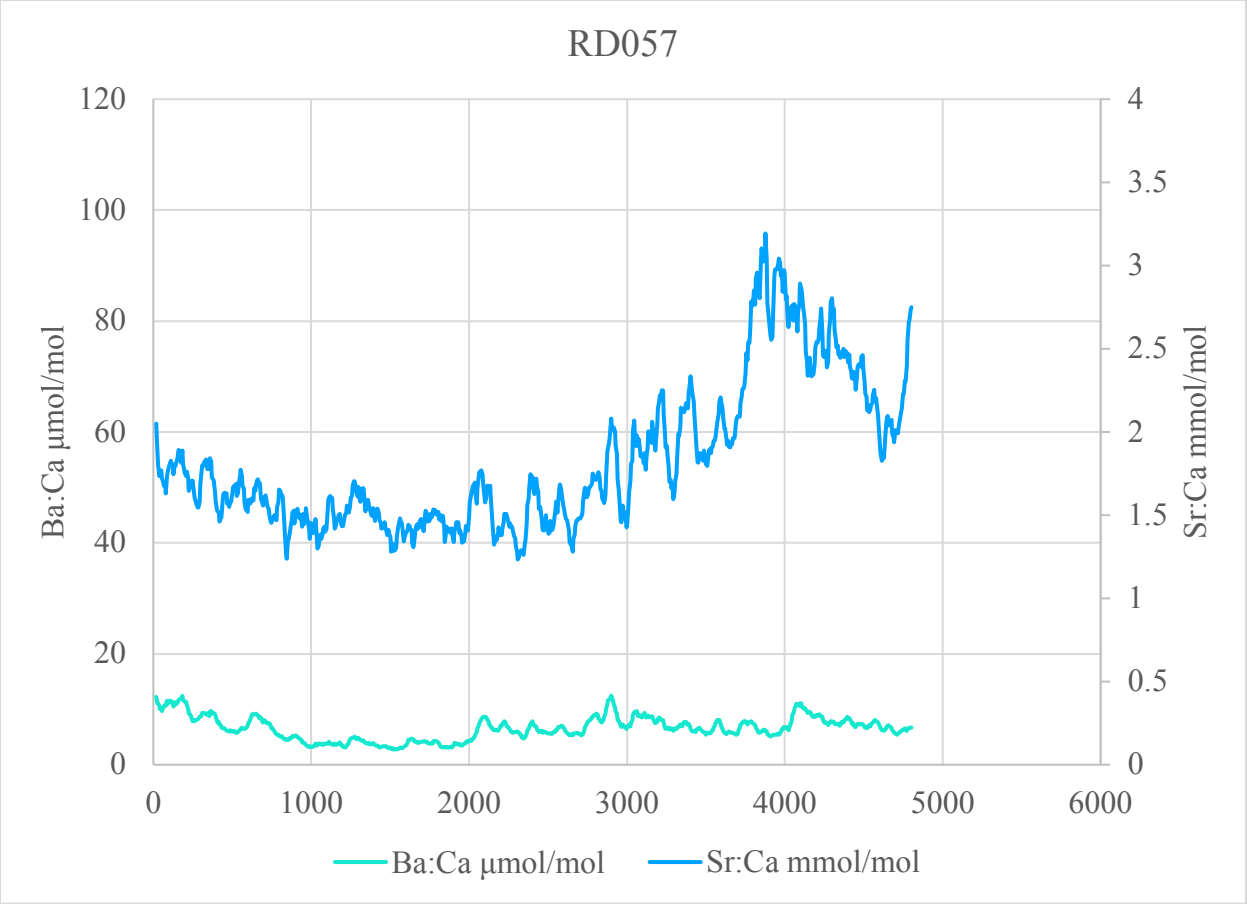

Figure A.57. The Ba:Ca and Sr:Ca life history profile of individual RD057.

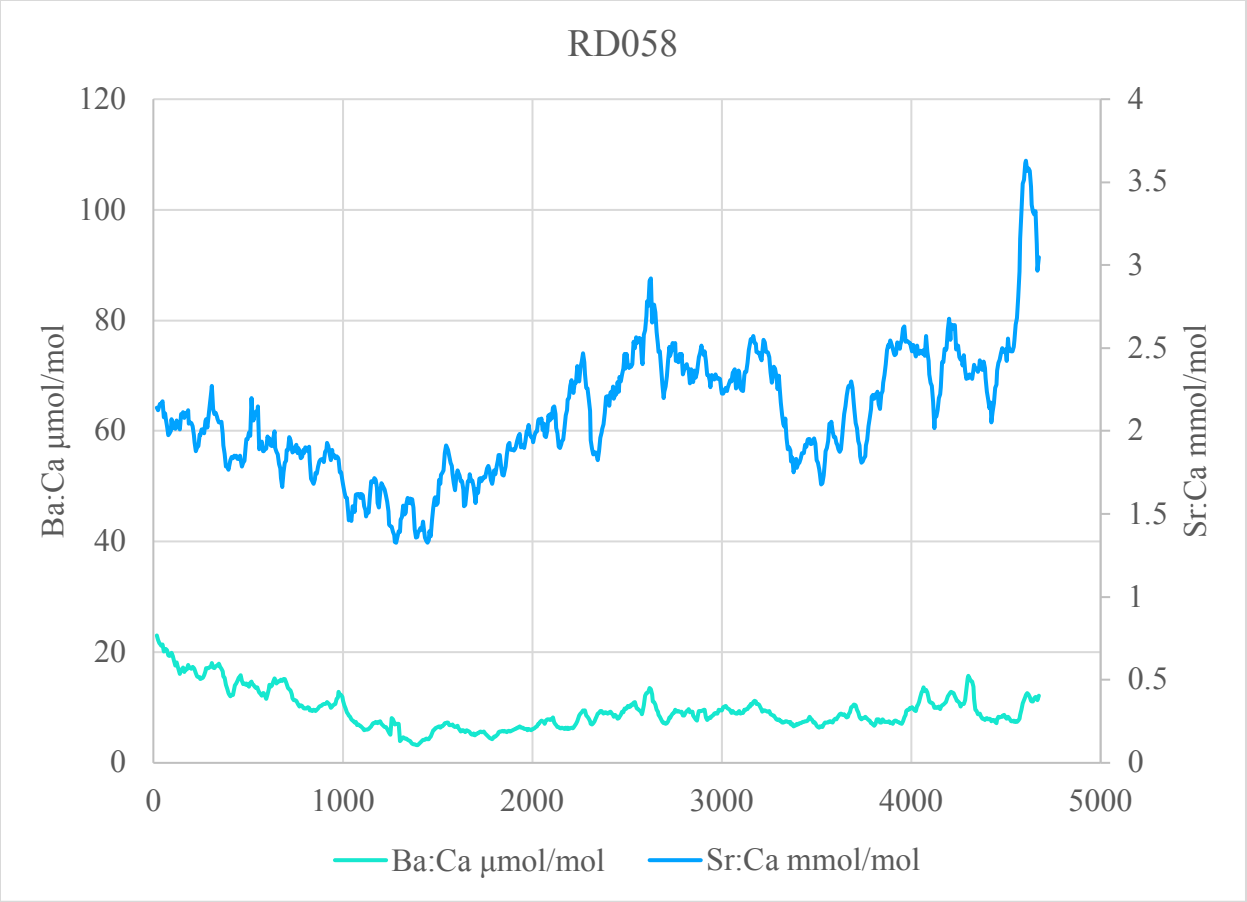

Figure A.58. The Ba:Ca and Sr:Ca life history profile of individual RD058.

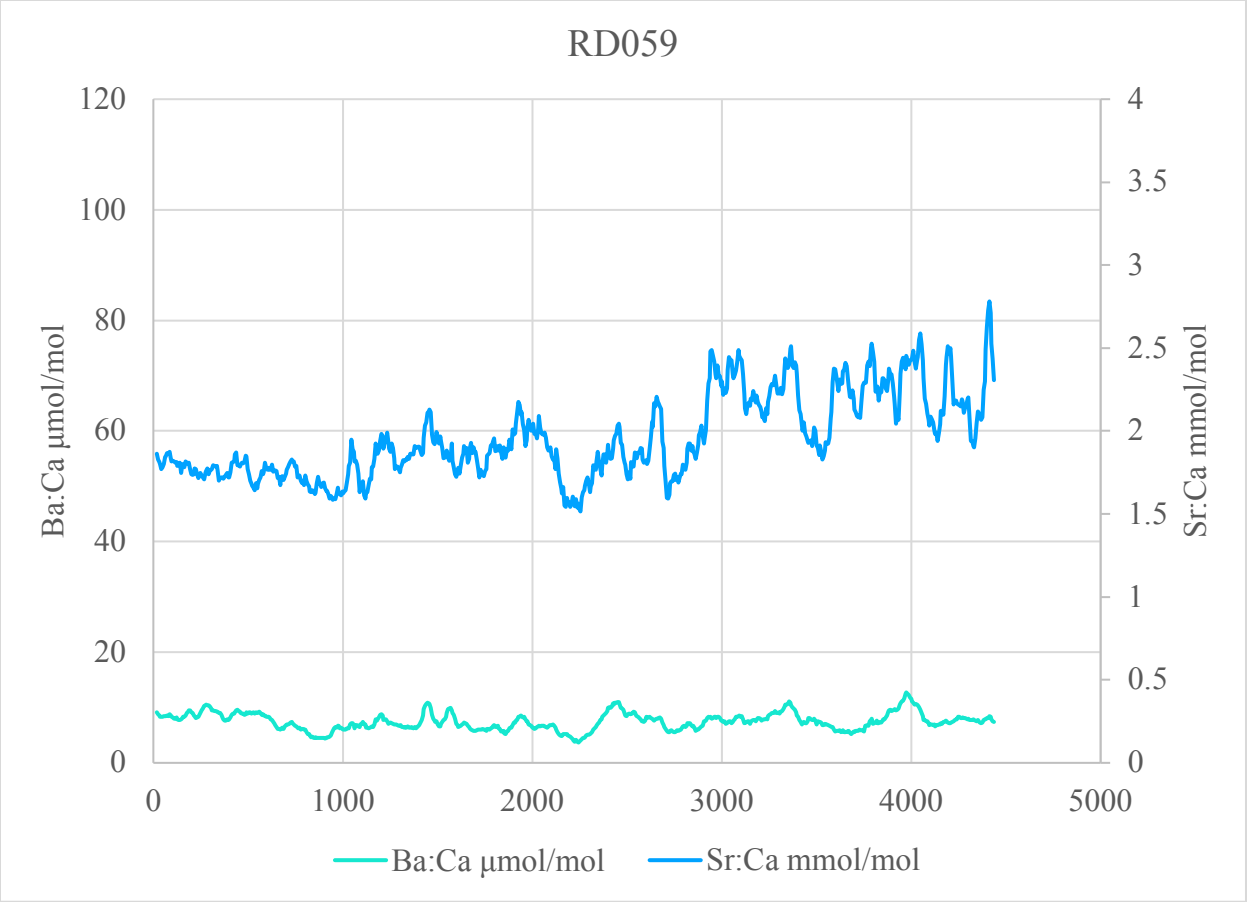

Figure A.59. The Ba:Ca and Sr:Ca life history profile of individual RD059.

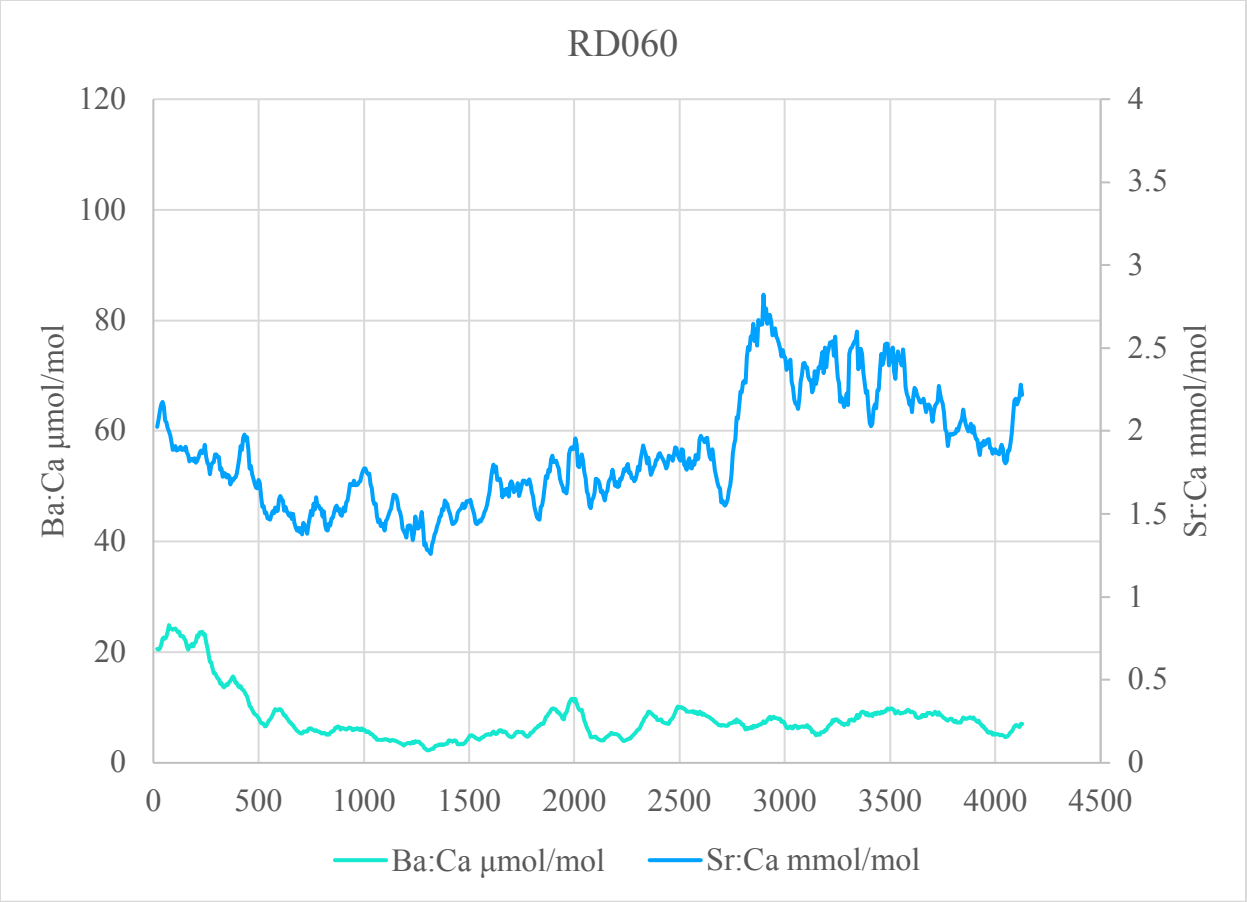

Figure A.60. The Ba:Ca and Sr:Ca life history profile of individual RD060.

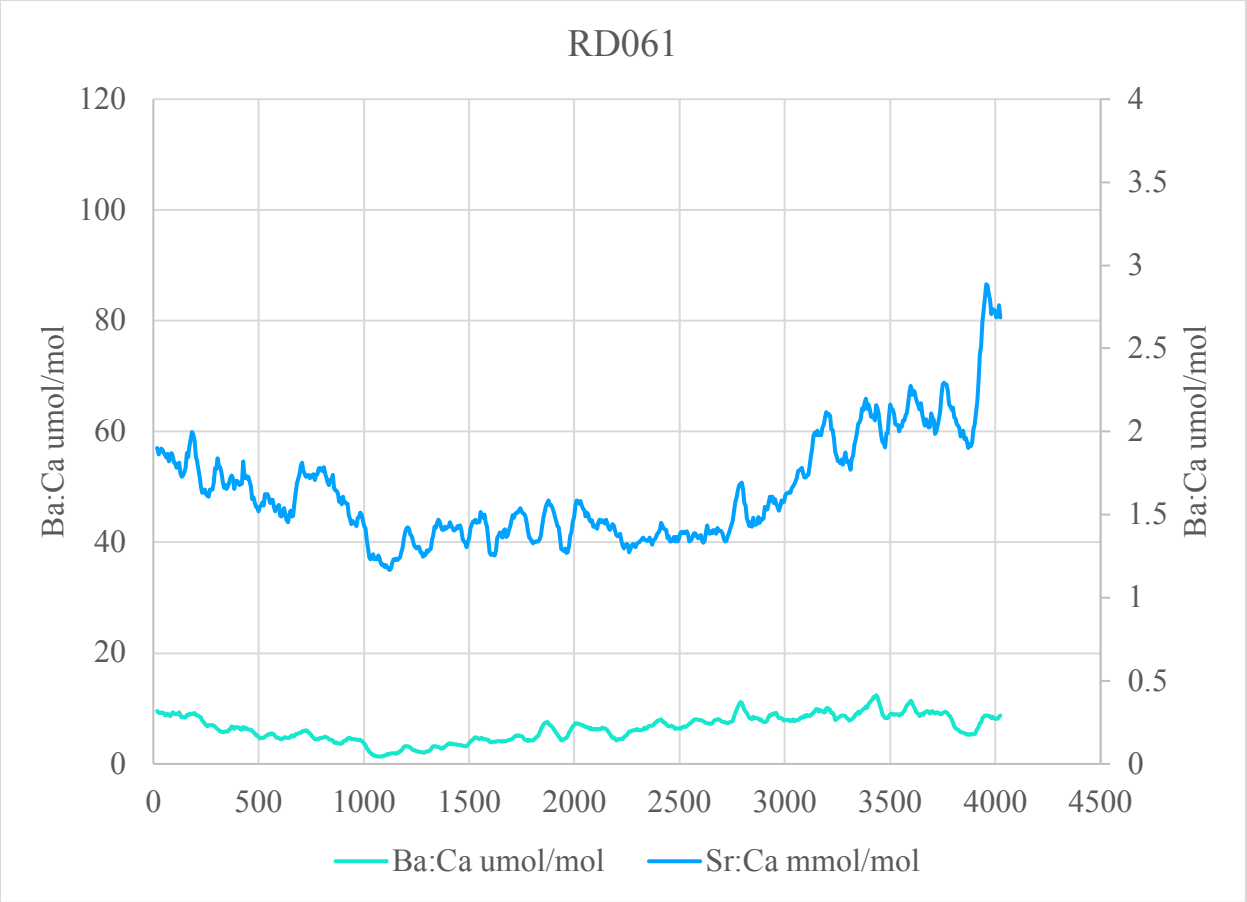

Figure A.61. The Ba:Ca and Sr:Ca life history profile of individual RD061.

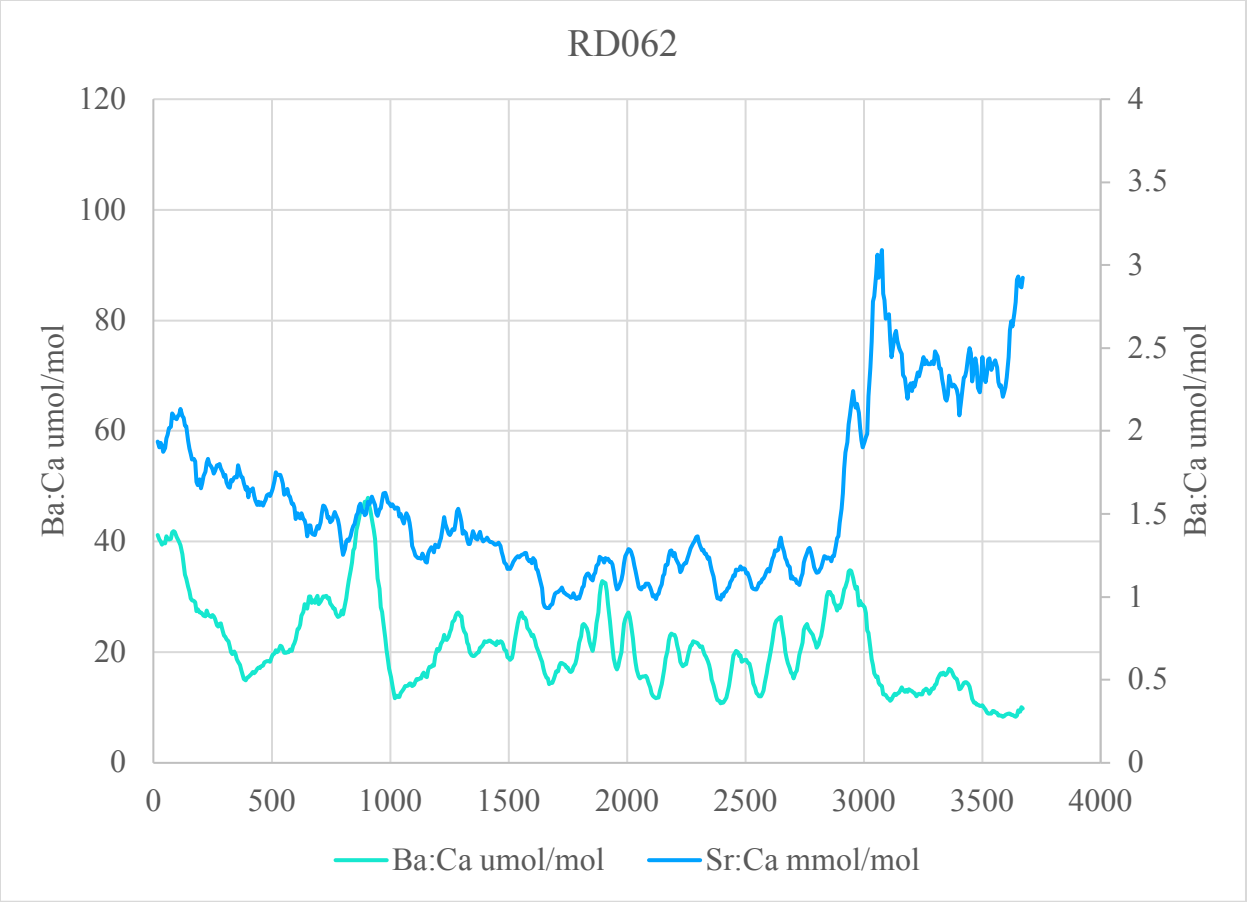

Figure A.62. The Ba:Ca and Sr:Ca life history profile of individual RD062.

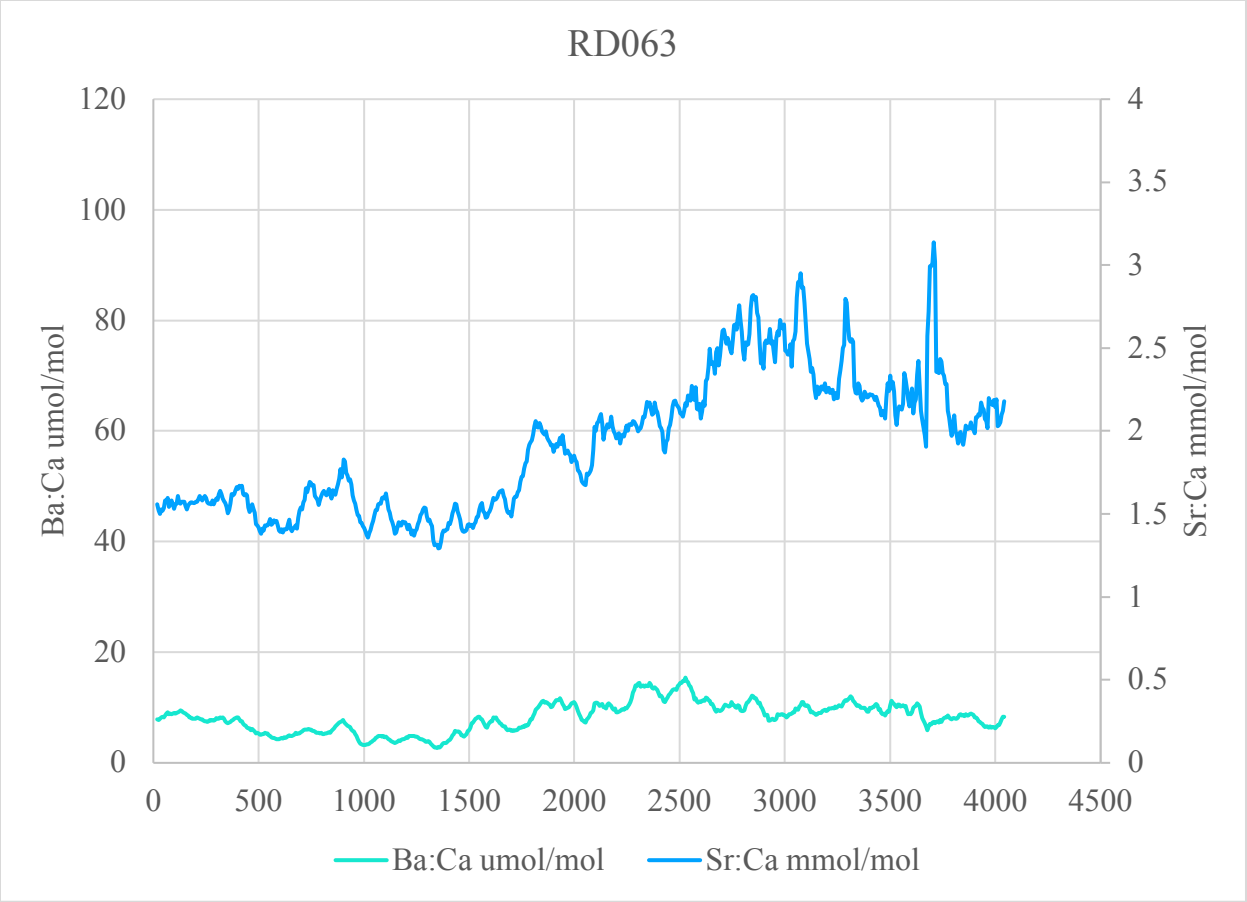

Figure A.63. The Ba:Ca and Sr:Ca life history profile of individual RD063.

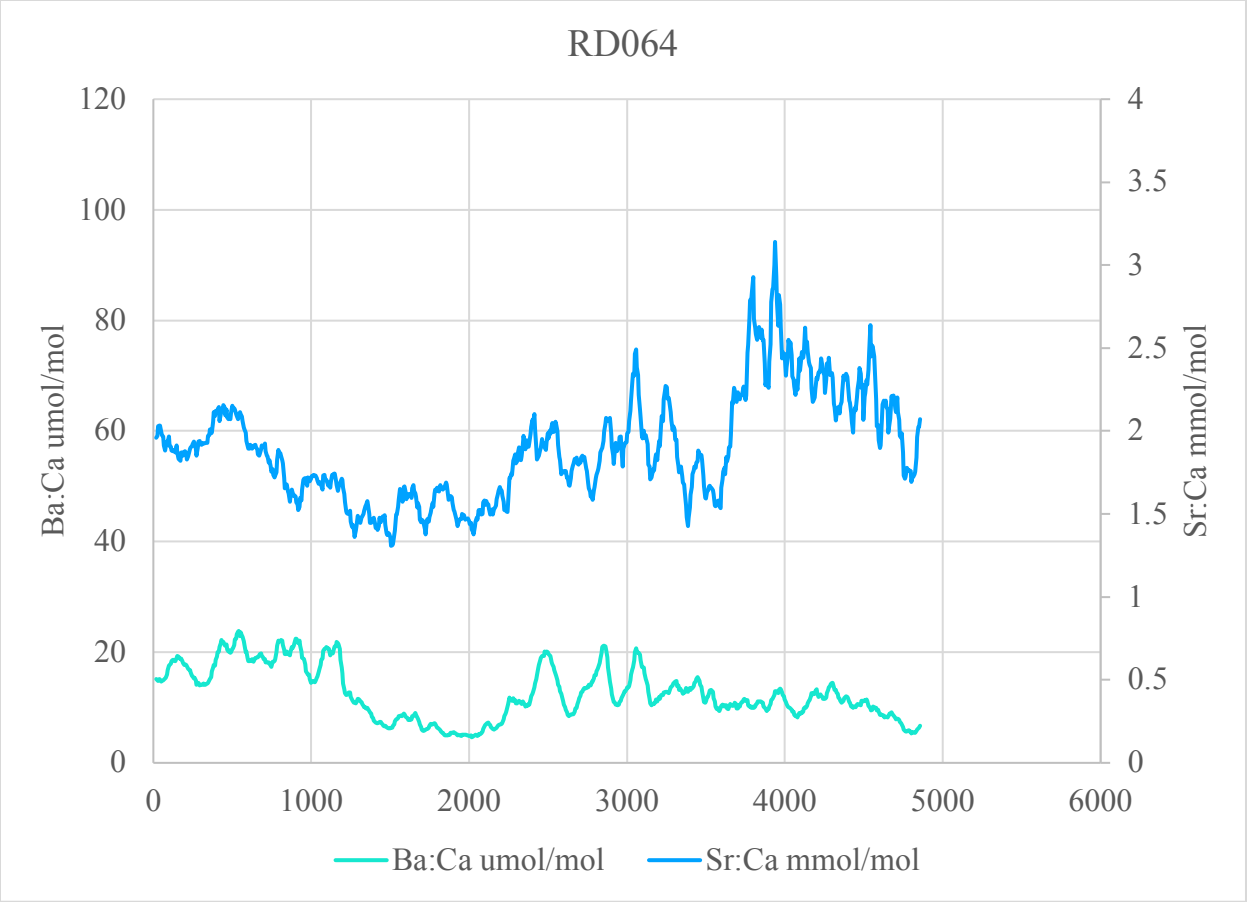

Figure A.64. The Ba:Ca and Sr:Ca life history profile of individual RD064.

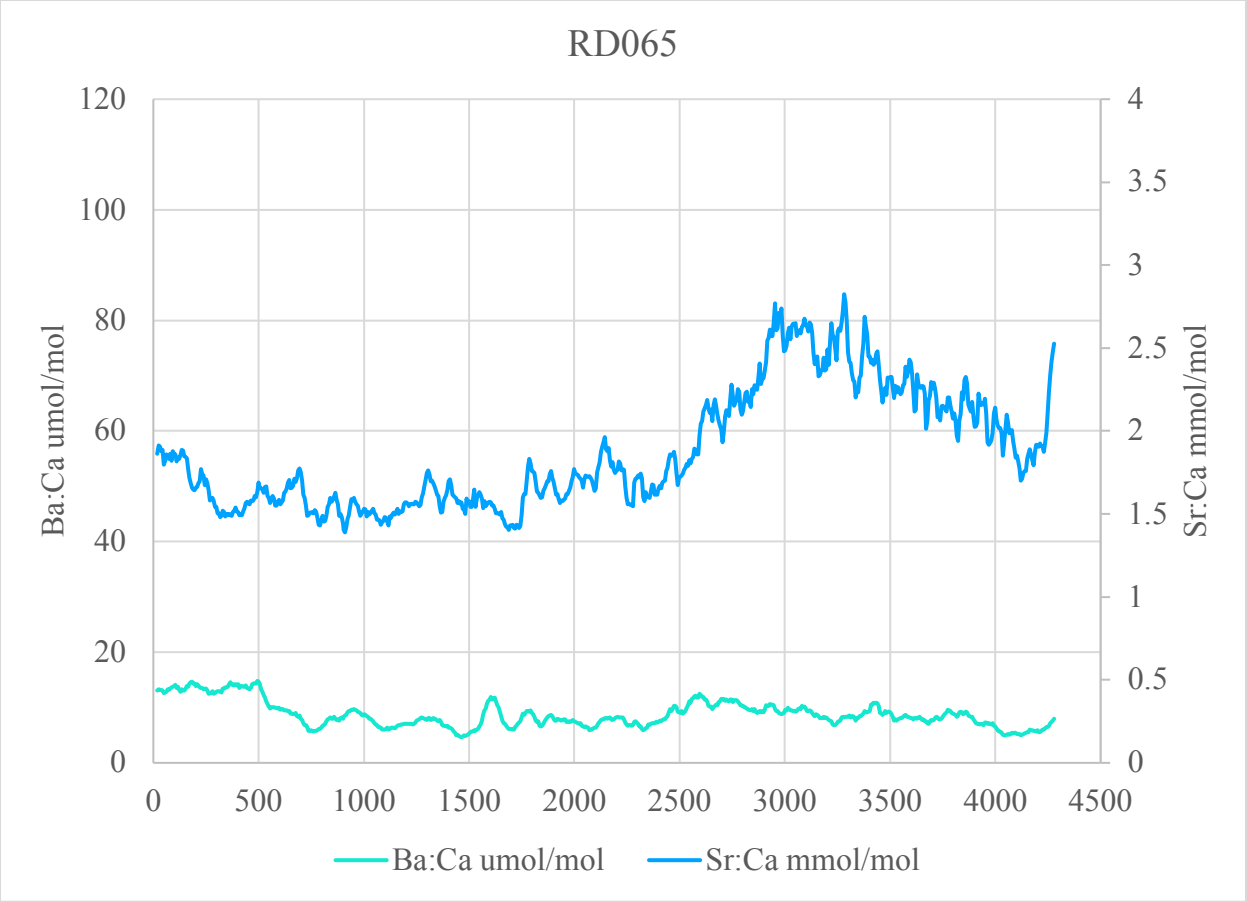

Figure A.65. The Ba:Ca and Sr:Ca life history profile of individual RD065.

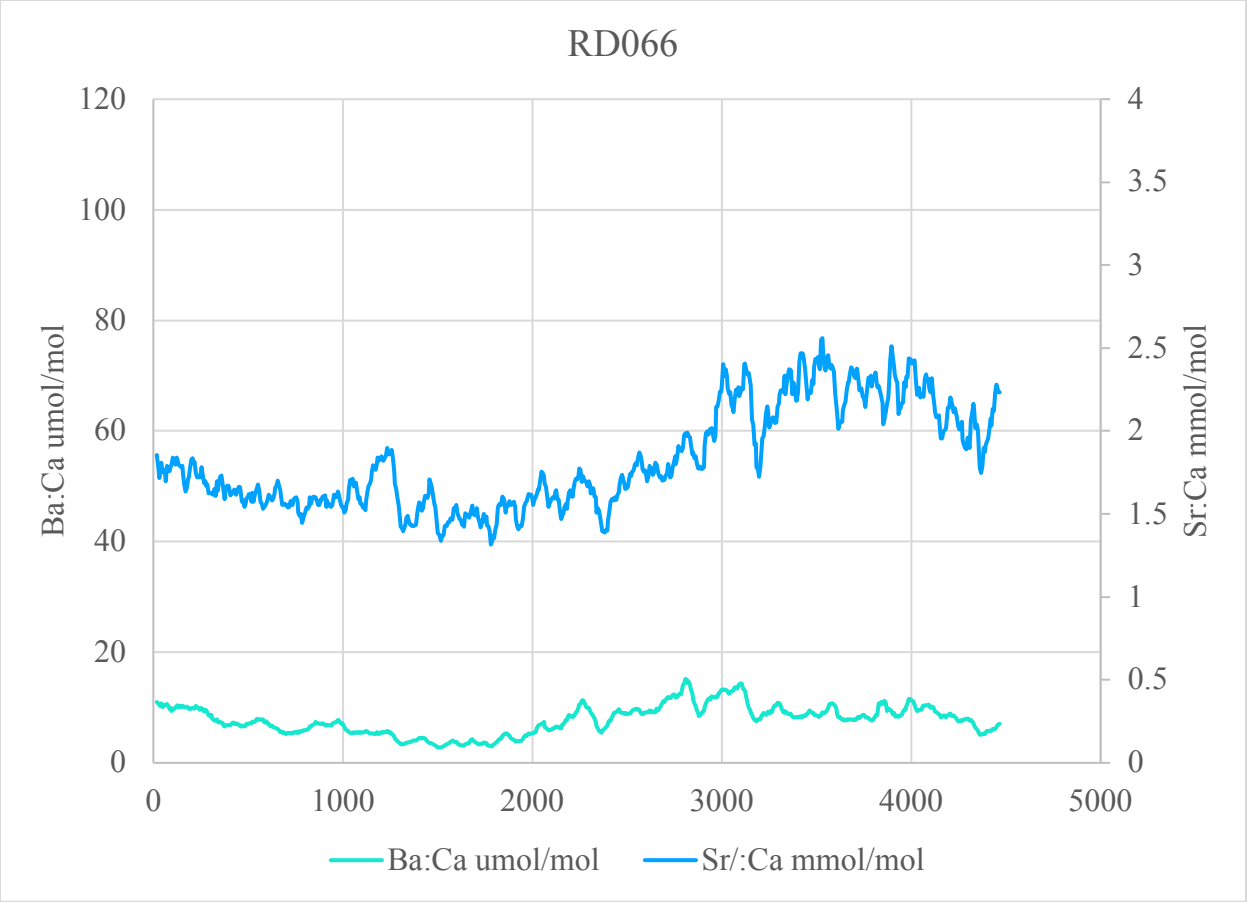

Figure A.66. The Ba:Ca and Sr:Ca life history profile of individual RD066.

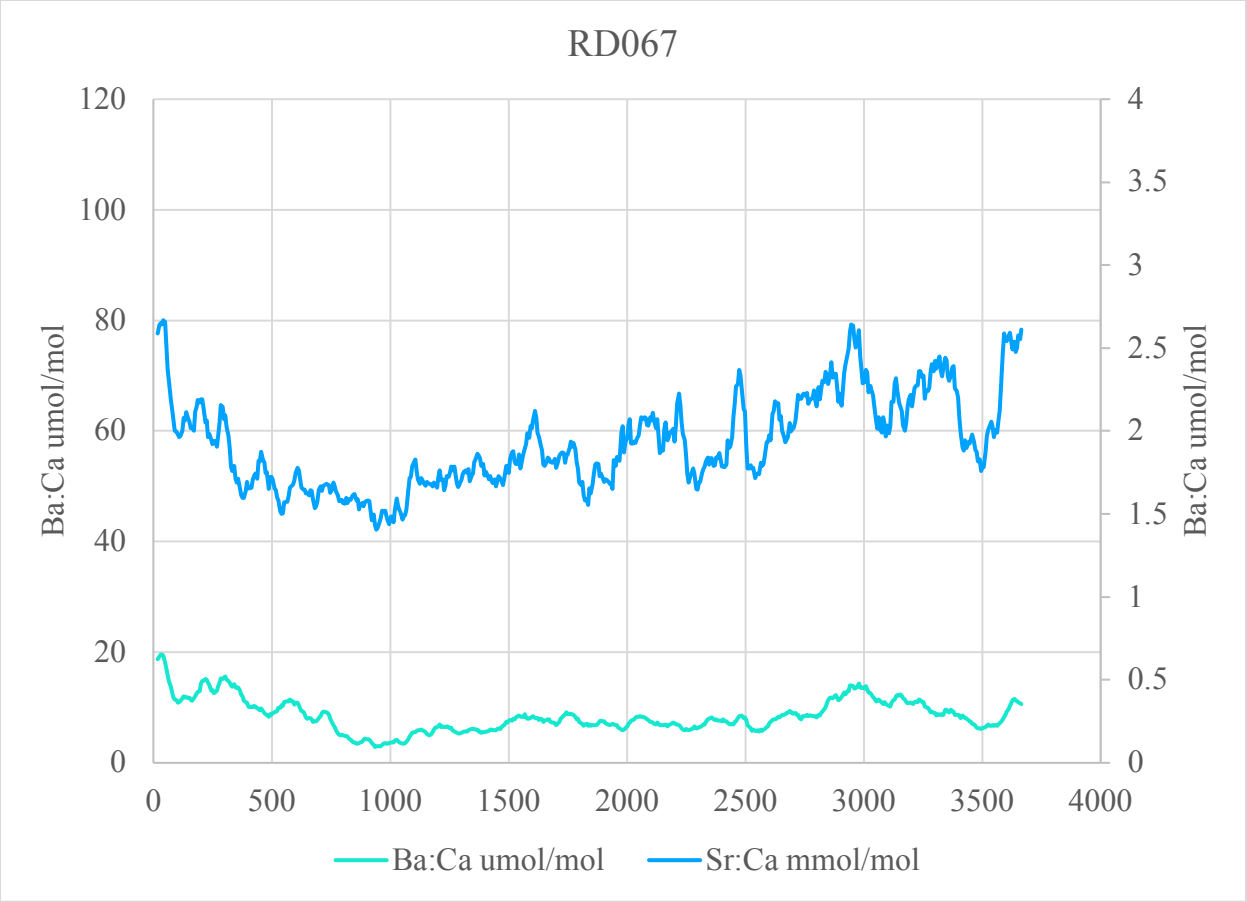

Figure A.67. The Ba:Ca and Sr:Ca life history profile of individual RD067.

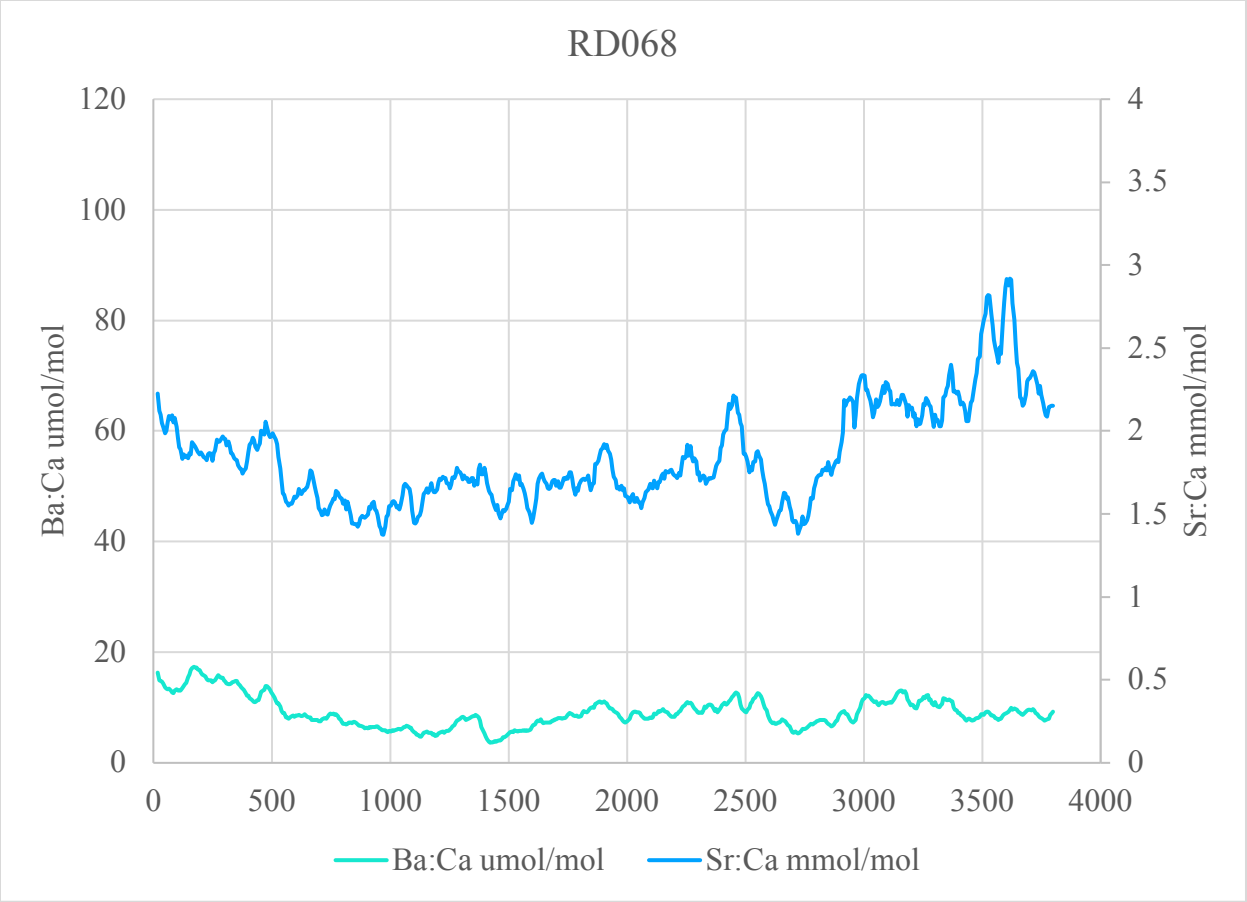

Figure A.68. The Ba:Ca and Sr:Ca life history profile of individual RD068.

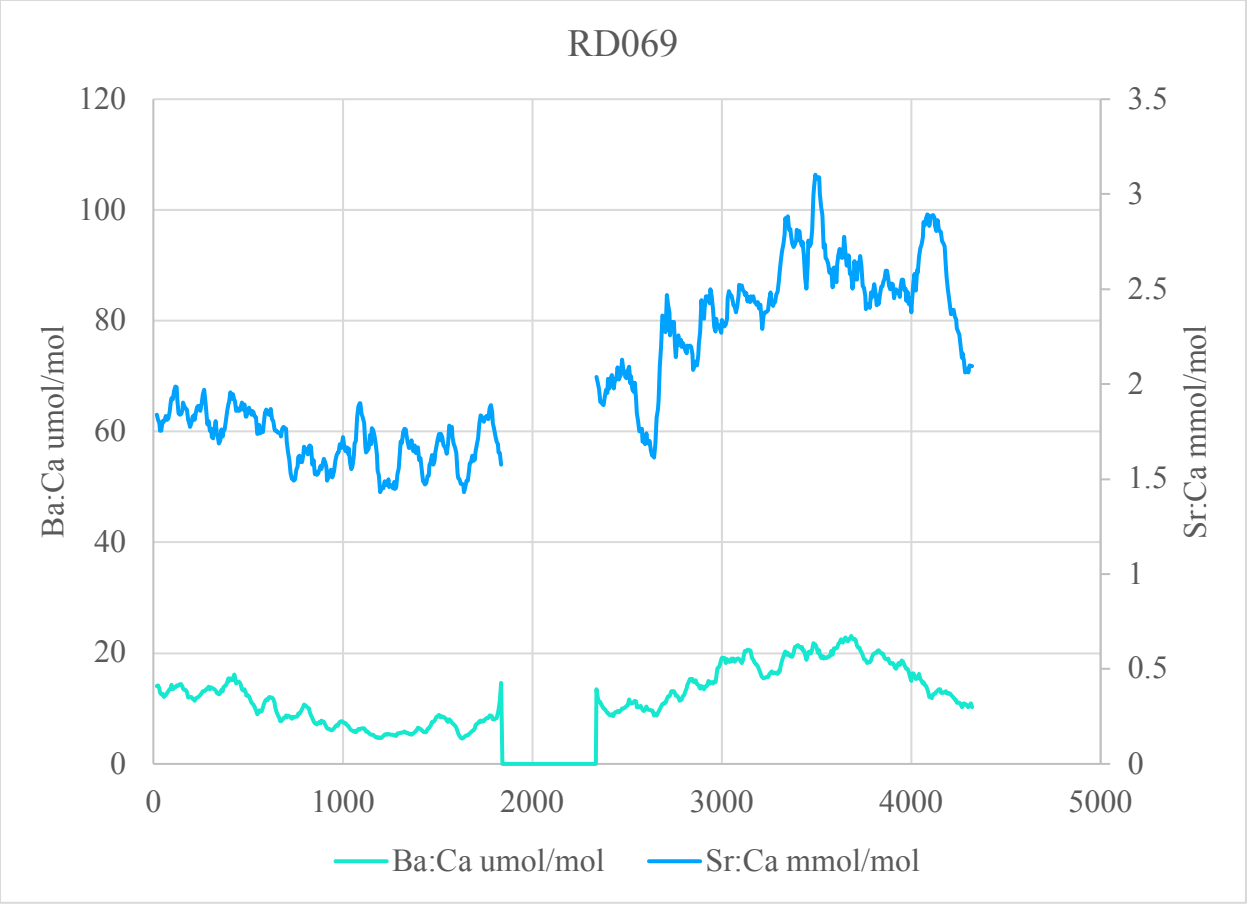

Figure A.69. The Ba:Ca and Sr:Ca life history profile of individual RD069. Note: values were removed for potential crack in otolith.

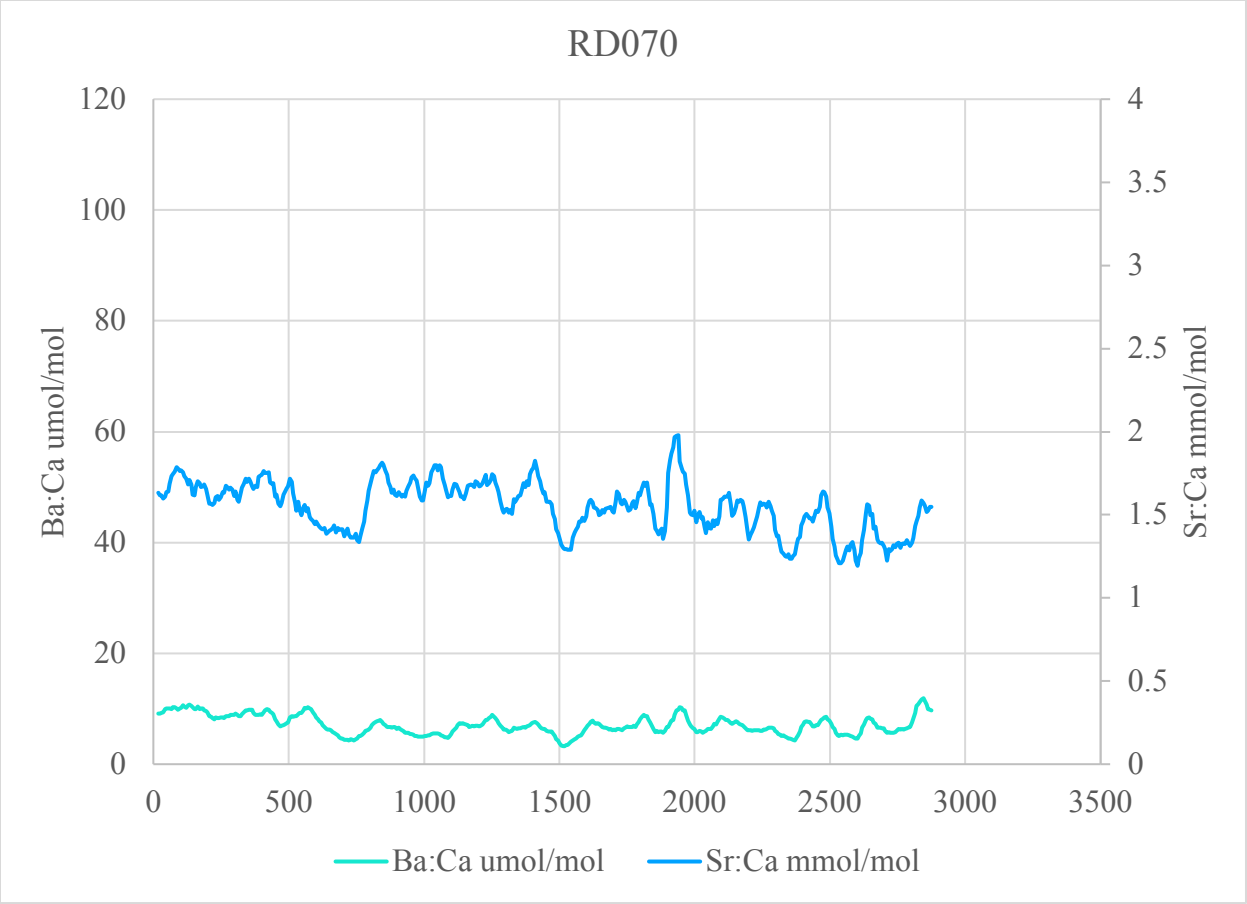

Figure A.70. The Ba:Ca and Sr:Ca life history profile of individual RD070.

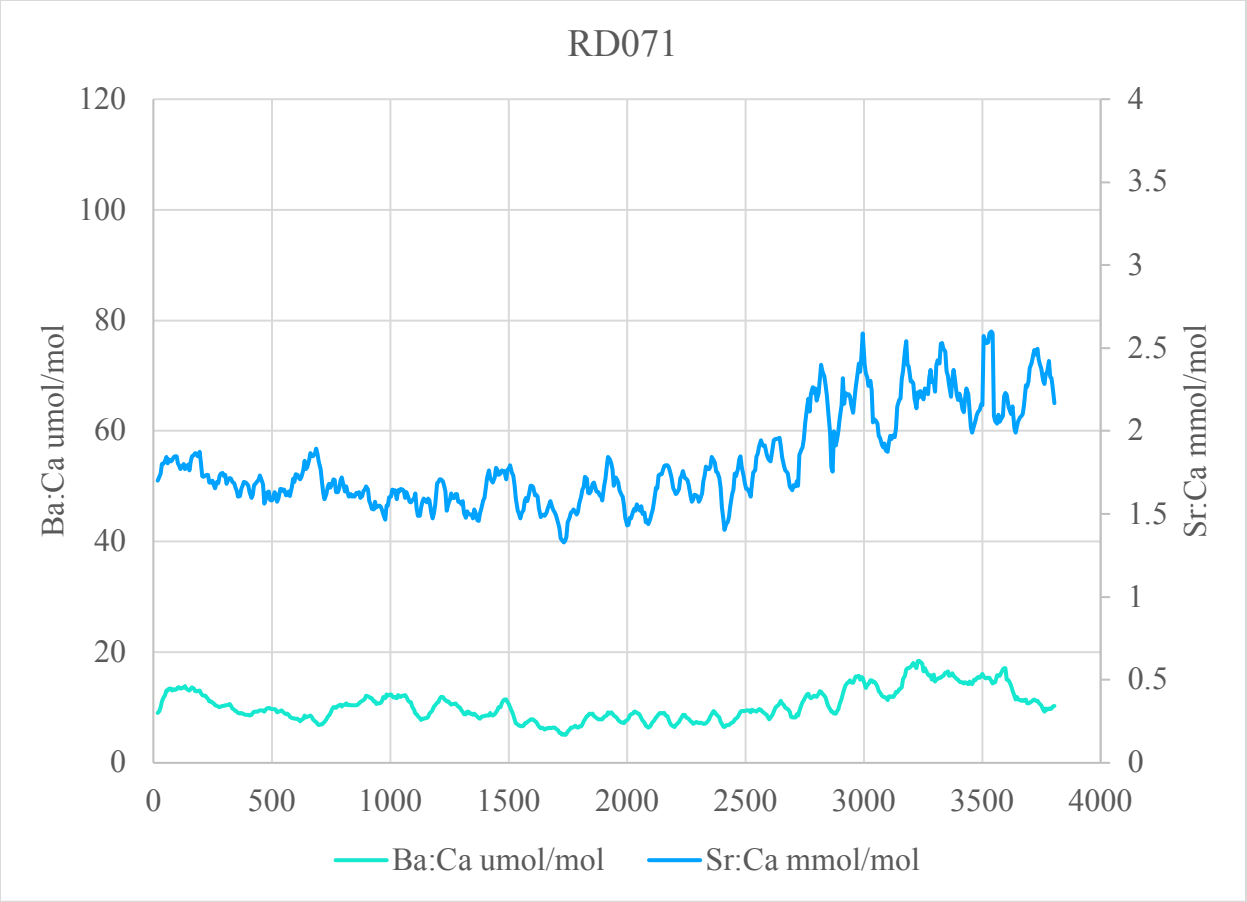

Figure A.71. The Ba:Ca and Sr:Ca life history profile of individual RD071.

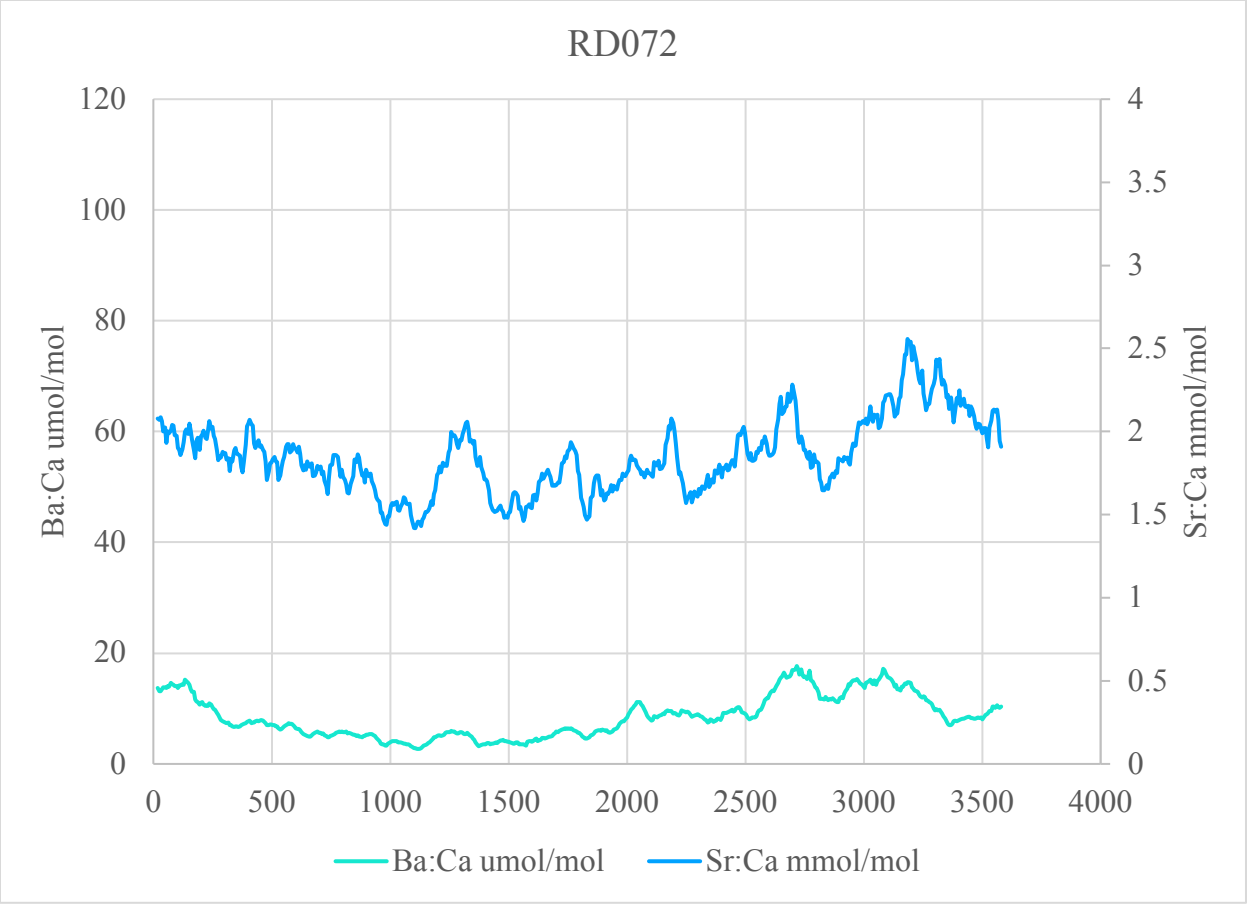

Figure A.72. The Ba:Ca and Sr:Ca life history profile of individual RD072.

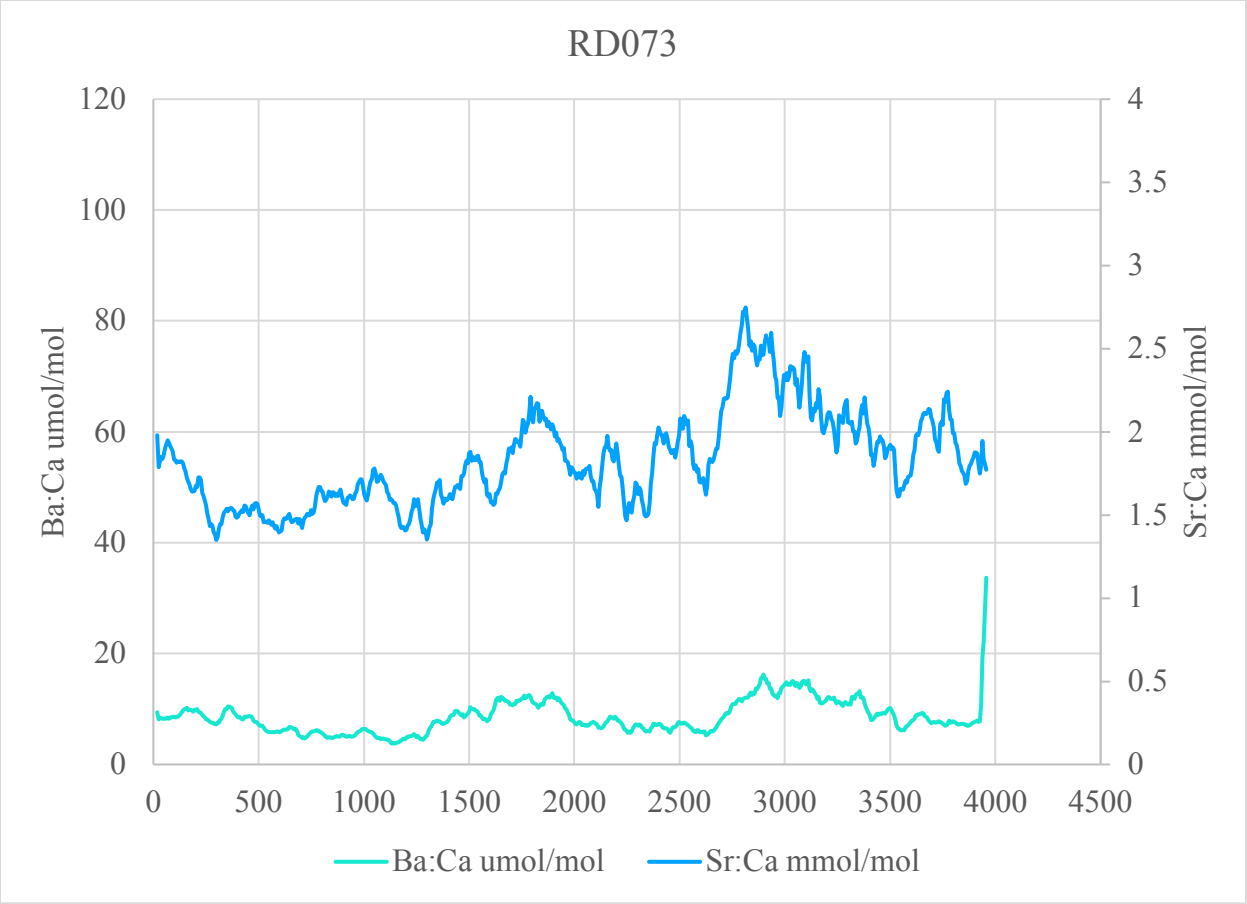

Figure A.73. The Ba:Ca and Sr:Ca life history profile of individual RD073.

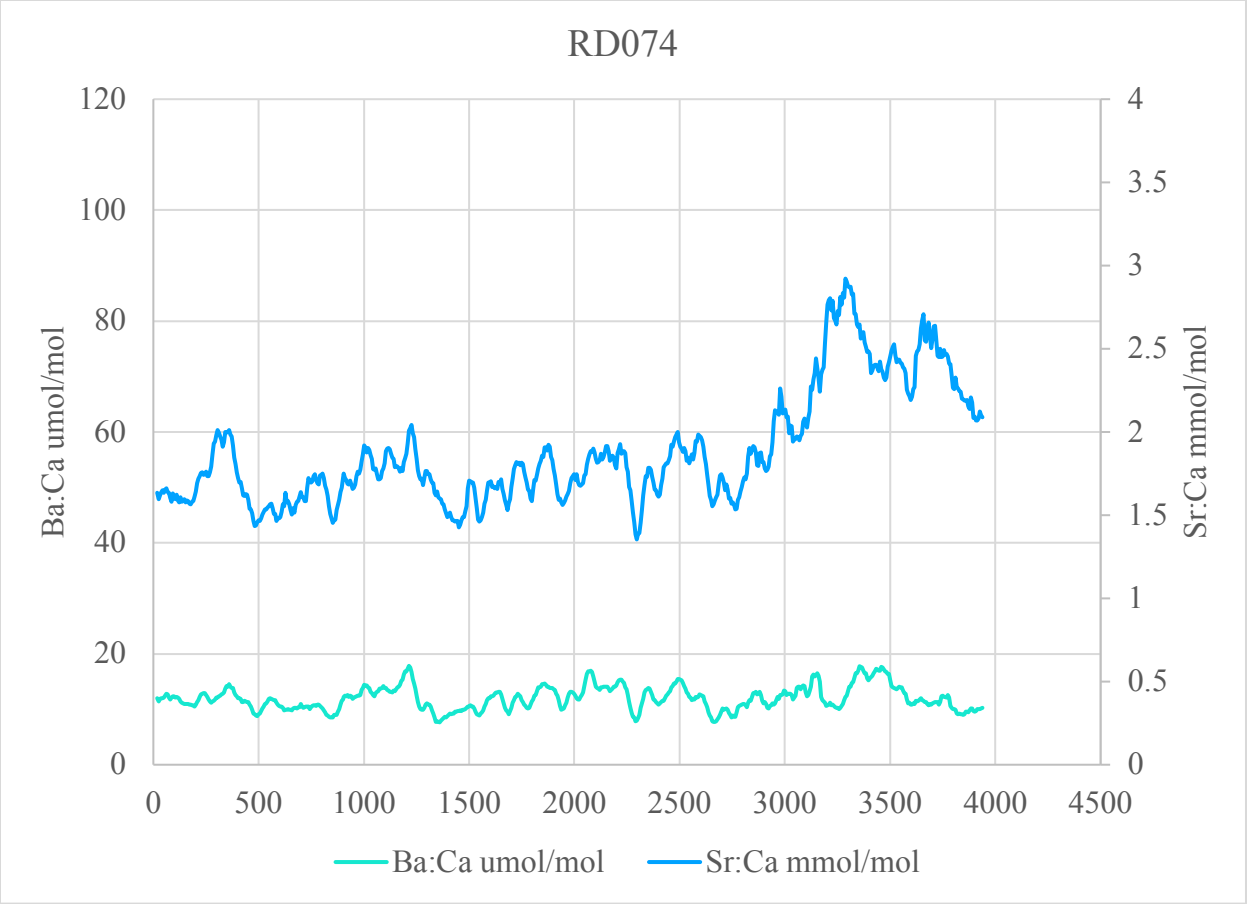

Figure A.74. The Ba:Ca and Sr:Ca life history profile of individual RD074.

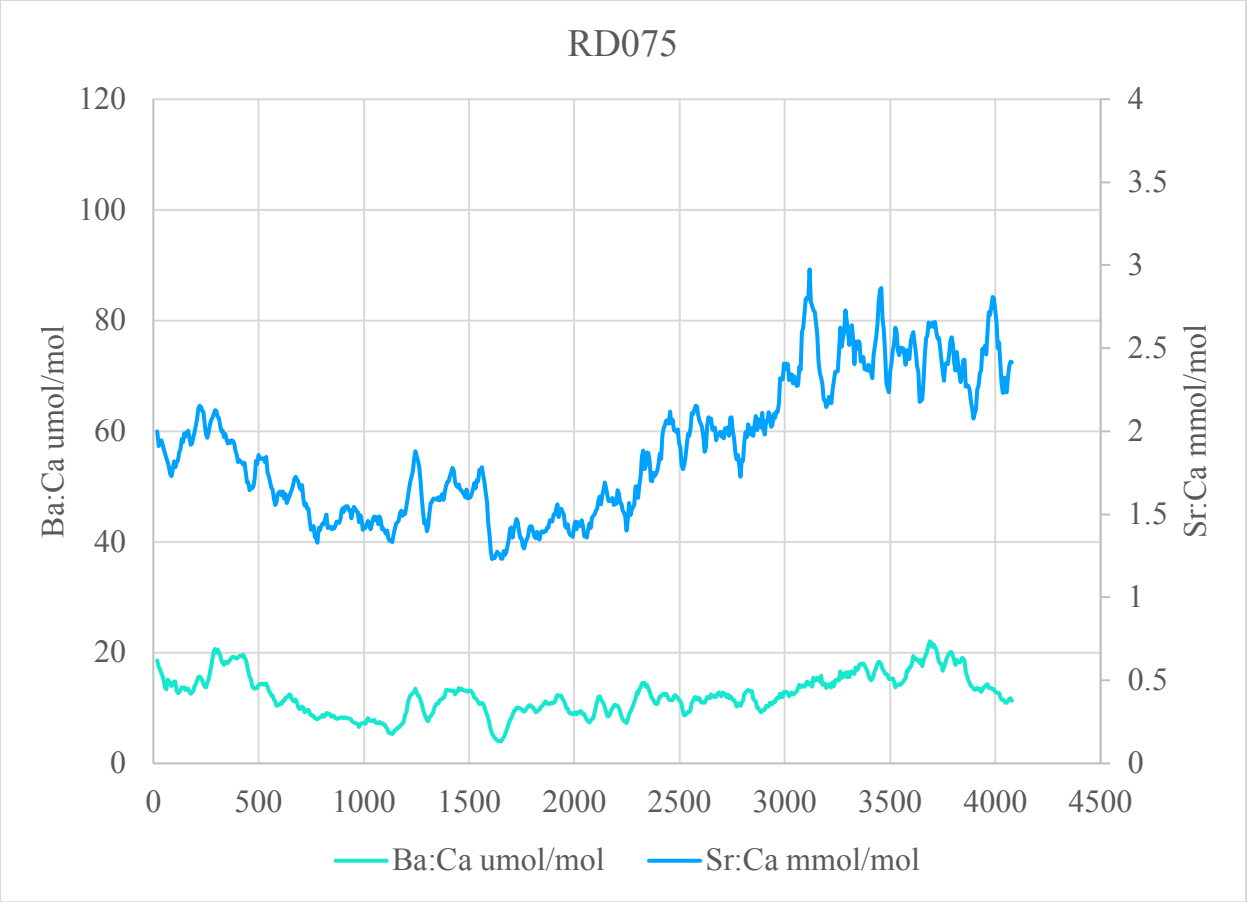

Figure A.75. The Ba:Ca and Sr:Ca life history profile of individual RD075.

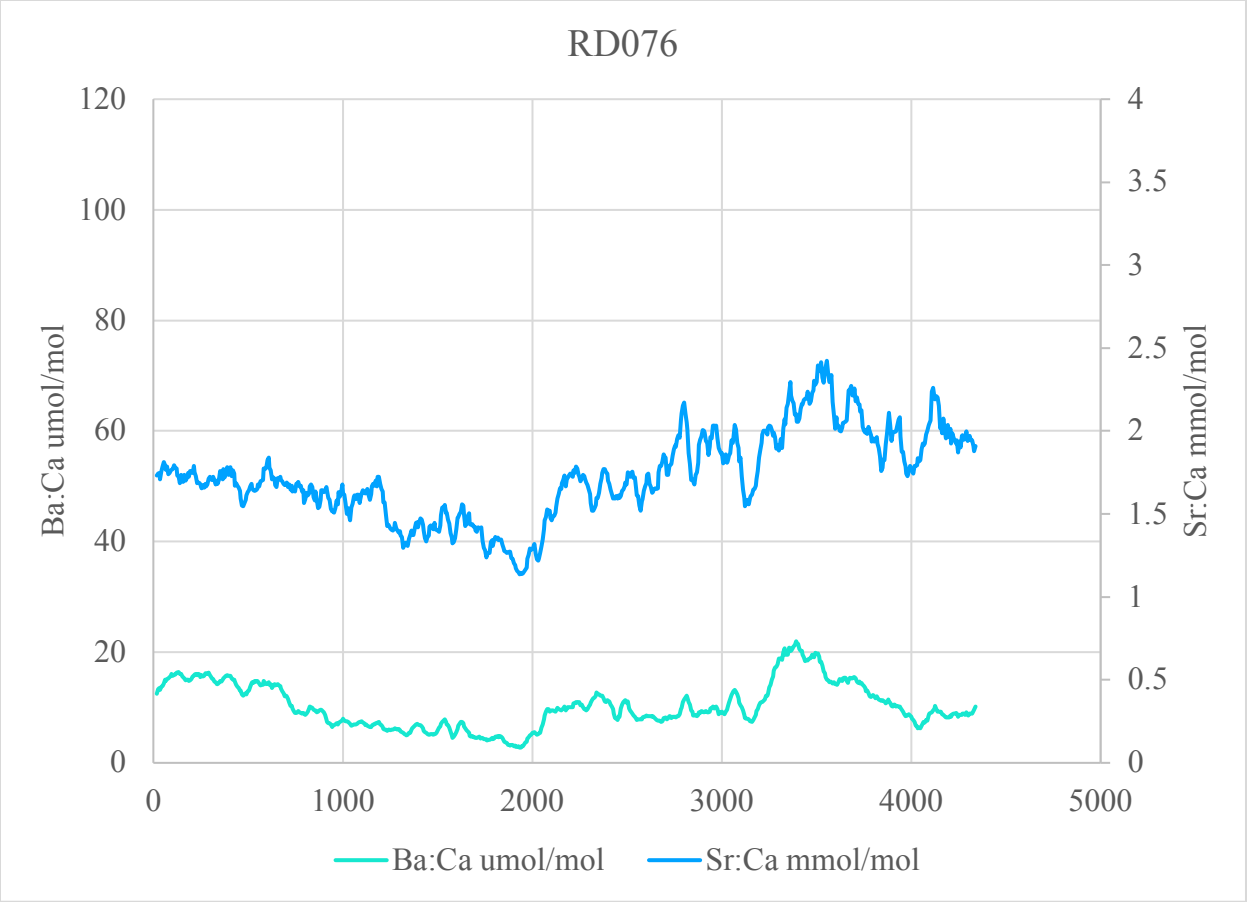

Figure A.76. The Ba:Ca and Sr:Ca life history profile of individual RD076.

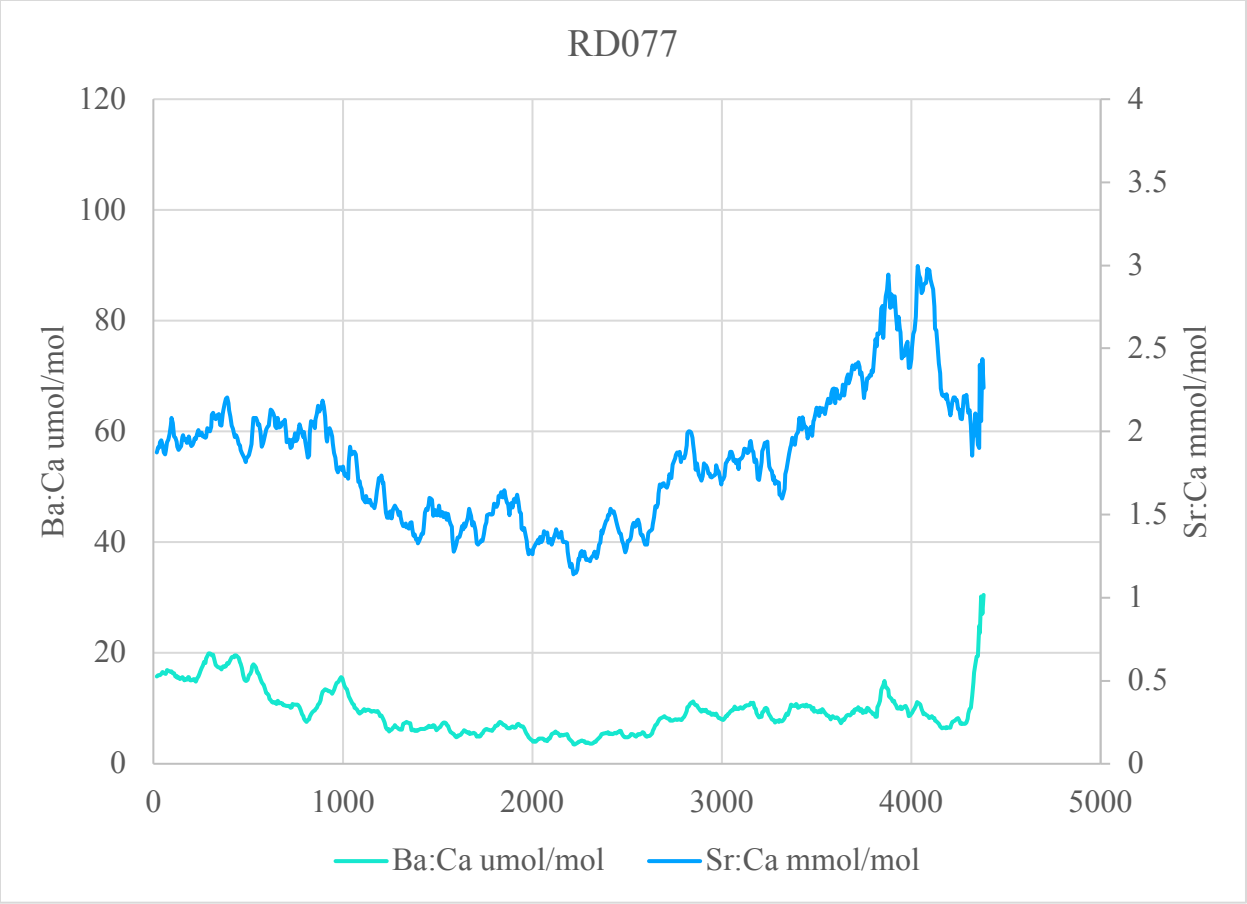

Figure A.77. The Ba:Ca and Sr:Ca life history profile of individual RD077.

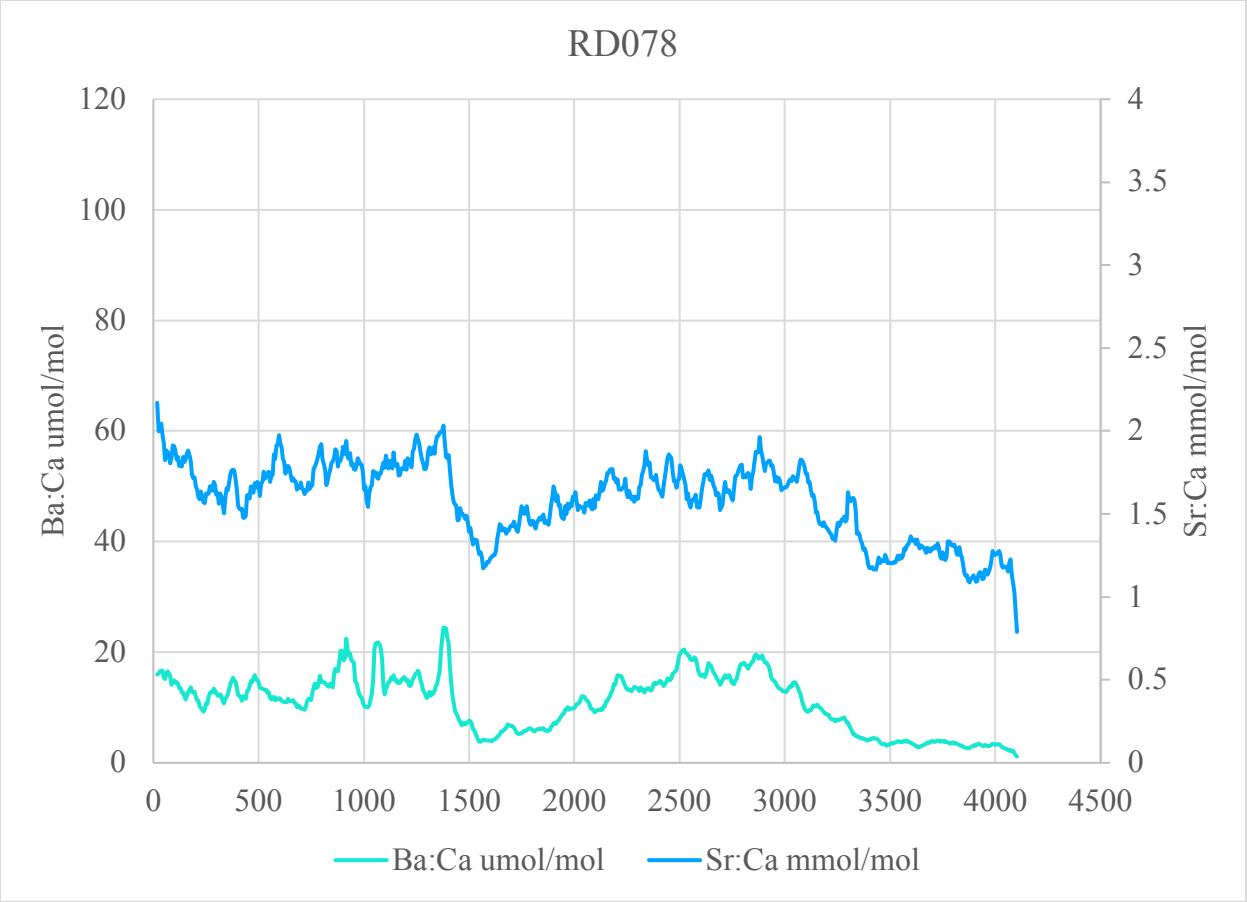

Figure A.78. The Ba:Ca and Sr:Ca life history profile of individual RD078.

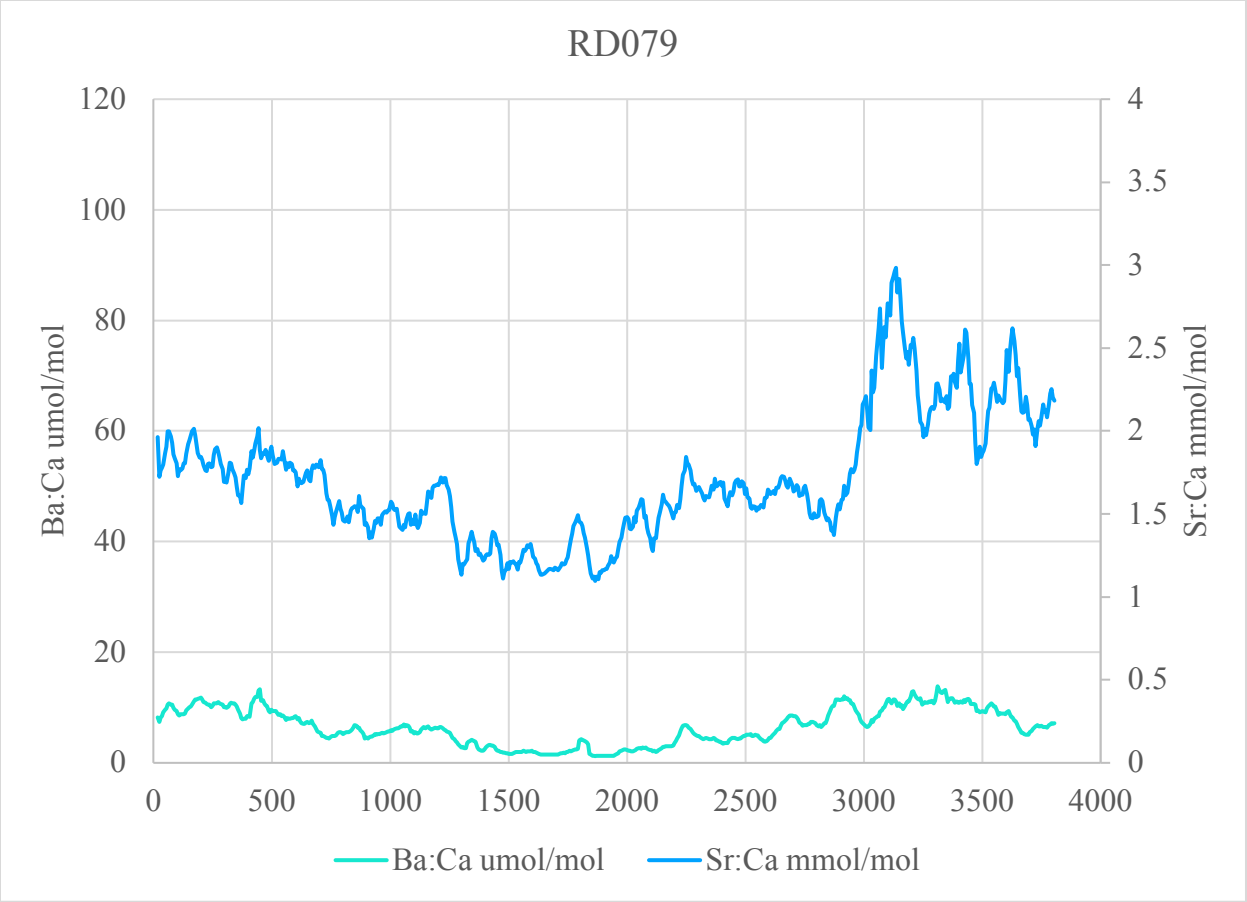

Figure A.79. The Ba:Ca and Sr:Ca life history profile of individual RD079.

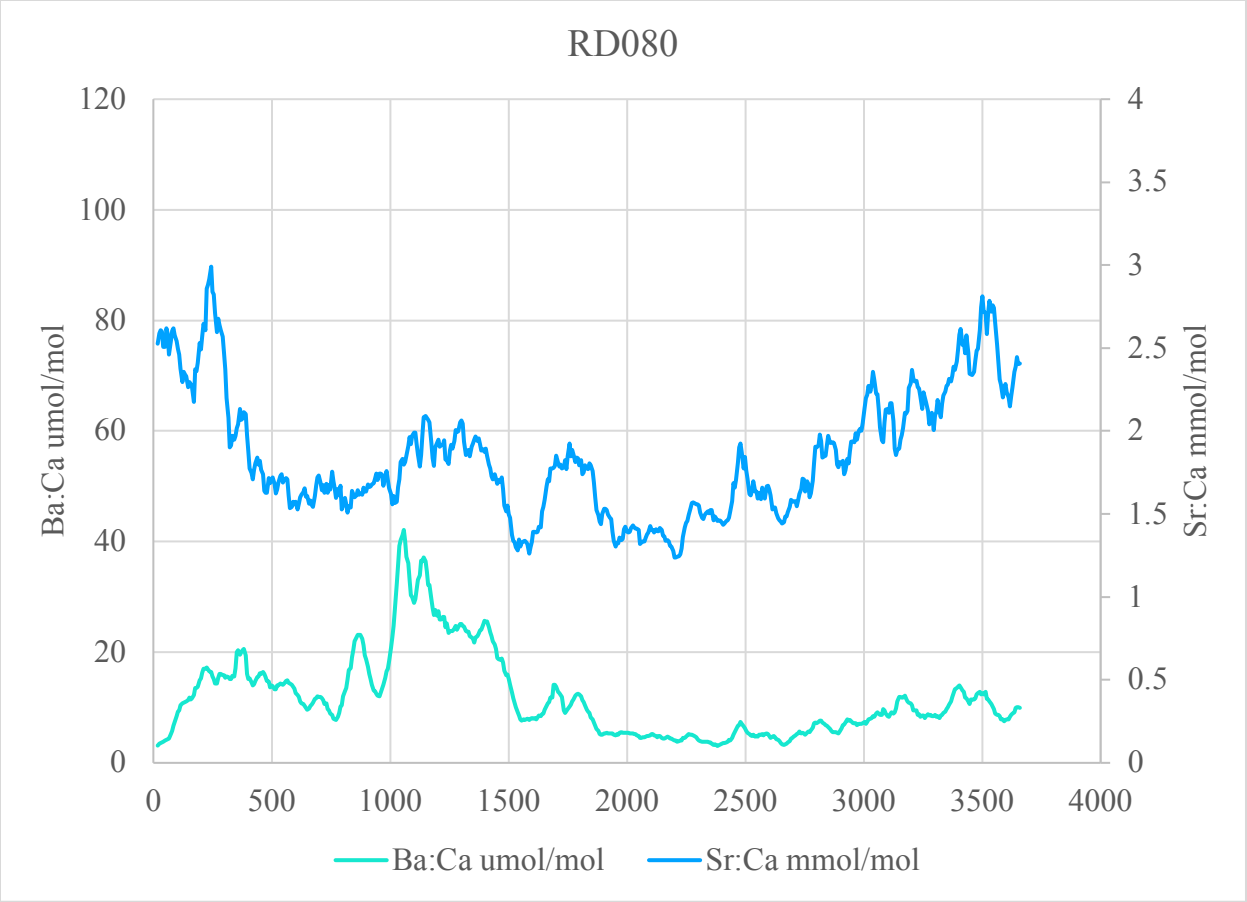

Figure A.80. The Ba:Ca and Sr:Ca life history profile of individual RD080.

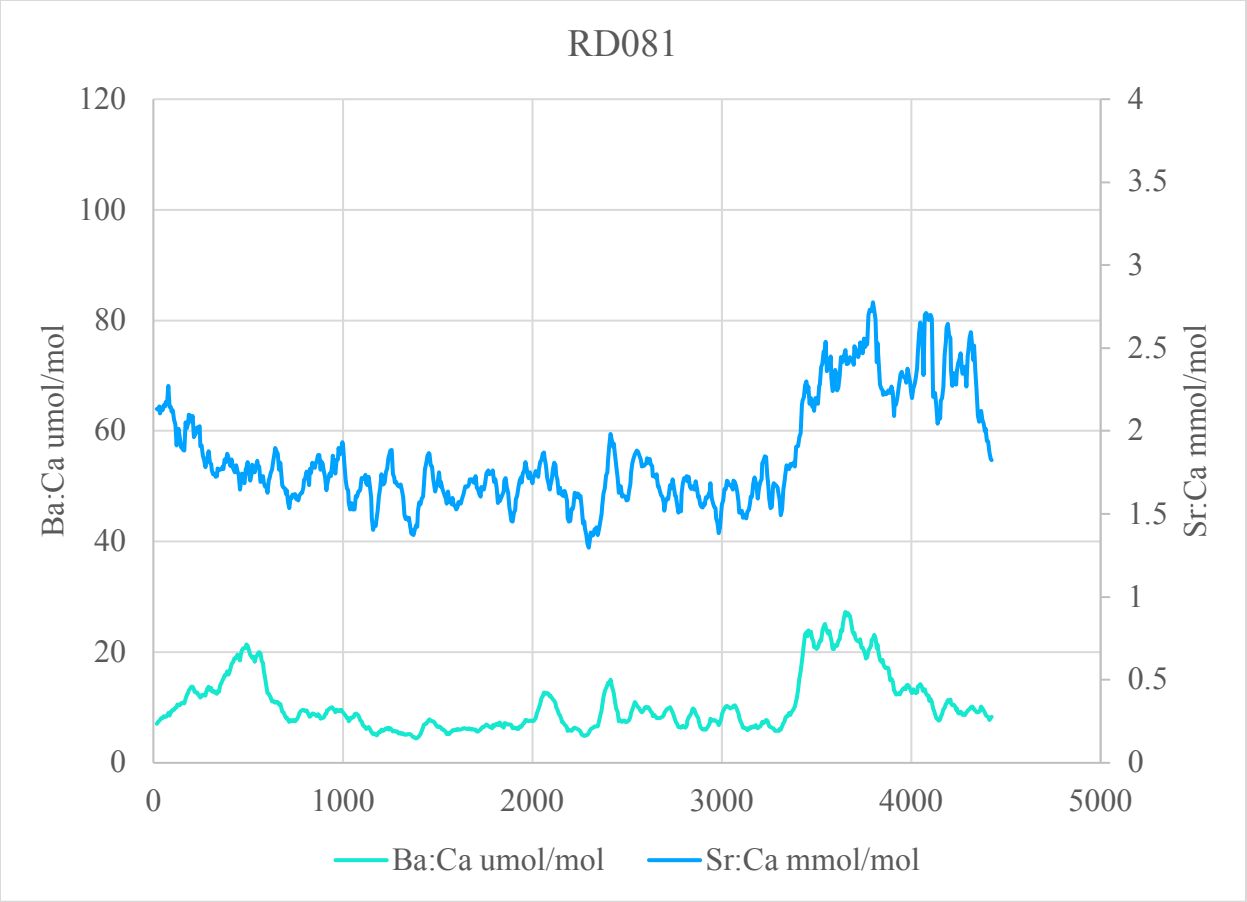

Figure A.81. The Ba:Ca and Sr:Ca life history profile of individual RD081.

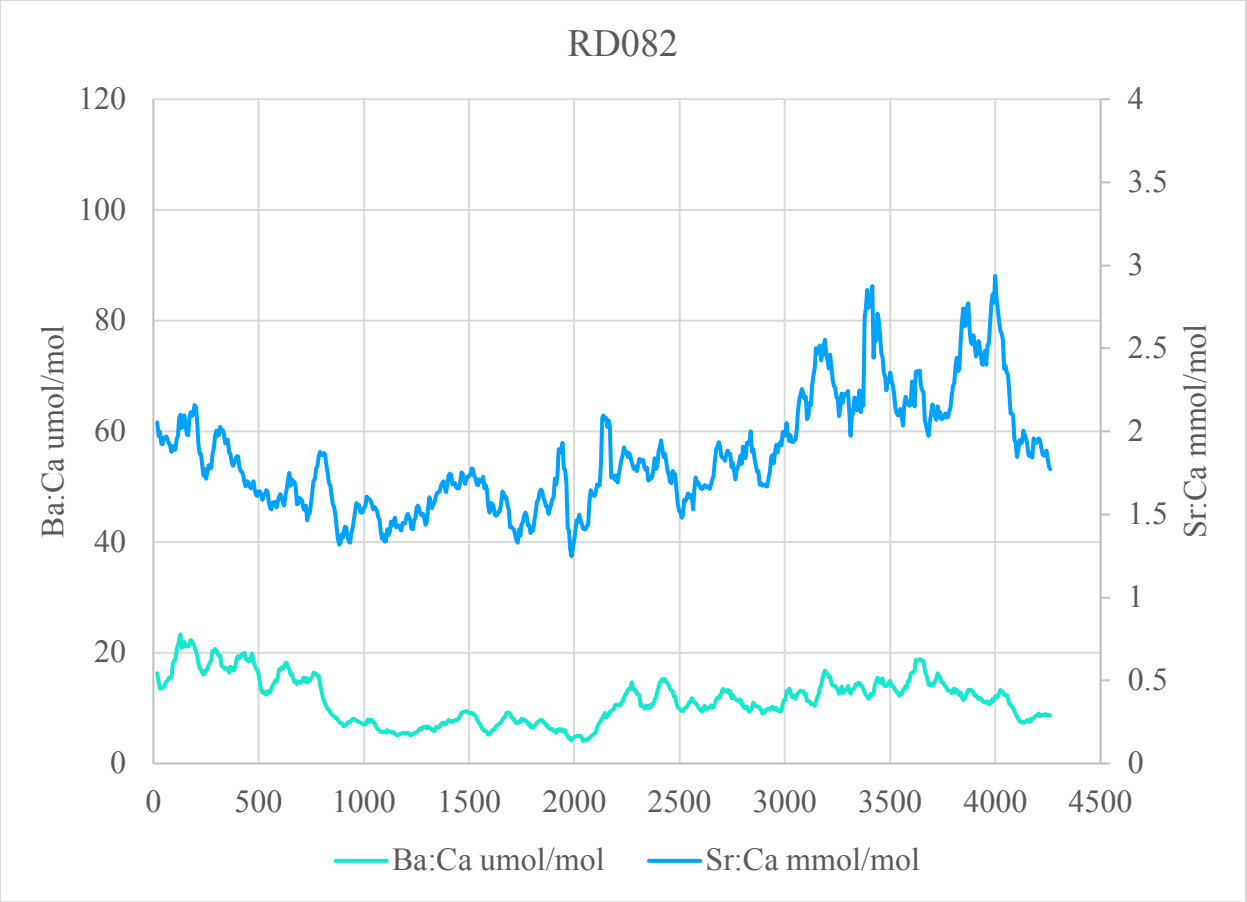

Figure A.82. The Ba:Ca and Sr:Ca life history profile of individual RD082.

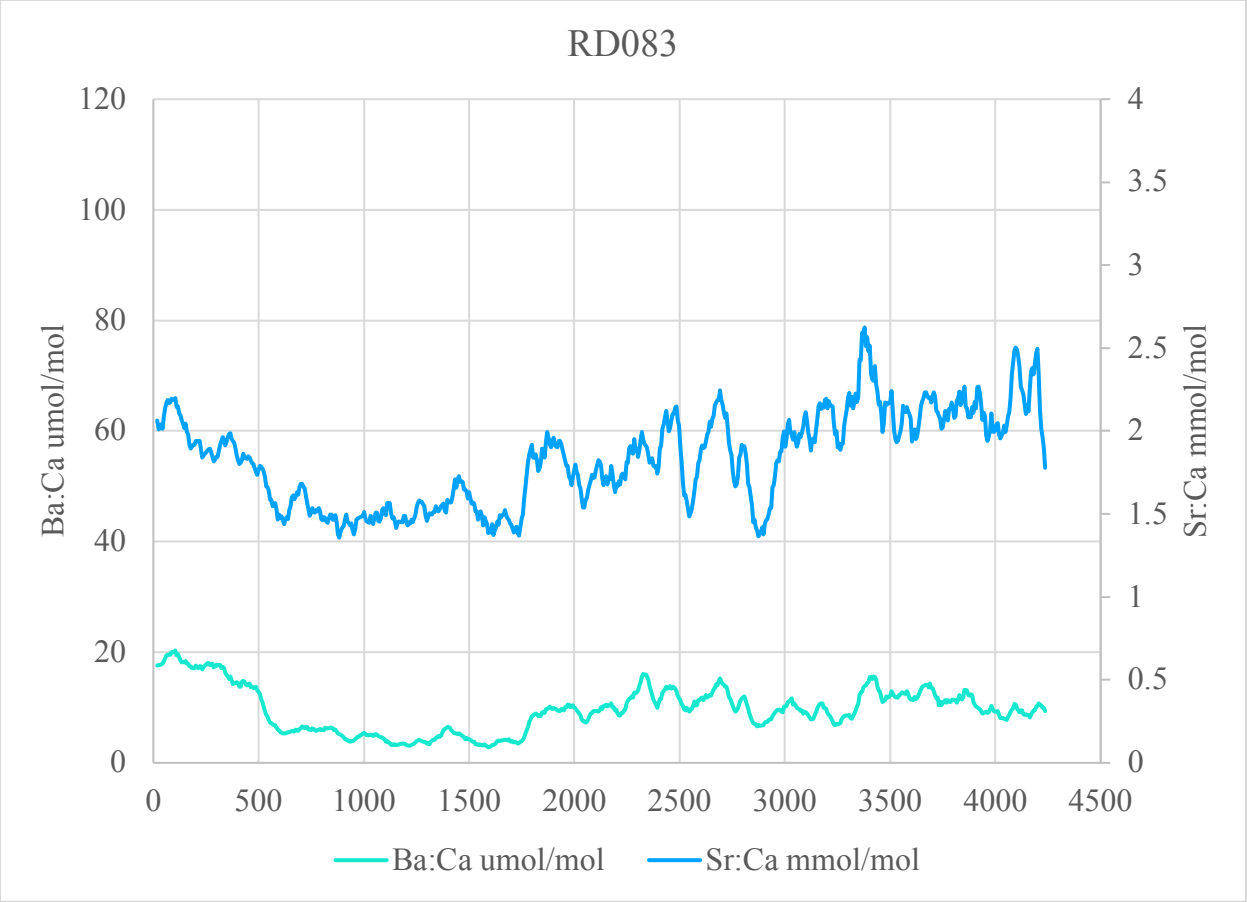

Figure A.83. The Ba:Ca and Sr:Ca life history profile of individual RD083.

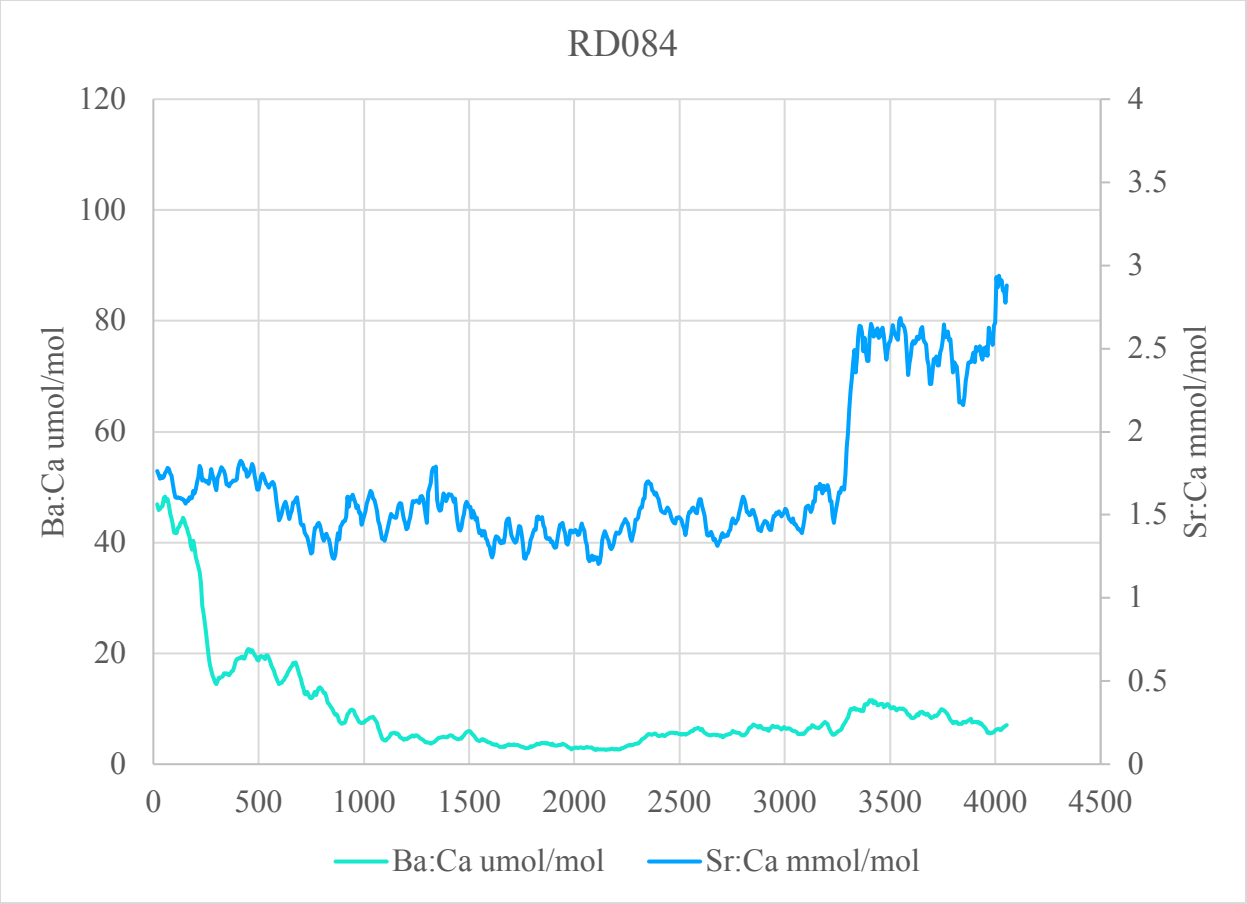

Figure A.84. The Ba:Ca and Sr:Ca life history profile of individual RD084.

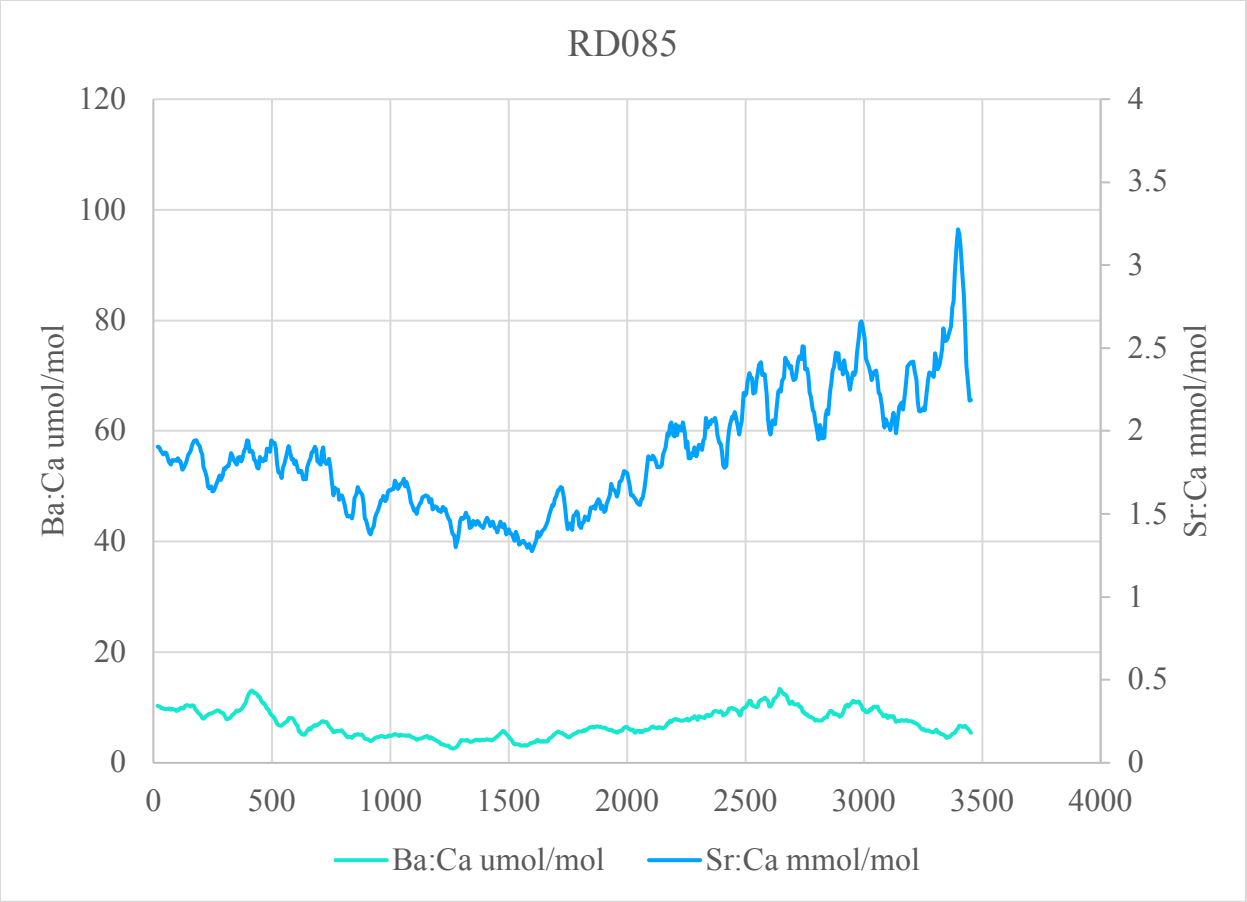

Figure A.85. The Ba:Ca and Sr:Ca life history profile of individual RD085.

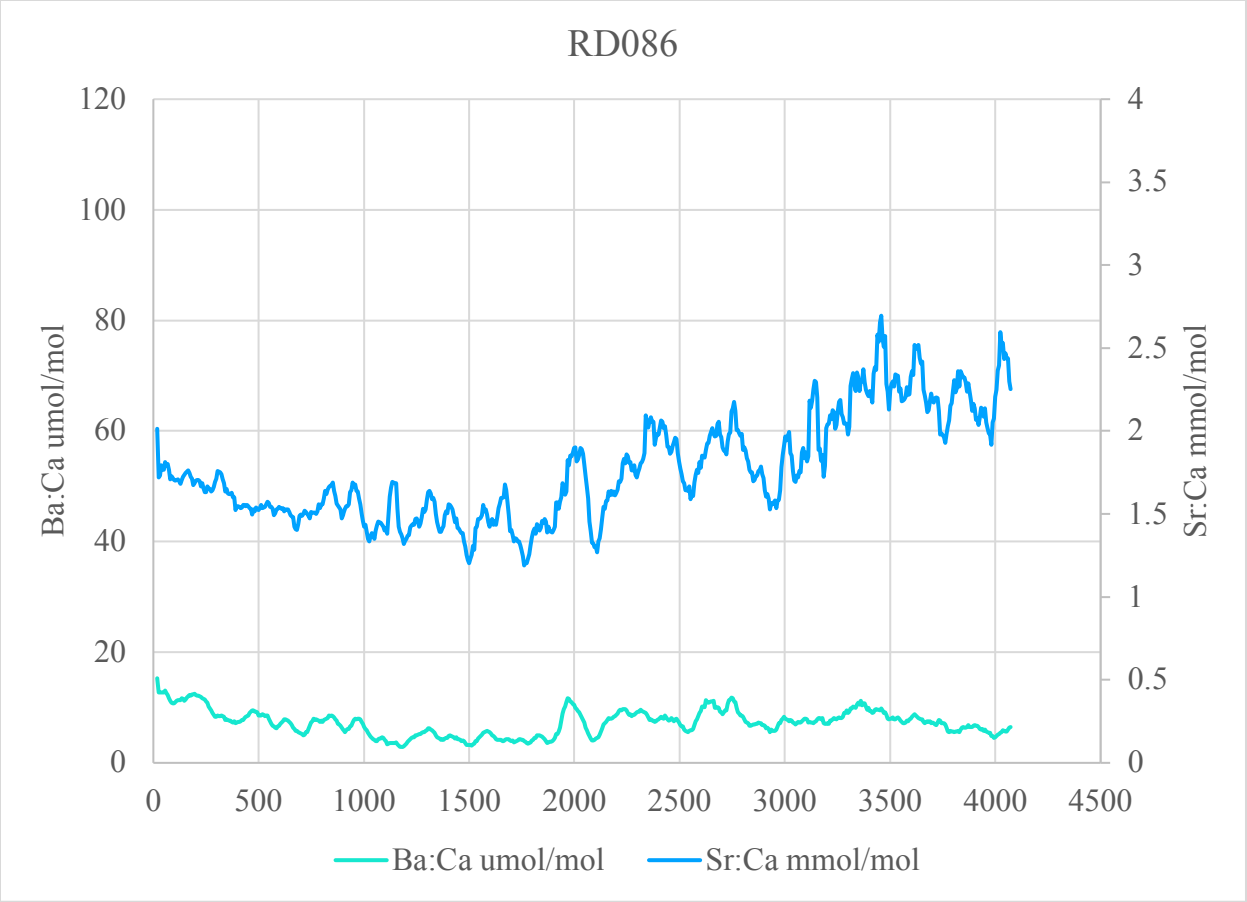

Figure A.86. The Ba:Ca and Sr:Ca life history profile of individual RD086.

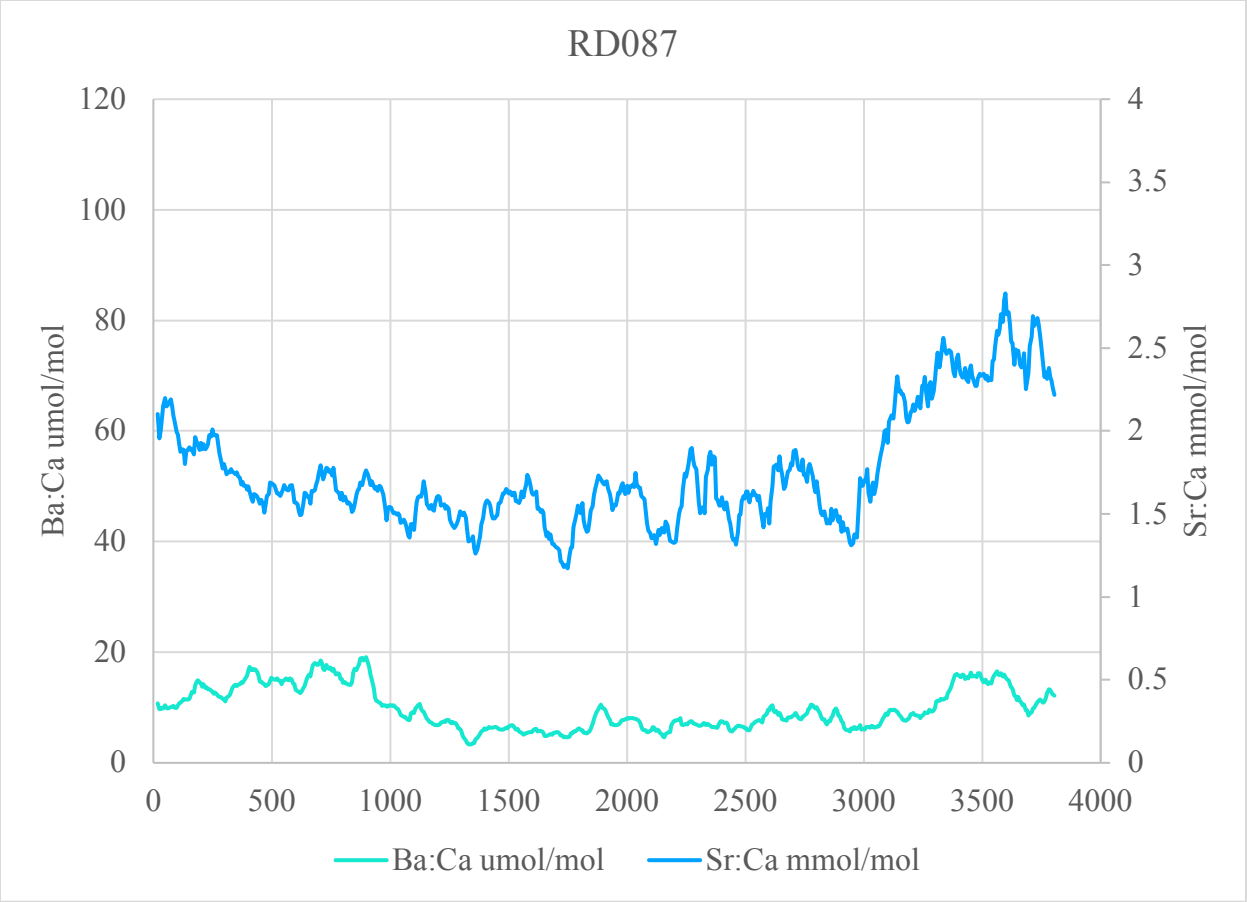

Figure A.87. The Ba:Ca and Sr:Ca life history profile of individual RD087.

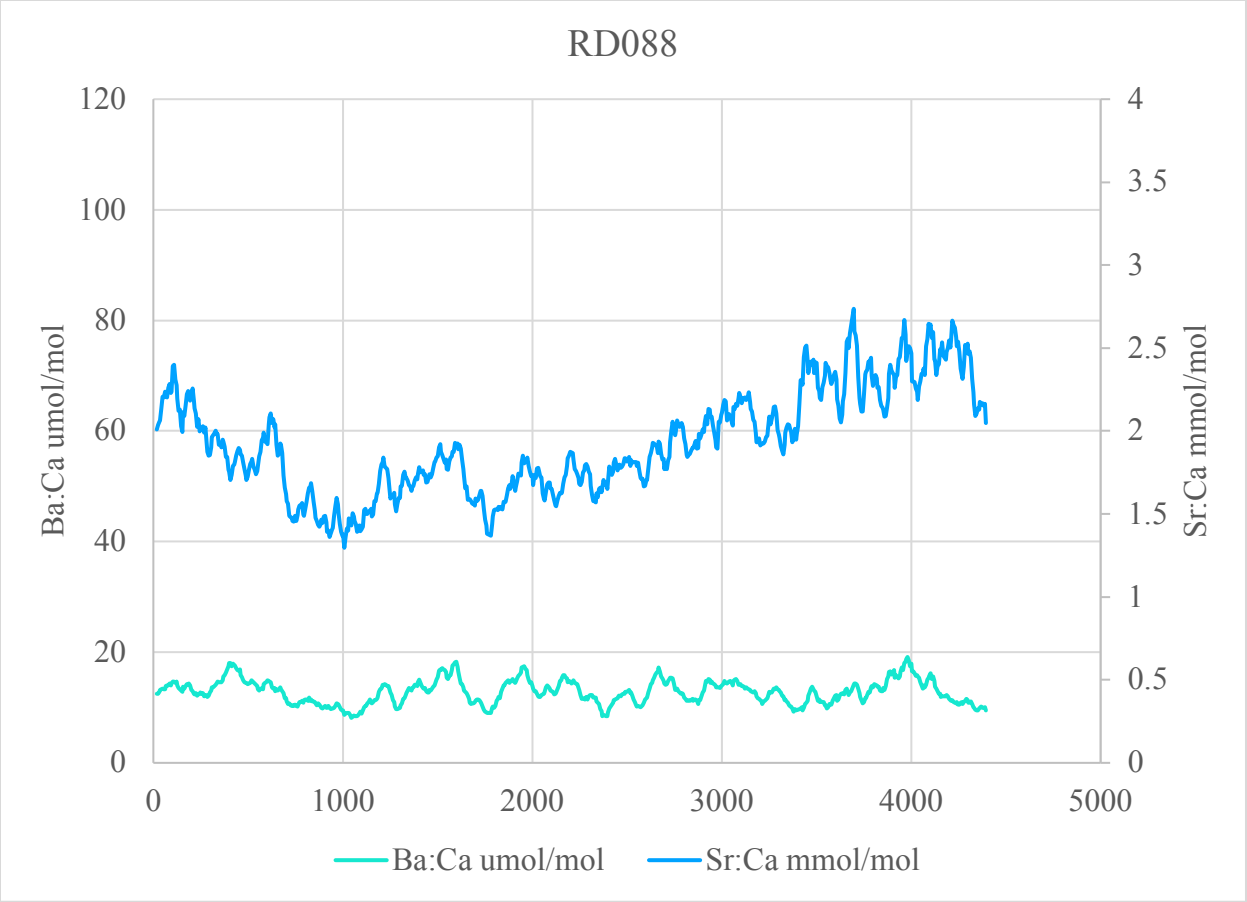

Figure A.88. The Ba:Ca and Sr:Ca life history profile of individual RD088.

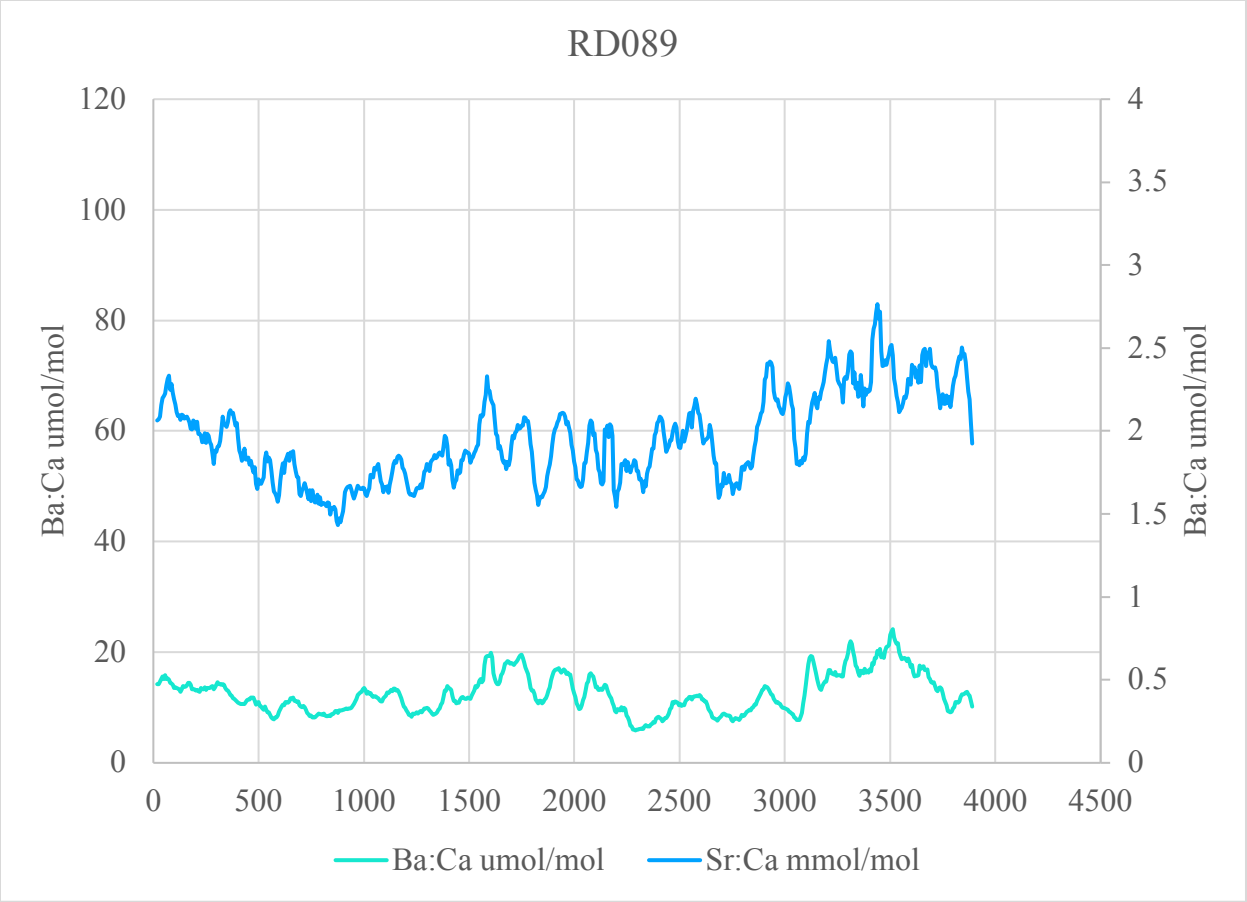

Figure A.89. The Ba:Ca and Sr:Ca life history profile of individual RD089.

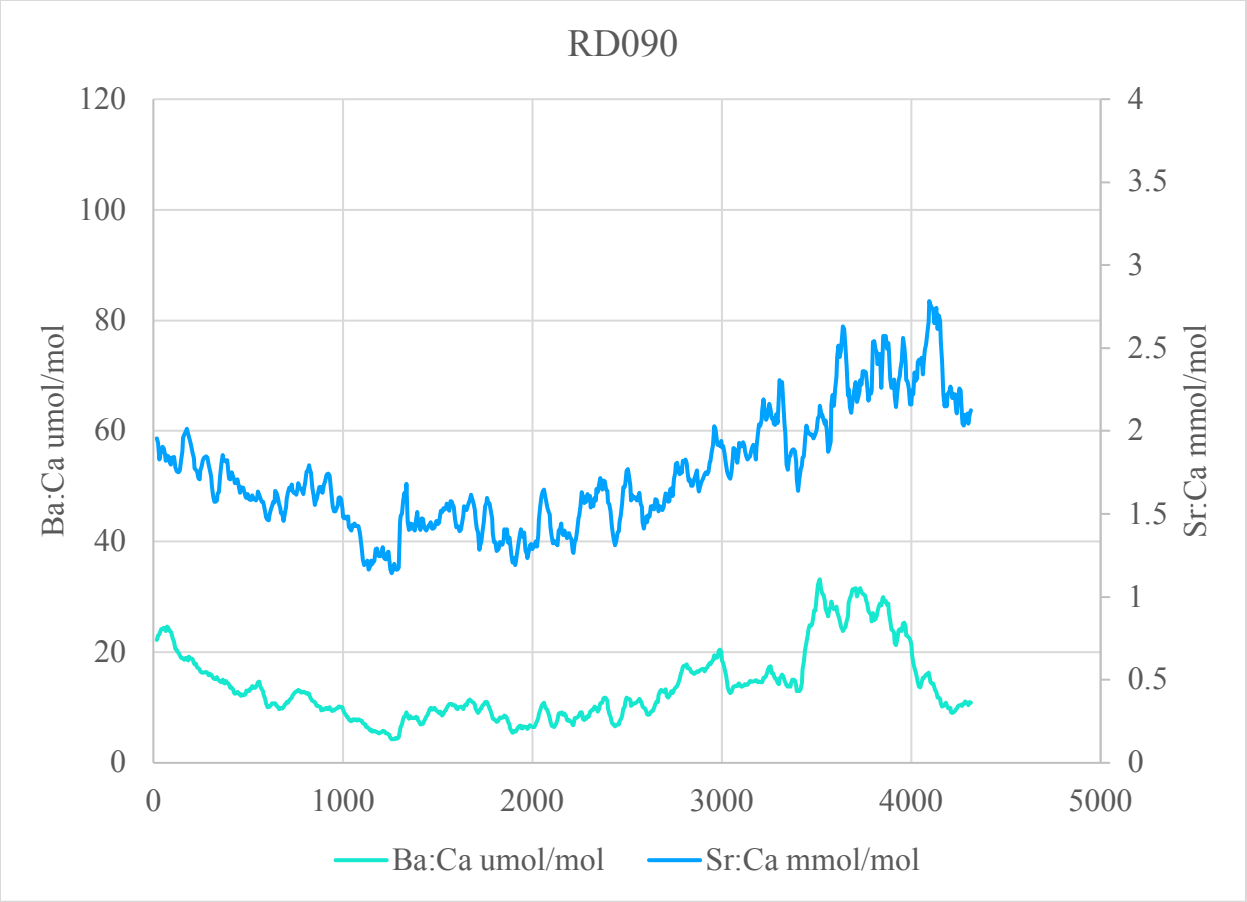

Figure A.90. The Ba:Ca and Sr:Ca life history profile of individual RD090.

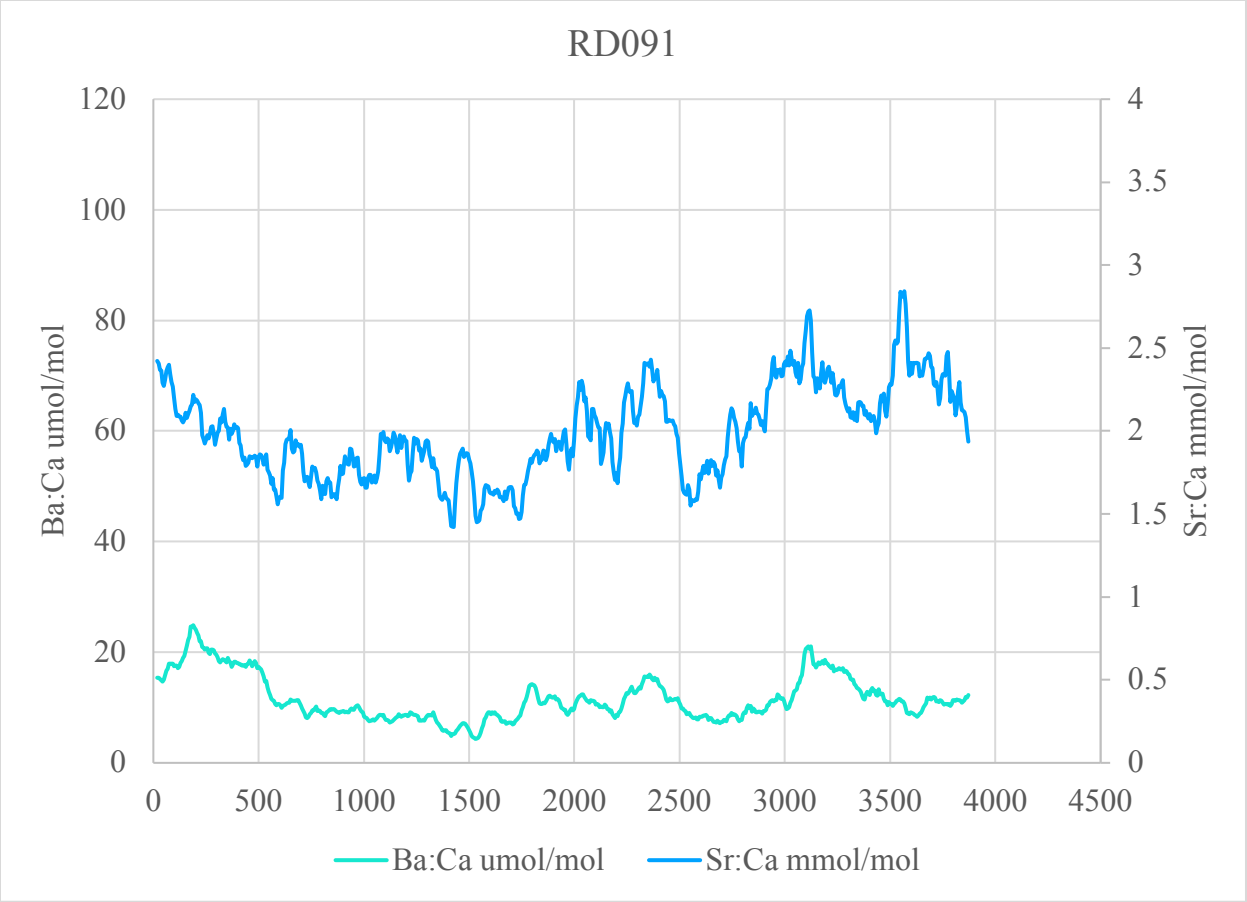

Figure A.91. The Ba:Ca and Sr:Ca life history profile of individual RD091.

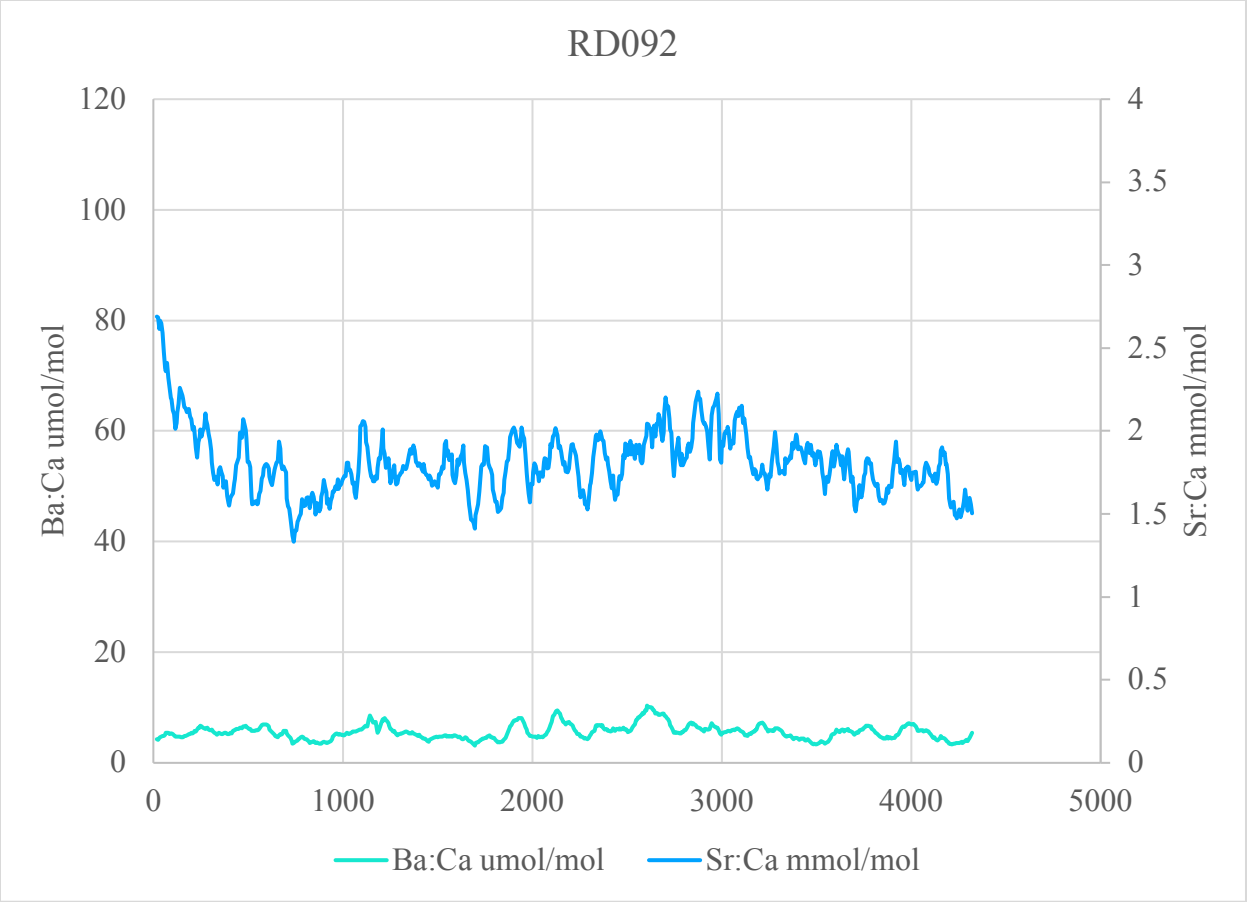

Figure A.92. The Ba:Ca and Sr:Ca life history profile of individual RD092.

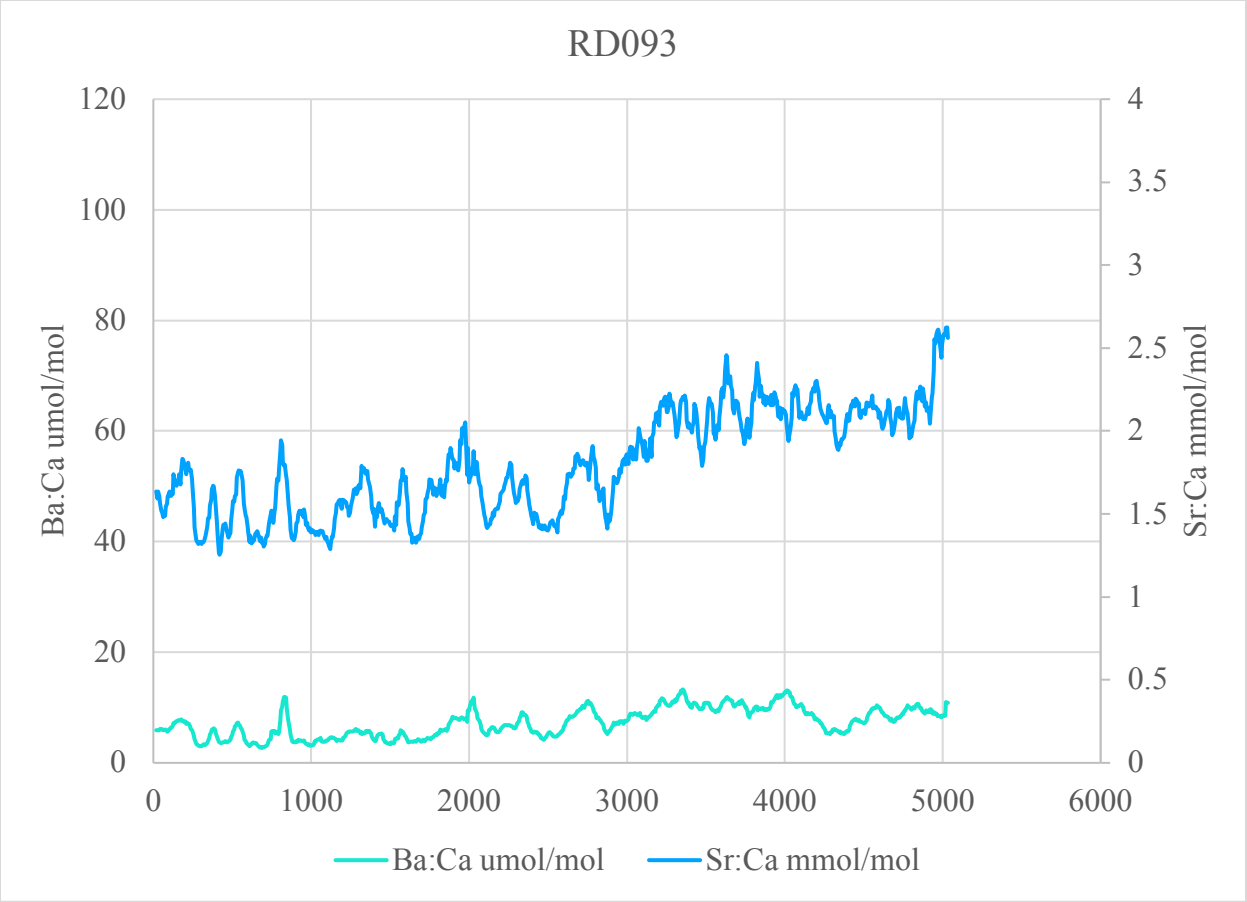

Figure A.93. The Ba:Ca and Sr:Ca life history profile of individual RD093.

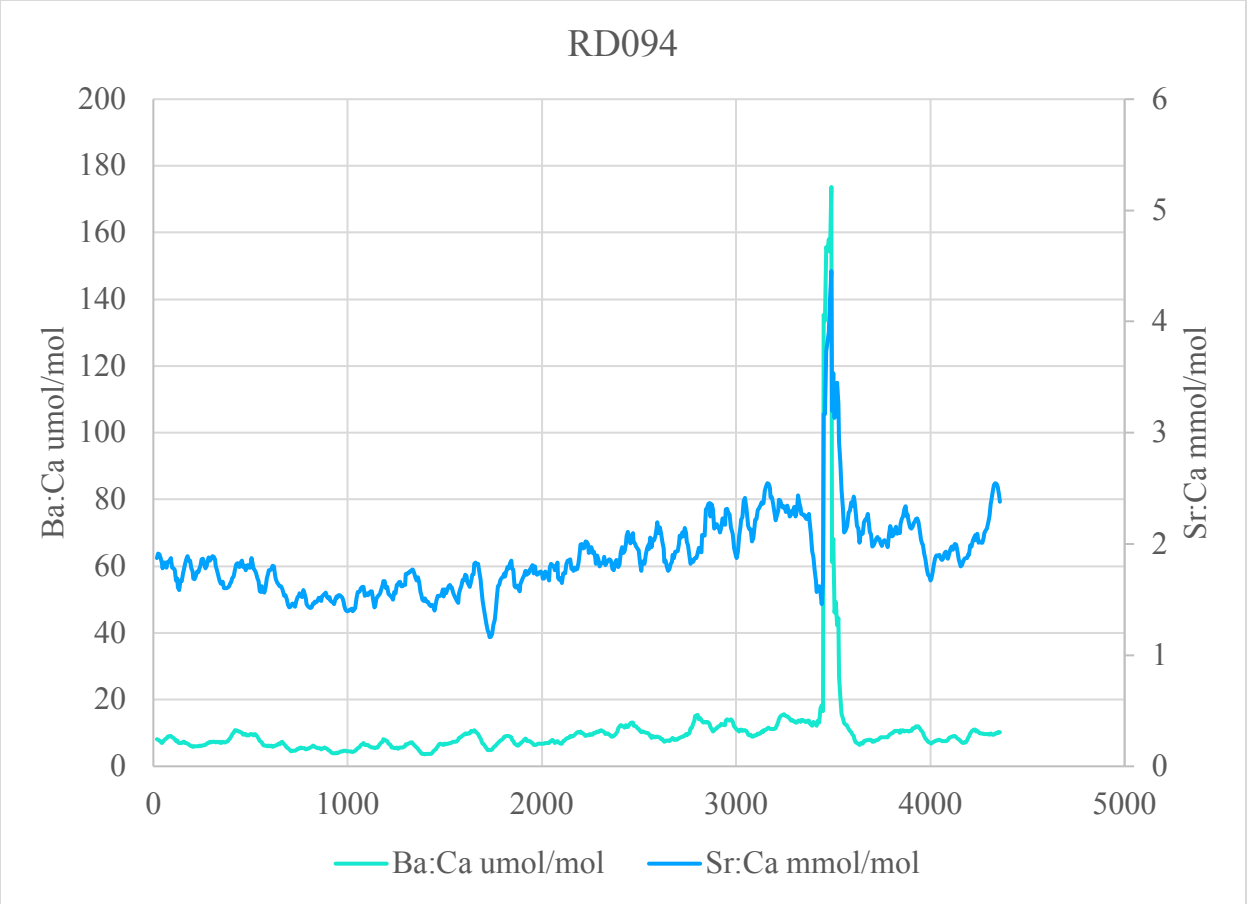

Figure A.94. The Ba:Ca and Sr:Ca life history profile of individual RD094.

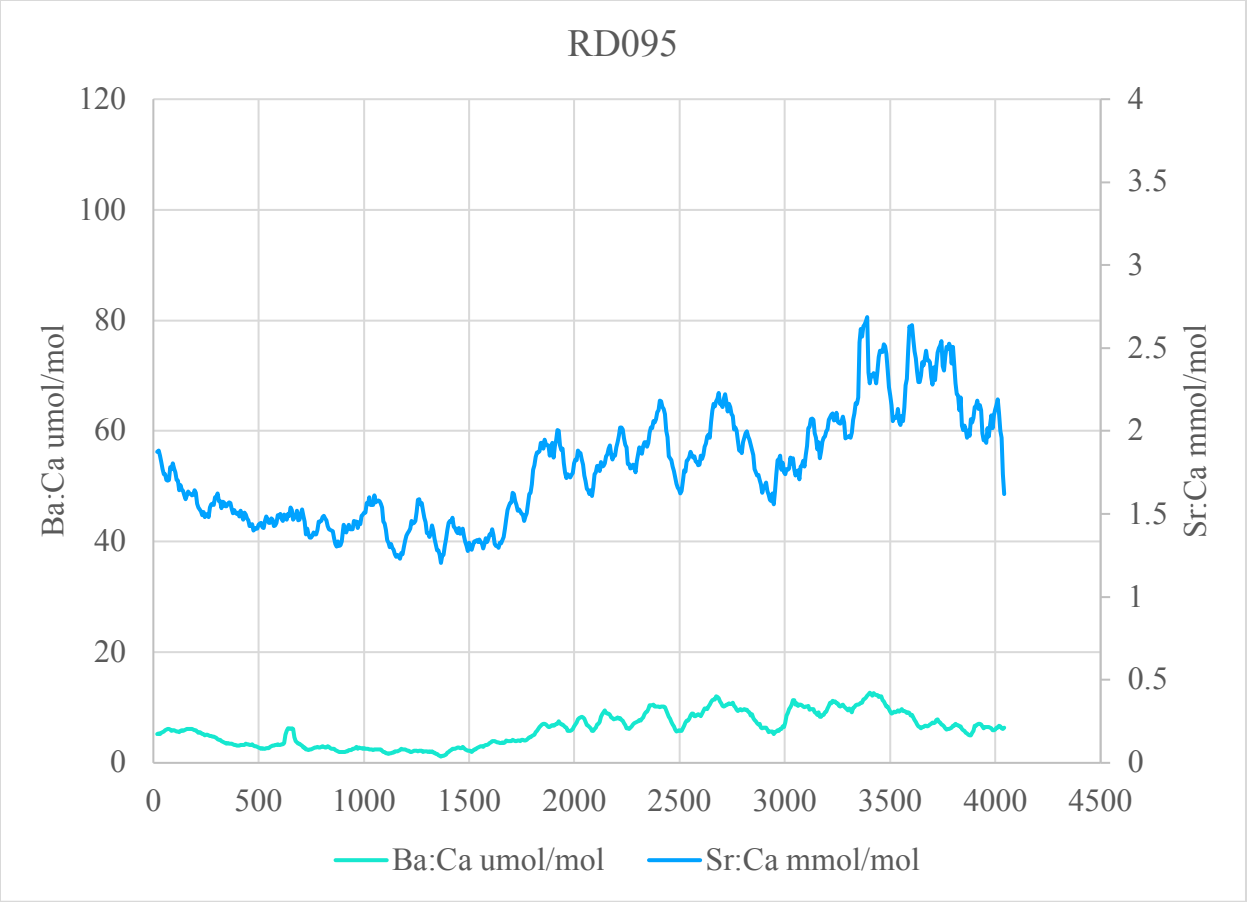

Figure A.95. The Ba:Ca and Sr:Ca life history profile of individual RD095.

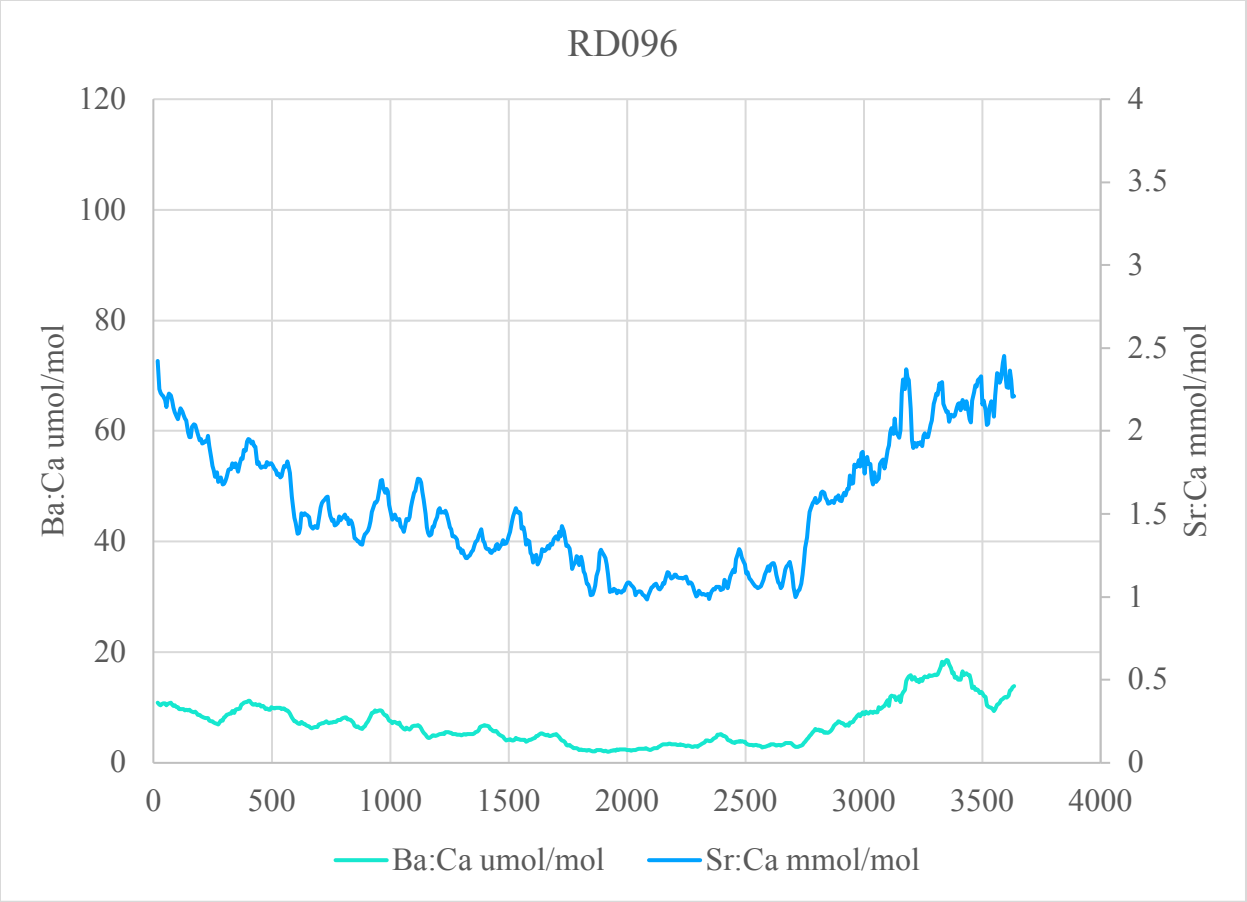

Figure A.96. The Ba:Ca and Sr:Ca life history profile of individual RD096.

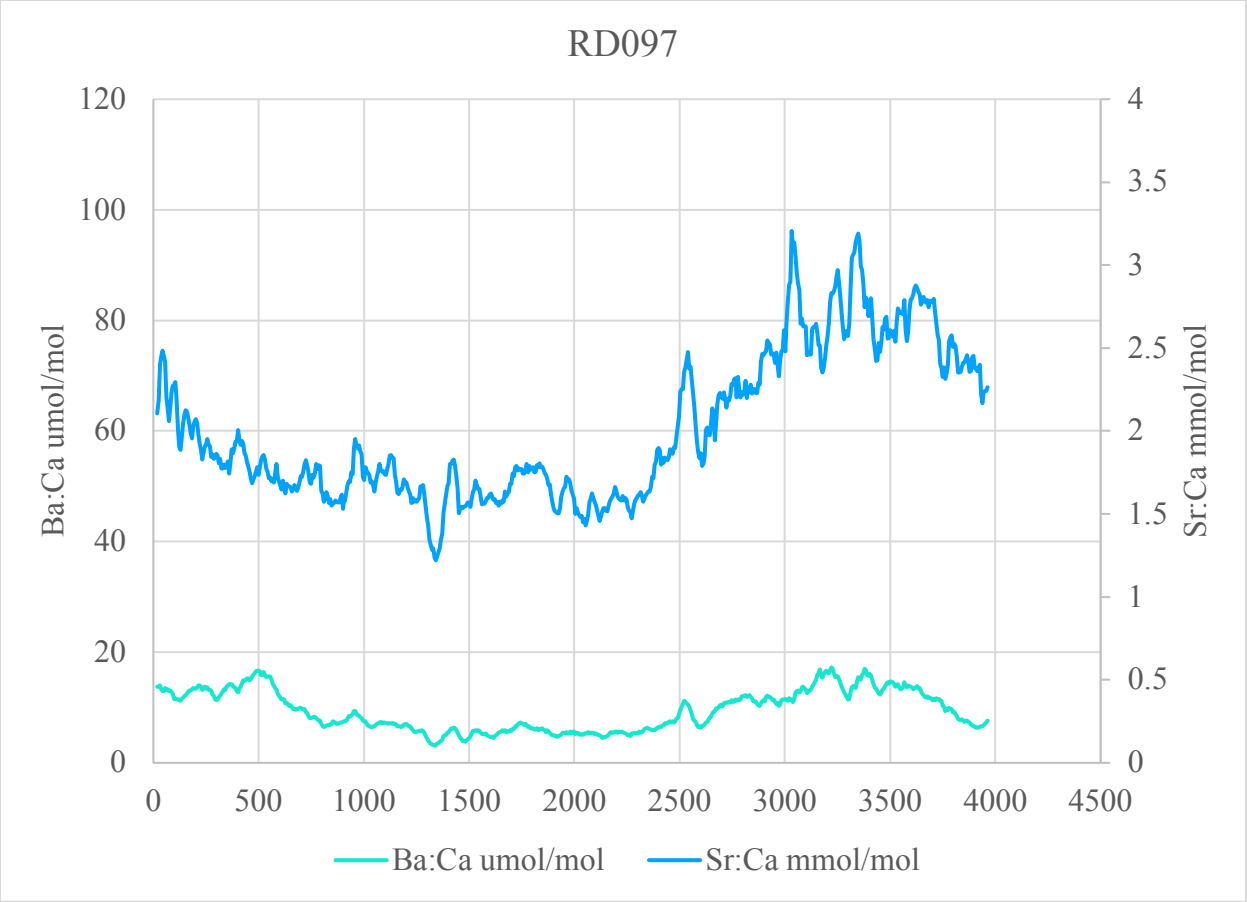

Figure A.97. The Ba:Ca and Sr:Ca life history profile of individual RD097.

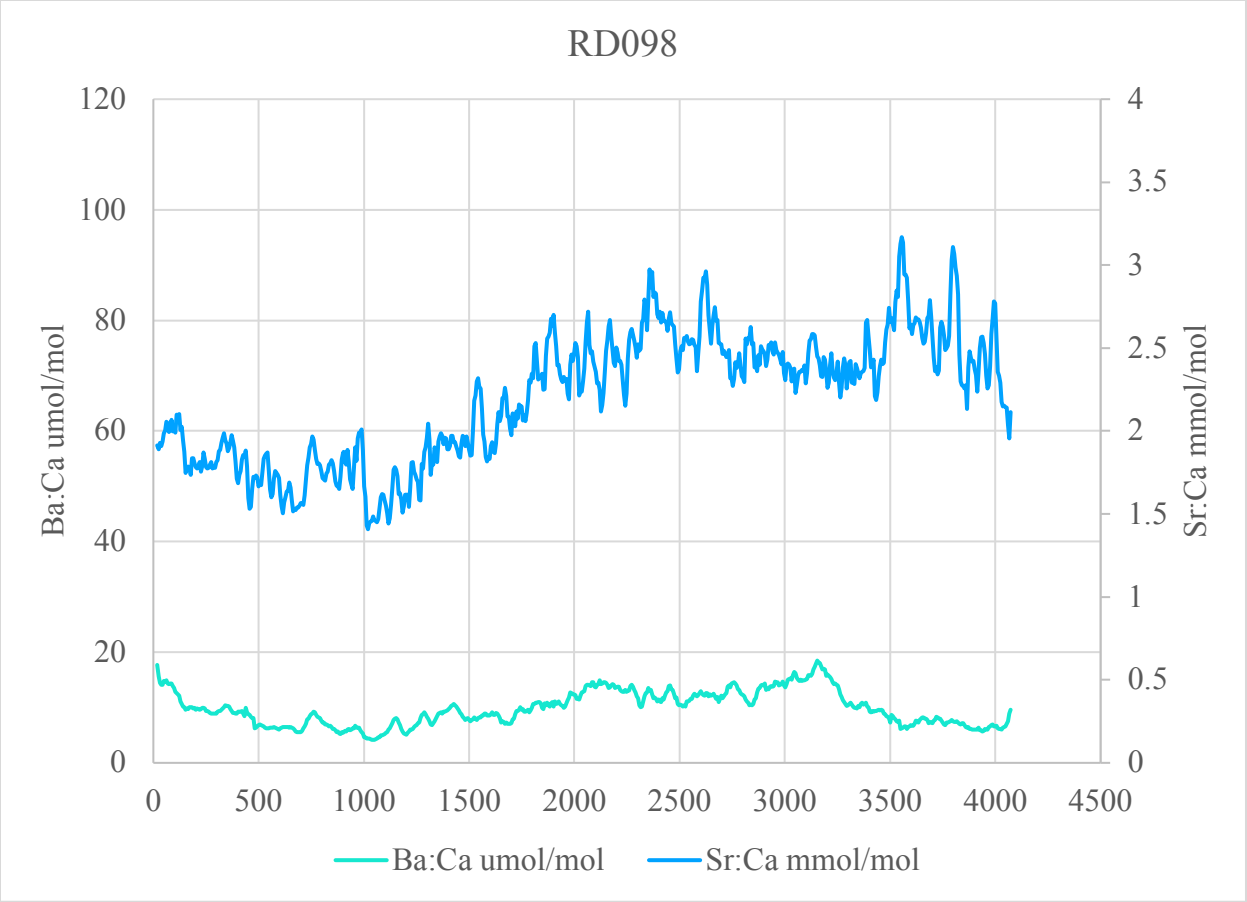

Figure A.98. The Ba:Ca and Sr:Ca life history profile of individual RD098.

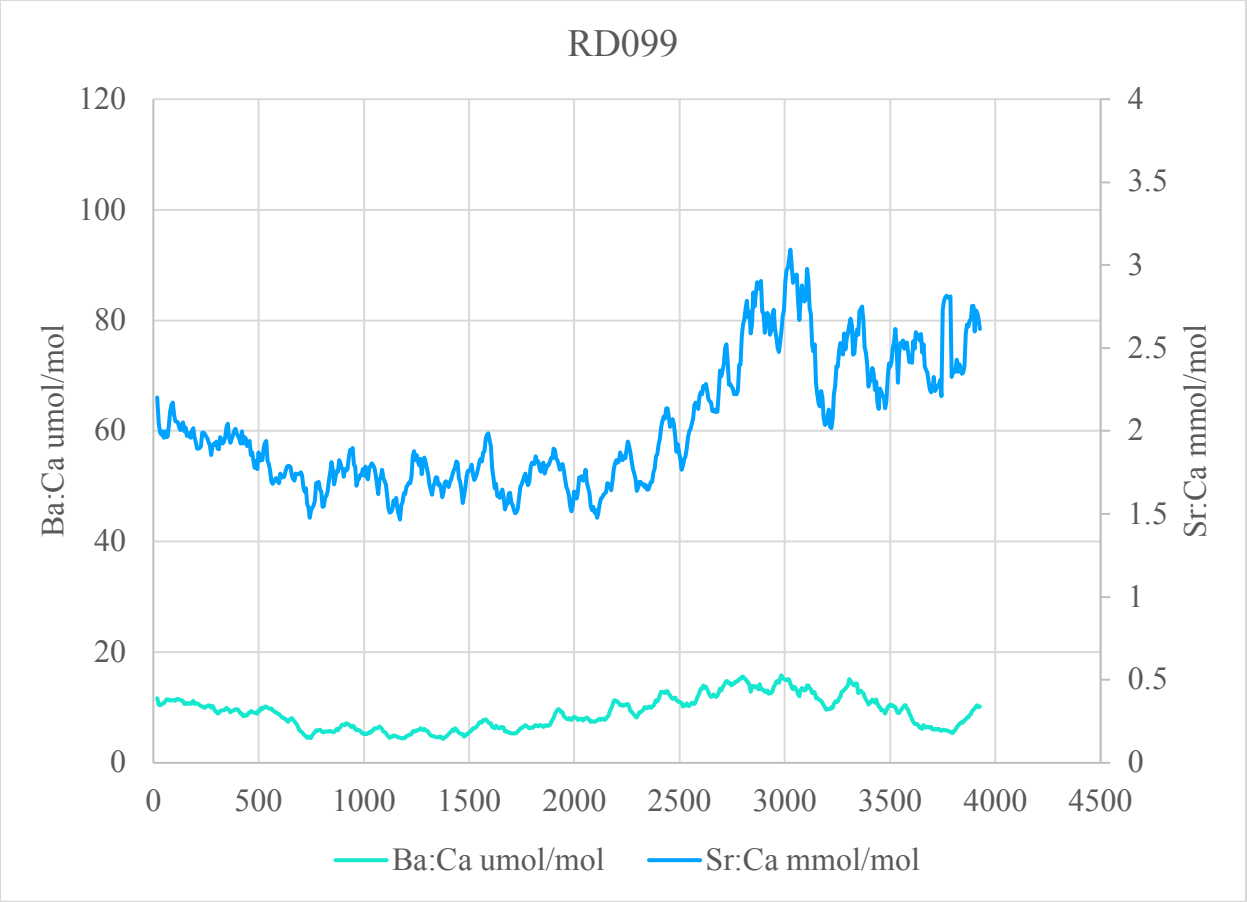

Figure A.99. The Ba:Ca and Sr:Ca life history profile of individual RD099.

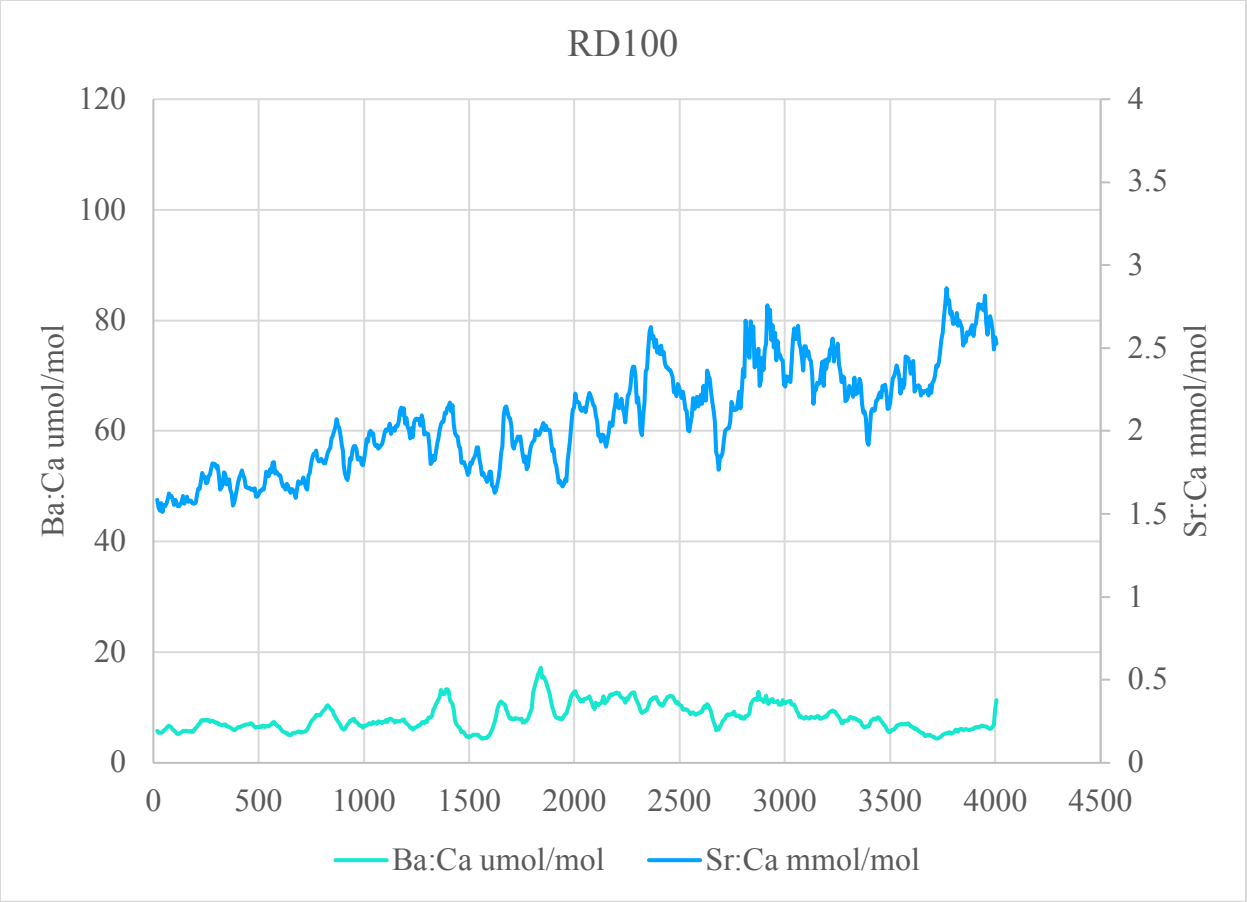

Figure A.100. The Ba:Ca and Sr:Ca life history profile of individual RD100.